Universitat Autònoma de Barcelona

DEPARTMENT of BIOCHEMISTRY and MOLECULAR BIOLOGY

Doctoral Program in Biochemistry and Molecular Biology

"PROTEOMIC APPROACH TO FLATFISH AQUACULTURE. STUDY OF THE REPRODUCTIVE BIOLOGY OF *SOLEA SENEGALENSIS.*"

IGNASI FORNÉ i FERRER

MAY, 2007

DEPARTMENT of BIOCHEMISTRY and MOLECULAR BIOLOGY

Doctoral Program in Biochemistry and Molecular Biology

Doctoral thesis presented by

IGNASI FORNÉ FERRER

to obtain the

Ph.D. IN BIOCHEMISTRY AND MOLECULAR BIOLOGY

This work has been carried out in the Proteomics Laboratory CSIC/UAB and in Oryzon Genomics under the supervision of Dr. Joaquín Abian and Dr. Joan Cerdà.

Ph.D. candidate	Ph.D. Supervisor
IGNASI FORNÉ i FERRER	Dr. JOAQUIN ABIAN MOÑUX CSIC Research Scientist
Department Tutor	Ph.D. Supervisor
Dr. JAUME FARRÉS VICÉN UAB Biochemistry and Molecular Biology Professor	Dr. JOAN CERDÀ LUQUE IRTA Research Scientist

Barcelona, May 2007

Veles e vents han mos desigs complir,
faent camins dubtosos per la mar.
Mestre i ponent contra d'ells veig armar;
xaloc, llevant, los deuen subvenir
ab llurs amics lo grec e lo migjorn,
fent humils precs al vent tramuntanal
que en son bufar los sia parcial
e que tots cinc complesquen mon retorn.

Bullirà el mar com la cassola en forn,
mudant color e l'estat natural,
e mostrarà voler tota res mal
que sobre si atur un punt al jorn.
Grans e pocs peixs a recors correran
e cercaran amagatalls secrets:
fugint al mar, on són nodrits e fets,
per gran remei en terra eixiran.

Ausiàs March (Veles e vents)

No importa el problema, no importa la solución,

me quedo con lo poco que queda, entero en el corazón.

Me gustan los problemas, no existe otra explicación.

Esta sí es una dulce condena, una dulce rendición.

Andrés Calamaro (Dulce condena)

En primer lloc agrair al Dr. Carlos Buesa i al Dr. Joaquin Abián la possibilitat de realitzar el treball de tesi doctoral conjuntament al Laboratori de Proteómica CSIC-UAB i a Oryzon Genomics, per la oportunitat que suposa combinar el dia a dia del creixement d'una empresa biotecnològica i la convivència en un entorn acadèmic de referència en espectrometria de masses i proteòmica.

Al Dr. Joaquín Abián (de nou) i al Dr. Joan Cerdà per la direcció de la tesis i per la seva implicació personal, dedicació, suport i esforç en tot moment.

A tota la gent que ha participat en el disseny i realització del projecte Pleurogene, en especial al Dr. Joan Cerdà per la coordinació general, i a la Dra. Tamara Maes per la direcció científica des d'Oryzon Genomics.

Al Dr. Jaume Farrés per la tutoria d'aquest treball, per la seva col·laboració i disponibilitat en tot moment.

A tota la gent que he conegut a Oryzon durant aquests gairebé quatre anys, especialment a la Maite del Hierro, per ser una persona i companya de laboratori excel·lent, per la seva responsabilitat i el seu humor (kapasao-i-yokezé!!); al Joaquin (darrer cop) per la seves dosis de moral, experiència i temps quan les coses anaven maldades; al Jaume Mercadé per la col·laboració en el darrer capítol i per les converses sobre cóm canviar el món; al Dr. Toni Espinosa per la seva col·laboració en el primer capítol i per estar sempre a punt per fer "*unas risas*"; a la Dra. Elisabet Rosell per la seva mà esquerra i l'optimisme que transmet; al Xavi Calvo pel seu ajut en l'apartat de microarrays i per cuidar-me la cadira durant les meves llargues absències; al Jaume, el Jordi, l'Elena, el Roger i el Ricard per compartir l'experiència de fer una tesi dins de la empresa (ànims, que hi ha una llum al final!!); i a tots els que heu participat en les tertúlies després de dinar, en una sessió de *youtube* o senzillament amb un somriure en un mal dia.

Als companys del Laboratori de Proteómica CSIC-UAB que ja hi eren quan vaig arribar, en especial a la Dra. Montse Carrascal pel temps i les energies dedicades (si hay que hacerlo, se hace…), i a la Dra. Carme Quero pels primers temps al lab; als que han passat deixant petjada, en especial al Miguel Trigo per la convivència al "zulo", i als que

us quedeu i encara m'acolliu de bon grat quan vinc de visita: Marina, David, Rebeca, Vanesa i Cristina.

Al Dr. Francesc Canals per facilitar-me l'ús del Laboratori de Proteómica de Vall d'Hebrón, a la Núria per les classes de Decyder i, junt amb la Cristina, per fer les hores de Decyder/Typhoon molt més amenes.

Al Dr. Jaume Planas per la cessió dels resultats de microarrays del segon capítol.

Al Miquel Daura de "Common Sense" pel disseny de la portada i del CD.

A tots els que m'heu ajudat a créixer dins del món de la investigació en els diferents centres on he tingut la sort de treballar, en especial al Dr. Cándido Juarez del Departament d'Immunologia de l'Hospital de Sant Pau, per les primeres passes en el món de la proteómica.

A tots els amics que heu col·laborat desinteressadament en el meu suport psicològic durant aquests anys, a la Cristina i al Miquel per la Vila del Pingüí (i per tantes altres coses…), a la Sónia i al Pedro per Madrids, Lisboas, París i Basileas, i a tots quatre per uns quants Munichs; al Jordi i al Natxo per estar sempre a punt; a la colla de l'ESM (ja sabeu qui sou…), per tant anys d'històries.

Al meu germà Oriol per tots els moments junts a casa, pistes, pavellons, gimnasos, bars i festes majors: per ser com és.

Als meus pares, Anna i Ernest, per educar-me i fer-me créixer amb generositat, convicció i amor, donant-me totes les oportunitats i les eines que m'han permès arribar fins aquí.

A la meva dona Alexandra, per tenir les mides perfectes de "Cherry Blossom Girl", de "Limón y Sal" i d'"Alegria"; i a la meva filla Paula pels moments únics que he viscut i espero viure. A totes dues, "I just want say "Hi" to the ones I love".

Table of Contents

Abbreviations

1-D:	one dimensional
2-DE:	two-dimensional electrophoresis
11-KT:	11-ketotestosterone
17α,20β-P:	17α,20β-dihydroxy-4-pregnen-3-ona
Δ:	increment
ACN:	acetonitrile
BLAST:	basic local alignment search tool
cAMP:	3'-5'-cyclic adenosine monophosphate
CHAPS:	3-[(3-cholamidopropyl) dimethylamonio]-1-propanesulfonate
CID:	collision induced dissociation
CV:	coefficient of variation
Cy:	cyanine fluorophore
Da:	Dalton (molecular mass)
DIGE:	differential in gel electrophoresis
DMF:	dimethylformamide
DTT:	ditiothreitol
EDTA:	ethylenediaminetetraacetic acid
ETD:	electron transfer dissociation
ESI:	electrospray ionization
EST:	expressed sequence tag
FSH:	follicle stimulating hormone
F0:	wild-grown fish
F1:	aquaculture-grown fish
FT-ICR:	Fourier transform ion cyclotron resonance (mass spectrometry)
Gc:	primary germ cell
GnRH:	gonadotropin releasing hormone
GnRHa:	gonadotropin releasing hormone agonist
GO:	gene ontology
GSI:	gonadosomatic index (gonad weight/body weight x 100)
GtH:	gonadotropin hormone
GUI:	Graphic user interface
HED:	2-hydroxyethyl disulfide
HPLC:	high-performance liquid chromatography
ID:	internal diameter
IEF:	isoelectrofocusing
IPG:	immobilized pH gradient
IS:	internal standard
IT:	ion trap
i-TRAQ:	isobaric tag for relative and absolute quantitation
L:	late spematogenesis stage
LC:	liquid chromatography
Lc:	Leydig cells
LH:	luteinizing hormone
m/z:	mass-to-charge ratio
MALDI:	matrix assisted laser desorption /ionization
M:	mid spermatogenesis stage
Mat:	functional maturation spermatogenesis stage
MeOH:	methanol
Mr:	relative molecular mass (dimensionless)
MS:	mass spectrometry
MS/MS:	tandem mass spectrometry
n-ESI:	nano electrospray ionization
NP40:	nonidet P-40
OA:	11-ketoandrostenedione
P:	p-value
PAGE:	polyacrylamide gel electrophoresis
PCR:	polymerase chain reaction

pI:	isoelectric point
PMF:	peptide mass fingerprinting
PMSF:	phenylmethylsulfonyl fluoride
PTM:	post-translational modification
RP:	reversed phase chromatography
S2S:	self-to-self analysis
Sc:	Sertoli cells
SCX:	strong cationic exchange chromatography
SD:	standard deviation
SDS:	sodium dodecyl sulphate
SEM:	scanning electron microscopy
Spc:	spermatocytes
Spd:	spermatides
Spg A:	spermatogonia type A
Spg B:	spermatogonia type B
Spz:	spermatozoa
st:	seminiferous tubules
TFA:	trifluororacetic acid
TIC:	total ion chromatogram
TL:	tubule lumen
TOF:	time-of-flight
TSQ:	triple stage quadrupole
Tris:	tris(hydroxymethyl) aminomethane
UV:	ultraviolet

Introduction

I.1 Flatfish species

Flatfishes, members of the order Pleuronectiformes, comprise a biologically interesting and commercially relevant group of marine fishes with a broad distribution from the Artic to Australasia, with a unique asymmetric body shape developed as an adaptation to a lifestyle living on the sea-bottom. During development, flatfishes reorient themselves to lie on one side, losing the bilateral symmetry characteristic of most living organisms. Such metamorphosis involves the migration of one eye to the other side of the body, the flattening of the body and the settling of the fish on the side vacated by the migrating eye. Flatfish metamorphosis requires a complex reorganization of skeletal, nervous and muscle tissues. In addition to this unique developmental event, flatfishes have long been a choice seafood, with many members of the group (i.e. halibuts, flounders, soles, turbot, plaice) having commercial value. With the general worldwide decline of wild fishery and an essentially stable wild catch of these fish species, investigations into producing them in aquaculture have been underway for the last twenty years. Aquaculture of some flatfish species like Japanese flounder, turbot, Atlantic halibut and others has now been successfully achieved, although improvements in the efficiency of production are still needed (Gibson 05).

The Senegalese sole (*Solea senegalensis*), a member of the Soleidae family (Actinopterygii class: ray-finned fishes) is a common, high-value marine flatfish recently adapted to aquaculture in Spain and Portugal. The fast development of eggs and larvae, and the improved growth of alevins under intensive culture conditions make the Senegalese sole a new species for aquaculture with a highly promising economic potential and an increasing strategic market in Spain and other Mediterranean countries (Dinis 99). For these reasons, there is a significant demand within the Spanish aquaculture industry for the development of an integrated culture technology for the Senegalese sole. This fish species is well-adapted to warm climates and it is commonly raised in the extensive culture conditions of salt marshes and earthen ponds along the south coasts of Spain and Portugal (Rodríguez 84; Drake 84; Dinis 92), where the reproductive biology of this species became a focus of research from the early 1980s (Rodríguez 82; Rodríguez 84; Dinis 92). However, some culture problems are still limiting the yield of the sole production process to a level that is not yet optimal for

commercialisation. Therefore, before a reliable technology for mass production of the Senegalese sole can be transferred to the industry, several aspects of its culture need to be solved and optimized. In consequence, this work aims to describe the Senegalese sole reproductive physiology by using modern chromatographic, electrophoretic and spectrometric techniques for shotgun and differential expression proteomics, in combination with DNA microarray analysis and bioinformatic tools.

I.1.1 Flatfish aquaculture

Species belonging to teleosts, one of three infraclasses of the ray-finned fishes, are of great interest for basic studies and commercial exploitation. Despite this importance and their ready availability as research subjects, the reproductive biology of relatively few species of teleosts has been adequately studied. Most of the current knowledge concerning reproductive physiology in fish originates also from a few species, some of them interesting for fish industry such as salmonids or the rainbow trout. However, research on key intracellular and molecular events has been often limited to small laboratory species that, despite being useful models for developmental biology, often lack of value as commercial species (Miura 03).

Reproduction represents the phase in the life cycle that links the new generation of offspring to the adult population for any living species. Successful reproduction is then vital for the continued existence of the fish population in its natural environment (Rijnsdorp 05). The main events related to reproduction are spawning, gonad development, fecundity and onset of sexual maturity. It is well known that certain commercially important species suffer from low fertilization and low hatching rates, and similar problems occurs when they are cultured in artificial environments under controlled conditions (Rottmann 91). Moreover, reproduction in fishes is regulated by external environmental factors that trigger internal mechanisms, which modulate the release of eggs and sperm and that result in spawning, the final event of the reproductive cycle. These external factors controlling the reproduction vary considerably among species. Factors like photoperiod, water temperature, water quality, water currents, moon cycles, nutrition, disease and parasites as well as the presence of other fishes have been involved in the reproductive cycle in an interrelated way. Unfortunately, this complex set of factors and equilibria that can affect spawning in natural conditions

can not be reproduced in captivity. In consequence, the artificial conditions inherent to aquaculture complicate the industrial exploitation of many species of interest.

In nature, *S. senegalensis* spawn mainly in spring and secondarily in autumn, although males can produce sperm almost any time through the year with a production of a few tens of microliters of sperm in overall (García 05). In captivity, however, spontaneous spawning is often associated with relatively low (45-60%; Anguis 05) or zero fertilization rates, especially in the F1 generation (Agulleiro 06). As egg quality from female individuals in aquaculture conditions is acceptable, such reproductive dysfunction might be related to impaired spermatogenesis and/or spermiation in captivity. This has been already observed in North Sea plaice, in which captive males produce abnormally dense milt and show plasma concentrations of sex steroids that are 100 times lower than those of wild-caught males (Vermeirssen 98). Thus, in *S. senegalensis,* abnormal spermatogenesis and/or the production of low quality sperm are the main obstacles that impair reproduction in captivity. To make things worse, basic knowledge on gametogenesis and the sexual cycle of wild and cultured *S. senegalensis* is scarce.

I.1.2 Teleost spermatogenesis

As in other vertebrates, the gonads of teleost fishes originally arise as paired structures in the dorsal lining of the peritoneal cavity. The gonads have two main functions: to generate germ cells through the processes of oogenesis (ovary) or spermatogenesis (testis), and to produce sex steroids and growth factors that are important for the regulation of reproduction. The testis size is highly variable among teleosts, ranging from 0,2 to 10% of total body weight (Coward 02). In the structure of the testis two different compartments can be differentiated. The first one, the interstitial compartment, consists on, fibroblasts, blood and lymph vessels, and Leydig cells. These cells possess enzymes involved in male steroid hormone synthesis (Miura 91).

The second compartment can show a lobular or tubular structure, depending on the particular species. Testes are classified as being lobular or tubular referring to the structure of this compartment. It contains three cell types: membrane basement cells, germ cells and somatic cells lining the periphery of the lobule/tubule (Nagahama 94). The somatic cells, known as Sertoli cells, attach to each other by specialized junction complexes to create the blood–testis barrier that provides the germ cells of physical

support and other factors needed for its survival, proliferation and differentiation (Weltzien 04). Functions of Sertoli cells seem to include metabolite transport (Grier 75; Billard 83) and phagocytosis of residual bodies (Grier 93).

A sperm duct, originated in the posterior region of each testis, leads to the urinary papilla located between the rectum and urinary ducts. The epithelial cells lining the sperm duct possess microvilli with numerous mitochondria and alkaline phosphatase activity, suggesting a role in the regulation of ionic composition, pH and osmotic pressure of the seminal fluid.

Spermatogenesis in teleosts takes place within the testicular spermatocyst (or cyst) formed by Sertoli cells involving a primary spermatogonium or germ cell (type A spermatogonia). Although development occurs synchronously within each cyst germ cell, spermatogenesis tends to proceed asynchronously in the lobules/tubules and therefore provides batches of germ cells at different stages of differentiation (Coward 02). This strategy seems to increase fecundation odds as it provides a longer period where a number of mature cells are exposed, thus not restricting the process to only one event.

During spermatogenesis, three major events occur in each spermatocyst. First, the spermatogonial germ cells undergo mitotic proliferation, leading to both new germ cells and differentiated spermatogonia (type B spermatogonia). After a differentiation process, spermatogonia transform into primary spermatocytes (spermatocytes I), which enter in two meiotic cell cycles, presenting in between an intermediate germ cell (spermatocytes II). The meiotic processes take place with one round of DNA duplication where the genetic information is recombined and distributed over the resulting genetically distinct haploid spermatids. Finally, spermatids turn into mature flagellated spermatozoa in a process referred as spermiogenesis. Spermatids are characterised by the loss of 80% of the cytoplasmatic volume (García 2005) and the replacement of histones by protamines, allowing optimal chromatin condensation (Schulz 00). Once maturation occurs, isogenic clones of spermatozoa are released by rupture of the cyst wall and collected in spermal ducts derived from cysts (figure i).

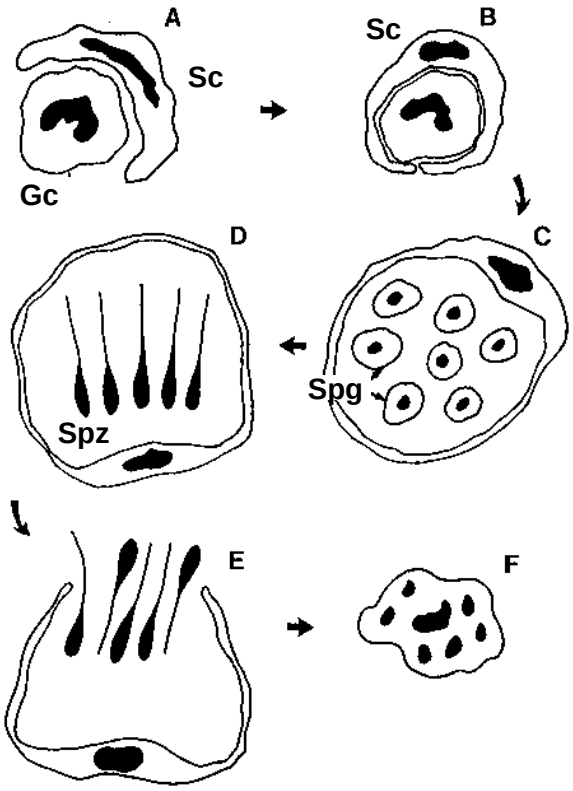

Figure i.- General features of cyst formation in teleosts. A: Initially, a Sertoli cell associates with a primary germ cell. B: The Sertoli cell completely surrounds the germ cell, becoming the wall of the new cyst. C: The germ cells undergo several mitosis to produce spermatogonia. D: Spermatogonia maturation proceeds then with the production of isogenic spermatozoa. E: Spermiation is accomplished by the rupture of the cyst. F: Finally the Sertoli cells undergo degeneration (adapted from Grier 93). Gc: germ cell; Sc: Sertoli cells; Spg: spermatogonia; Spz: spermatozoa.

At histological level, the process of spermatogenesis in teleosts can be separated into five stages, where germ cells are found in different developmental stages (Weltzien 02):

(a) Stage I: tubules/lobules contain spermatogonial stem cells associated to Sertoli cells and spermatocysts with early or late spermatogonia.

(b) Stage II: cysts with primary or secondary spermatocytes appear. The appearance of spermatocytes indicates the initiation of meiosis.

(c) Stage III: the tubule/lobule diameter increases and cysts with the spermatids appear.

(d) Stage IV: cysts containing spermatids and also spermatozoa are present. Spermatozoa appear in the lumen. Milt can be stripped from approximately 50% of the males in this stage.

(e) Stage V: testis in regression. All stages of developing germ cells may be present. This stage is characterized by the presence of Sertoli cells phagocytising spermatid residual bodies.

In the interstitial compartment of immature and early maturing testis (stages I and II), the Leydig cells are arranged in clusters, while in mature or maturating testis (stages III and IV), the Leydig cells become more dispersed and the Sertoli cells more flattened. After spermiation, the layers of Sertoli cells in the regressing testis (V) become thicker while the diameter of the lobule lumen decreases.

The way in which spermatogenesis occurs depends on the anatomical organisation of testis, on the relationship between germ cells and Sertoli cells during the spermatogenic cycle, and on the place where the fertilization takes place (external or internal). Also cold-blooded (poikilotherm) and warm-blooded (homeotherm) species show differences on the spermatogenesis process.

Testes, either lobular or tubular, can be classified in two main types depending on the distribution of the spermatogonia along the entire length of the tubule or lobule (figure ii). The unrestricted type is the most common one in teleost and is characterized by tubules/lobules with a patent lumen that results from a tubule/lobule lining up effect produced by cysts development at the onset of spermatogenesis. As more cysts burst, more spermatozoa are collected into the lumen. When required, sperm is finally released into the sperm duct (spermiation). A second pattern of organization found in teleost is the restricted spermatogonial testis type, presented only in lobular testes. Primary spermatogonia are confined in the distal region of the lobule. During spermatogenesis primary spermatogonia associate with Sertoli cells to form cysts. As germ cells mature, cysts migrate down the lobule toward the efferent sperm ducts. By the time spermatozoa have been formed, the cysts are located near the sperm duct and burst into the lumen of the sperm ducts (figure iii).

Unrestricted

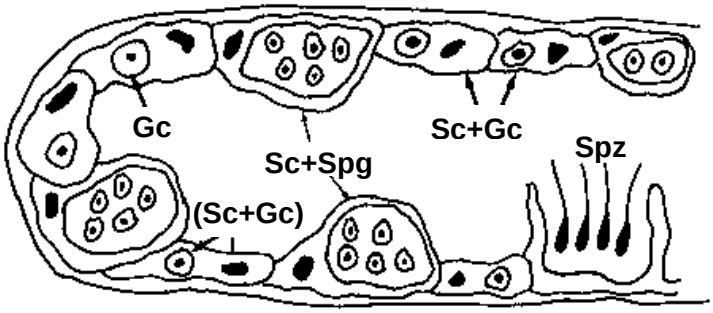

Restricted

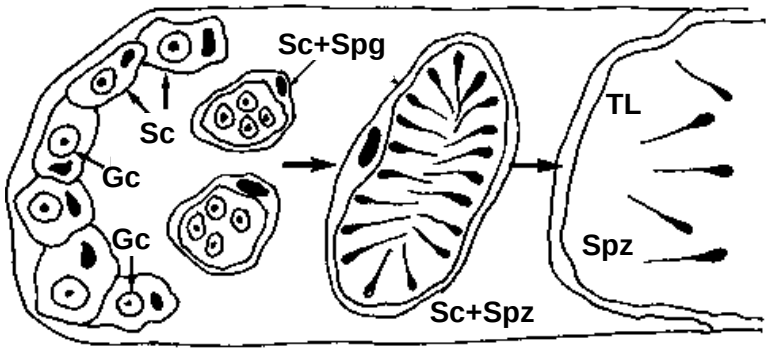

Figure ii.- Scheme illustrating unrestricted and restricted spermatogenesis in teleosts. Unrestricted spermatogenesis is characterized by the presence of germ cells along the lobule/tubule in testes. Cysts are formed when a Sertoli cell surrounds a germ cell. Cysts mature and line the lobule/tubule until rupture occurs, liberating spermatozoa (spermiation). In restricted spermatogenesis, germ cells are restricted to the distal end of the lobule. Cysts are also formed when a Sertoli cell surrounds a germ cell. As cysts mature they migrate towards the tubule lumen of efferent ducts. By the time cysts reach the tubule lumen, they contain spermatozoa. Spermiation results when the cyst fuses with the tubule lumen (adapted from Grier 93). Sc: Sertoli cell; Gc: germ cell; TL: tubule lumen; Spg: spermatogonies; Spz: spermatozoa.

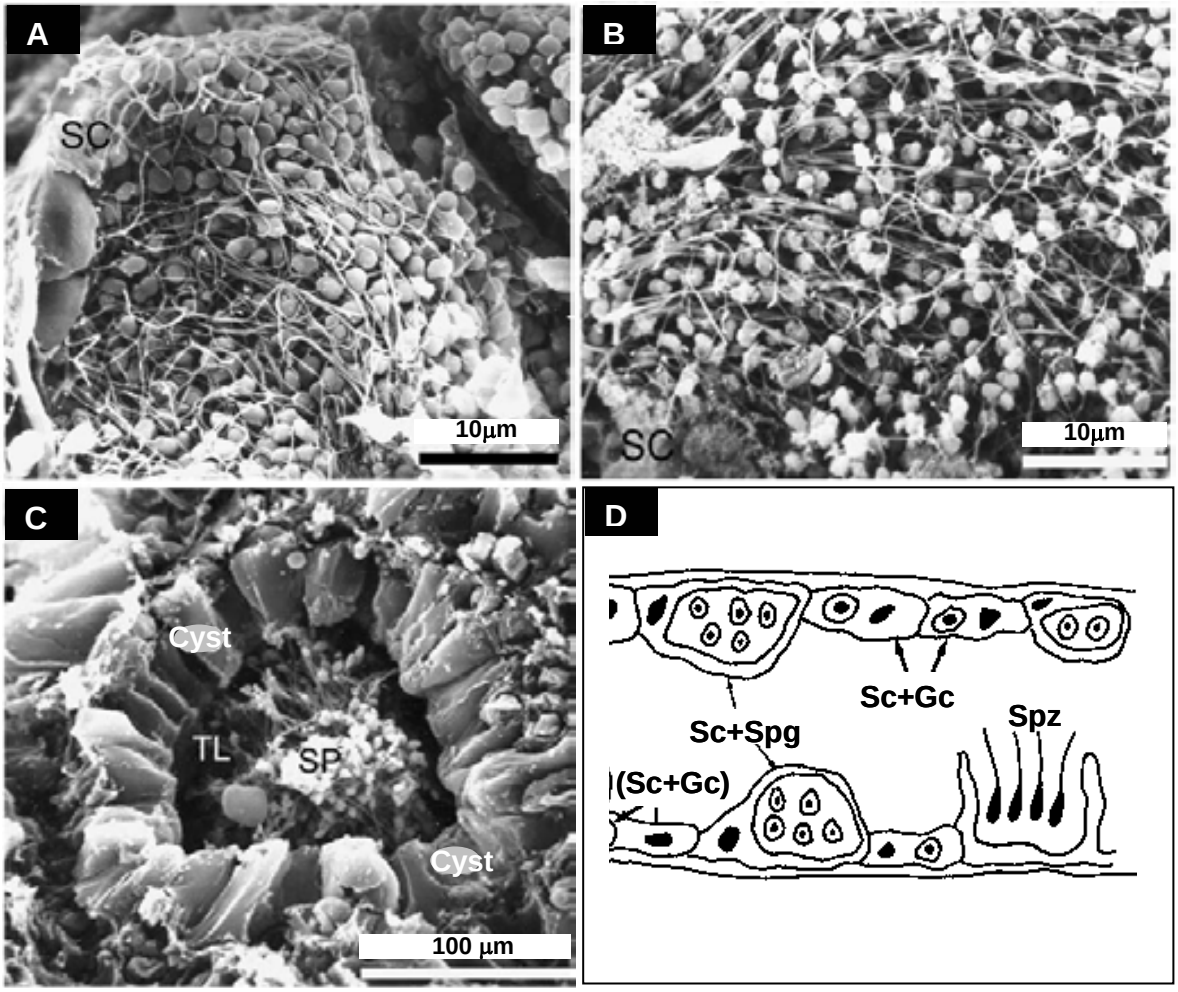

Figure iii.-. Scanning electron microscopy (SEM) of maturing spermatocyst (A), cyst opening with mature sperm (B) and tubule with ripe sperm (C) from a teleost fish (Cardinal fish). D: Spermatogenesis in unrestricted tubules. Sc= Sertoli cover over spermatocyst, Spz (SP in C) = spermatozoa, TL= tubule lumen. (A-C: adapted from Fishelson 2006; D: adapted from Grier 93).

I.1.3 Special features of *Solea senegalensis* spermatogenesis

The testis of the vast majority of teleost is elongated and accumulates a high quantity of sperm during maturation. Thus, in general, the gonadosomatic index (GSI, gonad weight/body weight x 100) varies significantly during spermatogenesis. In contrast, the testis of *S. senegalensis* presents a very small bilobulated structure with rounded seminiferous tubules. The GSI is ≥0.1 and it does not show marked changes during the reproductive cycle (García 06). In addition, the spermatogenesis process is of semi-cystic type, i.e., spermatocytes and spermatids are released into the seminiferous lobule lumen where they are transformed into spermatozoa (García 05). This unusual model of spermatogenesis is associated with the constant production of few tens of microliters of sperm. Spermiating males are thus observed almost all year around, with peak periods mainly in spring and secondarily in autumn (Rodríguez 84).

The structure and morphological localization of the Senegalese sole testis was recently described by García and co-workers (2005). It presents two main sections: the cortex and the medulla. The cortical region is composed by a thin connective capsule that covers the entire organ and the seminiferous lobules, the main location of spermatocysts (figure iv).

The seminiferous lobules are disposed transversally from the cortex to the medullar region. There, developing spermatocysts are scarce or inexistent and in some cases it is possible to find the efferent duct system that collects and stores the spermatozoa. Central efferent ducts leave the testicular lobule and open into the main deferent duct, that canalizes the sperm outwards. Both seminiferous lobules and ducts are surrounded and structurally supported by the testicular interstitial tissue. Within the interstitial tissue, myoid cells, collagen fibres, Leydig cells, amyelinic nerves, melanomacrophage centres, and capillaries can be observed. This structure has been reported for many other teleosts (García 05).

The germinal compartment, composed of germ and Sertoli cells, is separated from the interstitial tissue by a basement membrane. Extensions of Sertoli cells envelop germ cells forming spermatocysts. In *S. senegalensis* testis, Sertoli cells only enclose spermatogonia and spermatocytes, because at a certain time during the end of meiosis, spermatocysts open and spermatids are released into the seminiferous lobule lumen,

where they are transformed into spermatozoa. The spermatocysts (containing spermatogonia or spematids) are distributed all along the lobules. However, the majority of those containing type A spermatogonia are found at the distal part of the lobules.

The location of genital pores in both sexes, the dorsal surface in males (figure v) and the ventral surface in females, matches the believed spawning behaviour assumed for *S. senegalensis*. This is supposed to be similar to that reported in *Solea solea* (Baynes 94), where fish form pairs during spawning with the male always positioned under the female. In this way the genital pores were close together and gamete release takes place in an optimal position for extensive oocyte fertilization.

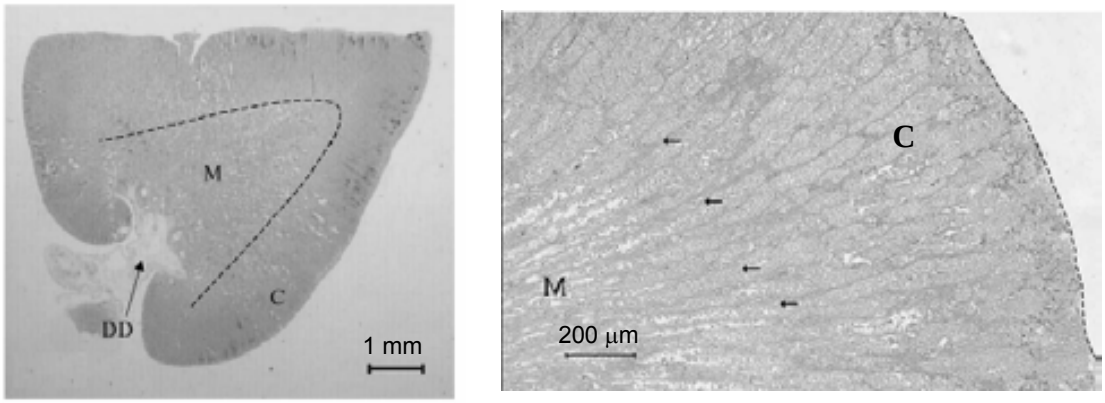

Figure iv.- Photomicrographs of a cross-section of *S. senegalensis* testis. Two main regions are observed: cortex (in the periphery of the organ; C) and medulla (internal or central region; M). Deferent duct (DD) is connecting testis to spermatic duct. The seminiferous lobules present a radial disposition (arrows) from the central medulla (M) to the *tunica albuginea* (broken line) at the cortex (C; adapted from García 05).

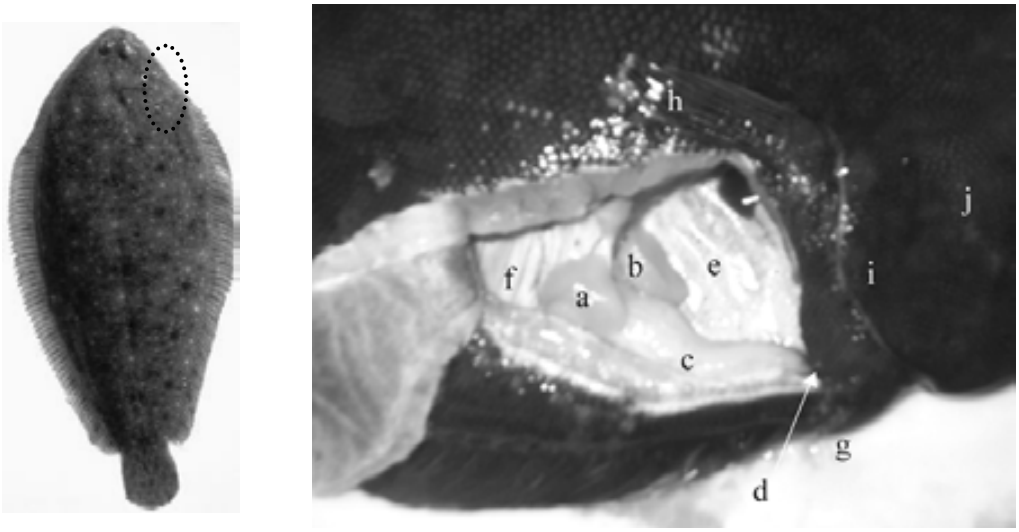

Figure v.- Anatomy of male reproductive system in adult *S. senegalensis*. a, ocular side testicular lobe; b, blind side testicular lobe; c, spermatic duct; d, urogenital pore; e, visceral cavity; f, central skeletal portion; g, pelvic fins; h, pectoral fin from the ocular side; i, operculum; j, head (adapted from García 05).

García-López *et al.* (2006) defined five stages in spermatogenesis for the Senegalese sole during spermatogenesis on the basis of the observed histological changes and the relative abundance of the different germ cell types. The main features of each stage are described below. The present study will refer to this classification when describing spermatogenesis states in testes from *S. senegalensis*.

Early spermatogenesis: The testis cortex is occupied by numerous germinal cysts, containing spermatogonia surrounded by Sertoli cells. A few spermatids can be present in the lumen of the seminiferous lobules. Spermatids and spermatozoa can be found in the medullar efferent ducts. Abundant empty spaces could be seen in both regions.

Mid spermatogenesis: Germ cells are present at all developmental stages. In the cortex, meiosis is initiated as signalled by the decline in the number of spermatogonia and the appearance of a large population of spermatocytes. Germinal cysts containing spermatocytes were distributed in the periphery of the seminiferous lobules, leaving a small central lumen filled by spermatides. In the medullar efferent ducts, some spermatids and spermatozoa can be observed.

Late spermatogenesis: The lumen of the cortical seminiferous lobules is almost fully filled by spermatids. Few cysts containing spermatocytes are still present. Spermatids are the most abundant cell type inside the testis. Spermatozoa become more abundant in the medullar efferent ducts.

Functional maturation: Spermatids are still very abundant in the cortical seminiferous lobules at the beginning of this stage, but their number decreased progressively as successive batches transform into spermatozoa. Ripe spermatozoa accumulate in large quantities in the medullar efferent ducts. Spermatogonia and associated Sertoli cells commenced to proliferate at the distal part of the cortical lobules, beneath the thin connective capsule that surrounds the organ.

Recovery: The number of spermatozoa slightly decreases in the medullar efferent ducts compared to functional maturation stage, while the number of spermatids is significantly reduced in the cortex. Spermatogonia and Sertoli cells are in active proliferation at the distal part of the cortical seminiferous lobules, leading to the appearance of numerous groups of these cells. Spermatocytes are totally lacking indicating the absence of meiotic processes.

I.1.4 Role of steroids during spermatogenesis and spermiation in teleosts

The regulation of the reproduction process in fish takes place along the brain-hypothalamus-pituitary-gonad axis and involves a complex mechanism (figure vi). Briefly, environmental stimuli of reproductive relevance are received and translated by the brain and routed to the hypothalamus. This brain region produces gonadotropin releasing hormone (GnRH), as well as gonadotropin release-inhibiting factors like dopamine (Vacher 00). GnRH is thought to stimulate the pituitary, a small gland located beneath the brain, to produce and release gonadotropin hormones (GtHs). The GtHs act on testes through the biosynthesis of gonadal steroid hormones, which in turn mediate various stages of spermatogenesis, sperm maturation and spermiation. The GtHs known in teleosts are the follicle-stimulating hormone (FSH) and the luteinizing hormone (LH) (Weltzein 03). FSH and LH (formely referred to as GtH I and II, respectively) are released into the circulation and stimulate the gonads by binding to specific membrane receptors. In the male gonad, FSH and LH receptors are probably located on Sertoli and

Leydig cells, respectively (figure vi). The gonad has two main functions. First, it produces germ cells during spermatogenesis. Second, it synthesises sex steroids (steroidogenesis) and growth factors that are important for the regulation of reproduction, either directly on gonadal tissues in a paracrine/autocrine manner, or through positive or negative feedback mechanisms on the hypothalamus and pituitary hormones in an endocrine fashion (Weltzein 04).

The two major gonadal sex steroid hormones described for teleosts are testosterone and 11-ketotestosterone (11-KT). In most studied teleosts, testis growth and development coincide with increased plasma levels of 11-KT, and to a lesser extent, testosterone. *In vivo* and *in vitro* studies show that 11-KT is most effective as a direct stimulator for spermatogenesis, while testosterone is most effective as a stimulator of hypothalamic and pituitary activity, leading to further testis activation. 11-KT is then considered to be the main androgen in teleost fish (Coward 02).

Spermatozoa that have completed the two meiotic divisions in the testis are not yet fertile, as they lack motility. In some teleosts, another steroid, 17α,20β-dihydroxy-4-pregnen-3-ona (17α,20β-P), seems to increase sperm duct pH, when spermatozoa pass through it. This pH variation in turn increases cAMP in sperm, allowing the acquisition of motility. Such event generally occurs in teleosts immediately before or during the spawning period (Miura 92). The 17α,20β-P hormone is supposed to be the testicular mediator of gonadotropin-induced spermiation. This compund is produced in sperm fluid, from a precursor steroid (probably 17α-hydroxyprogesterone) produced by testicular somatic cells under the influence of gonadotropin and 11-KT (Nagahama 94). Contrarily, it has been described that testosterone does not have a direct effect on gonadotropin-induced spermiation (Miura 92; figure vii).

Little is known about the specificities of the endocrine control of semi-cystic spermatogenesis in fish. In addition, few reports on the reproductive physiology of species from the genus *Solea* have been published to date. Recent studies in *S. senegalensis* (García 06) have integrated the histology of gonadal development with sex steroids profiles. These studies demonstrated the relationship between plasma levels of sex steroids (T, 11-KT, 17α,20β-P) with different phases of spermatogenic activity.

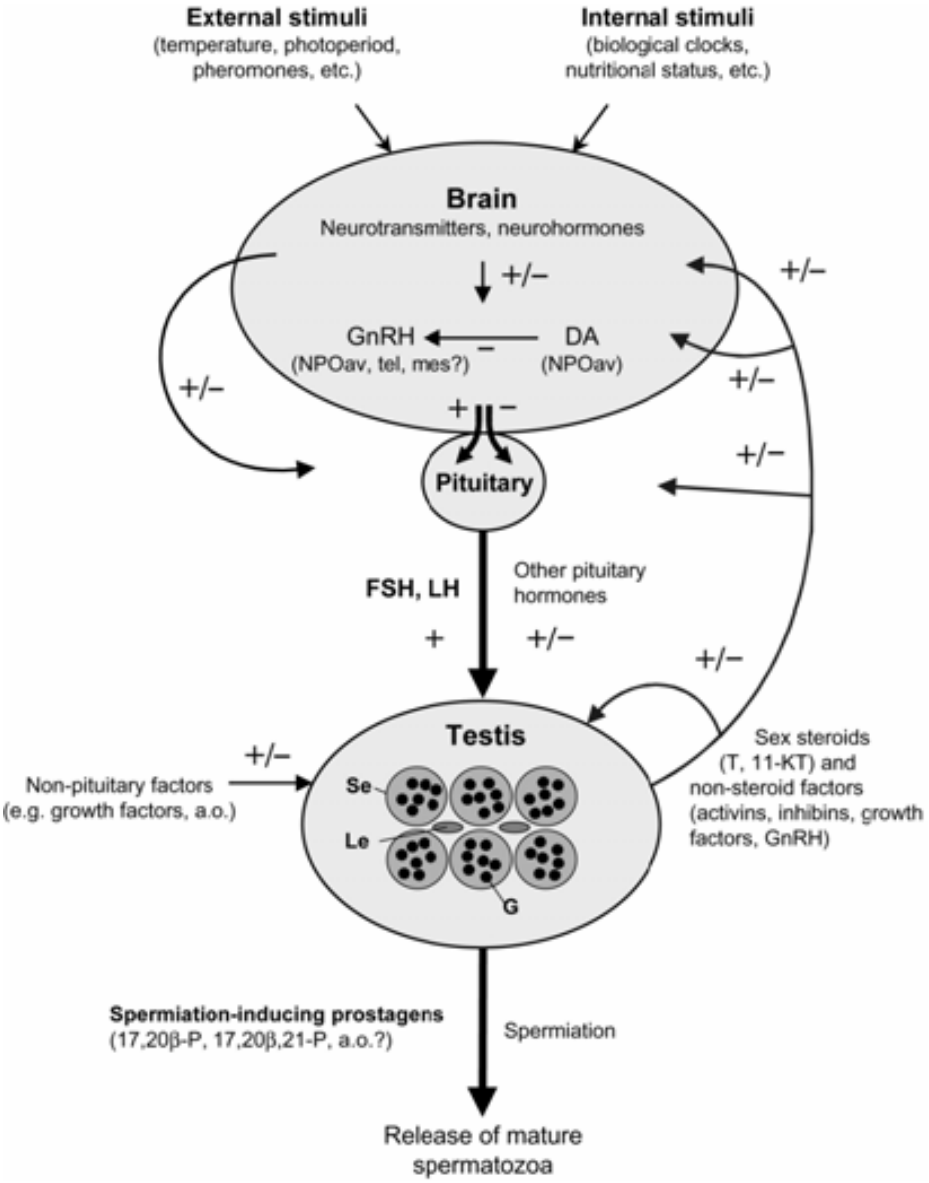

Figure vi.- The brain–pituitary–gonad (BPG) axis in male teleosts. NPOav, nucleus reopticus anteroventralis; tel, telencephalon; mes, mesencephalon; DA, dopamine; Se, Sertoli cell; Le, Leydig cell; G, germ cell (adapted from Weltzien 04).

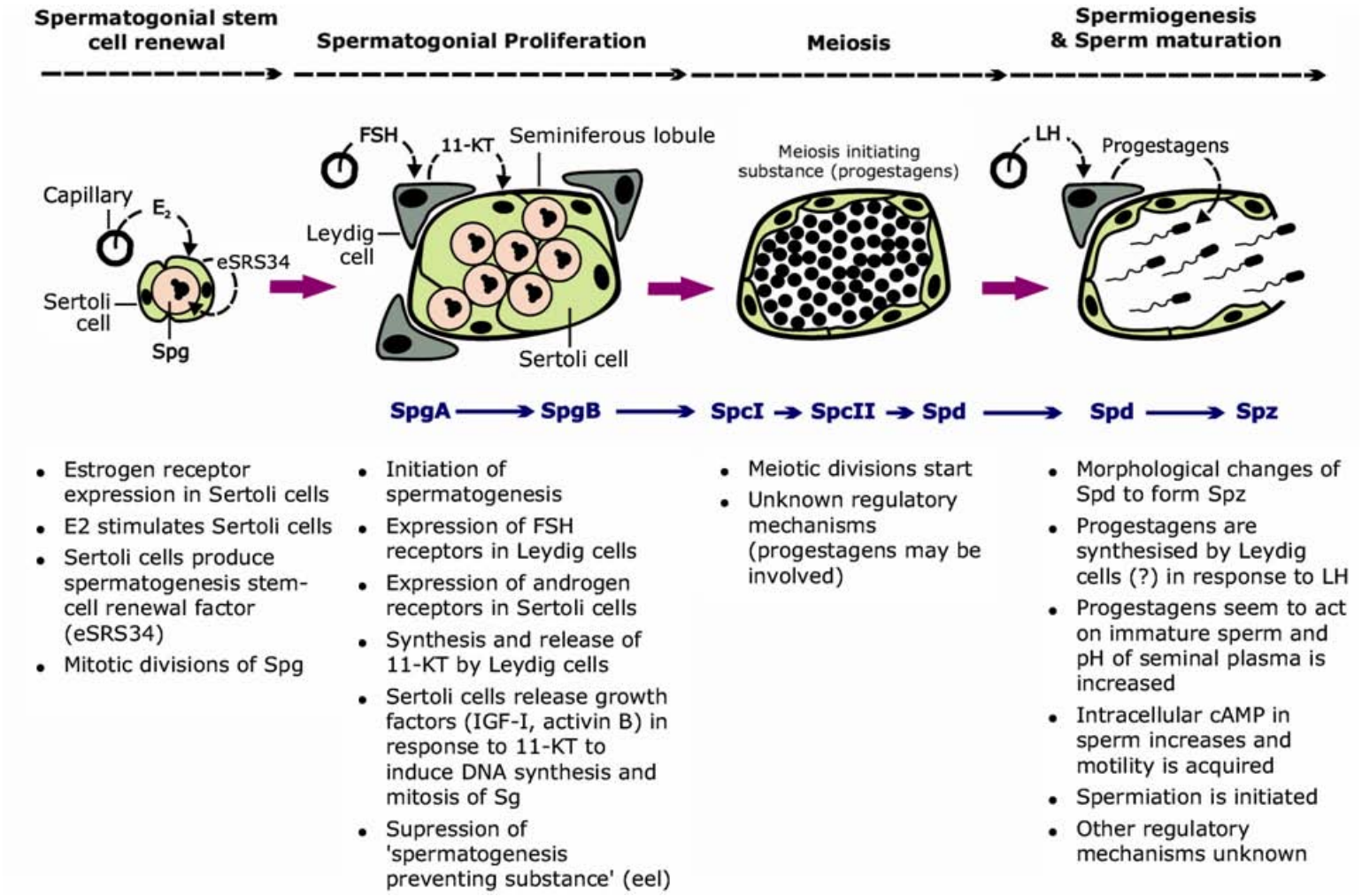

Figure vii.- Schematic diagram of the main molecular mechanisms during fish spermatogenesis. E2, 17□-estradiol; FSH, follicle-stimulating hormone; IGF-I, insulin growth factor I; 11-KT,11-ketotestosterone; LH, luteinizing hormone; Spg spermatogonia; SpgA, spermatogonia type A; SpgB, spermatogonia type B; SpcI, spermatocyte type I; SpcII, spermatocyte type II; Spd, spermatid; Spz, spermatozoa (provided by Dr. Joan Cerdà).

Plasma 11-KT and testosterone levels progressively increased in association with the progression of spermatogenesis, showing a peak in the late spermatogenic stage. Levels decrease dramatically in functional maturation stage when spermatozoa appear massively. On the other hand, high concentrations of 17α,20β-P were reported at any developmental stage. These hormone profiles are unusual in other pleuronectiform teleosts and may be related to the special type of spermatogenesis reported to resemble the pattern of oocyte development in group-synchronous ovaries (García 06). Further studies should be done to determine the role of 17α,20β-P in *S. senegalensis*.

I.1.5 Hormone treatment approaches on flatfish spermatogenesis

Treatment of flatfish with gonadotropin-releasing hormone agonist (GnRHa) generally increases plasma concentrations of androgens (Harmin 93; Vermeirssen 98, 00; Pankhurst 00; Moon 03; Agulleiro 06), C21 steroids (Baynes 85, Vermeirssen 98 and 00), milt hydration (Vermeirssen 98; Martin-Robichaud 00; Tvedt 01; Moon 03; Lim 04) and/or sperm motility (Clearwater 98; Vermeirssen 04). However, in the Senegalese sole and some other teleost species, GnRHa is apparently ineffective at enhancing milt production (Berlinsky 96, 97; Agulleiro 06). In fish, it is known that synthesis of 11-KT in the testis, as well as in extratesticular tissues, can occur from pregnenolone via progesterone, 17α-hydroxyprogesterone, androstenedione, 11β-hydroxyandrostenedione and 11-ketoandrostenedione (OA) (Mayer 90a; Goos 02). Accordingly, castrated fish treated with OA show elevated plasma 11-KT levels and restored secondary sexual characteristics (Mayer 90b; Borg 93). Also, treatment of intact males with OA or 11-KT can promote testicular development (Goos 02).

A recent study performed by Agulleiro and co-workers (2007) demonstrates that males treated with GnRHa in combination with OA show an enhancement of plasma levels of sex steroids, germ cell development and milt production in the Senegalese sole. The OA is an immediate precursor in the biosynthesis of 11-KT through its conversion by the enzyme 17β-hydroxysteroid dehydrogenase (17β-HSD), which is present in testis and other tissues in fish (Mayer 90a; Schulz 91). The authors hypothesized that GnRHa+OA administration in males could result in an additional source of 11-KT, independent of gonadotropin stimulation and hence of regulatory mechanisms at the brain-pituitary level, to potentiate the GnRHa effect on spermatogenesis.

I.2 Proteomics

The term proteome was first coined to describe the set of proteins encoded by a genome (Wilkins 96). Nowadays this term evokes a broader meaning that includes the full range of protein isoforms and modifications, the interaction between them, and the structural description of proteins and their higher-order complexes. Proteomics is a research area that studies the proteome components in a global and often quantitative manner. Together with other functional “omic” approaches, proteomics aims to provide a wide vision of cellular function (Zhu 03). In consequence, proteomics must deal with the vast and heterogeneous collection of proteins derived from alternative RNA splicing, pre- and post-translational modifications and other metabolic processes that compose a highly dynamic proteome, whose component distribution is further affected by the specific cell or tissue type as well as by interindividual, transient, developmental stages. This huge proteomic task is often further complicated by sample availability (such as biopsies), limited collections in banks of patience or unique sample preparations (Tyers 03).

Different disciplines are combined together to achieve a proteome wide vision: mass spectrometry (MS), arrays and separation nanotechnologies, structural proteomics, functional proteomics and bioinformatics. Some of these tools (MS-based proteomics and bioinformatics) will be discussed more in detail in the following lines, as they will be thoroughly applied in this work for the study of the Senegalese sole proteome.

I.2.1 Mass-spectrometry based proteomics

MS has increasingly become the method of choice for qualitative and quantitative analysis of complex protein samples. MS-based proteomics is possible because of advances in other several areas like genome sequence databases or technologies related to protein ionization for MS analysis. Electrospray ionization (ESI; Fenn 89, Abián 99) and matrix assisted laser desorption/ionization (MALDI; Karas 88) are the two most popular techniques for protein or peptide ionization in proteomics. ESI ionizes proteins from the liquid state, making this technique advisable for coupling MS to liquid-

based separations (for instance, liquid chromatography and capillary zone electrophoresis). On the other hand, MALDI ionizes the sample out of a crystalline matrix via laser pulses and it is then best suited for fast analysis of individual samples.

For proteomic purposes, ESI ion sources have mostly been coupled to three dimensional (3-D IT) and linear ion traps (LIT), quadrupole (Q) and, more recently, Fourier transform ion cyclotron (FT-ICR) analyzers. The 3-D IT is more sensitive and inexpensive in comparison to other MS equipment for proteomic studies, but shows a lower mass resolution than time-of-flight (TOF) analyzers. Recently commercialized devices such as the Orbitrap have substantially increased 3-D IT accuracy. However, The FT-ICR is still the analyzer presenting the higher potential in terms of sensitivity, dynamic range, accuracy and resolution, despite its economical cost and operational complexity have limited their use in proteomics (Aebersold 03).

These devices allow all the measurement of the m/z of intact protein or peptide ions, the production of fragments from those ions and its mass analysis. The latter capability, i.e. the mass analysis of fragment ions from peptide molecules, is the basis for MS-based protein sequencing. Ion fragmentation can be carried out by several procedures including collision induced dissociation -CID- or electron transfer dissociation –ETD. These processes can take place inside the analyzer (such as in ion traps and ICRs) or in especial collision chambers in tandem or hybrid instruments.

MALDI is usually coupled to TOF analyzers. The simplicity, mass accuracy, resolution and sensitivity of MALDI-TOF mass spectrometers made them the most common equipment to identify proteins by peptide mass fingerprinting (PMF, see below). New configurations of MALDI instruments have been coupled to linear ion traps, 3D ion traps (Viner 05), or to tandem TOF-TOF or hybrid mass spectrometers, allowing fragmentation of MALDI generated ions.

The identification of proteins by MS is based in two main methods: PMF and MS/MS sequencing (figure viii). In both cases, the initial step is the digestion of the protein with a specific enzyme like trypsin. In PMF a protein can be identified by comparing the list of the experimental masses from the digested peptides with those corresponding to the different peptide collections predicted from the protein sequences stored in a comprehensive database. This method requires purified target proteins, so previous

protein fractionation using 1-D or 2-D electrophoretic separation of the sampe is performed before MS analysis. In comparison, protein identification by MS/MS peptide sequencing does not require the isolation of the target protein and gives information about the peptide sequence in addition to the peptide mass. Trypsin digested peptides are medium length (500-2000 Da) and their carboxy-terminal residue is almost always Lys or Arg. This favours the production of doubly charged ions that yield fragmentation spectra which can be easily deciphered because of the presence of complementary series of b and y ions (see below) and that allows peptide sequence characterization and its correlation with known gene sequences stored in databases (Reinders 04).

The CID MS/MS fragmentation pattern of a peptide is a characteristic of the peptide sequence, the charge of the fragmented ion and the collision energy. In a MS/MS analysis, peptides can fragment in any of the peptidic bonds, generating fragments of different types, which can be grouped in two main series: a, b, c contains the amino-terminal, while series x, y, z contains the carboxi-terminal (figure ix, Roepstorff 84).

In addition, the breakdown of two peptide bonds generates ion fragments denominated internal ions. Typical ions of this class are the immonium ions that contain only one aminoacid residue. In consequence, immonium ions are useful markers for the presence of some aminoacids. Depending on the aminoacid composition, fragments derived from a loss of water (S, T, D o E) or ammonium (Q, K, R) from *y* and *b* ions can also be detected.

The relative intensity of the ionic fragments depends on the aminoacids present in the peptide chain, as well as on other experimental parameters like collision energy and pressure. Some peptidic bonds like Gly-Gly or Gly-Ala are especially stable. Fragments derived from the breakdown of these bonds are thus difficult to observe in the spectra. This makes sometimes sequence assignation difficult because the molecular mass of Gly-Gly is identical to Asn and Gly-Ala to Gln/Lys. Other cases of special fragmentation pattern are caused by the presence of proline (Maux 02), aspartic followed by an arginine, (Wysocki 00), or the formation of disulfide bonds between cysteine (Carrascal 05).

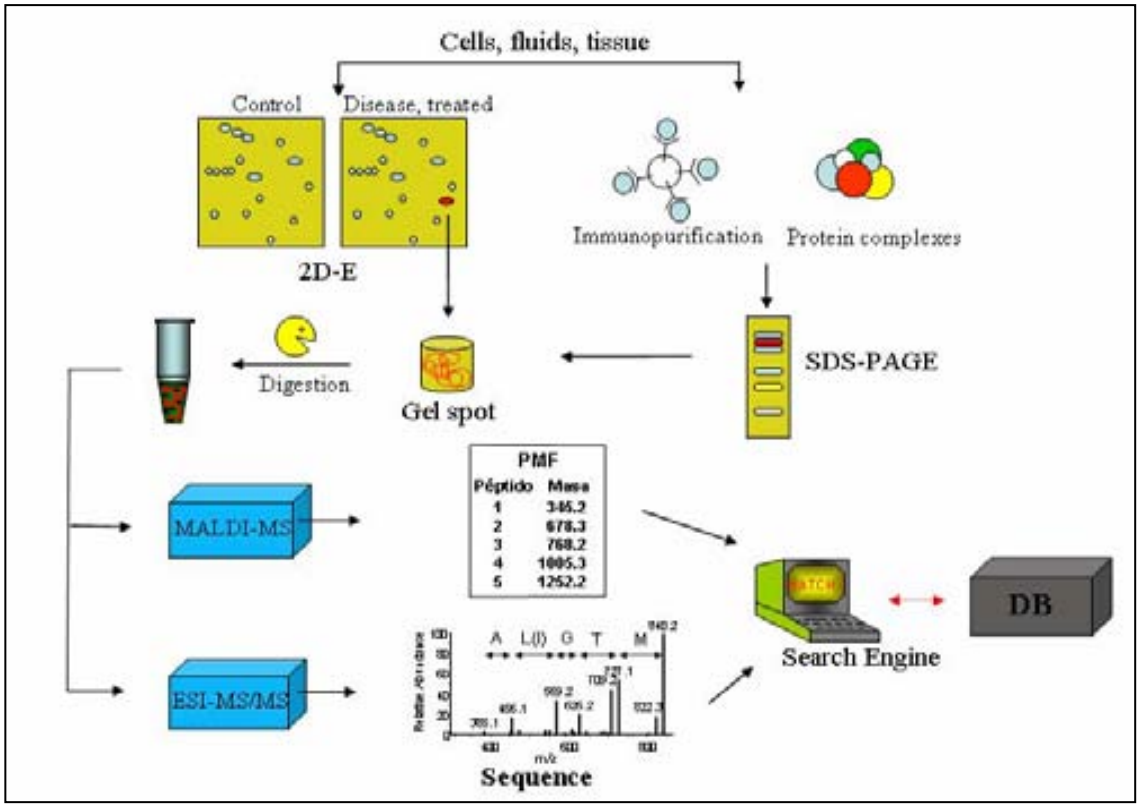

Figure viii.- Generic MS–based proteomics experiment. First, proteins are isolated by physicochemical fractionation or bioaffinity selection, and then separated in a 1-D gel or 2-D gel. Proteins are then digested, usually by trypsin, leading to peptides with C-terminal protonated aminoacids. Resulting peptides are then analysed in a MALDI-TOF mass spectrometer and protein identification performed via peptide mass fingerprinting. In parallel, analysis by MS/MS can also be performed for protein identification (adapted from J. Abián in “Tratado de Medicina Interna Rodés-Guardia” Ed. Massons 2004).

When the peptides derive from known protein or gene sequences, the determination of partial sequences or tags is sufficient to identify the original proteins in a database. Once the protein is found, the complete sequence of the peptide can be deduced from combining the information from the tag, the aminoacid sequence next to the tag region and the molecular weight of the analysed peptide. In this manner peptides can be matched between real peptide sequences and sequences stored in databases, even when spectra are difficult to interpret completely or when only a poor spectra is obtained.

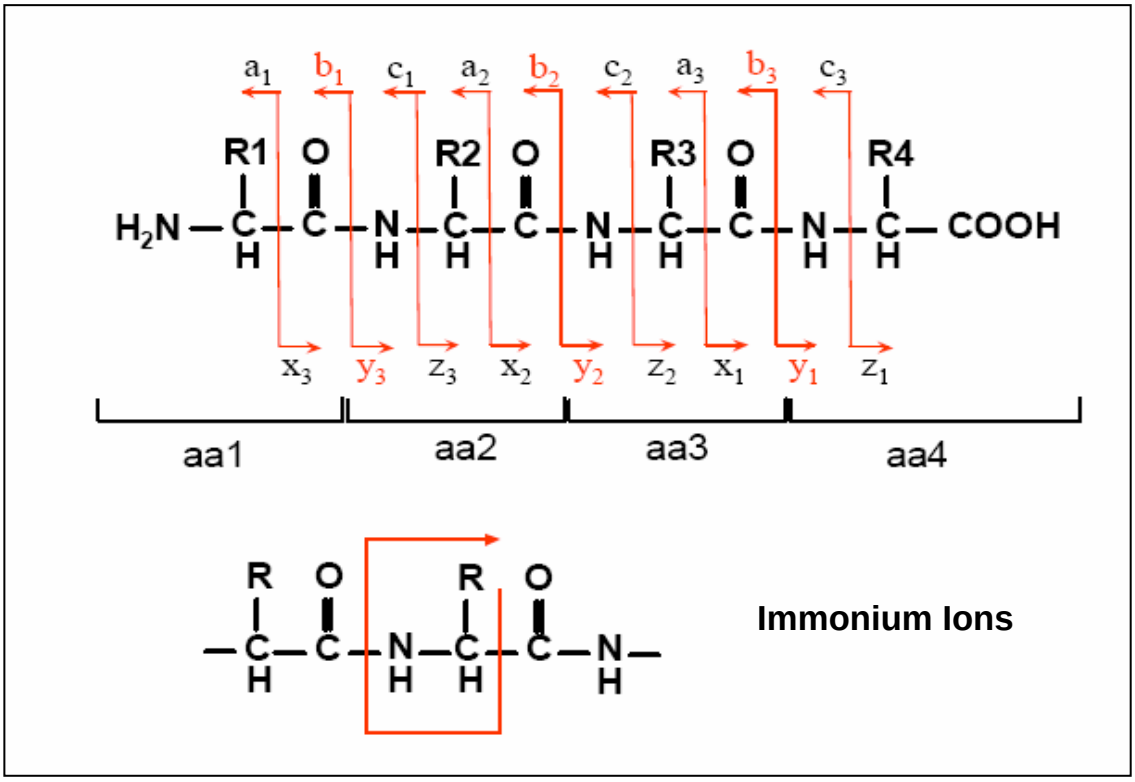

Figure ix.- Scheme of MS/MS peptide fragmentation by low energy collisions.

Fragmentation spectra can be interpreted either manually or using dedicated software. Available software packages can be classified in two main groups depending on the need for a database to determine sequences from fragmentation spectra. Most database-dependent softwares are based in an approach similar to PMF. The complete set of proteins from a database is digested and a theoretical *in silico* fragmentation spectra is generated. The experimental spectrum is then compared with the generated spectra in order to find possible candidates. On the other side, de *novo* sequence softwares analyses spectra applying mathematical algorithms that calculate possible sequences fitting the experimental spectra without comparing to any sequence database (Hernández 06).

I.2.2 Differential expression analysis in proteomics

The two-dimensional electrophoresis analysis is one of the current approaches to determine differences in the protein expression of biological samples (Görk 04). Proteomes from samples submitted to different conditions, in different physiological

situations or developmental stages are separated orthogonally by isoelectric point (*pI*) and molecular mass (*Mr*) in polyacrylamide supports. The full 2-DE expression analysis procedure can be divided in six main steps: sample preparation, isoelectrofocusing (IEF), SDS-polyacrilamide gel electrophoresis (SDS-PAGE), gel staining, image analysis and protein identification.

There are many variations in the experimental procedures for sample preparation, but they normally include: 1) tissue or cell disruption (either mechanical and/or chemical), protein precipitation using TCA/acetone, methanol-chloroform (Wessel 84) or optimized commercial kits, 2) protein resuspension in 2-D compatible buffer and 3) protein quantification (Shaw 03). IEF is currently run with commercially available plastic baked immobiline strips, although in the past other supports have been used (O'Farrell 77, Bjellqvist 82) The introduction of these strips (Patel 88) increased the reproducibility of the 2D-gel experiments and also allowed to extend the length of proteome vision, to analyse small *pI* regions (zoom strips) and basic proteins (Görk 04).

For expression studies, SDS-PAGE is generally performed in a gel format of about 24 cm wide x 20 cm long. Mini-gels (approximately 7x7 cm) can be also used in some cases, especially for result validation (Rodríguez 06). Visualization of separated proteins can be carried out using various labelling or staining methods (Westermeier 05). Among them, silver staining has been the more used technique in proteomics, despite some of its limitations: restricted dynamic range, impaired linearity and staining variations between proteins depending on their chemical structure (Rabilloud 94). Staining methods based on fluorescent dyes are also used to overcome some of the silver drawbacks providing at the same time similar sensitivities. However, fluorescence reading requires scanners with extra features (Miller 06). Moreover, spot excision from fluorescent stained gels requires spot pickers with compatible cameras or a further step to silver stain the gels.

The analysis of the gel images is partially automated with available software. These packages include spot detection algorithms that allow the characterization of hundreds of protein spots usually present in the images, methods to match spots among all the experiment gels, and statistical and data analysis tools to determine expression variations (Marengo 05)

Recently, the DIGE technology has been introduced to overcome some of the problems of reproducibility, spot detection and matching of the classical gel approach (Alban 03). This technology is based upon the specific properties of three different fluorescent dyes of the cyanine family (CyDye), which enable multiplexing of separate samples on the same 2-D gel. Common DIGE protocols involve the multiplexing of two different samples and one internal standard (IS) per gel. This IS consists of a pool including all of the samples within the experiment.

In DIGE, each protein spot in a sample can be compared to its counterpart within the IS on the same gel, to generate a ratio of relative protein levels. Quantitative comparisons of samples between gels are made based on the relative change of sample to its in-gel internal standard. This process effectively removes the gel-to-gel variation enabling accurate quantitation of biological induced changes. These characteristics also help to reduce the number of gels replicates required per experiment. Besides, spot matching between different gels in the DIGE approach is more straightforward. As the IS image is common between all gels in an experiment, matching process can be performed between IS images, which have similar or nearly identical spot patterns (Marouga 05). On the contrary, conventional 2-D electrophoresis requires matching between different samples on different gels, which introduces differences in spot patterns from sample-to-sample and gel-to-gel variation. Matching between IS in DIGE allows matching between identical samples, so variations in spot patterns are due only to electrophoretic differences. Additionally, the scanner that is used for imaging accepts gel sandwiches including the low fluorescent glass plates. As occurs with plastic-backed gels for silver staining, this reduces the variation between gels, and the risk of damaging or destroying them.

Whichever the method used for protein visualization, the spots of interest are finally excised from the gel and submitted to an in-gel digestion with enzymes with known restrictions points. The resulting peptides are used to identify the protein of origin by PMF. When this approach does not result in any protein identification, digested peptides can be sequenced by nano-electrospray ionization coupled to tandem mass spectrometry (n-ESI/MS-MS), as described above (figure viii; de Hoog 04).

Despite the usefulness of 2-DE analysis, it is well known that only a fraction of the proteome can be observed by this procedure. Proteins with extreme *pI* and *Mr* as well

as low solubility proteins are not detected in conventional analyses. In addition, the dynamic range of concentrations of the proteome components and the detection limit of the staining methods determine that only the more abundant proteins can be observed (Gygi 99). Several improvements have been performed in sensitive staining methods, large-format resolving gels and sample fractionation to diminish, although not eliminating, these restrictions from the 2-DE/MS approach.

The shotgun proteomic approach aims to circumvent some of the limitations of 2-DE in determining protein expression differences and to provide a complementary, less biased and more global view of the proteome. This approach is based in liquid chromatography coupled to mass spectrometry (LC-MS) with two main variants: non-labelling and labelling techniques. The first set of technologies requires a highly reliable LC-MS system, able to process a great number of samples at different times under controlled and repetitive conditions. Variations between samples are obtained after samples run on different analysis are compared (Old 05).

The labelling techniques overcome this reproducibility requirement by analysing at the same time a mixture of samples that were labelled separately with different chemical tags. These tags are based on an unique chemical reagent that is synthesized with different isotopical compositions (Leitner 05, Frohlich 06). For a given peptide, the derivatives produced from these reagents differ only in its isotopical composition, so that physicochemical properties are practically identical and the same protein or peptide in different samples behave in like manner, when enzymatically digested or submitted to a chromatographic separation. Relative differences between analysed samples are revealed in the mass spectrometer, where the mass differences due to the isotopical variations allows the separation of the corresponding peptide signals. In both approaches specially designed bioinformatic tools are mandatory to extract results from the data generated by the LC-MS system (Ong 05).

As indicated above, the LC-MS technique presents advantages over the gel experiments. Briefly, proteins in a larger dynamic range can be studied, the set of analysed proteins is opened to membrane and other insoluble proteins, as well as to a wider range of *pI* and *Mr*, and the change ratios of the same peptide in the different analyzed samples are more accurate and reproducible. However, there are practical difficulties in LC-MS that made 2D-gel analysis more popular. The acquisition and

maintenance costs of the mass spectrometer, as well as the required experience to run LC-MS instruments, are among them (Hanash 03, Neverova 04).

More recently, the microarray technology is also finding its way into quantitative proteomics through various formats, which promise to allow a rapid interrogation of protein activity at proteomics level. Protein-detecting microarrays are currently performed using many different affinity reagents (recombinant proteins, antibodies, peptides, small molecules, single-stranded oligonucleotides) arrayed at high spatial density on a solid support. Each surface-bound molecule captures its target protein from a complex mixture (such as serum or cell lysate), and the captured proteins are subsequently detected and quantified. Detection and quantification is normally achieved by labelling the compared samples with different cyanines (i.e. Cy3 and Cy5) and measurement of the array fluorescence. Other approaches go further and identify the captured proteins by MALDI-TOF MS (Finnskog 04, Ekstrom 01).

Protein microarray technology has been tested successfully in the study of several human cancer or human autoimmune diseases (Miller 03, Haab 03, Joos 00, Graham 04). In contrast to less specific separation methods such as gel electrophoresis and liquid chromatography, affinity-based approaches enable the investigator to direct the experiment. If the goal of the experiment is to study a particular biological process, only those proteins involved in that process need to be examined. The downside, of course, is that this approach requires both a prior knowledge of the proteins to be studied and appropriate affinity reagents. This highlights the importance of efforts directed at the rapid selection of recombinant antibodies, phage display ligands and small molecules.

I.2.3 Annotation of DNA databases using peptidic ESTs

Organism genome annotation has been classically approached with genomic techniques that pursue the continuous nucleotide sequence which encodes genes. Databases containing nucleotide sequences are the mandatory framework for different applications in genomics, proteomics and interactomics.

However, complete genomic sequences of many organisms are still not available, and even for those that are known, modifications such post-translational chemical changes are rarely inferable from the genetic sequence. Thus, complete characterization or just an early approach to primary protein structure may require determination of protein sequence with minimal or null assistance from genomic data, a strategy so-called *de novo* protein sequencing (Standig 03). Moreover, the recent technical advances outlined above in this introduction allow the effective application of proteomic approaches to implement gene annotation (Tanner 07). These new tools include highly efficient soft ionization methods for the analysis of peptides and proteins, availability of new types of ion-mass analyzers providing increased mass accuracy, resolution and scan speed as well as an important improvement in software tools for high throughput data analysis.

Several liquid phase separation techniques that can be directly coupled to mass spectrometers and are capable of resolving hundreds of compounds per analysis, like capillary liquid chromatography and capillary zone electrophoresis, have also evolved in parallel with these advances. In order to cope with the complexity inherent to the direct analysis of whole proteomes, several separations steps have to be arranged in two-dimensional liquid chromatography (2-D LC) setups. These systems make use of two or more orthogonal separation methods (often an ion exchange chromatography followed by a reversed phase separation) to further increase the chromatographic separation power. Patterson and co-workers (Davis 01) demonstrated the utility of 2-D LC in the analysis of the proteome human brain glioma cells characterizing 213 proteins (869 unique peptides sequences). These authors used two chromatographic separations, a strong cationic exchange chromatography (SCX) followed by a reversed phase (RP) column and an intermediate reversed phase C18-column trap to optimize the capture of the SCX fractions and their separation in the reverse phase column. The on-line 2-D LC system was directly coupled to an LCQ ion trap mass spectrometer.

In a simpler experimental scheme, the different separation processes can be carried out off-line through the collection of chromatographic fractions that are individually analyzed in other systems. In 2003, Gygi and co-workers (Peng 03) described the yeast proteome using an off-line 2-DLC experimental scheme. Eighty fractions were collected after the SCX chromatography and each was analysed by RP-LC MS/MS in a LCQ Deca ion trap mass spectrometer, identifying up to 1504 proteins (7537 unique peptides). Both options have their pros and cons. On-line coupling is preferable to off-line separation, as it allows complete automation and diminishes sample losses. On the other side, the off-line option is proposed as a flexible experimental approach where sample amount and chromatographic conditions can be optimized for each separation step. In fact, as the loading capacity of the first fractionation step is not restricted, in practice, this approach is able to produce a higher number of peptidic tags than the on-line approach where the amount of starting sample have to be limited (Gygi 02, Vollmer 04).

The state-of-the-art of the 2-D LC approach allows processing of around 10000 peptide fragmentation spectra from a crude proteome tryptic digest in less than two hours[1]. Additional previous sample fractionation procedures provide of an extended proteome description. As a consequence, the huge volume of generated data makes necessary the use of bioinformatic tools in order to extract the maximum amount of relevant information (MacCoss 05, Gaspari 06).

[1] The state-of-the-art of electrospray coupled ion traps is nowadays in its third generation. The work in this PhD was performed with the first generation of ion traps acquired in the 1995 by the CSIC/UAB Proteomics Laboratory.

I.3 Applying proteomics to *Solea senegalensis*

Up to the present, the application of proteomic technologies for differential expression analysis in fish species, either wild or cultured, has been scarce and mainly focused on the model organism zebrafish (*Danio rerio*; Link 06a-b, Tay 06, Knoll-Gelida 06, Love 04, Shrader 03), the rainbow trout (*Oncorhynchus mykiss*; Russell 06, Smith 05, Rime 04, Martin 03, Hogstrand 02) and, in less extend, to other species like the Atlantic salmon (*Salmon salar;* Provan 06, Booy 05), the Sea bass (*Dicentrarchus labrax*; Monti 06), or the flatfish dab (*Limanda limanda*; Stentiford 05). Other fish-related research areas have also taken advantatge of proteomic tools, like marine ecology (López 07), the description of fish allergens, the identification of species among fish families (i.e. *Merluccius sp*.) or fish quality control (Carrera 06, Martínez 04, Piñeiro 03).

The present study will approach for the first time the flatfish *S. senegalensis* with some of the above-mentioned proteomic technologies (2-D LC MS/MS, 2-DE, 2-D DIGE), focusing on the reproductive biology in wildness and captivity. This novel study will provide a new insight at molecular level into the reproductive biology of this species and will constitute groundwork for further studies on reproductive aspects of flatfish aquaculture.

Objectives

About the Pleurogene Project: understanding the frame of this PhD work

The Senegal sole (*Solea senegalensis*) and the Atlantic halibut (*Hippoglossus hippoglossus*) are two flatfish yielding high value market products with the potential for production in aquaculture. Currently, the culture of Senegal sole in Spain and other European countries is seriously impaired primarily because of difficulties in controlling reproduction in captivity. Atlantic halibut aquaculture is somewhat more advanced, with commercial aquaculture production occurring in Norway, Iceland, Scotland and Canada, but there are still improvements to make, particularly with regard to judging when to spawn females, selecting genetically superior broodstock and enhancing disease resistance. Thus, between these two species, there are a series of production-related problems that would be more easily solved with improved knowledge of several basic biological processes: reproduction, development, nutrition, genetics and immunity.

In order to overcome hurdles in the development of these species for aquaculture, the Pleurogene project aims to set up a high-throughput, genome- and proteome-based technology for the identification and characterization of genes and proteins important for sex differentiation, reproduction, larval development, immunity and nutrition, both in the Senegal sole and the Atlantic halibut. With this purpose, a comprehensive EST survey has been performed to become the basis of a microarray for the study of flatfish gene expression during reproduction, development and under different environmental, hormonal and dietary conditions. The microarray analysis of gene expression has been complemented with other molecular approaches, such as tissue laser capture microdissection, *in situ* hybridization and Real-Time PCR. Proteomic technologies played a main role in the analysis of specific abnormal phenotypes of gonads and larvae to identify differentially expressed proteins as biomarkers of quality.

All the genetic and molecular information obtained in this project has been integrated into Pleuromold, an interactive bioinformatic platform specifically developed for this project. This platform reconstructs an *in silico* flatfish with a tissue-specific gene/protein expression-based atlas. The platform will help to identify crucial genes/proteins and regulatory pathways involved in reproduction and development in the Senegal sole and the Atlantic halibut, and will contribute with the generation of new genomic, proteomic and bioinformatic tools for flatfish research in the control of reproduction and

optimization of larval health and nutrition in these species, and other related flatfish, under intensive culture conditions.

The focus of this thesis work is on the study of the reproduction of *Solea sengalensis* in captivity and especially in the description of the proteins involved in spermatogenesis. The study of several phenotypes of testis of wild and cultured animals has been performed in order to unravel biochemical pathways related to morphological and functional defects of gonads from male Senegal soles in captivity. The effect of hormonal treatments to solve these deficiencies has been also analysed to define biomarkers of gamete quality in captivity.

As indicated in the introduction, the spermiation process in *S. senegalensis* involves important physiological changes especially focused on testes. The study of these molecular changes is essential for the understanding of the mechanisms and factors involved in these physiological processes. The proteomic approach has been demonstrated to be a powerful tool for the global study of complex systems. A classic proteomic tool, the expression analysis based on 2-D electrophoresis gels, could help to determine differences along the physiological evolution in a process like spermatogenesis.

Comparative analyses in testis have been performed using proteomic and genomic technologies, in order to combine information of both approaches and obtain a general vision of the studied situations. All the proteomic-derived have been placed in Pleuromold, which also includes the genomic based data generated in the DNA microarray analysis. The fruitful combination of information and tools from different technologies in this thesis project has been only possible through the inclusion of this work inside the interdisciplinary Pleurogene project.

The aim of this thesis is described in the following individual purposes:

- Annotate the proteome of pre-metamorphic larva and testis tissue of *Solea senegalensis* using two-dimensional liquid chromatography coupled to tandem mass spectrometry.

- Determine the proteome variations in testis during the different spermatogenesis stages in wild and cultured *Solea senegalensis*.

- Compare the classical and the DIGE approaches for measuring proteome variations in testis from *Solea senegalensis*.

- Determine the proteome expression changes in testis of *Solea senegalensis* after different hormonal treatments.

- Integrate the data generated in the 2-D LC MS/MS and 2-D gel experiments on *Solea senegalensis* tissues into a comprehensive bioinformatic platform.

Chapter 1

De novo peptide sequencing of *Solea senegalensis* larva and testis proteome using two-dimensional liquid chromatography coupled to tandem mass spectrometry.

In this chapter, proteins from larva and testis of *Solea senegalensis* are characterized using a proteomic shotgun approach, i.e., proteome digestion followed by peptide separation and sequencing by 2-D LC coupled to mass spectrometry. This set of sequenced peptides will be of great interest to help the annotation of *S. senegalensis* databases and will complement the set of expressed sequence tags (ESTs) obtained by other Pleurogene partners. Thus, the results obtained in the characterization by shotgun proteomics of protein sequences of *S. senegalensis* will help in further experimental procedures when studying important biological processes like sexual maturation or larval metamorphosis.

After considering the different technical approaches that could be applied (see general introduction) it was decided to use an on-line SCX-RP LC setup and the “salt-plug” method for the sequencial desorption and separation of the peptide mixtures. In this type of system, samples of interest are usually injected automatically. Most sample components are retained in the first column, a SCX cartridge, while others such as molecules of low *pI* or even anionic species with a low number of negative charges escape the cartridge and are trapped in a RP pre-concentration cartridge at the exit of the SCX column. These molecules will be desorbed from the RP cartridge and submitted to the second chromatographic step as described later, while the SCX-retained peptides will wait until the first step of the salt desorption cycle begins. Thus, using the 'salt-plug' procedure the SCX-retained peptides are gradually eluted from the first cartridge by injections of ammonium acetate solutions at increasing concentration. In each salt step, a few microlitres of the salt solution enter to the system and pass through the SCX column eluting a peptide fraction that will be trapped in the pre-concentration cartridge. This process is repeated until a concentration of 0.25-2M, depending on the case, is achieved. At this salt concentration most peptides have been already eluted from the column. The number of salt steps used varies depending on the desired resolution, although in practice, a compromise between resolution and cost must be taken.

Peptides eluted from the SCX cartridges are trapped in the RP cartridge, where they are concentrated and suffer a buffer exchange step that eliminates salt residues and optimizes the next analytical separation in the RP analytical column. For this second chromatographic separation, the peptides concentrated in each cycle are eluted from the pre-concentration cartridge to the analytical column using an acetonitrile gradient.

Peptides separated in the analytical column enter directly into the mass spectrometer ion source, so that its mass and sequence analysis takes place in real time. Three different steps are carried out automatically before obtaining a fragmentation spectrum. First, the spectrometer acquires a full scan mass spectrum of the material eluting from the chromatographic system at a given moment. Then, it acquires a second spectrum with a short m/z range (zoom spectra) centered at the m/z value of the highest m/z peak in the full scan, and finally, it fragments by CID the peptide ion corresponding to this target peak. This triple scan process is performed in a relatively short time. Depending on the experimental conditions, it could take from milliseconds to a few seconds. The full process can generate from 1000 to 10000 fragmentation spectra depending mainly on the MS speed, the number of different salt steps used, the length of the acetonitrile gradient and the amount and complexity of the injected sample.

The set of MS/MS spectra is further processed with bioinformatic tools to obtain tentative peptide sequences, polish this tentative sequences, assign a corresponding protein through a BLAST comparison, query other bioinformatic tools, and finally create a database summarizing all the information related to each fragmentation spectrum. The information deduced from peptide sequencing can then be used in combination with genomic sequence database to complete and, when necessary, correct the available information to describe an organism.

A similar homology-driven approach was proposed and automated by Shevchenko and co-workers to describe proteomes of species without sequenced genome (*Xenopus laevis*; Liska 04), using cross-species references from *Homo sapiens*, *Mus musculus*, *Danio rerio*, *Salmo salar*, *Droshopila auria*, *Gallus gallus* and *Paralichtchys olivaceus*, among others.

1.1 Materials and methods

1.1.1 Sample processing

Protein from 100 mg of testis tissue was obtained from three wild-caught individuals of *S. senegalensis* fished in Cadiz Bay (Spain) in spring 2004. Approximately 70 mg of 10-days old pre-metamorphic larvae of *S. senegalensis* were obtained from eggs spawned in captivity and cultured as described (Cañavate 99). Fifty milligrams of protein were mixed with 500 μl of TNE buffer (50 mM Tris HCl pH 7.6, 150 mM NaCl, 2 mM EDTA pH 8,0, 1 mM Na_3VO_4, 1 μM Leupeptin, 2 μM Pepstatin A, 0,1 μM Aprotinin) and mechanically disrupted. NP40, DTT and PMSF were added to a final concentration of 1% v/v, 1 mM and 2 mM, respectively. Proteins were precipitated with methanol/chloroform as described elsewhere (Wessel 84) and dissolved in 400 μl of 6 M Urea, 50 mM Tris pH 8.0, 4 mM DTT buffer. Sample quantification was done using the RcDc kit (Bio-Rad). Two hundred fifty micrograms of protein extract dissolved in 2,5 ml of 6 M urea, 50 mM Tris pH 8 and 10 mM DTT were incubated 30 minutes at 30ºC. Afterwards, 25 μl of 500 mM iodoacetamide were added and incubated 30 minutes at 30ºC. The sample was digested overnight at 37ºC with 1,3 μg Trypsin Gold (Promega) in 50 mM NH_4HCO_3 pH 7,8. After digestion, tryptic peptides were extracted using C18 Bond Elut LRC columns (3 mg Varian), following supplier instructions. Peptides were eluted with ACN/H_2O 1:1 0,25% TFA and the resulting extract was fully dried in a centrifugal evaporator-concentrator (Savant).

1.1.2 Two-dimensional LC MS-MS

Protein extracts were redissolved in 40 μl (testis) or 30 μl (larva) of SCX buffer (5 mM K_2HPO_4, 5% ACN pH 3.0). Twenty microliters of each sample (volume equivalent to 83 μg testis protein and 166 μg larva protein assuming a 100% recovery process) were injected. A custom-made 2-D LC MS/MS system was used for analysing larva and testis samples (figures 1.1 and 1.2). The first dimension separation was carried out using a Kontron 325 System (Kontron Instruments). An Agilent HP1100 automatic injector was used for the injection of both the sample and the salt plugs required for desorption. The

mobile phase consisted on 5 mM K_2HPO_4, 5% ACN, pH 3 at 0,2 ml/min). Five salt steps were loaded using 20 μl of ammonium acetate solutions at increasing concentration (10, 50, 100, 250 and 500 mM ammonium acetate in SCX-buffer). The second dimension chromatography of these salt fractions was done using a HP1100 (Agilent Technologies) provided of an automatic injector for sample and salt steps injection, and a UV detector with a Z-cell for microflow working.

Both HP1100 systems were controlled by a HP Chemstation. The SCX chromatography used a BioX-SCX 500 μm ID x15 mm cartridge (LCPackings) and the reverse phase chromatography used a preconcentration C18 300 μm ID x 5 mm cartridge (LCPackings) and a Kromasil C18 5 μm, 5 cm x 180 μm custom-built as described before (Carrascal 03). Separation on the C18 capillary column was carried out at 10 μl/min using a solvent gradient that started at 10 min from 0% to 60% solvent B in 60 min. (A: H_20/CAN 95/5 v/v 0,05% TFA; B:H_2O/ACN 20/80 v/v 0,05% TFA). The eluted material was analysed on-line with a LCQ ion trap mass spectrometer (Thermo Electron). Electrospray ionization voltage was set at 2,5 kV and entrance capillary temperature at 140ºC. LCQ acquisition parameters were set as follows: maximum injection time 20 ms, 8 accumulated microscans, automatic gaining control on and multiplier voltage at –910V. A continuous series of acquisition data containing each a scan spectrum, a zoom scan spectrum and a MS/MS fragmentation spectrum, were acquired automatically by the LCQ under the control of the Xcalibur 1.0 software (figures 1.3 and 1.4).

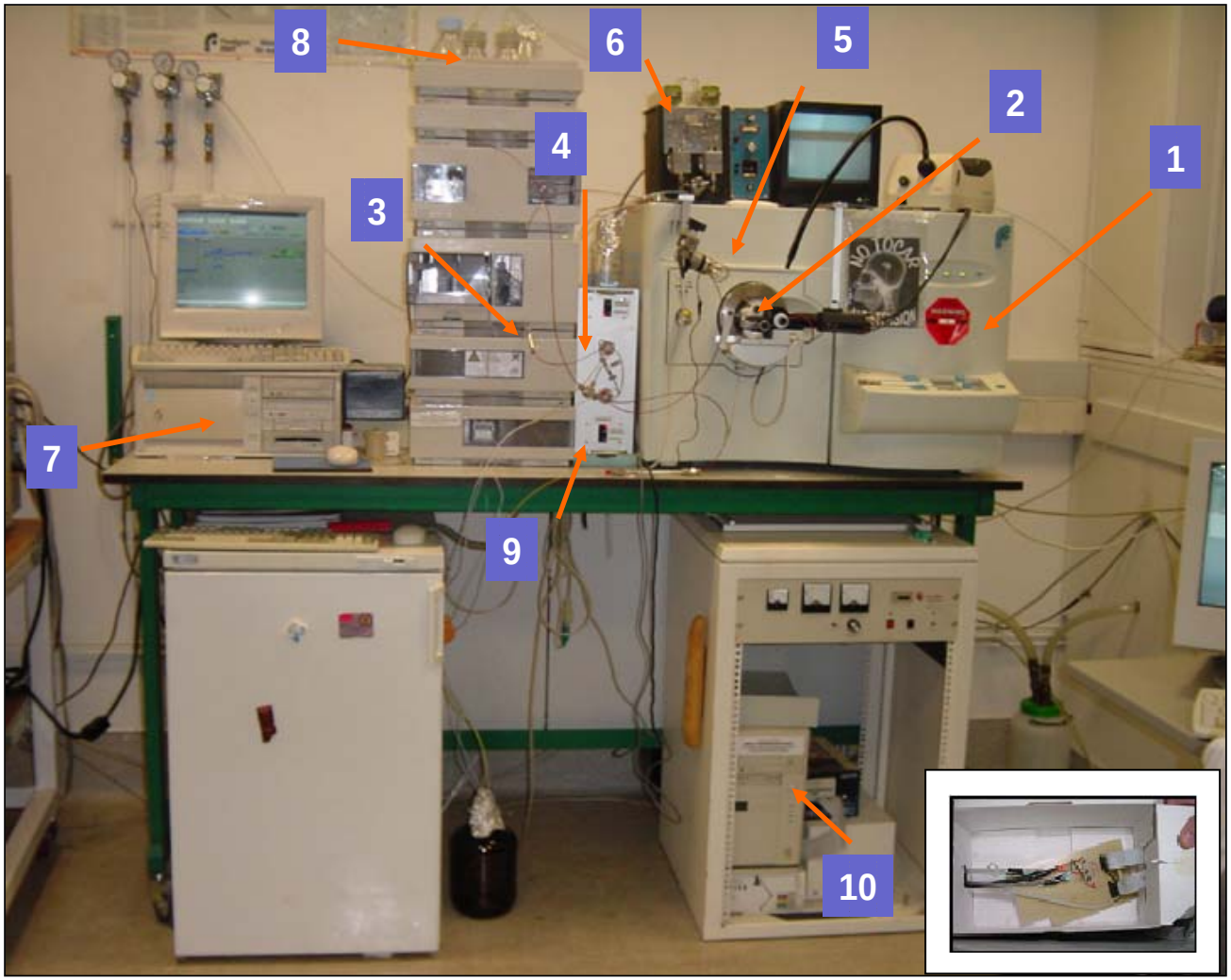

Figure 1.1.-Overview of the on-line 2-D LC system. *Mass Spectrometer:* (1) LCQ Classic Ion trap Mass Spectrometer with (2) Protana micrometric positioner. *Columns*: (3) SCX precolumn: BioX-SCX 500µm IDx15mm (LC Packings); (4) C18 precolumn: C18 300 µm ID x 5mm (LC Packings). (5) Analytical column: Home-made fused silica with Kromasil C18, 5 µm. *Pumps*: (6) HPLC pump 1: Waters 2000 isocratic pump; (7) HPLC pump 2: HP 1100 BinPump, HP UV Detector and (8) Degasser G1312A, controlled by HP ChemStation software. *2-D LC valve-switch system*: (9) Home-made with two Valco VICI valves. *System control*: (10) Custom built hard- and software for system control through open-close electric switches. A pentium 100 computer with I/O card and extern signal converter coordinate all the 2-D LC elements. A C++ software controls the events of the equipment involved (valves, mass spectrometer, chromatographic system).

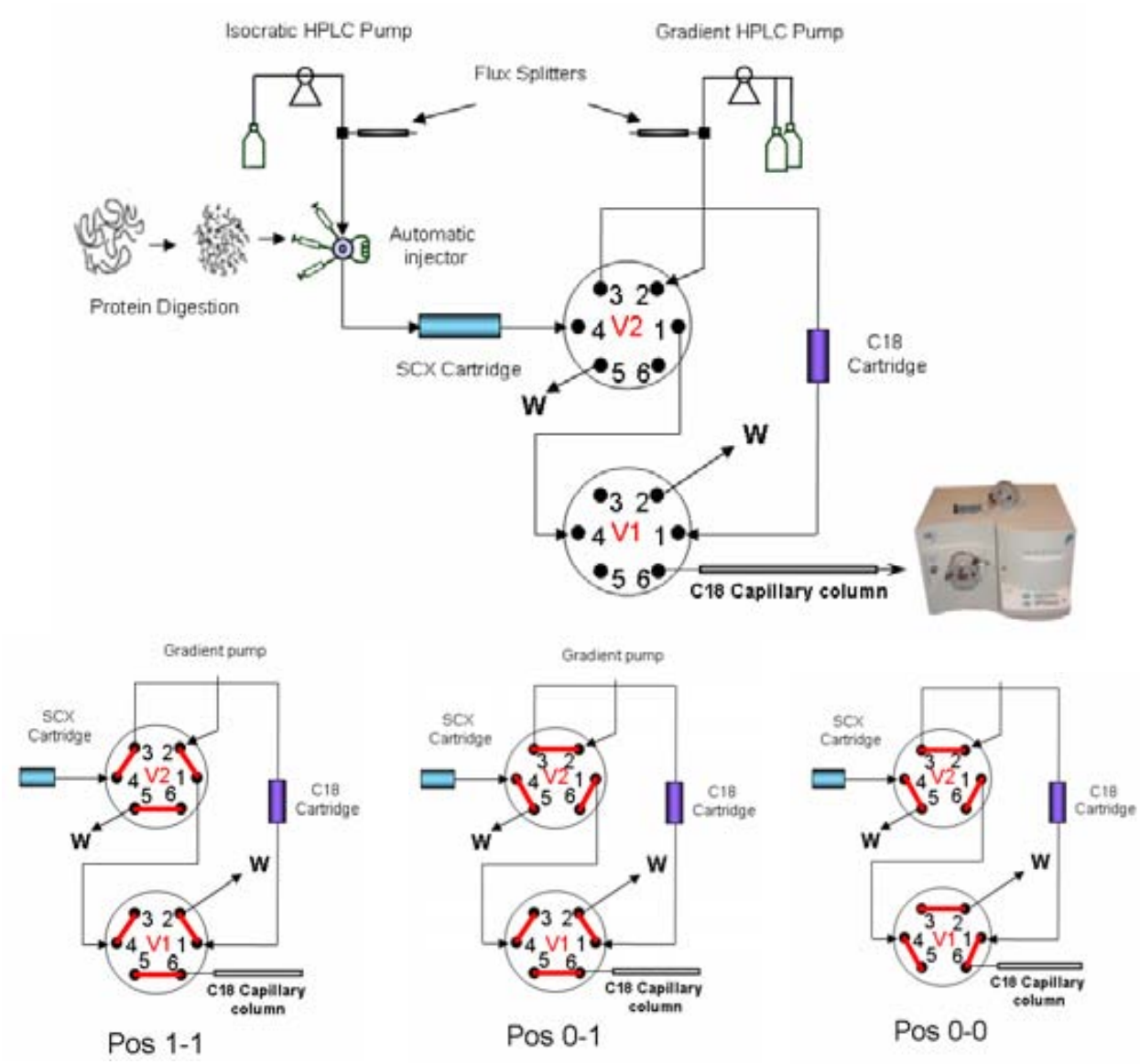

Figure 1.2.-Overview of the on-line 2-D LC system used in this work. The SCX cartridge absorbs the injected sample. This material is stepwise desorbed using solvent trains of increasing salt concentration. Each SCX fractions is directed to a RP concentration cartridge and then desorbed, separated by an acetonitrile gradient in a capillary column and analysed in a mass spectrometer. The 2-D LC system uses two Valco electromechanic valves of 6 ports and 2 positions (0 and 1). When valve configuration is 1-1 (valve1 in position 1 and valve 2 in position 1) sample or salt trains go to SCX cartridge, when 0-1 they run to C18 precolumn and when 0-0 sample elute from precolumn to analytical C18 and mass detector

1.1.3 Data processing and refinement

Xcalibur 1.0 generated 7 total ion chromatograms (TICs) per sample, one for each salt step and another from the initial SCX-non retained fraction. Then, the Sequest 1.0 software (Thermo Electron) was used in order to extract the information encoded in the fragmentation spectra of each TIC. Sequest data processing produces files in dta format. Dta files are ASCII files that include information about the precursor peptides mass and charge and the fragment ions m/z and intensity values. Two different *de novo* sequencing softwares, Peaks Studio 2.4 (Bioinformatic Solutions) and Lutefisk97 (free software developed by Richard Johnson and Amgen Inc. with Graphic User Interface designed by Dr J. Abian; Johnson 97) were used to produce a maximum of 5 candidate peptide sequences per each 2-D LC dta file. *De novo* sequencing conditions for Peaks were: Parent mass error tolerance 0.5; Fragment mass error tolerance 0.5; Enzyme and PTM Trypsin with Cam; Instrument IonTrap. Lutefisk used options were: Parent mass error tolerance =0.6; Fragment mass error tolerance =0.6; Peak width= 1; Enzyme and PTM = Trypsin with Cam; Instrument=LCQ.

A BLAST search (Altschul 90) was performed for each Peaks result file, looking for short related, nearly exact matches in 3 Ensembl fish fasta peptide databases (*Takifugu rubripes* September-2004; *Danio rerio* September-2004; *Tetraodon nigroviridis* September-2004). In order to automate the BLAST search, Orynovo, a perl script developed at Oryzon Genomics by Dr. A. Espinosa was used. When the resulting BLAST protein description did not indicate protein function, a tentative one was looked for through a pBLAST against NCBI databases (www.ncbi.nlm.nih.gov/BLAST). BLAST and sequence information from Peaks and Lutefisk were individually revised and integrated in the 2-D LC sequence database. Lutefisk results were used for validation of Peaks–derived candidates, and therefore only Peaks candidates were processed with Orynovo. The data processing scheme is depicted in figure 1.5. Charge at pH 3 was also calculated for each sequence using the “iep function” based on aminoacids pKas present in the EMBOSS package (Rice 00; bioinfo.cnio.es/EMBOSS/gui/).

Four protein-containing databases (December 2003 NCBI entries containing any of the words “danio”, “rerio”, takifugu”, “rubripes”, “tetraodon”, “nigroviridis” or “fish”; September 2004 Ensembl fish fasta peptide databases for *Takifugu rubipres*, *Danio rerio* and *Tetraodon nigroviridis*) were digested *in silico* with a Python 2.4 script designed by Dr.

Abián. Trypsin-like cleavages, a minimum peptide length of 5 aminoacids, and none missing cleavages were set as working conditions. Peptide length distribution was calculated for both experimental and database peptides. Charge at pH 3 was calculated based on aminoacids pKas (web.indstate.edu/thcme/mwking/amino-acids.html). The charge distribution at pH 3 of *S. senegalensis* peptides was also calculated with this Python script.

When available at NCBI web site (www.ncbi.nlm.nih.gov/entrez), human and, occasionally, mouse Unigene number were used to query DAVID (apps1.niaid.nih.gov/david) and get gene ontology (GO) charts. The resulting information was compared with GO charts already published for *Tetraodon nigroviridis* (Jaillon 04), *Takifugu rubripes* (Jaillon 04), and *Oncorhynchus mykiss* (rainbow trout; Rexroad 03). GO classifications from literature were obtained from cDNA (*Oncorhynchus mykiss)* or complete sequenced genome *(Tetraodon nigroviridis*, *Takifugu rubripes).*

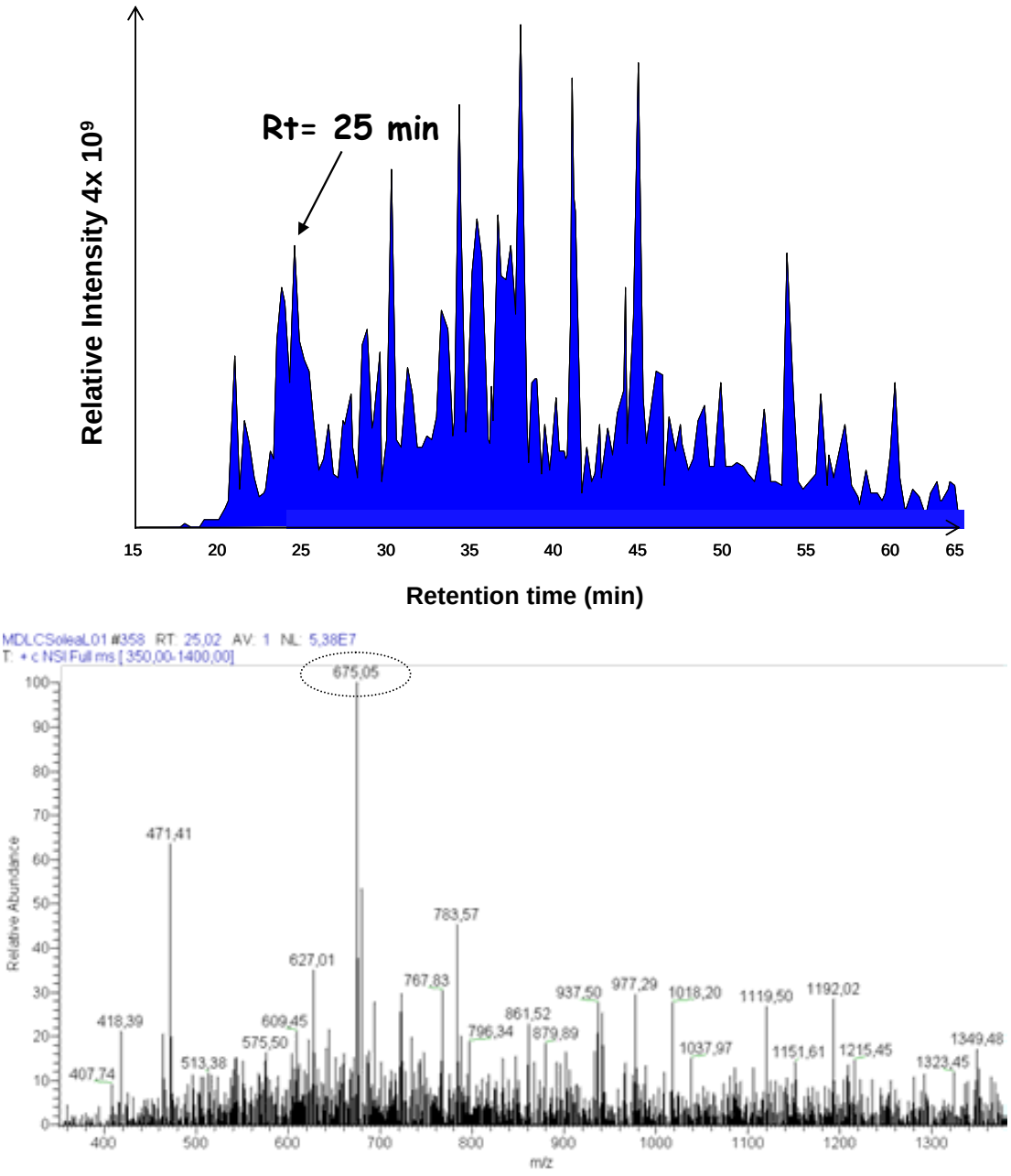

Figure 1.3.- Automated MS/MS analysis of peptides eluted from de 2-D LC system. A peptide eluting from the analytical column at minute 25 (up), is detected as the major component in the full mass scan spectrum acquired at that retention time (down). The mass spectrometer identifies on the fly the most abundant ions in each spectrum and performs MS/MS spectra centered on the corresponding masses (see figure 1.4).

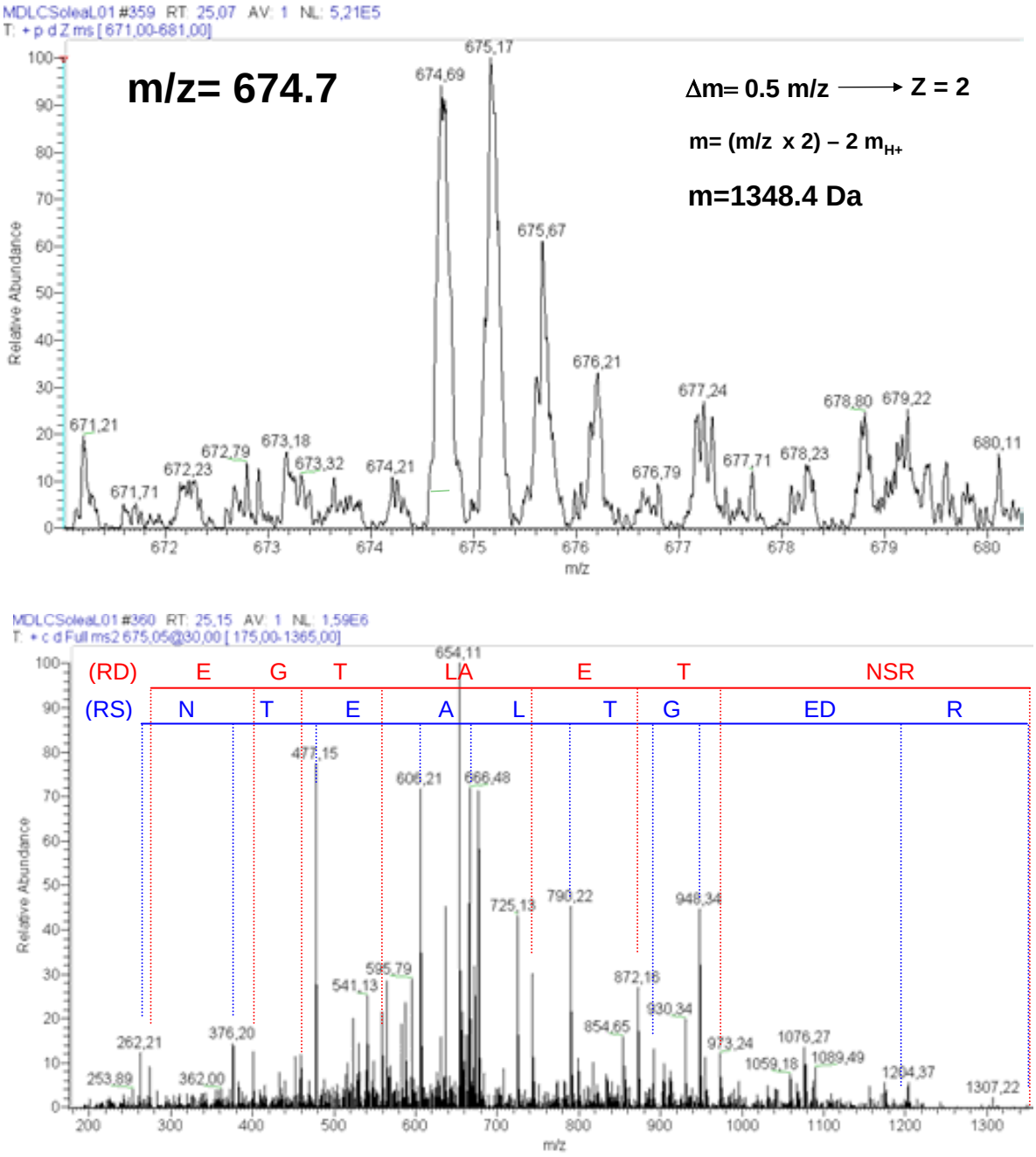

Figure 1.4.- The MS/ MS analysis over the eluted peptides (II): The zoom scan spectrum allows the determination of the peptide mass (up) previous to peptide fragmentation (down). The sequence of the analysed peptide (RDEGTLAETNSR) can be calculated from this spectrum using a *de novo* sequencing software.

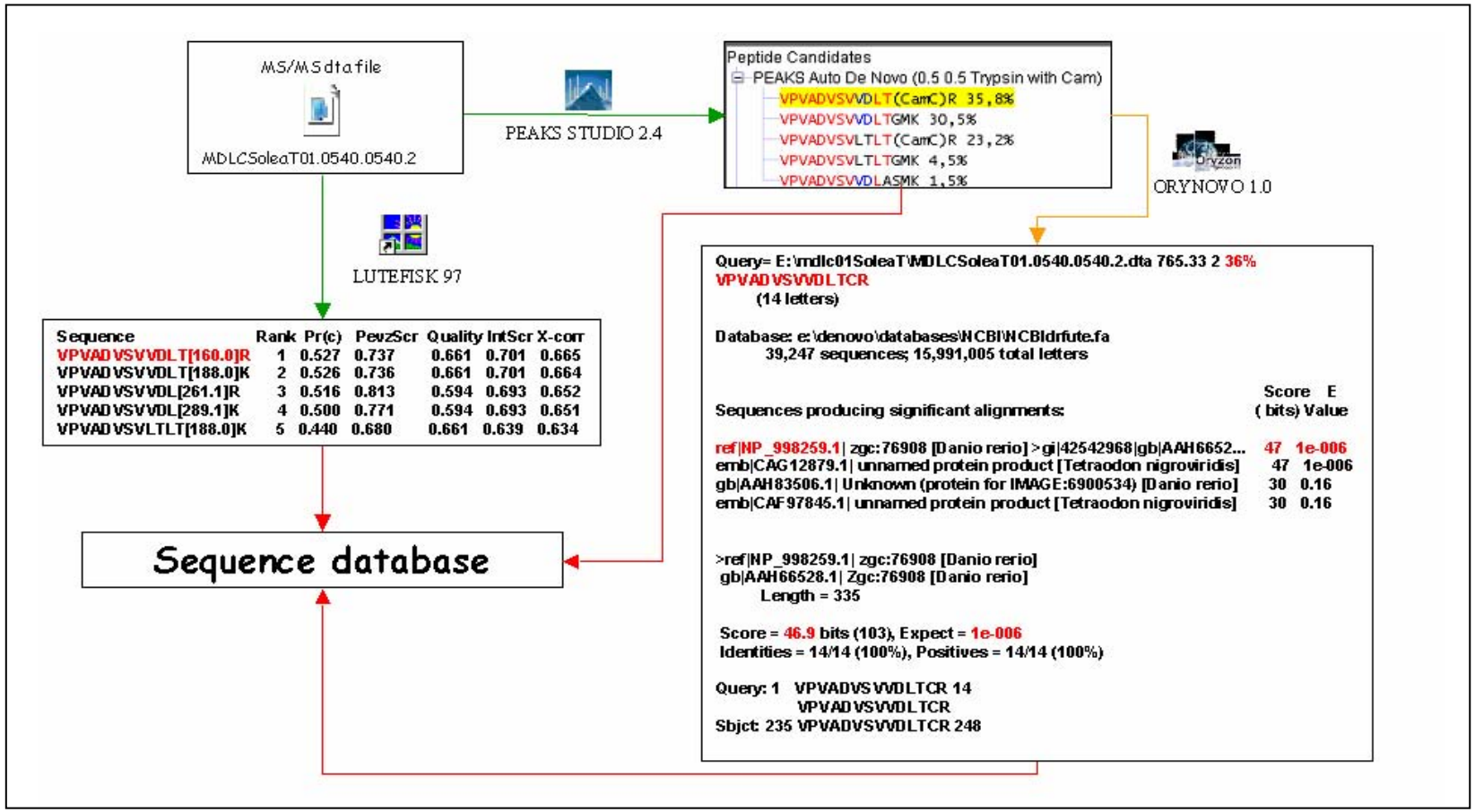

Figure 1.5.- The informatics process over the MS/MS fragmentation spectra. Each recorded TIC is processed by the SEQUEST software to generate a collection of dta files, one per each MS/MS spectrum. Each dta file is submitted to *de novo* sequencing using Peaks Studio 2.4 and Lutefisk 97. Lutefisk97 entries are used as confirmation data for Peaks candidates. Each candidate sequence produced by Peaks Studio output file is compared with fish genomes using ORYNOVO 1.0, a BLAST based software. The information coming from the Peaks, Lutefisk and ORYNOVO output files is finally integrated and the best sequence corresponding to every initial dta file is annotated in a database (figure 1.7).

1.2 Results

1.2.1 Two-dimensional LC, *de novo* sequencing and BLAST comparison

Two-dimensional chromatography analyses resulted in seven TICs per sample (figure 1.6). From these data, 954 and 815 peptide tags for testis and larva, respectively, were obtained by *de novo* sequencing. After these sequences were refined using BLAST, a database containing 1298 selected entries was generated (figure 1.7). Database annotation for each peptide tag include the source dta file, the mass and charge of the MS/MS fragmented ion, the name of the protein that had been related with the resulting sequence by BLAST and the charge of the sequence peptide at pH 3 calculated using EMBOSS. Information related with the bioinformatic analysis was also annotated including tentative sequences and scores, obtained using Peaks Studio 2.4 and Lutefisk97, the sequence of the protein database which gives the best BLAST comparison and the score of this comparison (tables 1.1 and 1.2).

Fragmentation spectra could present regions where it is difficult to deduce the aminoacid sequence and its relative order. Both *de novo* softwares, Peaks and Lutefisk, provide of alternative solutions in order to fit the final precursor ion mass. Lutefisk introduces a mass value in brackets ([Da]), indicating that any aminoacid combination with this mass value could be placed in that sequence region. On the other hand, Peaks calculations results in the placement of a series of high mass aminoacids, mainly tryptophans and tyrosines, at the C-terminal or N-terminal of the tentative sequence, to fill the undefined mass gap. This is obviously an artifact and thus, this type of sequence terminations have to be considered carefully. When BLAST matches from Peaks-derived sequence tags are available, the tag giving the best macht for a given entry is underlined to define relevant aminoacids in the corresponding tentative sequences. The complete and detailed sequence database is available in the information found on the attached CD.

1.2.2 Methodological analysis: peptide charge distribution among 2-D LC

The charge distribution at pH 3 of *S. senegalensis* peptides was calculated with the EMBOSS “iep function“, and they were then classified depending on the salt step of elution and the charge of the peptide (figure 1.8 and Annex I.3). The charge distribution at pH 3 of *S. senegalensis* peptides was also calculated with a Python script designed by Dr. Abián. The four protein databases containing fish entries were digested *in silico* and the charge at pH 3 of the resulting peptides calculated with the same Python script. (figures 1.9 and 1.10).

1.2.3 Biological analysis: GO charts

In order to determine the extent of the proteome description performed by the 2-D LC approach, GO description of *S. senegalensis* and GO classifications for other fish species available in the literature were compared. GO classifications in literature were performed from genomic data of *Tetraodon nigroviridis*, *Takifugu rubripes*, *Oncorhynchus mykiss* (rainbow trout). The molecular function classification at level 1 for the four fish species was compared in a bar diagram to determine similarities in protein description with data available in the literature (figure 1.12). Annex I.1 contains the detailed comparison between *S. senegalensis* testis and larva and *Oncorhynchus mykiss* GO charts for every classification level at hierarchical level 1.

The available Unigene ID numbers for the proteins described by the 2-D LC approach were introduced at DAVID gene ontology tool (203 Unigene ID for larvae and 242 for testis). Resulting GO charts are depicted in the Annex I.2 for the available classification modes: Biological Process, Molecular Function and Cellular Component.

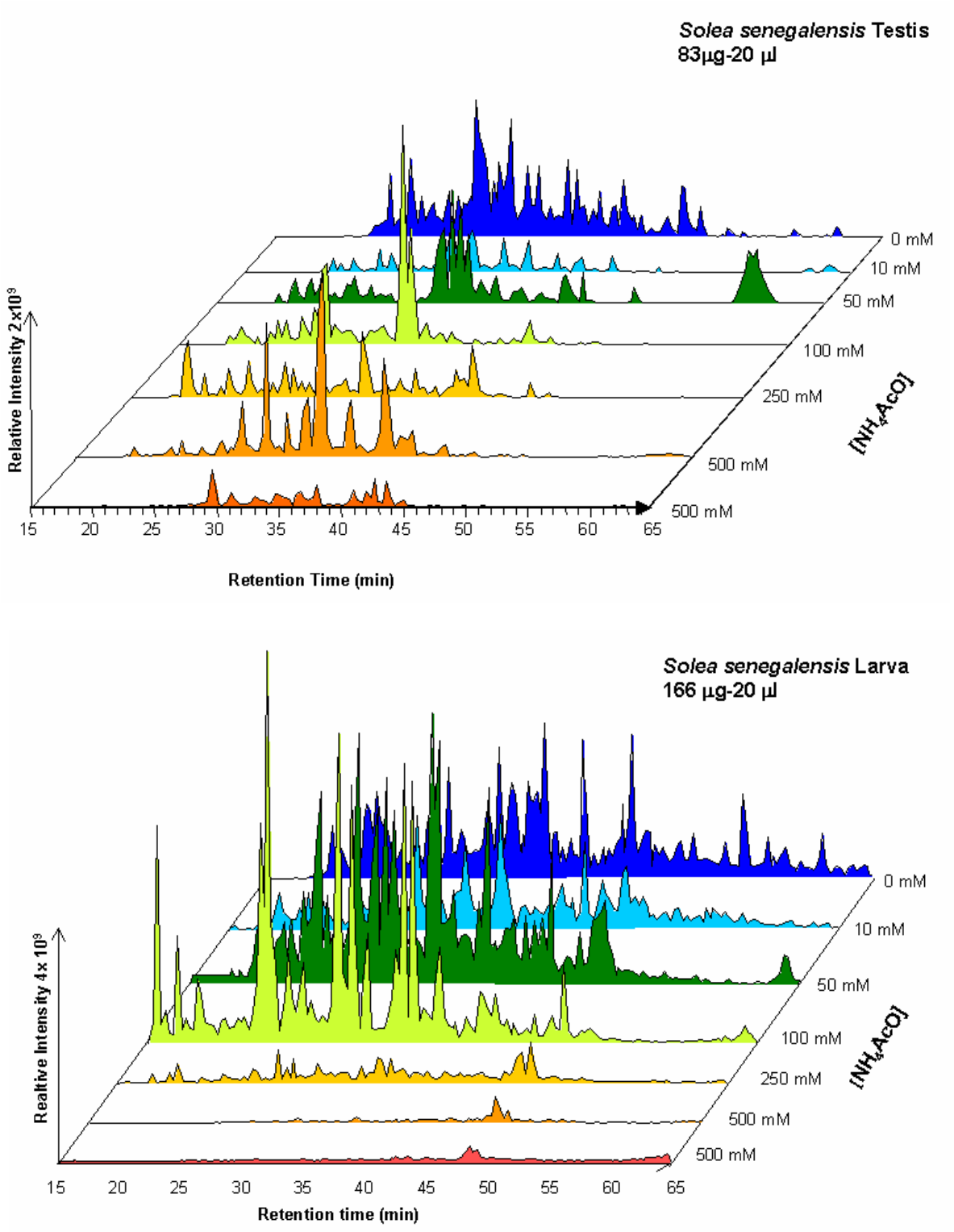

Figure 1.6.- Two-dimensional LC total ion chromatograms of larva (above) and testis (below) samples. The X-axis represents the reversed phase LC retention time, the Y-axis the ion intensity and the Z-axis the ammonium acetate (NH_4AcO) concentration for the corresponding SCX desorption cycle.

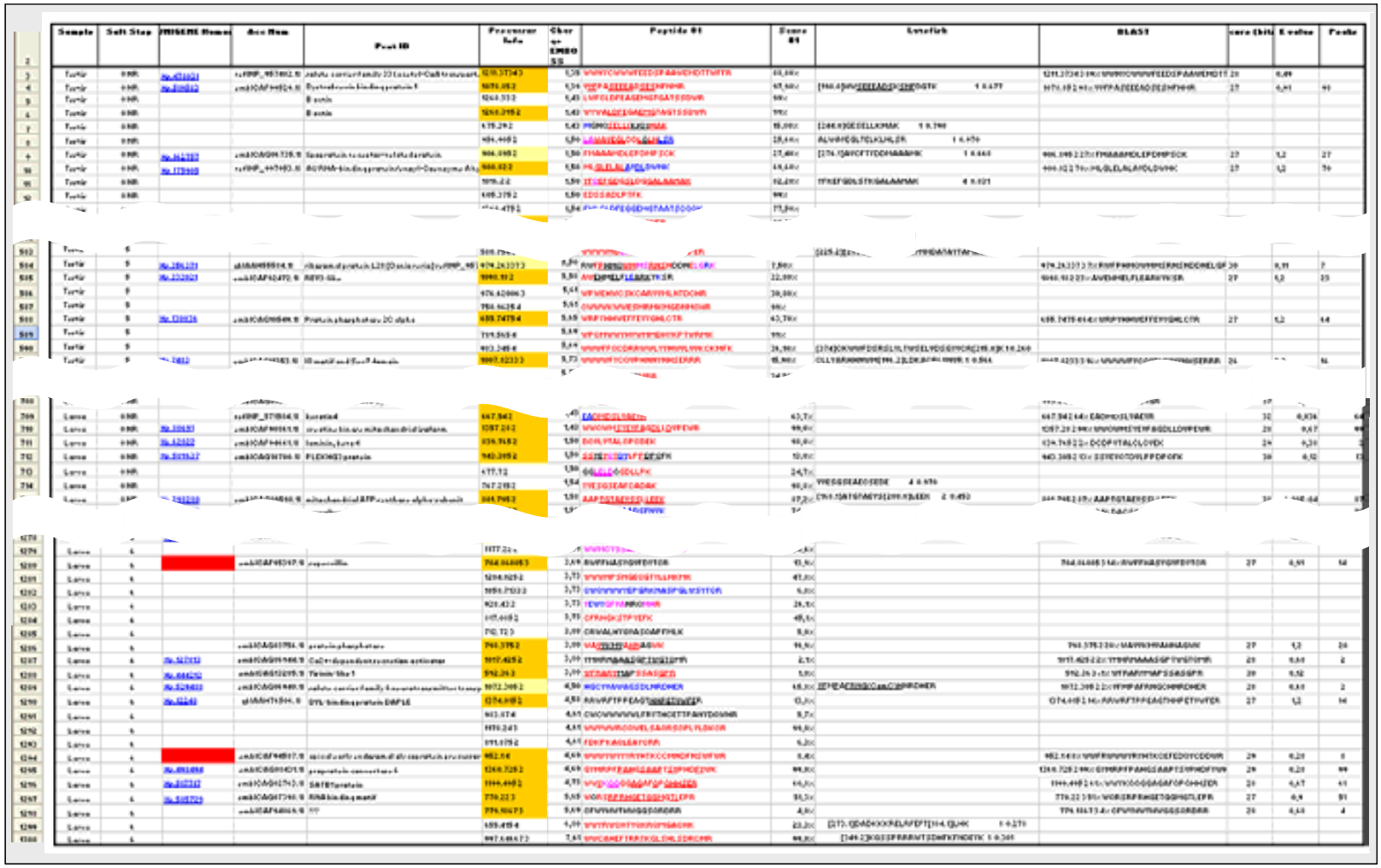

Figure 1.7.- *Solea senegalensis* peptide tags database: Overview of the 1298 entries. All entries from larva and testis peptide tags were introduced in the database after processing as described in figure 1.5. Detailed explanation of each field can be found in tables 1.1-1.2.

Tabla 1.1.- The Sequence Database (I). The validated sequences are introduced to a database where different information is integrated. *Sample* and *Salt step* identify the analyzed fraction; *Unigene Human*, *NCBI* and *Prot ID* give information about the protein that has been related with the resulting sequence by BLAST comparison; *Precursor Info* describes the mass in Da and charge of the MS/MS fragmented ion described in every dta file. BLAST matches are indicated with an orange background; *charge (EMBOSS)* of each Peptide#1 sequence is calculated at pH 3 using EMBOSS; *Peptide #1* and *Score#1* are the sequence and the score indicating the confidence of the *de novo* calculated sequence, obtained using Peaks Studio 2.4. Peptide sequences are also colour coded to indicate the confidence of different sequence tags: Red = 99-80%; Blue= 79-60%; Cyan= 59-40%; Black=<40%. Underlined tag sequences are common with the *BLAST* sequence. When present, Peptide *#2* and *Score#2* show a second, different high probability sequence provided by the *de novo* program.

Sample	Salt Step	UNIGENE Human	NCBI	Prot ID	Precursor Info	Charge (EMBOSS)	Peptide #1	Score #1
Testis	0 NR		NP_001001409.2	Actin, alpha 2	895.865 2	3.93	SYELPDGQVLTLGNER	88.10%
Testis	0 NR			Protein-kinase, interferon-inducible double stranded	1245.315 2	3.98	FWYQEAVTVLSAMEVECWNK	1%
		Hs.503315	NP_001002680.1|	RNA dependent inhibitor, repressor of (P58 repressor)				
Testis	0 NR	Hs.75514	NP_998476.1	Purine nucleoside phosphorylase	596.29 2	4.11	TADWLLDQTK	10.10%
Testis	0 NR	Hs.248017	NP_998259.1|	Glyceraldehyde 3-phosphate dehydrogenase	765.33 2	4.11	VPVADVSVVDLTCR	35.80%
Testis	0 NR	Hs.480653	emb|CAF92142.1|	Annexin A5	851.89 2	4.18	GLGTFPDALLELLTSR	1%
Testis	0 NR	Hs.180141	emb|CAG09506.1|	Cofilin 2 (muscle)	990.785 2	4.18	AWVQVAMEVLSLFNDMK	6.10%
Testis	0 NR	Hs.434255	emb|CAG05091.1|	Pleckstrin and Sec7 domain containing	912.36 2	4.18	FQSVFTPDLPATFPEK	17%
Testis	0 NR	Hs.153322	CAG02823.1	Phospholipase C	671.29 2	4.18	WPSPPDCAEQR	23%
Testis	0 NR		NP_851847.1	Heat shock 60 kD protein 1	601.22 2	4.26	NAGVEGSLVVEK	5.30%

Table 1.2.- The Sequence Database (II). *NCBI* gives information about the protein that has been related with the resulting sequence by BLAST comparison in the NCBI protein database; Lutefisk presents the sequence or sequence tag provided by this algorithm, rank among the five resulting candidates and the general score. This score indicates probability to be true from 1 (maximum value) to 0 (minimum value). Underlined tag sequences are common with the Peaks (*Peaks#1*); BLAST contains the m/z precursor info, Score#1 (see table 1.1) of the Peaks candidate giving the best BLAST comparison, and the matched database protein fragment; Score and E value are the BLAST scores.

NCBI	Lutefisk	Rank	Score	BLAST	Score (bits)	E value	Peaks
ref|NP_001001409.2|				895.865 2 88% SYELPDGQVLTLGNER	47	1.00E-06	88
ref|NP_001002680.1|	[243.1][260.0]CFAVTVLSAMWE[154.1]N[234.1]	1	0.331	1245.315 2 <1% FWYQEAVTVLSAMEVECWNK	32	0.027	
NP_998476.1				596.29 2 10% TADWLLDQTK	28	0.52	10
ref|NP_998259.1|	VPVADVSVVDLT[160.0]R	1	0.527	765.33 2 36% VPVADVSVVDLTCR	47	1.00E-06	36
emb|CAF92142.1|	WAADEDALLELLTSR	1	0.97	851.89 2 <1% GLGTFPDALLELLTSR	27	1.2	
emb|CAG09506.1|	[144.0]LVKVSDEVLSLFNDMK	5	0.762	990.785 2 6% AWVQVAMEVLSLFNDMK	30	0.12	6
emb|CAG05091.1|	FKSVFTPDLPATFPEK	3	0.691	912.36 2 20% FQSVFTPDLPTFAPEK	29	0.28	20
CAG02823.1				671.29 2 23% WPSPPDCAEQR	26	2.2	23
NP_851847.1	NAGVEGSLVVEK	2	0.97	601.22 2 5% NAGVEGSLVVEK	38	4.00E-04	5

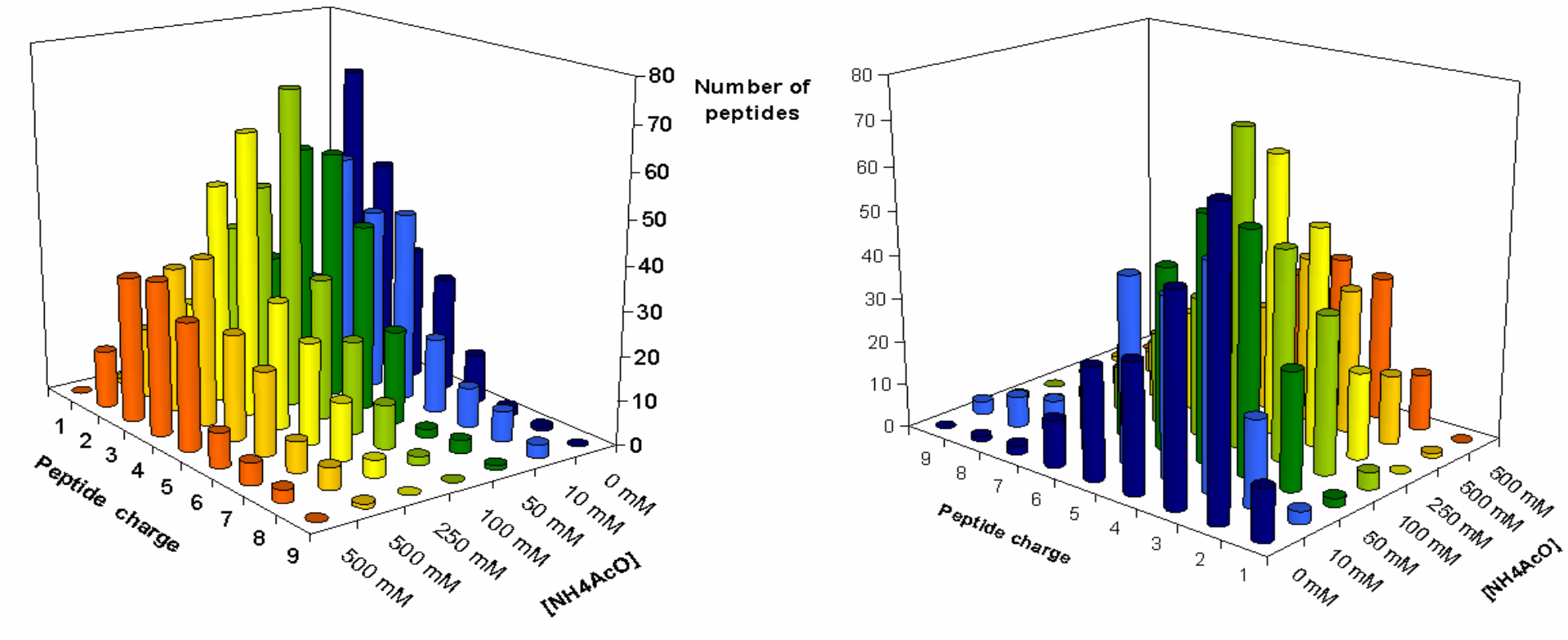

Figure 1.8.- Peptide charge distribution for the *Solea senegalensis* sequenced peptides. The peptide charge distribution of the sole testis and larva peptide sequences described with the 2-D LC approach are represented relative to the salt step where they were acquired. Both panels show the same figure from opposite perspectives.

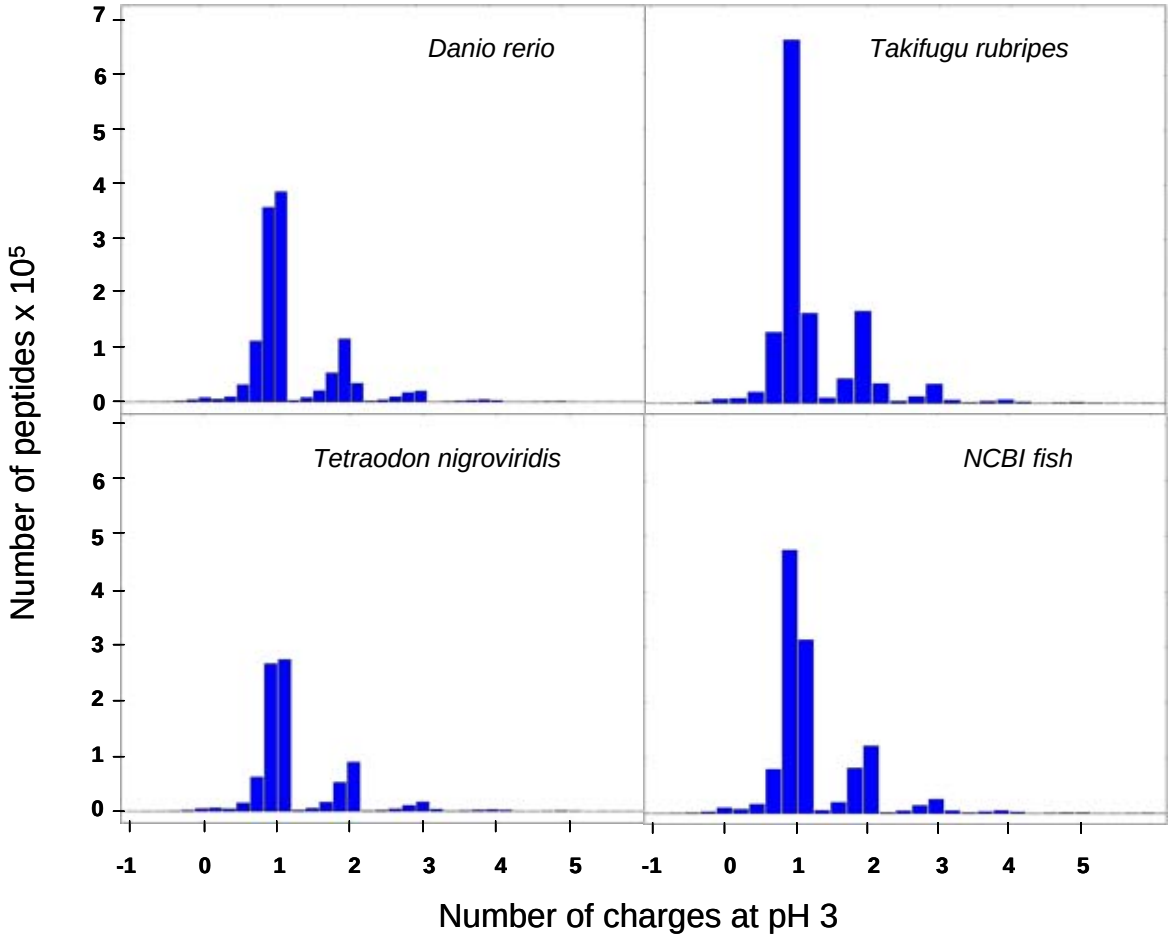

Figure 1.9.- Peptide charge distribution at pH 3 for the *in silico* Trypsin-digested database genomes. Ensembl peptide databases for *Takifugu rubripes*, *Danio rerio* and *Tetraodon nigroviridis* and the NCBI fish related database.

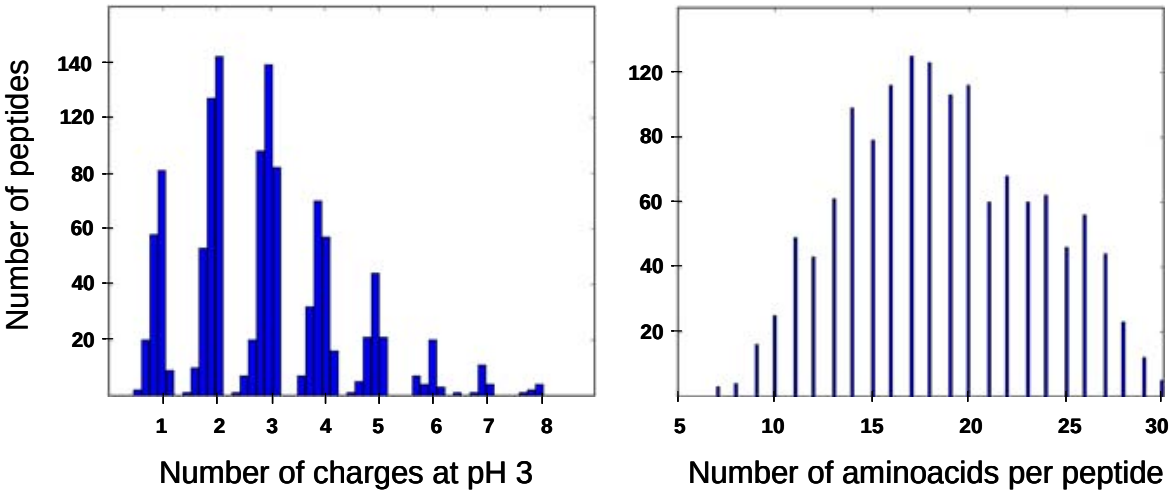

Figure 1.10.- Peptide charge and length distribution for the Senegalese sole experimental sequences.

1.3 Discussion

The goal of this chapter was the description of the proteome of testis and larva of the Senegalese sole. To achieve this objective, proteins were obtained from testis and larva tissue, digested with trypsin and the resulting peptides analysed in a 2-D LC system coupled to an ion trap mass spectrometer. Resulting MS/MS spectra were processed with several bioinformatic tools to generate a set of tentative peptide sequences. These sequences were further compared with existing proteins to find a possible identification. The information related to MS/MS, *de novo* sequencing and protein identification were introduced in a peptide tag database. This database, that currently contains around 1300 entries, comprises the first source of proteomic information for the Senegalese sole available for further investigations in reproductive biology and larval development of this species.

1.3.1 Methodological analysis

Chromatography of testis and larva samples was carried out at pH 3. In these conditions, most peptides are positively charged and their interaction with the SCX sorbent is favoured. To determine the charge profile of the 2-D LC experiment, the charge at pH 3 of the resulting 1298 peptides was calculated using the “iep function” of the EMBOSS software.

The distribution of peptide charge along the different salt steps where the peptide was detected shows roughly the expected trend: as the salt concentration increases, the calculated charge of the peptides eluting in that fraction also increases (Alpert 88, Zhu 91). Nevertheless, some biases or exceptions to this main trend can be observed. For example, the amount of double charged peptides showed an steady increase between 100 and 500 mM, despite the major concentration of these sort of peptides was found in the non-retained fraction (0 mM) Also, the salt step with a maximum of peptides at five, eight and nine charges was 10 mM, although this maximum was expected at a higher concentration, probably, about 100 mM and 250-500 mM for 5 and 8 or 9 charges respectively, in agreement with the tendency observed in the graph. These biases may be the result of other factors involved in the separation process such as hydrophobic interactions (Peng 03) or peptide length effects (Gillar 05).Charge distributions from the

four studied fish databases and the 2-D LC MS/MS obtained sequences presented significant differences (figures 1.9 and 1.10). The *S. senegalensis* data indicates a more spread distribution, with a maximum for 2 and 3 positively charged peptides, while the fish databases present a maximum for peptides around one positive charge.

This effect could be caused by the different peptide length distribution between database and experimental data (figures 1.10 and 1.11). The great number of short peptides resulting after the digestion of the proteins in the four databases may generate a maximum at one positive charge, as observed in figure 1.9. For this reason, new distributions for the databases were calculated, restricitng the length of the peptides resulting from digesting *in silico* the database. No changes were observed between both approaches, concluding that differences in charges distributions should be caused by other factors explained below.

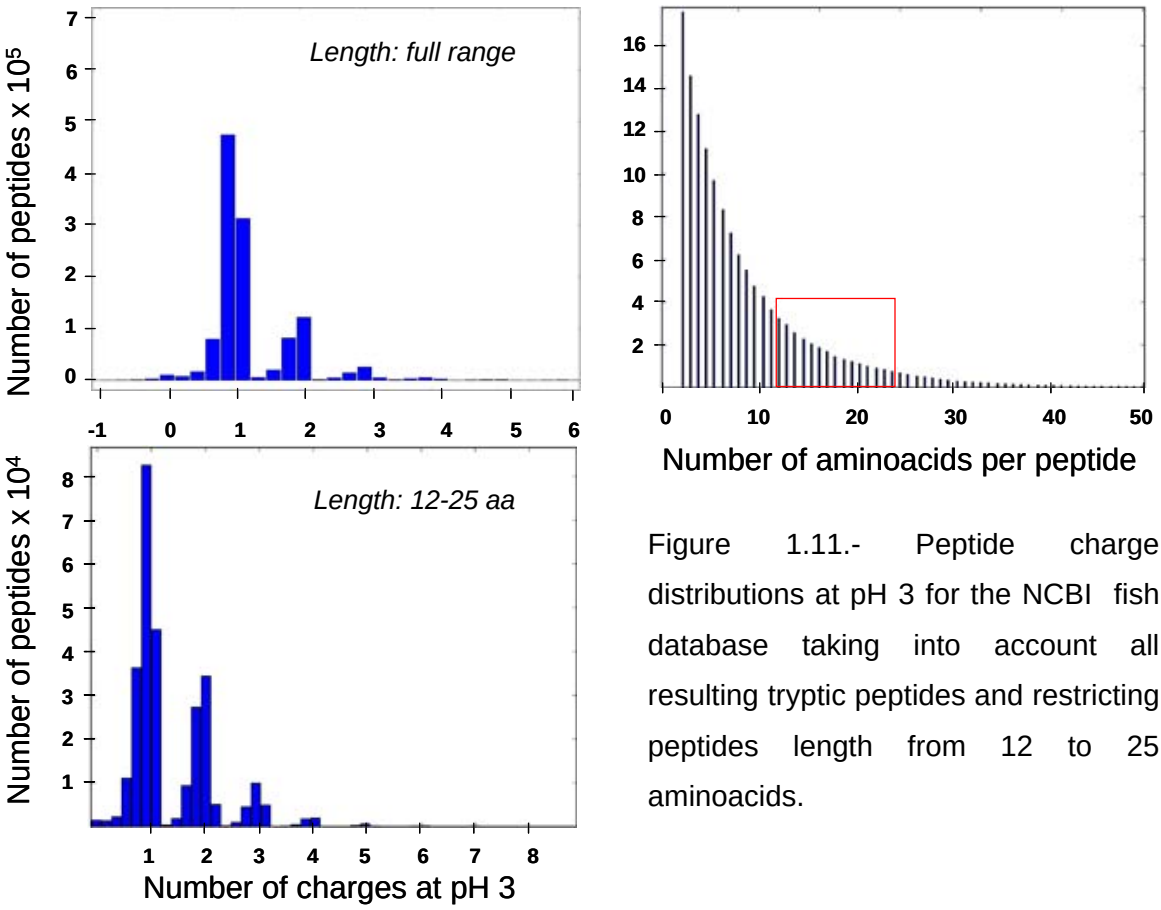

Figure 1.11.- Peptide charge distributions at pH 3 for the NCBI fish database taking into account all resulting tryptic peptides and restricting peptides length from 12 to 25 aminoacids.

Three main reasons might explain this bias between the shotgun-derived peptide repertory and the protein databases. First, tryptic digestion of proteins commonly produces a fraction of incompletely digested peptides. These peptides were not considered in the *in silico* calculation. As a result, experimentally determined sequences, and especially those with a large number of aminoacids, could have additional charges derived for the presence of internal K or R residues. This fact may produce a bias relative to the *in silico* peptide population. Second, the 2-D LC setup in this study could be selective for some groups of peptides, as the SCX step traps more effectively peptides with multiple positive charges. And finally, MS analysis and detection could understimate peptides with negative or small positive charge, because the response in the electrospray positive ion mode is greater for basic compounds. All these facts together should contribute to underestimate the multiple charged peptides in the *in silico* calculated distribution.

As observed in figures 1.9-1.11, taking into account a unit of charge, the possible values for a set of experimental or *in silico* peptides describes a distribution, where some of them are more probable than others, and even some values present almost null probability of ocurrence. This distribution was consistent over the different modifications tested in the Python script, and may be caused by the fact that charge for peptides is restricted to a certain values resulting from the combination of a limited number of pKa values of the aminoacids. A similar distribution of probabilities was described and applied to peptide identification by Mann and Zubarev (Mann 95; Zubarev 96) regarding to the possible masses that a peptides could present in function of the masses of the aminoacids. Several approaches have taken advantatge of this property to discrimate between peptides and contaminants in MS analysis (Dods 06, Kaur 06, Fukai 00, Blom 97). On the other hand, the observed property on charge distribution will not be so profitable for peptide discrimination, but it is still of interest for theoretical and experimental calculations of peptide charge.

The shotgun technology has been successfully applied to human samples (Davis 01; MacCoss 02; Shen 04), yeast (Wolters 01; Washburn 02; Peng 03), *Xenopus sp*. (Liska 04), some plants like *Oryza sativa* (Koller 02) or different bacterias (Choe 05; Wolff 06). Descriptions for any fish proteome (tissue or whole organism) using this technology were not available in the literature by the time of the current study.

Testis from other species has been also described using a similar 2-D LC MS system composed by an off-line SCX-RP chromatography coupled to a LCQ Deca (*Rattus norvegicus;* Essader 04). This study obtained over 6500 unique peptides and around 2600 proteins from 1 mg of digested testis proteome. As explained in the general introduction, the broadness of the description obtained by 2-D LC coupled to MS/MS depends principally on the election of an off-line (*R. norvegicus*) or an on-line system (*S. senegalensis*), on the scan speed of the mass spectrometer (LCQ Deca vs. LCQ, second and first generation of IT-MS by Thermo Electron, respectively) and, obviously, on the amount of sample analysed (1 mg for *R. norvegicus* against less than 0,1 mg for *S. senegalensis*). These three factors made the description of the testis proteome of *R. norvegicus* much more extensive than the performed in this study for the testis of *S. senegalensis*. On the other hand, the description of *R. norvegicus* was facilitated by the presence of genome databases for the same species or for very close homologous animals. In the case of *S. senegalensis,* proteome was described by peptide sequencing without database support and homology-driven protein identification.

Different improvements on the shotgun system of the current study could be performed to extent the description on *S. senegalensis*. For instance, loaded sample should be increased either by changing the SCX cartridge for another column with higher capacity or by turning to an off-line system. The range of salt-plugs can also be wider, especially in the low concentration range, where the majority of peptides were identified, or the length of the RP gradient could be adjusted to expand the time region where peptides elute. Another major upgrade would be the usage of the last generation of IT mass spectrometers (i.e. LTQ Orbitrap). Considering the expertise and know-how acquired during this first approach, and that much of these experimental requierements are already available, these ameloriations will provide in a near future a further and deeper step into the description of *S. senegalensis* proteome.

1.3.2 Biological analysis

The GO description of the Senegalese sole proteome was compared with the descriptions available in the literature for other fish species (*Tetraodon nigroviridis, Takifugu rubripes* and *Oncorhynchus mykiss)*. These GO classifications had been performed using predicted proteins translated from a cDNA library (*Oncorhynchus*

mykiss) or full genome sequences (*Tetraodon*, *Takifugu*), and correspond to the larger GO data collections available for fishes. The entries used in GO classifications were 450, 25625, 10841 and 9885 for *Solea*, *Oncorhynchus*, *Tetraodon* and *Takifugu,* respectively (Rexroad 03, Jaillon 04).

Protein distributions were similar between the four fish species despite differences in the methodological origin and size of the datasets (figure 1.12). Major discrepancies were observed in the "enzyme regulator" and "nucleic acid binding" groups of the rainbow trout. Interestingly, in the case of the Senegalese sole, the group of proteins in the "signal transducer" group was more numerous than in any of the other species. This increased proportion of proteins involved in pathway signalling could be related to the specific samples analyzed in the case of *S. senegalensis*, as expected for tissues involved in growing and metamorphosis processes (larva; Kimmel 01) or spermatogenesis (testis; Ethier 01; Welt 02).

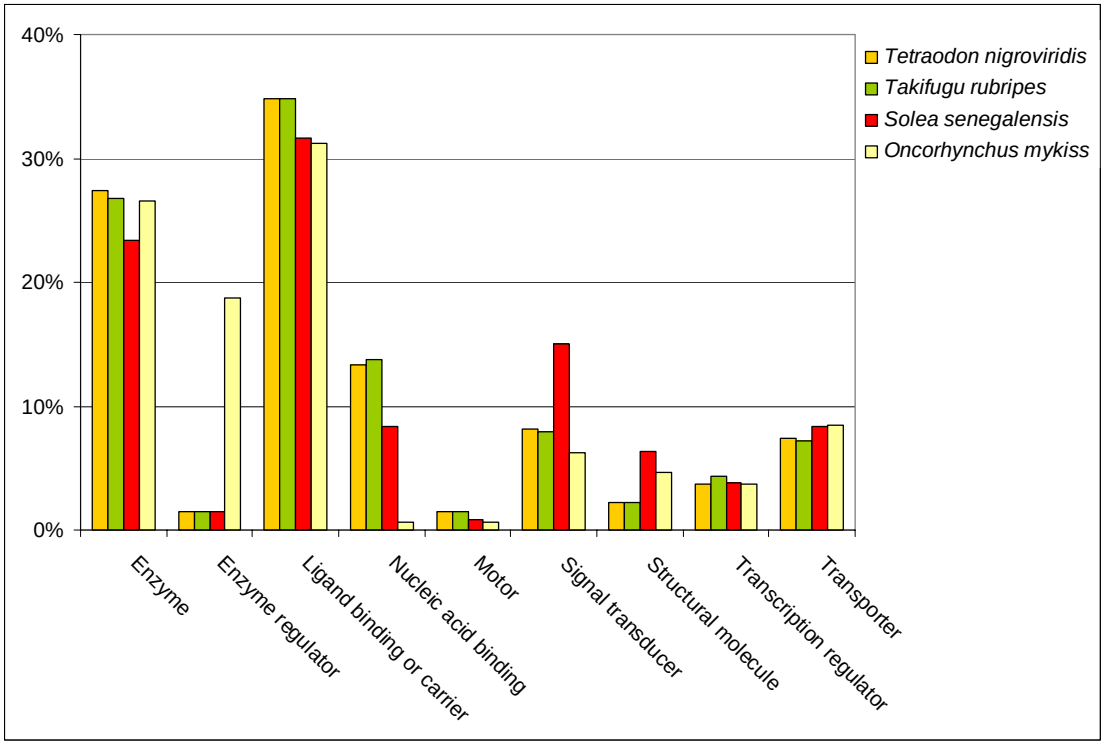

Figure 1.12.- Molecular function geneontology comparison for different fish species. Comparison of the *Solea senegalensis* GO results for Molecular Function at level 1 compared with those described in the literature for *Tetraodon nigroviridis*, *Takifugu rubripes*, *Oncorhynchus mykiss* (rainbow trout). Proteins classified under the "Unknown" term in GO results were not taken into account to calculate the percentatges of the other groups.

The comprehensive GO comparison between the Senegalese sole and the rainbow trout (Annex I.1) showed that, proportionally, less sole entries were determined as “unknown” at any classification level. These differences coud be produced by the different methodologies used for sequence analysis (2-D LC MS/MS peptide sequencing and mRNA-cDNA sequencing for sole and trout, respectively) and the relative size of the two data collections (1300 peptides vs 25625 cDNA sequences). The 2-D LC approach detects with more probability peptides derived from high abundant proteins, while cDNA sequenciation is not so conditioned by the abundance of the mRNA, as the genomic material is amplified by PCR. Then, the cDNA trout dataset probably present more sequences representing low abundant proteins, which in turn have a lower chance of having annotated functions than highly expressed molecules.

In summary, a set of about 1300 peptides from *S. senegalensis* testis and larva has been described for the first time by an LC-MS shotgun approach. This experimental design yielded a peptidic repertory where double and, more generally, multiple charged peptides were overrepresented relative to monocharged or acidic sequences. Despite this bias, the functional description obtained from the 2-D LC-derived data was comparable to other descriptions performed with larger genomic datasets, validating the shotgun methodology in terms of the protein groups represented by the obtained peptide repertory in *Solea senegalensis*.

Chapter 2

Proteomic analysis of differentially expressed proteins in wild and cultured *Solea senegalensis* during the spermatogenesis process.

In this chapter, proteome variations during spermatogenesis were compared between wild-caught and F1 generation in captivity of *Solea senegalensis*. The Senegalese sole F1 males often present an impaired production of sperm and morphological abnormalities in spermatozoa, which decrease the fecundation rates with respect to those observed in wild-caught fish. An approach that detects differences at the protein level in testis and/or sperm of both wild and F1 animals during spermatogenesis will be of great interest to increase the current knowledge on flatfish spermatogenesis and the factors which modulate this process. Therefore, a proteomic study was carried out on testis from wild and F1 animals at different stages of spermatogenesis, i.e., mid, late and functional maturation.

In collaboration with the research groups of Dr. J. Planas and Dr. J. Cerdà, the testes from wild animals used in this study were also analyzed by using an oligonucleotide-based microarray as a complementary expression analysis tool. Both proteomic and transcriptomic analyses were performed using the same biological material to provide data without interindividual variations. These studies will be of interest to describe expression changes at protein and mRNA level in the spermatogenic process in the wild Senegalese sole.

The whole process of microarray analysis was carried out in the genomic platform of Oryzon Genomics as described by Cerdà *et al*. (in preparation). The proteomic analysis was performed using the facilities of the CSIC/UAB Proteomic Laboratory as described in *Materials and methods.*

2.1 Materials and methods

2.1.1 Biological samples

Testis tissue was obtained from 9 wild (F0) adult individuals of *S. senegalensis* fished in the salt marshes of the Cadiz bay (Spain) in March and April 2004, and then maintained in the facilities of "CICEM El Toruño" in tanks under natural conditions of photoperiod and temperature for 30 days until sacrifice. Testis samples were also obtained in April 2005 from 6 cultured (F1) *Solea senegalensis* adult fish reared from eggs spawned by wild-caught fish adapted to captivity. These individuals were fed *ad libitum* for one year once a day with commercial pellets (Proaqua, Spain), and kept under natural photoperiod and temperature in 12,000-liter rectangular tanks in the Centre of Aquaculture-IRTA. The morphometric data of all the studied individuals are described in table 2.1.

Fish were sacrificed by stunning and decapitation, the testes were dissected and weighed and the GSI was calculated. For each animal, the testis was divided in different parts for further genomic, proteomic and histological analysis. For genomic and proteomic purposes, samples were frozen in liquid nitrogen and kept at –80ºC. Transport of these samples was always done in dry ice.

2.1.2 Histological analysis

Histological analysis was carried out to determine the stage of spermatogenesis. Pieces of testis were fixed in modified Bouin solution (75% picric acid and 25% formaline) for two hours, dehydrated, embedded in paraplast, sectioned at 5 μm and stained with eosin/hematoxilin. Testes were classified into three stages depending on the relative abundance of germinal cells as described by García-López *et al*. (2005).

Table 2.1.- Morphometric data of the studied individuals. Group= Experimental group in which each individual was classified for 2-D analysis. F0 and F1 stands for wild and aquacultured, respectively; the following key letters in the group name (M, L or Mat) indicate spermatogenesis stage. F0=wild, F1=cultured, M=mid spermatogenesis stage, L=late spermatogenesis stage, Mat=functional maturation.

Animal ID	Weight (g)	Length (cm)	Spermatogenesis Stage	Growth Environment	Group
4	740	43,5	Mid	Wild	F0M
10	511	38,2	Mid	Wild	F0M
12	716	40,7	Mid	Wild	F0M
1	566	39	Late	Wild	F0L
2	685	43,2	Late	Wild	F0L
3	758	44	Late	Wild	F0L
6	414	45,7	Functional maturation	Wild	F0Mat
7	537	41,1	Functional maturation	Wild	F0Mat
11	546	41	Functional maturation	Wild	F0Mat
2F8E	746	0,056	Late	IRTA	F1L
13C9	899	0,093	Late	IRTA	F1L
149F	833	0,113	Late	IRTA	F1L
L77	639	0,087	Functional maturation	IRTA	F1Mat
L5530	1164	0,083	Functional maturation	IRTA	F1Mat
L55	750	0,080	Functional maturation	IRTA	F1Mat

2.1.3 Protein extraction

Protein extracts were obtained from 3 testis samples per histological stage. According to male origin (F0 or F1) and the criterions to determine spermatogenesis state (García 05), five classes were defined: F0 Mid (F0M), F0 Late (F0L), F0 Functional maturation (F0Mat), F1 Late (F1L) and F1 Functional maturation (F1Mat). Fifty milligrams of tissue per individual fish in table 2.1 were disrupted mechanically in 400 μl of TNE buffer (50 mM Tris-HCl pH 7,6; 150 mM NaCl; 2 mM EDTA pH 8,0; 1 mM Na_3VO_4; 1 μM Leupeptin; 2 μM Pepstatin; 0,1 μM Aprotinin).

Then, samples were sonicated in a water bath at 4ºC for 10 min and NP40, PMSF and DTT were added to achieve 1% v/v, 1 mM and 2 mM respectively. Proteins from 100 μl of the resulting homogenate were precipitated using the Wessel-Flugge method (Wessel

84). The precipitated proteins were dissolved with 100 µl of 2-D rehydration buffer (7M urea, 2M thiourea, 2% CHAPS, 40 mM Tris-Cl, 1,2% HED (DeStreak, GE Healthcare) and 0,5% ampholites 3-10 pI (GE Healthcare)). Each sample was quantified individually using the RcDc kit (Bio-Rad).

2.1.4 Two-dimensional electrophoresis

Each sample was analysed twice by 2-DE. IPGstrips (3-10 L, 18 cm. GE Healthcare) were loaded with 100 µg of protein each. These IPGstrips were processed in an IPGphor II following a seven step voltage program during approximately 24 hours (table 2.2 and figure 2.1; 10 h at 50 V, 1:30h at 500 V, increase to 1000 V during 1:30h, increase to 2000 V during 1:30h, increase to 4000 V during 1:30h increase to 8000 in 2 hours and focus at 8000 V until 70000 Vhr). Strips were frozen at -40 ºC until equilibration or immediately equilibrated during 15 minutes with 10 ml of 50 mM Tris-HCl pH 8,8, 6 M urea, 30% v/v glycerol, 2% w/v SDS, 10 mg/ml DTT and 0.1% bromophenol blue, 15 minutes more with 10 ml of 50 mM Tris-HCl pH 8,8, 6 M urea, 30% v/v glycerol, 2% w/v SDS, 25 mg/ml IAA and then loaded over a 12% polyacrylamide gel. Samples ran through the polyacrylamide gels in an Ettan Dalt VI electrophoresis unit (GE Healthcare) at 20 ºC (Hetofrig CB refrigerator, Heto) under standard conditions (30 minutes at 2,5 W/gel and 16 W/gel for 4 hours). Gels were then stained as described before (Moertz 01) and images acquired in a GS-800 Calibrated Densitometer (Bio-Rad)

Table 2.2.- Isoelectrofocusing steps programmed on the IPGphor to separated proteins of gonad proteome samples by *pI*.

Step	Process	Voltage (V)	Time (hh:mm)	Volts-hour (Vhr)
1	Voltage assisted rehydration and sample loading	50	10:00	--
2	Sample loading and focusing	500	1:30	--
3	Sample focusing	1000	1:30	--
4	Sample focusing	2000	1:30	--
5	Final sample resolution	4000	1:30	--
6	Final sample resolution	8000	2:00	--
7	Final sample resolution	8000	--	70000

Current was 50 µA/IPGstrip and temperature was set at 20ºC during the whole process

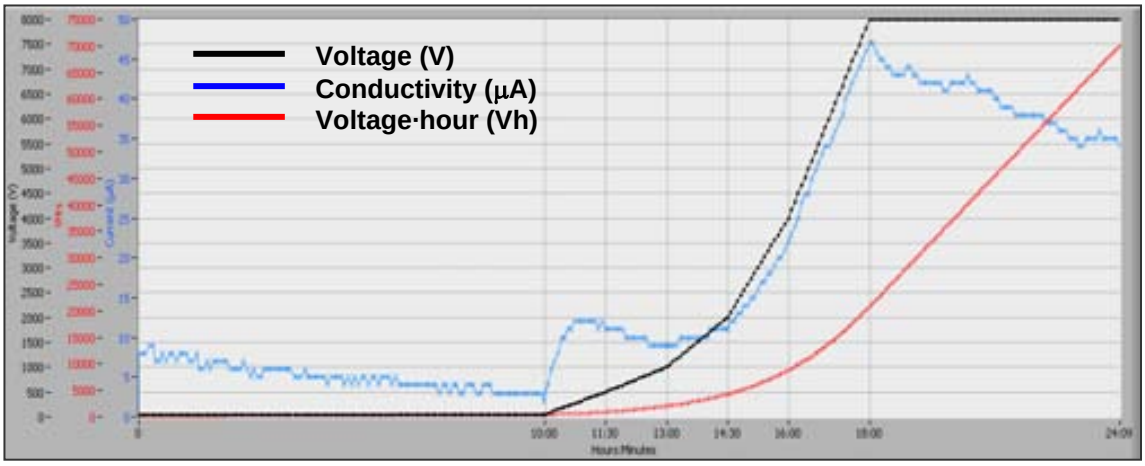

Figure 2.1.- Evolution of the electrical parameters monitored for the IPG separation of a protein extract from a male sole gonad. These graphics were used as quality controls for the IEF processes involved in this study. Voltage, conductivity and voltage·hour were recorded every 5 minutes during the 24 hours of the process and plotted against time (Hours: Minutes). The vertical lines delimitate the seven steps described in table 2.2.

2.1.5 Differential expression analysis and clustering

The expression analysis was done using the Image Master Platinum 5.0 software package (IMP 5.0, GE Healthcare). Spots were detected automatically fixing saliency between 1000-2500, and minimum area and smooth at 5 and 2, respectively. Spot detection was further refined manually for each gel to ensure good quality results. Matching was done using one of the gel replicates from individual number 3 (F0 Late) as the reference gel, with 10 landmark uniformly distributed and further manual checking. Six different comparisons were performed between the previously defined classes (F0M vs. F0L; F0L vs. F0Mat; F0M vs. F0Mat; F1L vs. F1Mat; F0L vs. F1L; F0Mat vs. F1Mat), to determine spots with changing protein levels. Normalized volume (%Vol) of spots was used to determine differences. This value corresponds to the volume of a certain spot in a gel divided by the summatory of the volumes of all the spots detected in the same gel. The degree of difference between two groups of spots is expressed as the average ratio. The average ratio value indicates the normalized volume ratio between the two groups. Values are displayed in the range of $-\infty$ to -1 for decreases and +1 to $+\infty$ for increases in protein abundance. Values between -1 and +1 are not represented, hence a two-fold increase and decrease is represented by 2 and -2, respectively (instead of 2 and 0,5).

Determination of the significance of the differences on %Vol between two groups was performed using the Student's t-test option provided in the IMP 5.0 package. Only groups presenting differences with Student's t-test values greater than 3 in one of the comparisons were used for further identification steps. A Student's t-test value greater than 3 with 6 gels per state (10 degrees of freedom) corresponds to a p-value < 0.05.

Normalized volume data for spots present in all gels was referred to F0Mat values and hierarchical clustering perfomed using Cluster 3.0 (developed by Michael Eisen and updated by Michiel de Hoon) with centred correlation and complete linkage conditions. Resulting clusters were visualized with Java TreeView 1.0.7 (Saldanha 04).

2.1.6 Determination of gel variation: *Mr* and *pI* variation

Six spots were chosen to study variation of *Mr* and *pI* coordinates during the experiment. Coordinates were calculated relative to the values of 10 spots taken as reference spots along the 30 gels. The *Mr* values of these 10 spots were interpolated from an experimentally determined relationship between the log *Mr* and electrophoretic mobility of molecular mass markers added to the 2D separation in the performed gels. *Mr* for these molecular mass markers was referred to the dye front. The *pI* values were deduced from the linear relationship between pH and length of the IPGstrips. The mean, the standard deviation (SD), and the coefficient of variation (CV) of *Mr* and *pI* values for these six spots were calculated in all the 30 performed gels.

2.1.7 Determination of gel variation: Normalized volume variation

A collection of spots that where present in all 30 gels (488 items) were chosen to study reproducibility of the normalized volumes in gels. The standard deviation and the coefficient of variation of the normalized volume for these spots were calculated in all the gels from the same state. The mean for the CV of all the spots of the same state (CV Mean Value) was also obtained.

2.1.8 Protein identification

Target spots were manually excised in a laminar flow cabin and placed in a digestion plate (Proxeon Biosystems). A multiscreen vacuum manifold (Millipore) was used to digest samples with trypsin. The procedure for in-gel digestion was as follows. First, gel slices were washed 3 times with 50 μl of 25 mM NH_4HCO_3 at pH 8 and dehydrated by washing them three times with acetonitrile. Gel slices were then incubated 1 hour at 37ºC with 50 microliters of 10 mM DTT in NH_4HCO_3 (25 mM, pH 8). Afterwards slices were incubated one hour at 25 ºC in a dark place with 50 μl of 55 mM iodoacetamide in NH_4HCO_3 (25 mM, pH 8) to carbamidomethylate the reduced cysteines. Gel fragments were washed with NH_4HCO_3 (25 mM, pH 8) and dehydrated again with acetonitrile. Five to fifteen microliters of 50 ng/μl trypsin (Promega) were added to each gel slice, depending on the volume of the excised spot, incubated 45 minutes at 4ºC and then the non absorbed trypsin removed. Gel fragments were covered with NH_4HCO_3 (25 mM, pH 8) and digestion took place during 16 hours at 30ºC (Carrascal 02). For the peptide extraction, gel slices were washed three times with ACN/H_2O 1/1 v/v 0,25% TFA and three times with acetonitrile. The resulting liquid (80-120 μl) containing the digested peptides was totally evaporated, redissolved with 5 μl de MeOH/H_2O 1/2 v/v 0,1% TFA and stored at –80 ºC until mass spectrometry analysis.

The digested sample (0,5 μl) was analysed with a Voyager De PRO MALDI–TOF mass spectrometer (Applied Biosystems). The instrument was run in reflectron mode with an average resolution of 12,000 full-width half-maximum at *m/z* 1500 and laser intensity between 1800 and 1900 V. A 5 mg/ml α-cyano-4-hydroxycinnamic solution was used as MALDI matrix. Spectra were externally calibrated using a standard peptide mixture (des-Arg1-bradykinin (904,46 Da), Glu1-fibrinopeptide B (1570,68 Da), angiotensin-1, (1296,69 Da), ACTH 1-17 (2093,09 Da), ACTH 18-39 (2465,20 Da), ACTH 7-38 (3657,93 Da)). Samples and calibration mixtures were spotted in alternate lines of a 96 x 2 sample positions MALDI plate. Each sample was externally calibrated with the standard peptide mix in the corresponding top left position in the plate. When the ions corresponding to already known trypsin autolytic peptides (*m/z* 842,5100 and 2111,1046) were detected, a second automatic internal calibration of the spectra was performed using these ions as reference.

The resulting spectra were used to select the peptides susceptible to be analysed by tandem mass spectrometry. Previously to this analysis, samples were desalted using ZipTip C-18 micropippete tips (Millipore) following these steps: chromatographic phase conditioning with 5x 10 µl ACN/H_2O 1/1 and 5 x 10 µl H_2O 0.1% TFA, sample load, sample wash with 3 x 10 µl H_2O 0.1% TFA and 3 x 10 µl H_2O; peptide elution with 5 µl of 70% methanol 1% acetic acid. A volume of 2-3 µl of sample was loaded into a nanoESI spray capillary (Proxeon Biosystems) and analysed by n-ESI ITMS/MS using a LCQ mass spectrometer (Thermo Electron) equipped with a nanospray interface (Protana). The instrument parameters were set with five standard peptides of molecular weights between 1296 and 2149 (angiotensin I and substance P and 3 synthetic peptides of 1758, 1911 and 2149 Da, respectively). Applied electrospray voltage to create electrospray was 0,8 kV and capillary temperature was set at 110 ºC.

For MS/MS experiments, the isolation window was 3 mass-units wide, and the relative collision energy was 20–45%, depending on the charge of the precursor ion. Resulting information contained a scan spectrum, a high resolution spectrum or zoom scan and a fragmentation spectrum or MS/MS spectrum. In the scan spectrum the signals corresponding to the different charge states from the present peptides were detected, while in the zoom scan the m/z and charge state of the ions to be fragmented were observed with precision. The MS/MS spectrum is used to determine the peptide sequence of each analyzed ion.

2.1.9 Bioinformatic analysis of MS/MS spectra

The information encoded in the fragmentation spectra of each peptide was extracted using the SEQUEST software (Thermo Electron) and transformed into dta format. Further analysis using Peaks 2.4 and Lutefisk97 and were performed as described in Chapter 1.

For each spectrum, the tentative *de novo* sequences derived from Peaks were sent together for a BLAST homology search, looking for short related, nearly exact matches (Altschul 90, www.ncbi.nlm.nih.gov/BLAST). In case of more than one BLAST match, Lutefisk candidates were used to confirm or suggest the final tentative sequence. When

resulting BLAST protein description did not indicate any protein function, a new search was performed against the NCBI database using pBLAST.

2.1.10 Comparing sequenced peptides and identified proteins with *S. senegalensis* ESTs

An EST database for the Senegalese sole was generated in the Pleurogene project by sequencing approximately 11000 clones from a normalized cDNA library generated by combining different cDNA libraries. These libraries were from intestine, stomach, liver, larvae at different metamorphic stage, brain (including pituitary), ovary, testis, and undifferentiated gonads (Cerdà, in preparation).

The peptide sequences from all spots were translated to genomic ATG code. All the possible degenerated combinations were taken into account for further steps. The resulting genomic sequences for each spot were compared using tblastn ([pam30] matrix; protein query vs. translated database, six frame translation) with a set of 10000 ESTs from the Senegalese sole. For each sequence a maximum of three possible hits were reported. The ESTs were also compared to the NCBI protein database using blastx ([blosum62] matrix; translated query vs. protein database with six frame translation). For each EST a maximum of three possible hits were reported.

Both results (peptide sequences vs. ESTs, ESTs vs. NCBI database) were combined to confirm relationships of MS/MS sequenced peptides and identified proteins. The 3 resulting ESTs for each peptide sequence were searched against the result list of the ESTs vs. NCBI comparison. In that list, each EST presents 3 protein hits. Those proteins were compared with the original protein assignation made after peptide sequencing (figure 2.2).

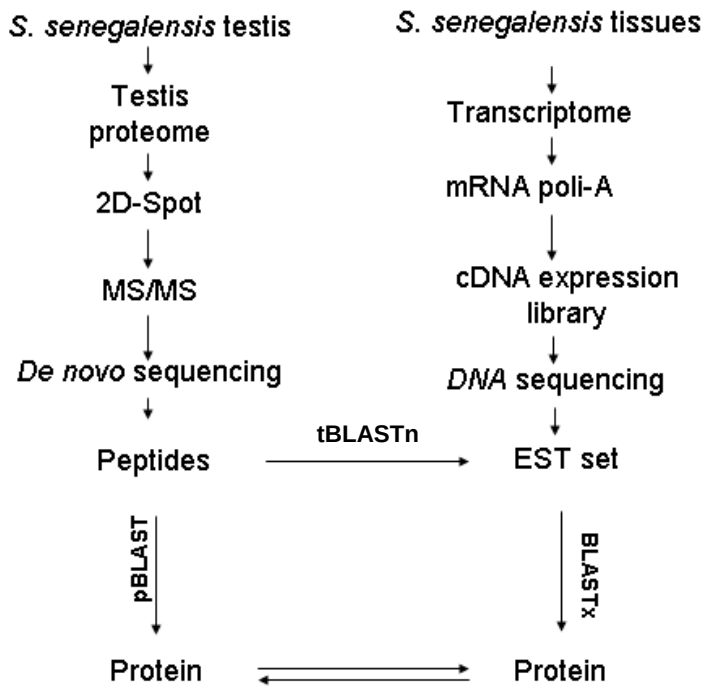

Figure 2.2- Confirmation of protein identification by comparing peptide sequences, EST and protein databases. The scheme shows the experimental procedures to obtain peptide sequences from *S. senegalensis* and ESTs from different tissues of *S. senegalensis*. For peptide sequences, differential spots were determined after testis proteome was analysed using 2-D gels. Tryptic peptides were analysed using a MS/MS mass spectrometer and *de novo* sequencing software. For ESTs, mRNA from different adult tissues and larvae was extracted, reverse transcribed to cDNA, and cloned into an expression library. An aliquot of the different cDNA libraries were combined into a master library, normalized, and clones were sequenced from the 3' end to produce the ESTs set. Three different comparisons were made: Peptides against ESTs; ESTs against protein database; Peptides against protein database. Finally, protein results obtained in the two described manners were compared.

2.2 Results

2.2.1 Histological analysis

Samples from F0 (wild) and F1 (cultured)) fish were divided into mid, late and functional maturation depending on the relative abundance of germinal cells as described by García-López *et al*. (2005). In mid spermatogenesis germ cells at all the different developmental stages were present. In the cortex, there was a decline in the number of spermatogonia and the appearance of a high population of spermatocytes (Fig. 2.3, A and B). Germinal cysts containing spermatocytes were distributed in the periphery of the seminiferous lobules, leaving a small central lumen filled by spermatides. In late spermatogenesis, the lumen of the cortical seminiferous lobules was almost fully filled by spermatides (figure 2.3, C-D). Few cysts containing spermatocytes were visible. Spermatides were the most abundant cell type inside the testis, and spermatozoa became more abundant in the medullar efferent ducts. In the final functional maturation stage, spermatides were still very abundant in the cortical seminiferous lobules, but their number decreased progressively as successive batches transformed into spermatozoa (figure 2.3, F and G). Ripe spermatozoa accumulated in large quantities in the medullar efferent ducts. This classification was used to divide the samples into the five states of this study: Mid wild (F0M), Late wild (F0L), Functional maturation wild (F0Mat), Late cultured (F1L) and Functional maturation (F1Mat).

2.2.2 Two-dimensional electrophoresis

Two gels per sample were performed (figure 2.4), scanned with a 300 dots per inch (dpi) resolution and introduced in an Image Master Platinum project, in order to analyse differences in protein expression between the different stages of spermatogenesis. The main features of each gel were evaluated taking into account all the spots considered for analysis (table 2.3). The reproducibility of the gels across the performed gels was determined by studying the variations in *Mr* and *pI* of six spots. These spots presented variations of their expression in the different experimental groups (figure 2.5 and 2.6). The standard mean deviation of normalized volume of 488 spots with representation in all thirty gels was also calculated to determine variability of normalized volume inside the same experimental group (figure 2.7). Mean value of CV in each state was 54%, 42%,

55%, 36% and 38% for F0M, F0L, F0Mat, F1Mat and F1L, respectively. From this data it was assumed that only variations greater than ±1,6 must be taken into account for further expression analysis.

2.2.3 Differential expression analysis and clustering

The %Vol of the detected spots was compared between F0 Mid and F0 Late; between F0 Mid and F0 Functional maturation; between F0 Late and F0 Functional maturation; between F1 Late and F1 Functional maturation; between F0 Late and F1 Late; and between F0 Functional maturation and F1 Functional maturation. The spots showing significant changes are indicated in the gel images depicted in figure 2.8. The corresponding statistical data is given in table 2.4, and the bar diagrams represent the relative changes in the five different stages in figure 2.10. Bar diagrams in this latter figure are grouped depending on the criteria described in figure 2.9. Briefly, histograms were visually analysed to determine whether a positive or negative variation occurs between “state A” and “state B”. In case it was positive (increase) a number 1 was annotated, while in the case of a negative variation a number 2 was chosen. Number 0 indicates no significant variation between states. The comparisons between spots in mid, late and functional maturation F0 gels were analysed together and in this case a code from 1 to 6 was given to represent the six different evolution patterns observed. Spots could then be grouped on the basis of the four-number code that was built after these comparisons (Table 2.5) The first number is related to the evolution through the mid, late and functional maturation F0 states (F0 MLMat), the second one is the comparison between F1Mat and F1L (F1Mat-F1L) states, the third stands for the differences found in the F0L- F1L analysis (F0 Late-F1 Late), and the last one for the F0Mat-F1Mat comparison (F0Mat-F1Mat).

Table 2.3.- Number of analysed spots per each experimental group. SD and CV: mean standard deviation and coefficient of variation of the spots of each experimental group, respectively.

	Experimental group				
	F0M	**F0L**	**F0Mat**	**F1Mat**	**F1L**
Spots	1055	1155	1135	1148	769
SD	188	299	108	238	183
CV	17,8	25,8	9,5	20,8	23,8

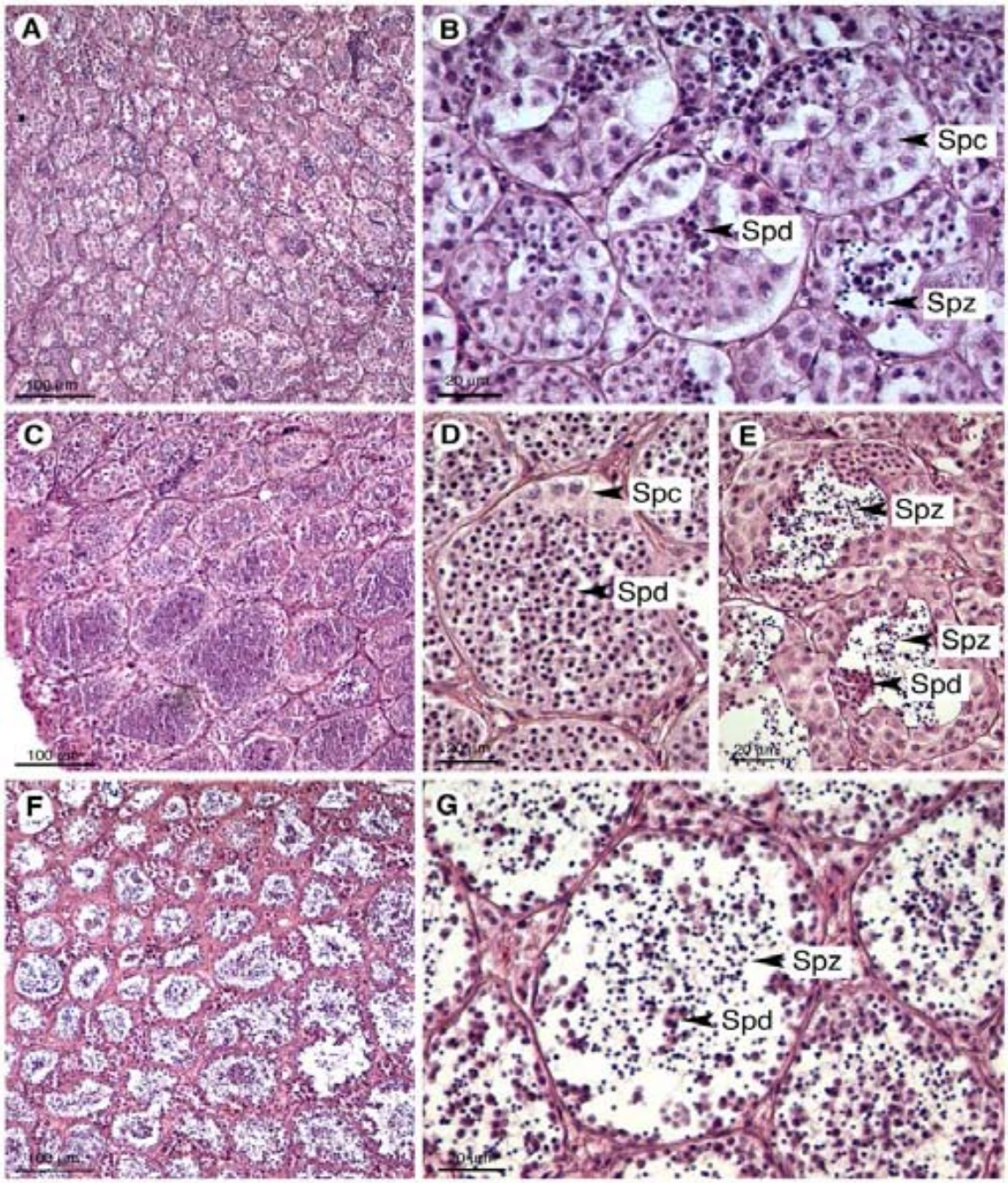

Figure 2.3.- Photomicrographs of histological sections of Senegalese sole testis at different stage of spermatogenesis. *Panels A-B*: Testis at mid spermatogenesis where spermatocytes (Spc) and spermatides (Spd) are the main germinal cells observed in the seminiferous tubules. The lumen of the seminiferous lobules is narrow, and some start to show some spermatozoa (Spz). *Panels C-E:* Testis at late spermatogenesis in which the lobules are almost fully filled of Spd, and Spc are restricted to the periphery of the lobules. (D). In the medullar area of the testis, the lobules show a bigger lumen filled by Spd and Spz (E). *Panels F-G*:, Testis at the functional maturation stage in which lobules show much bigger lumen containing much more Spz and few Spd. The Spc almost disappear of the periphery of the seminiferous lobules.

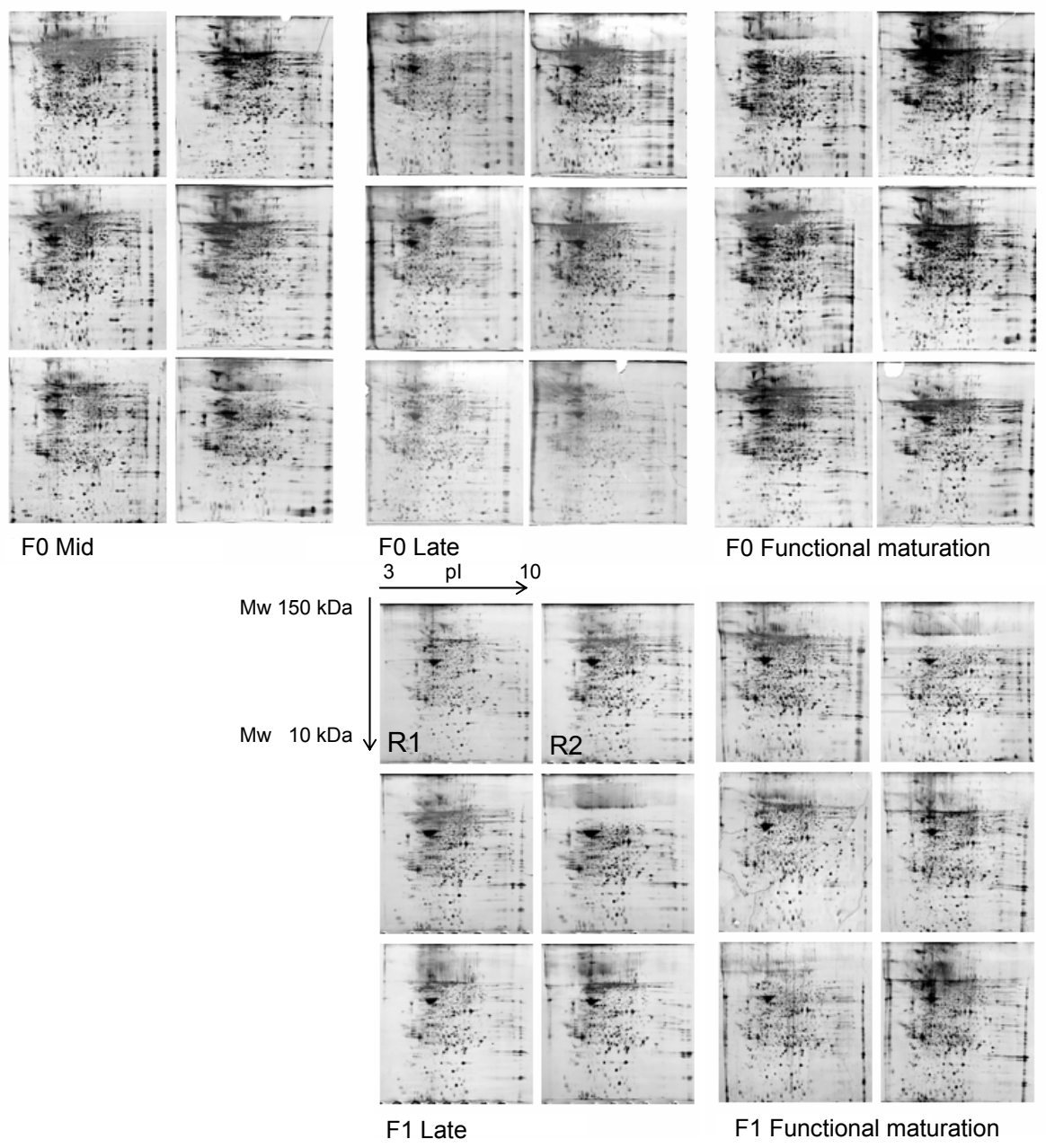

Figure 2.4.- Two dimensional electrophoresis gels obtained from Senegalese sole testis. Each sample was analysed twice. In the figure, these duplicates (R1, R2) are placed one next to the other inside each group of six gels with the same state. 2-DE separation was carried out in the 3-10 range of *pI* and in the 10-150 kDa range for *Mw*. The specimen code is, top to bottom in each group: F0 Mid = 4, 10, 12; F0 Late = 1, 2, 3; F0 Functional maturation = 6, 7, 11; F0 Late 2F8E, 13C9, 149F; F1 Functional maturation = L77; L5530, L55.

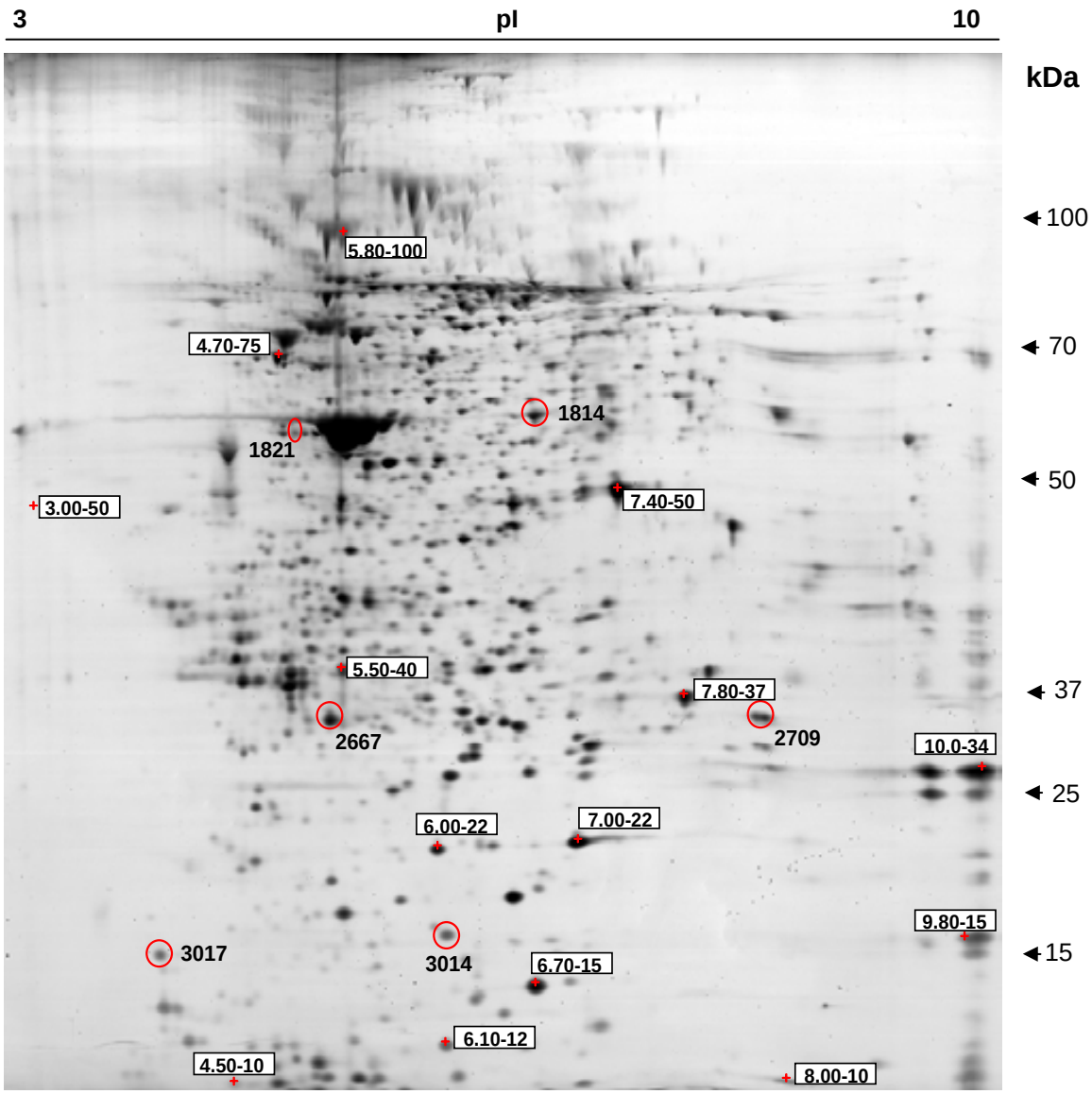

Figure 2.5.- Reproducibility of gel analysis: *Mr* and *pI* variations across the experiment. The variation of *Mr* and *pI* coordinates of six spots (in red circles: 1821, 1814, 2667, 2709, 3017 and 3014) was studied during the experiment (figure 2.6). Coordinates were calculated relative those 10 reference spots (indicated in the white squares as *Mr-pI* pairs).

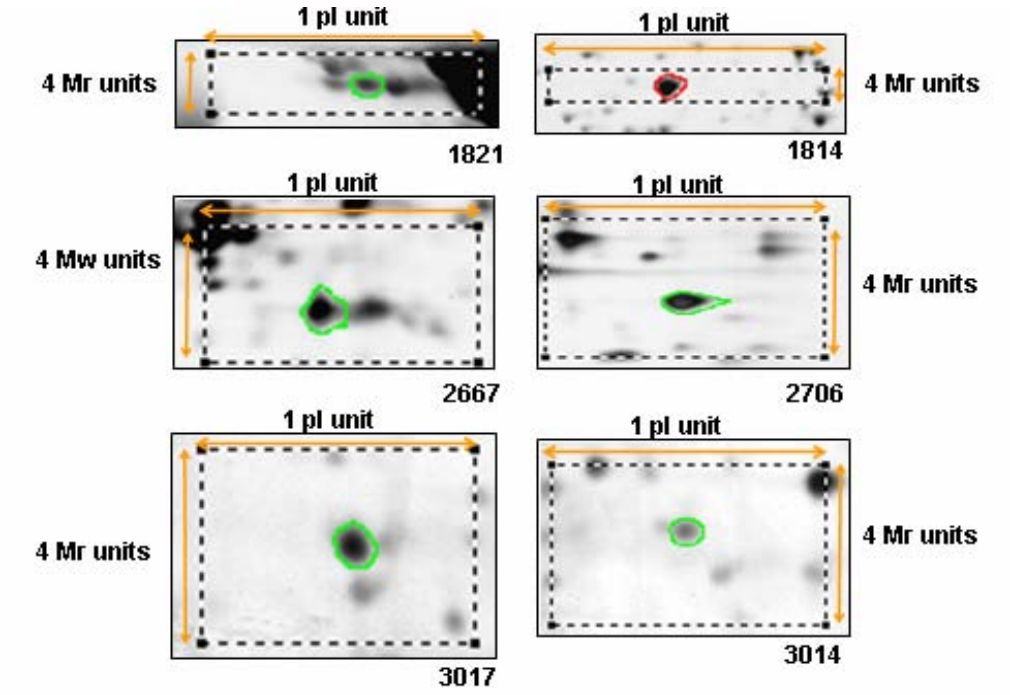

	Mr			*pI*		
Group ID	**Mean**	**SD**	**CV**	**Mean**	**SD**	**CV**
1821	61,5	2,2	4,7	4,7	0,07	0,01
1814	61,7	2,5	6,3	6,7	0,04	0,00
2667	37,0	0,5	0,2	5,3	0,03	0,00
2709	36,1	0,3	0,1	8,5	0,05	0,00
3014	17,8	0,4	0,1	6,1	0,09	0,01
3017	17,1	0,3	0,1	3,7	0,12	0,01

Figure 2.7.- Reproducibility of gel analysis. Top: Gel image areas containing the six selected spots are depicted indicating 4 *Mr* units wide and 1 *pI* unit high reference window. Bottom: The mean, the standard deviation (SD), and the variation coefficient (CV) of *Mr* and *pI* values for these spots in the 30 performed gels.

Table 2.4 *Part A*.- Protein abundance changes for the spots submitted to protein identification. Δ: variation value. Variation was calculated as vali/valj where vali=max (val1, val2) and valj=min (val1, val2). Variation is indicated as a positive value in case of overexpression and as a negative value in case of subexpression. Abundance changes higher than 2 fold are highlighted in yellow. Changes with confidence higher than 95% are indicated in bold; *T-test*: t-test value; *p*>: probability in percentage of obtaining the observed difference not because of stochastic variation (only probabilities <95% are described); Number code (NC): Group for each variation as explained in figure 2.8.

Spot	Prot ID	F0M - F0L		F0L - F0Mat		F0M - F0Mat		NC
		T-test / p >	Δ	T-test / p >	Δ	T-test / p >	Δ	
1942	Phosphoserine aminotransferase 1	0,5	+1,1	1,8	+1,6	**2,9 / 99**	+1,7	3
1963	Olfactory receptor Olr653	**4,3 / 99,5**	**-3,8**	**3,3 / 99,5**	**+2,5**	0,6	-1,5	2
1966	Serine (or cysteine) proteinase inhibitor	0,7	-1,4	0,1	-1,0	0,7	-1,4	4
2006	No ID	**2,3 / 95**	+1,6	**3,1 / 99**	-19	1,1	-1,2	1
2055	Isocitrate dehydrogenase 3 (NAD+) alpha	0,1	+1,0	0,1	-1,0	0,04	-1,0	0
2126	Malate dehydrogenase 1	0,4	+1,1	0,01	1,0	0,3	+1,1	0
2174	Polymerase (RNA) II (DNA directed) polypeptide C	**2,2 / 95**	**-2,2**	1,4	+1,5	0,8	-1,4	2
2176	Acidic ribosomal phosphoprotein P0	**3,6 / 95**	**+23,5**	1,6	**-26,6**	0,4	-1,1	1
2243	Uridine phosphorylase 1	0,9	+1,3	0,1	+1,0	0,5	-1,3	4
2275	Pyruvate dehydrogenase E1-beta subunit	**2,5 / 95**	**+2,3**	**2,8 / 99**	**-2,6**	0,3	-1,1	1
2339	Hydroxysteroid (17-beta) dehydrogenase 4	0,04	-1,0	0,6	-1,2	1,0	-1,2	0
2436	No ID	**2,5 / 95**	**-4,6**	1,4	-1,8	**3,4 / 99,5**	**-7,8**	6
2499	14-3-3 protein	0,5	+1,3	1,7	-2,0	1,12	-1,6	1
2521	6-phosphogluconolactonase	**3,2 / 99**	-1,6	**2,7 / 95**	+1,5	0,7	-1,1	2
2578	Carbonic anhydrase	0,8	+1,1	0,3	-1,1	0,4	+1,1	0
2587	Purine-nucleoside phosphorylase or Proteasome subunit alpha	1,4	+1,3	**5,8 / 99,9**	1,0	2,6	+1,3	1
2591	Carbonic anhydrase	0,8	+1,3	0,1	-1,2	0,8	+1,1	1
2603	Methionine sulfoxide reductase A	1,2	-1,3	**4,0 / 99,5**	**+3,6**	**3,2 / 99**	**+2,8**	2
2650	Glutathione S-transferase	1,1	+1,4	0,2	+1,1	2,8	+1,5	5
2667	Ubiquitin C-terminal hydrolase	**3,1 / 99**	-1,6	**3,5 / 99,5**	+1,8	0,5	+1,1	2
2685	Glutathione peroxidase	1,0	-1,3	**3,1 / 99**	+1,8	1,0	+1,5	2
2686	No ID	1,1	+1,9	**9,0 / 99,9**	**-3,6**	**2,0/ 95**	-1,9	1
2696	No ID	1,1	+1,2	**3,3 / 99,5**	-1,5	1,8	-1,3	1
2717	No ID	**3,1 / 99**	+1,7	**2,6 / 95**	-2,0	0,6	-1,1	1
2723	Peroxiredoxin 3 or Translin	0,1	+1,0	0,5	-1,1	0,4	-1,1	0
2738	Proteasome subunit beta	**2,4 / 95**	+1,4	**3,4 / 99,5**	-1,6	1,4	-1,2	1
2759	Apolipoprotein A-IV4	0,6	-1, 7	0,5	-1,4	0,9	**-2,3**	0
2778	Proteasome beta 4 subunit	**1,8 / 95**	+1,5	**2,5 / 95**	-1,5	0,1	-1,0	1
2784	No ID	0,5	-1,6	0,4	-1,5	0,7	**-2,3**	0
2820	No ID	**2,3 / 95**	+1,4	**2,7 / 95**	-1,4	0,3	+1,0	1
2837	Heterochromatin-specific nonhistone protein	**2,3 / 95**	**-6,4**	**2,0 / 95**	**+5,2**	0,2	-1,2	2
2877	Histidyl-tRNA synthetase	**3,4 / 99,5**	-1,5	**2,1 / 95**	+1,3	0,1	-1,2	2
2897	Cofilin	**12,4 / 99,9**	**-10,7**	**12,2 / 99,9**	**+9,5**	0,3	-1,1	2

Table 2.4 *Part A* (continuation).- Expression changes for the spots submitted to protein ID.

Spot	Prot ID	F0M - F0L		F0L – F0Mat		F0M - F0Mat		NC
		T-test / p >	Δ	T-test / p >	Δ	T-test / p >	Δ	
2898	Cofilin 2	0,4	+1,4	**3,1 / 99**	**-2,0**	**2,3/ 95**	-1,4	1
2908	Myosin regulatory light chain 2	1,4	+1,7	**3,2 / 99**	+1,9	0,3	+1,1	2
2909	Unnamed protein product	0,3	+1,2	**3,9 / 99,5**	**-2,1**	**3,5 / 99,5**	-1,7	1
2912	No ID	0,2	-1,1	0,5	-1,2	0,8	-1,3	6
2918	Myosin light chain	**1,8 / 95**	+1,9	**2,7 / 95**	**+2,2**	0,3	+1,1	2
2972	Cofilin 2	**10,5 / 99,9**	**-∞**	**8,7 / 99,9**	**+18,8**	1,0	**-∞**	2
3013	Transgelin 2	**4,0 / 99,5**	**+4,3**	**6,5 / 99,9**	**-4,6**	0,4	-1,1	1
3022	No ID	**5,0 / 99,9**	**-2,3**	**4,9 / 99,9**	**+2,1**	0,4	-1,1	2
3089	Nucleoside diphosphate kinase	0,9	+1,1	0,9	-1,2	0,5	-1,1	0
3122	Myosin light chain alkali	**3,6 / 99,5**	**-3,6**	**3,9 / 99,5**	**+2,4**	0,7	-1,5	2
3159	Myosin alkali light chain 6	1,8	-1,4	**4,9 / 99,9**	**+3,8**	0,8	**+2,8**	2
3233	Profilin 2 or Cytochrome c oxidase Vb	1,2	+1,3	**3,7 / 99,5**	+1,8	1,1	+1,4	2
3649	Apolioprotein A1 or Serin protease 35	0,6	+1,3	1,0	-1,6	0,4	-1,2	1
3675	No ID	1,6	+1,5	1,6	-1,7	0,4	-1,1	1
3676	No ID	0,5	+1,3	**2,2 / 95**	**+7,0**	**2,5 / 95**	**+8,9**	3
3690	Proteasome subunit alpha	**2,6 / 95**	+1,9	**2,2 / 95**	-1,8	0,4	-1,1	1

Table 2.4 *Part B*.- Expression changes for the spots submitted to protein ID. See "*Part A*" for legend.

Spot	Prot ID	F1L - F1Mat			F0L- F1L			F0Mat - F1 Mat		
		T-test / p >	Δ	NC	T-test / p >	Δ	NC	T-test / p >	Δ	NC
1942	Phosphoserine aminotransferase 1	1,6	+1,3	1	0, 8	+1,2	2	0,2	-1,0	0
1963	Olfactory receptor Olr653	**2,7 / 95**	**-3,1**	2	0,9	**+4,6**	2	1,5	-1,7	1
1966	Serine (or cysteine) proteinase inhibitor	**2,5 / 95**	+1,3	1	**4,6 / 99,9**	**-2,3**	1	**2,8 / 99**	-1,7	1
2006	No ID	**3,6 / 99,5**	**-3,7**	2	**3,3 / 99,5**	**+4,2**	2	**4,1 / 99,5**	**+2,1**	2
2055	Isocitrate dehydrogenase 3 (NAD+) alpha	**3,4 / 99,5**	**+2,1**	1	**3,1 / 99**	**-2,6**	1	0,7	-1,2	1
2126	Malate dehydrogenase 1	**5,3 / 99,9**	+1,8	1	**5,5 / 99,9**	**-2,7**	1	**1,8 / 95**	-1,5	1
2174	Polymerase (RNA) II (DNA directed) polypeptide C	**5,1 / 99,9**	**-7,0**	2	**2,5 / 95**	**+7, 7**	2	1,4	-1,4	1
2176	Acidic ribosomal phosphoprotein P0	0,1	-1,1	2	**9,3 / 99,9**	**-31,1**	1	**1,9 / 95**	-1,3	1
2243	Uridine phosphorylase 1	**3,8 / 99,5**	**+2,1**	1	**3,8 / 99,5**	**-3,1**	1	1,3	-1,6	1
2275	Pyruvate dehydrogenase E1-beta subunit	**5,0 / 99,9**	**+4,2**	1	**2,0 / 95**	**-4,1**	2	**3,1 / 99**	**+2,6**	2
2339	Hydroxysteroid (17-beta) dehydrogenase 4	0,02	1,00	0	1,5	+1,6	2	**3,3 / 99,5**	**+2,0**	2
2436	No ID	1,2	+1,9	1	0,9	+1,5	2	**3,0 / 99**	**+4,7**	2
2499	14-3-3 protein	**5,2 / 99,9**	**+3,5**	1	0,3	**-2,2**	2	**2,8 / 99**	**+3,2**	2
2521	6-phosphogluconolactonase	1,4	-1,5	2	**2,6 / 95**	+1,8	2	1,0	-1,2	1
2578	Carbonic anhydrase	**5,2 / 99,9**	**-2,5**	2	0,9	+1,3	2	**3,1 / 99**	-1,7	1
2587	Purine-nucleoside phosphorylase or Proteasome subunit alpha	1,0	-1,2	2	**2,6 / 95**	-1,4	1	1,1	-1,6	2
2591	Carbonic anhydrase	**4,5 / 99,9**	**+2,1**	1	1,4	-1,3	2	**2,0 / 95**	+1,9	2
2603	Methionine sulfoxide reductase A	0,8	-1,2	2	**2,6 / 95**	+1,6	2	**2,5 / 95**	**-2,7**	1
2650	Glutathione S-transferase	1,1	-1,4	2	1,0	-1,4	1	**3,7 / 99,9**	**-2,2**	1
2667	Ubiquitin C-terminal hydrolase	1,4	-1,3	2	**2,5 / 95**	+1,5	2	**2,4 / 95**	-1,5	1
2685	Glutathione peroxidase	1,1	+1,2	1	1,1	-1,3	1	**4,7 / 99,9**	-1,9	1
2686	No ID	0,2	+1,1	0	1,6	**-2,1**	1	**2,5 / 95**	+1,8	2
2696	No ID	0,4	-1,1	0	**1,9 / 95**	-1,8	1	1,2	-1,3	1
2717	No ID	0,5	-1,2	0	**1,9 / 95**	**-2,1**	1	1,1	-1,2	1
2723	Peroxiredoxin 3 or Translin	**2,8 / 99**	+1,7	1	**4,7 / 99,9**	**-2,1**	1	0,9	-1,2	1
2738	Proteasome subunit beta	0,8	+1,1	1	1,4	-1,2	0	**3,0 / 99**	+1,4	2
2759	Apolipoprotein A-IV4	1,4	-1,3	2	**3,7 / 99,5**	**-9,8**	1	**15,0 / 99,9**	**-9,6**	1
2778	Proteasome beta 4 subunit	**3,7 / 99,5**	+1,6	1	**2,1 / 95**	**-2,0**	2	1,4	+1,2	2
2784	No ID	**4,6 / 99,5**	**-15,1**	2	1,3	**+3,7**	2	**2,1 / 95**	**-2,8**	1
2820	No ID	**2,6 / 95**	+1,5	1	**4,3 / 99,9**	-1,9	1	0,3	+1,0	0
2837	Heterochromatin-specific nonhistone protein	**4,4 / 99,9**	**-6,4**	2	**2,0 / 95**	**+5,2**	2	**4,4 / 99,9**	**-6,5**	1
2877	Histidyl-tRNA synthetase	**2,2 /95**	**-2,1**	2	**3,0 / 99**	**+2,5**	2	1,1	-1,1	0

Table 2.4 *Part B* (continuation).- Expression changes for the spots submitted to protein ID. See "*Part A*" for legend.

Spot	Prot ID	F1L - F1Mat			F0L- F1L			F0Mat - F1 Mat		
		T-test / p >	Δ	NC	T-test / p >	Δ	NC	T-test / p >	Δ	NC
2897	Cofilin	0,4	-1,1	2	0,4	+1,1	0	**6,2 / 99,9**	**-9,7**	1
2898	Cofilin 2	**2,5 /95**	+1,4	1	**2,4 / 95**	-1,6	1	**3,2 / 99**	+1,7	2
2908	Myosin regulatory light chain 2	1,6	-1,4	2	**2,7 / 95**	+1,8	2	**2,0 / 95**	-1,5	1
2909	Unnamed protein NCBI gi|47218822	0,9	-1,1	2	0,9	-1,2	1	**2,7 / 99**	+1,5	2
2912	No ID	**4,2 /99,9**	**$-\infty$**	2	**3,5 / 99,5**	**$+\infty$**	2	0,7	+1,3	2
2918	Myosin light chain	**2,9 / 99**	-1,6	2	**2,2 / 95**	+1,7	2	**3,3 / 99,5**	**-2,0**	1
2972	Cofilin 2	0,6	-1,2	2	**2,3 / 95**	+1,6	2	**4,4 / 99,9**	**-14,1**	1
3013	Transgelin 2	1,2	-1,6	2	0,7	-1,3	0	**3,2 / 99,5**	**+2,2**	2
3022	No ID	0,2	-1,0	0	**5,9 / 99,9**	**+2,2**	2	0,2	+1,0	0
3089	Nucleoside diphosphate kinase	1,5	+1,2	1	**4,7/ 99,9**	-1,6	1	0,8	-1,2	0
3122	Myosin light chain alkali	**6,6 / 99,9**	**-2,5**	2	**2,5 / 95**	+1,5	2	**7,5 / 99,9**	**-3,9**	1
3159	Myosin alkali light chain 6	**2,6 / 95**	-1,9	2	**3,1/ 99**	**+2,3**	2	**4,7 / 99,9**	**-3,3**	1
3233	Profilin 2 or Cytochrome c oxidase Vb	**2,2 / 95**	-1,2	2	0,2	+1,7	2	**4,8 / 99,9**	+1,2	1
3649	Apolioprotein A1 or Serin protease 35	**8,6 / 99,9**	**+2,4**	1	**4,2 / 99,9**	**-3,8**	1	0,01	1,0	0
3675	No ID	**5,3 / 99,9**	**+5,1**	1	1,7	-1,7	1	**4,2 / 99,9**	**+5,1**	2
3676	No ID	0,5	**-2,0**	0	**2,2 / 95**	**+6,0**	2	0,5	**-2,4**	1
3690	Proteasome subunit alpha	**11,0 / 99,9**	**$+\infty$**	1	**2,3 / 95**	-1,7	1	**7,1 / 99,9**	**$+\infty$**	2

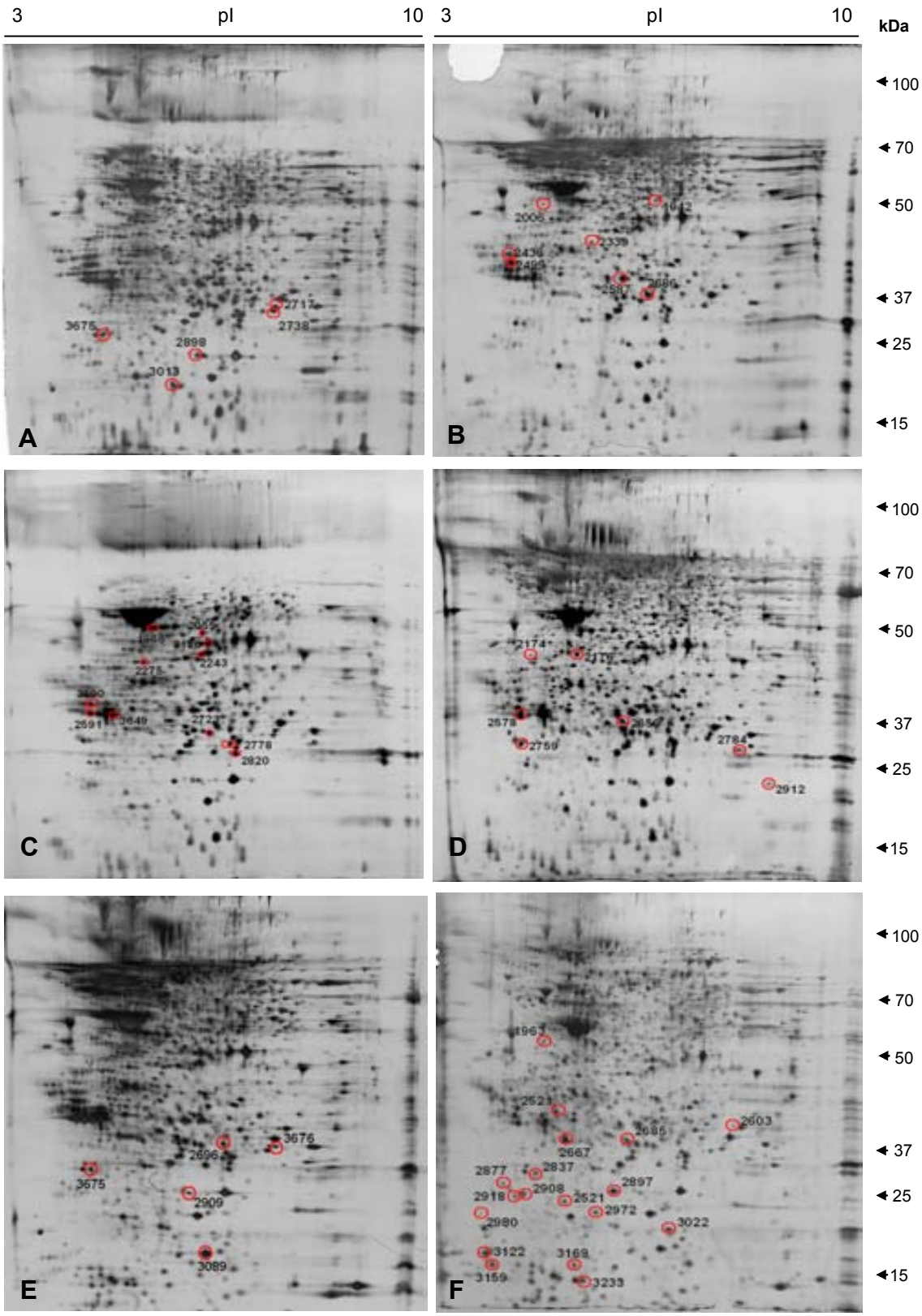

Figure 2.8.- Differential spots excised for identification in the spermatogenesis studies (A:04_150904; B: 06_160904; C: 02_160904; D: 01_210305; E: 05_060605; F: 05_060605)

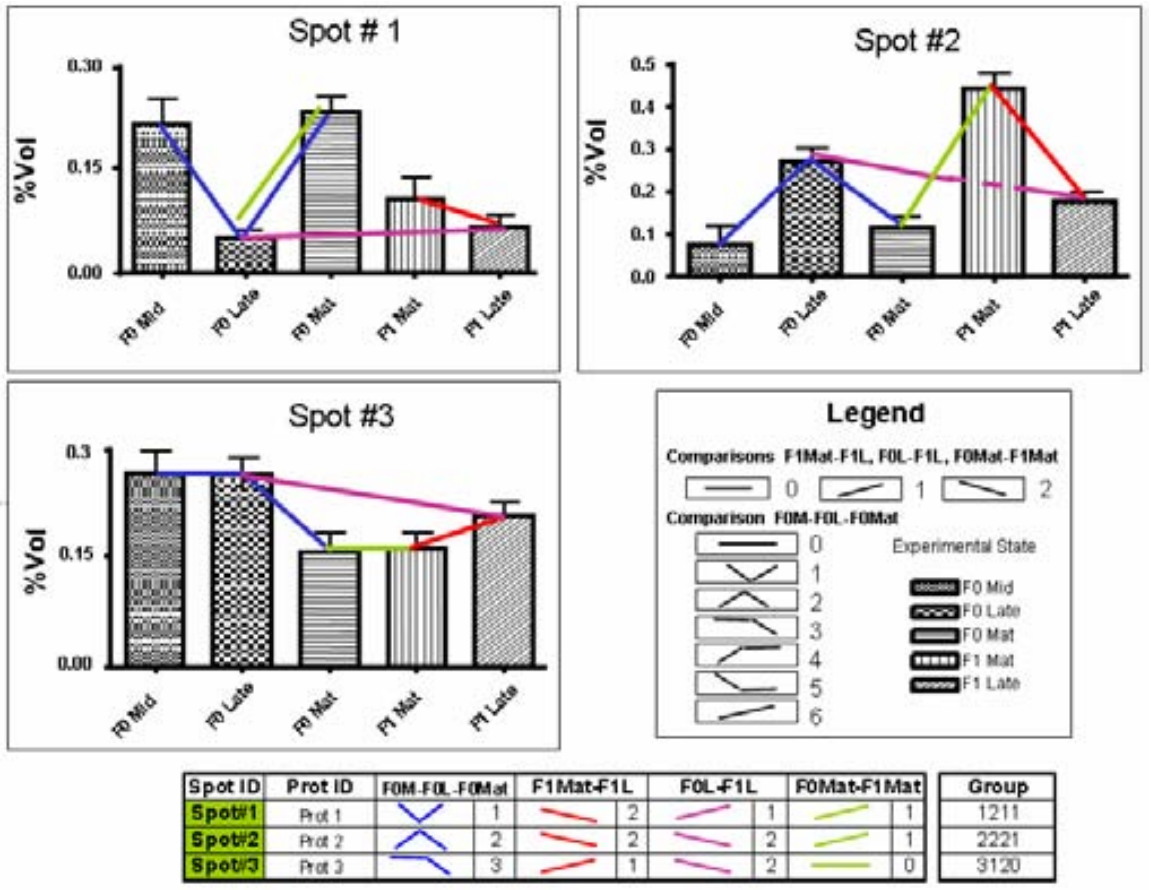

Spot ID	Prot ID	F0M-F0L-F0Mat		F1Mat-F1L		F0L-F1L		F0Mat-F1Mat		Group
Spot#1	Prot 1		1		2		1		1	1211
Spot#2	Prot 2		2		2		2		1	2221
Spot#3	Prot 3		3		1		2		0	3120

Figure 2.9.- Classification of spots relative to their protein abundance profile along the stages of development. The five %Vol data from each spot submitted to protein identification were arranged into a bar diagram. The comparisons between experimental states are represented with a line (blue for F0M- F0L - F0Mat; red for F1 L- F1M; purple for F0 L-F1 L; green for F0Mat-F1Mat). These lines are connecting the bars corresponding to the experimental groups considered in each comparison, showing graphically the relationship between them. A number is assigned to each line profile (Legend). The combination of the four numbers assigned to each bar diagram constitutes the code of the group in which every spot is classified on Figure 2.10. The examples in the figure represent spot#1, spot#2 and spot#3, classified in group 1211, 2221 and 3120 respectively (F0 = wild; F1= cultured; M= Mid; L=Late; Mat = Functional maturation).

Table 2.5.- Classification of proteins depending on their expression behaviour in the four comparisons. Spots chosen for mass spectrometry identification after image analysis were classified as described in figure 2.9. Comparison codes: (0) No significant differences between state A relative to state B; (1) Increase between state A relative to state B; (2) Decrease between state A relative to state B; The comparisons between spots in mid, late and functional maturation F0 gels were analysed together, giving four new patterns which were assigned to 3, 4, 5 and 6 (figure 2.9).

Spot ID	Prot ID	COMPARISON				Group Class
		F0M-F0L-F0Mat	F0Mat- F0L	F0L-F1L	F0Mat- F1 Mat	
2339	Hydroxysteroid (17-beta) dehydrogenase 4	0	0	2	2	**0022**
3089	Nucleoside diphosphate kinase	0	1	1	0	**011X**
2055	Isocitrate dehydrogenase 3 (NAD+) alpha	0	1	1	1	
2126	Malate dehydrogenase 1	0	1	1	1	
2723	Peroxiredoxin 3 or Translin	0	1	1	1	
2759	Apolipoprotein A-IV4	0	2	1	1	**02X1**
2578	Carbonic anhydrase	0	2	2	1	
2784	No ID	0	2	2	1	
2717	No ID	1	0	1	1	**101X**
2696	No ID	1	0	1	1	
2686	No ID	1	0	1	2	
3649	Apolioprotein A1 or Serin protease 35	1	1	1	0	**1110**
2820	No ID	1	1	1	0	
2738	Proteasome subunit beta	1	1	0	2	**11X2**
2898	Cofilin 2	1	1	1	2	
3690	Proteasome subunit, alpha	1	1	1	2	
2275	Pyruvate dehydrogenase E1-beta subunit	1	1	2	2	
2499	14-3-3 protein	1	1	2	2	
2591	Carbonic anhydrase	1	1	2	2	
2778	Proteasome beta 4 subunit	1	1	2	2	
3675	No ID	1	1	1	2	
2176	Acidic ribosomal phosphoprotein P0	1	2	1	1	**12XX**
2587	Purine-nucleoside phosphorylase or Proteasome subunit alpha	1	2	1	2	
2909	Unnamed protein NCBI gi|47218822	1	2	1	2	
3013	Transgelin 2	1	2	0	2	
2006	No ID	1	2	2	2	
3022	No ID	2	0	2	0	**2XXX**
2685	Glutathione peroxidase	2	1	1	1	

Table 2.5 (continuation).- Classification of proteins depending on their expression behaviour in the four comparisons.

Spot ID	Prot ID	COMPARISON				Group Class
		F0M-F0L-F0Mat	F0Mat- F0L	F0L-F1L	F0Mat- F1 Mat	
2877	Histidyl-tRNA synthetase	2	2	2	0	**2221**
2521	6-phosphogluconolactonase	2	2	2	1	
2603	Methionine sulfoxide reductase A	2	2	2	1	
2667	Ubiquitin C-terminal hydrolase	2	2	2	1	
2837	Heterochromatin-specific nonhistone protein	2	2	2	1	
2897	Cofilin	2	2	0	1	
2908	Myosin regulatory light chain 2	2	2	2	1	
2918	Myosin light chain	2	2	2	1	
3122	Myosin light chain alkali	2	2	2	1	
3159	Myosin alkali light chain 6	2	2	2	1	
3233	Profilin 2 or Cytochrome c oxidase subunit Vb	2	2	2	1	
2972	Cofilin 2	2	2	2	1	
1963	Olfactory receptor Olr653	2	2	2	1	
2174	Polymerase (RNA) II (DNA directed) polypeptide C	2	2	2	1	
3676	No ID	3	0	2	1	**3XXX**
1942	Phosphoserine aminotransferase 1	3	1	2	0	
1966	Serine (or cysteine) proteinase inhibitor	4	1	1	1	**4111**
2243	Uridine phosphorylase 1	4	1	1	1	
2650	Glutathione S-transferase	5	2	1	1	**5-6XXX**
2436	No ID	6	1	2	2	
2912	No ID	6	2	2	2	

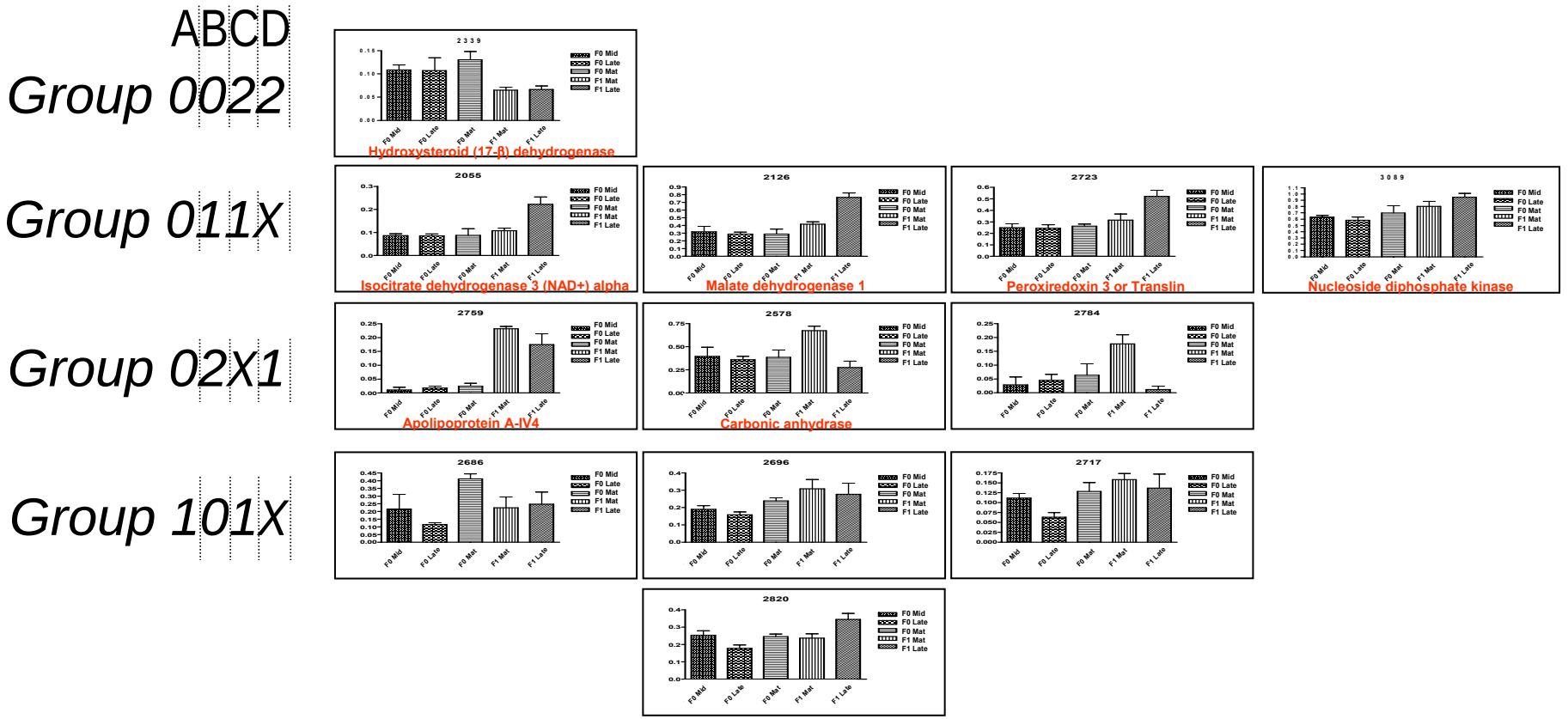

Figure 2.10.- Selected spots after differential expression analysis. The mean %Vol oif the spot in each studied state and its SD are displayed in each bar diagram, together with the name of the identified protein, when available. The bar diagrams are classified in several groups depending on the result of the comparisons made through the different states (see Figure 2.9). The symbol “X” in the code means that any code number is possible at that position. (Comparison A= F0MLMat, B=F1Mat-F1L, C=F0L-F1L, D=F0Mat-F1Mat; F0 = wild; F1= cultured; M= Mid; L=Late; Mat = Functional maturation)

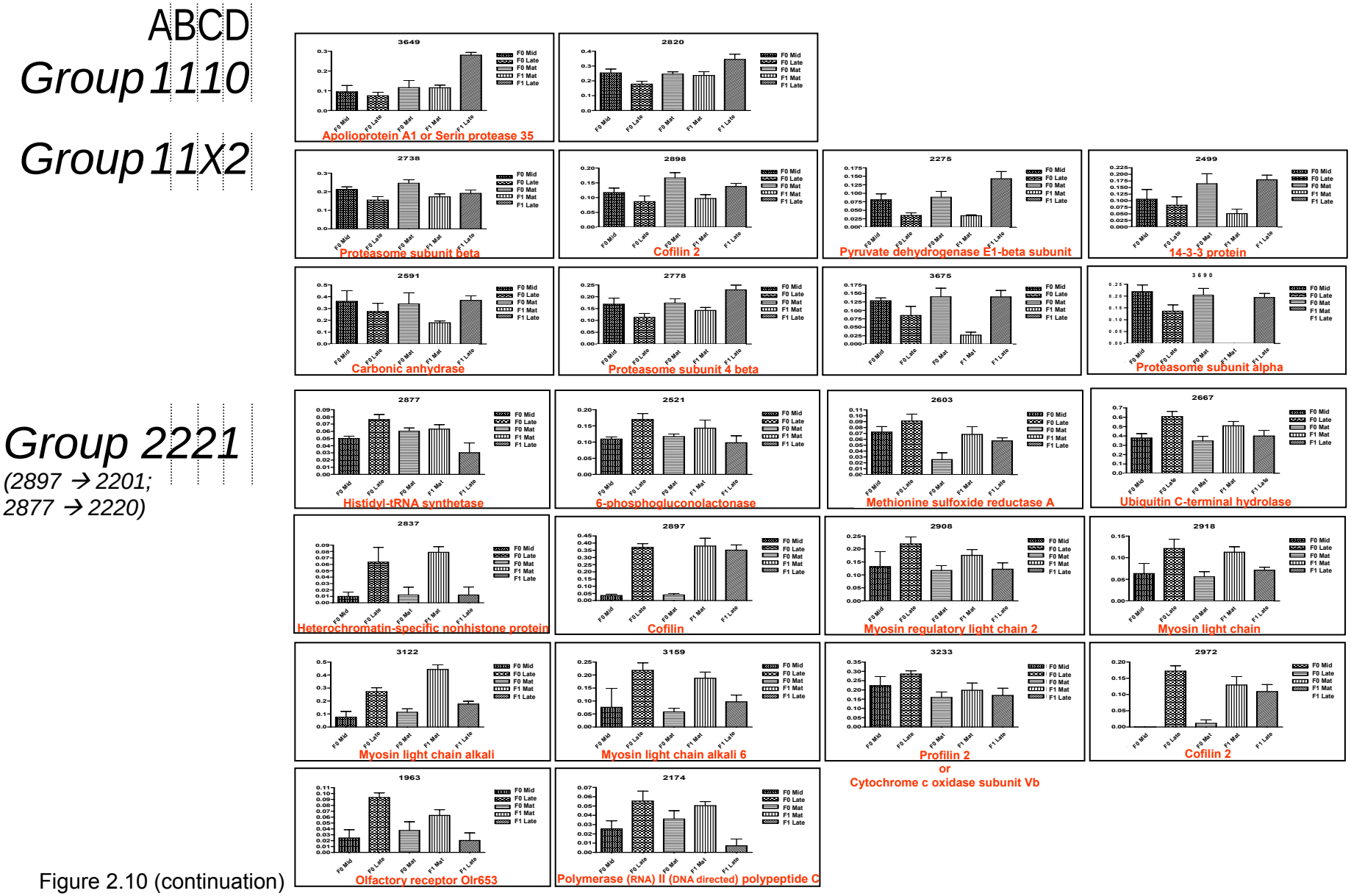

Figure 2.10 (continuation)

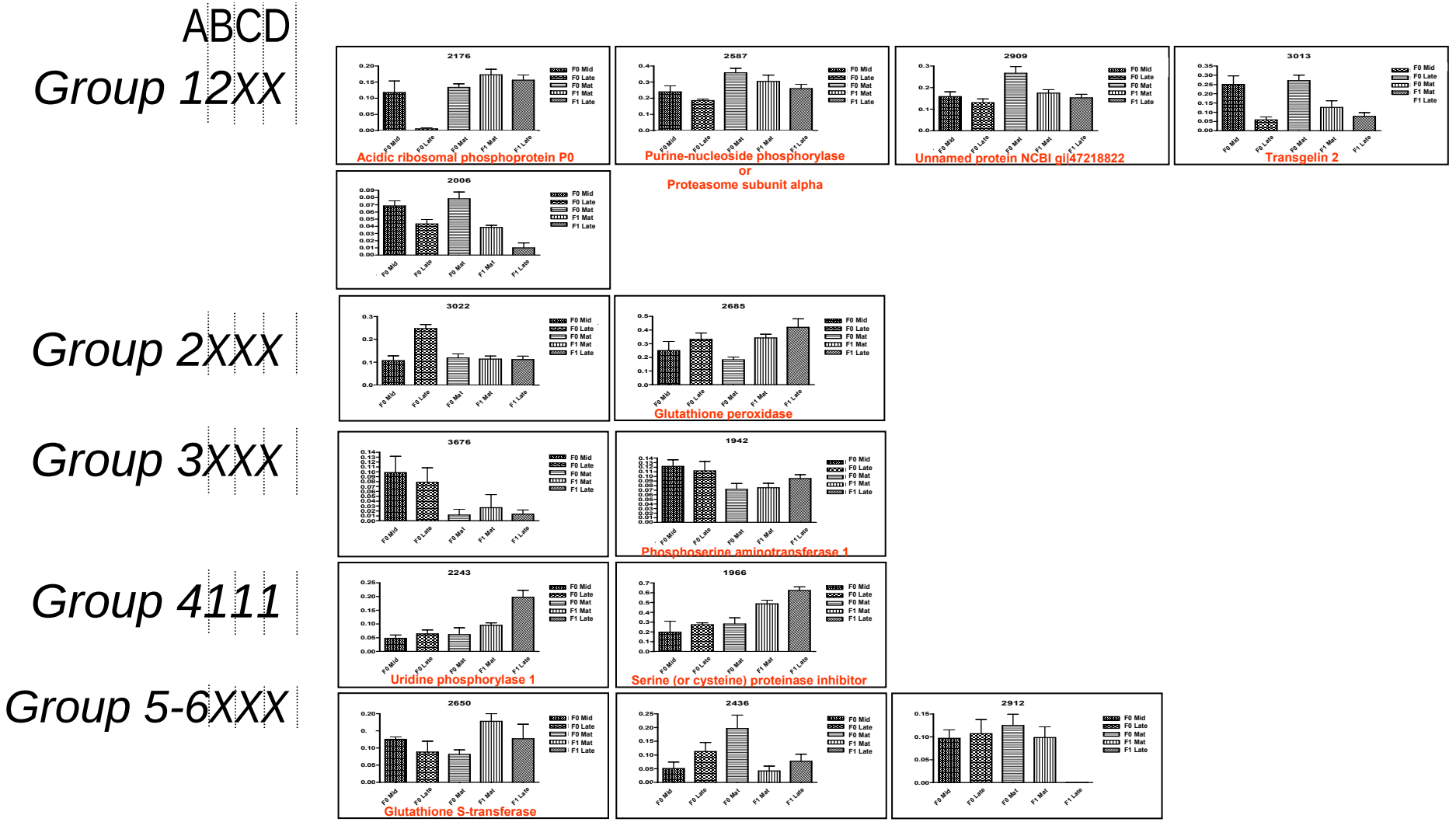

Figure 2.10 (continuation).

Normalized volume data of spots present in all gels along the spermatogenesis stages study was referred to F0Mat state values. Clustering of these expression data was performed with Cluster 3.0 and visualized with Java TreeView 1.0.7, unveiling six main subtrees of spots (figure 2.11). Identified proteins included in each subtree are described in table 2.6. Resulting classification of spots either in the manual or in the informatic clustering showed similar patterns of spot distribution (see colour legend in table 2.6). For instance, subtrees 1 and 2 included mainly spots from groups 2221, 2XXX and 3XXX of figure 2.10, while subtrees 5 and 6, present principally spots from groups 011X, 1110 and 11X2 of the same figure. From both clustering methods, manual approach (see fig 2.9) was used as a main guide to relate spots by their similar expression profile (informatic clustering used as confirmatory), when discussing biological function of spots with similar protein abundance patterns.

Table 2.6. MS/MS analyzed spots from 2-DE gels present in expression data clustering subtrees. Spots were highlighted to display the classification group in figure 2.10. *Legend* = : Groups 2221-2XXX-3XXX; : Groups 0022-101X-12XX-5-6XXX; : Group 4111; : Groups 011X-1110-11X2; : Group 02X1.

Subtree	Spots	Protein ID
1	1942, 2972, 3159, 2603, 2918, 2667, 2908, 2650, 2578	Phosphoserine aminotransferase 1, Cofilin 2, Myosin alkali light chain 6, Methionine sulfoxide reductase A, Myosin light chain, Ubiquitin C-terminal hydrolase, Myosin regulatory light chain 2, Glutathione S-transferase, Carbonic anhydrase.
2	1963, 2521, 3233, 3022, 2877, 2006	Olfactory receptor Olr653, 6-phosphogluconolactonase, Profilin 2 or Cytochrome c oxidase Vb, No ID, Histidyl-tRNA synthetase, No ID.
3	2685, 3122, 1966, 2759, 2176, 2717, 2696	Glutathione peroxidase, Myosin light chain alkali, Serine (or cysteine) proteinase inhibitor, Apolipoprotein A-IV4, Acidic ribosomal phosphoprotein P0, No ID, No ID.
4	3013, 2587, 2686, 2909, 2339, 2436, 2738,2898	Transgelin 2, Purine-nucleoside phosphorylase or Proteasome subunit alpha, No ID, Unnamed protein product, Hydroxysteroid (17-beta) dehydrogenase 4, No ID, Proteasome subunit beta, Cofilin 2
5	2275, 2243, 2723, 2055, 2126, 3649, 2820, 2778, 3089	Pyruvate dehydrogenase E1-beta subunit, Uridine phosphorylase 1, Peroxiredoxin 3 or Translin, Isocitrate dehydrogenase 3 (NAD+) alpha, Malate dehydrogenase 1, Apolioprotein A1 or Serin protease 35, No ID, Proteasome beta 4 subunit, Nucleoside diphosphate kinase
6	2499, 3675, 2591	14-3-3 protein, No ID, Carbonic anhydrase.

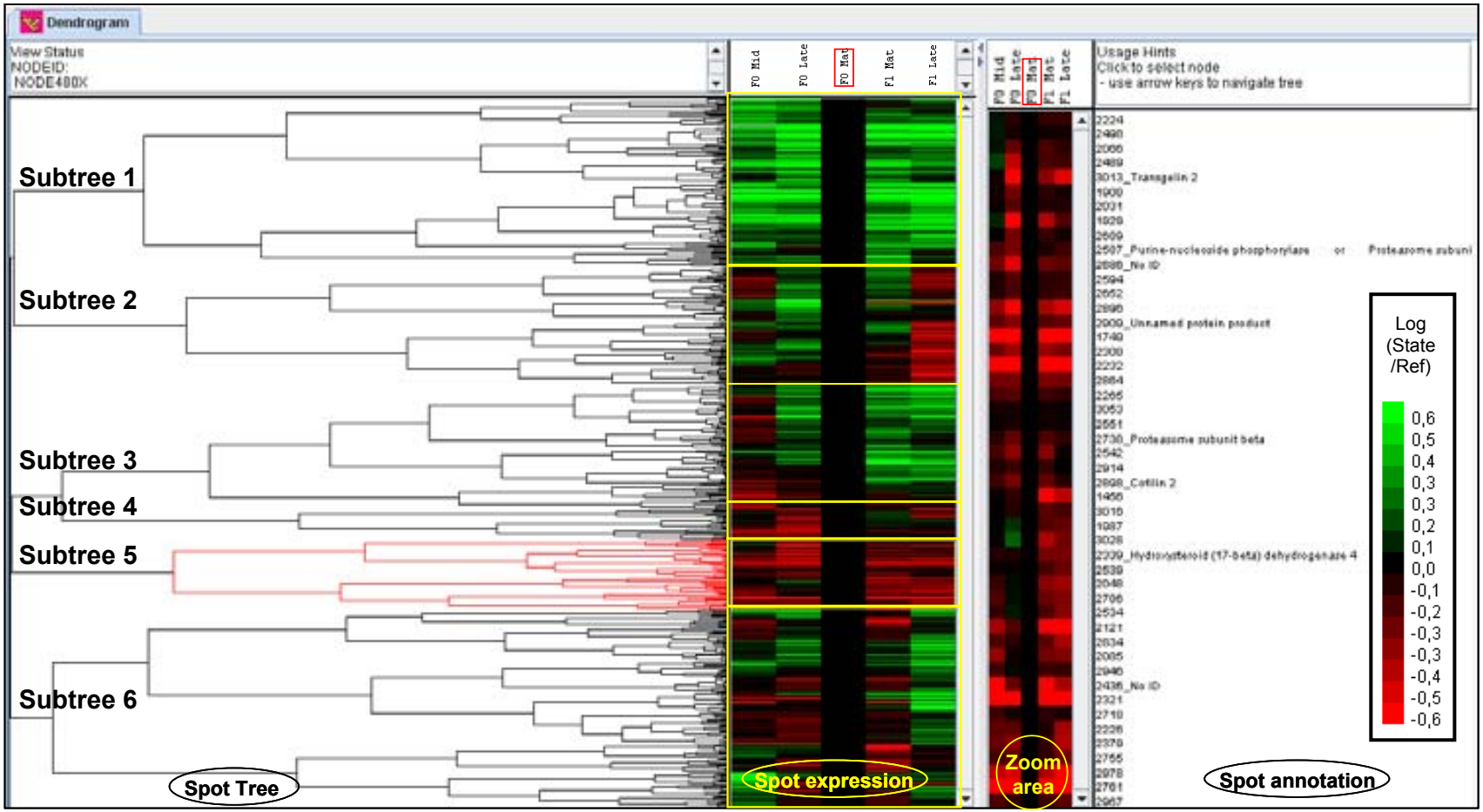

Figure 2.11.- Dendrogram of the spots present in all gels from the spermatogenic stage study. Six subtrees are visible from the “Spot tree“ panel. Relative spot expression to F0 Mat state (red squared) is displayed in the “Spot expression” panel, where Subtrees are divided by yellow lines. The “Zoom area” and “Spot annotation” panel are focused on the subtree 5. Spot belonging to this subtree are displayed with ID when available. Colour code: Green= overexpression; red= underexpression; black= no change.

2.2.4 Mass spectrometry and Bioinformatic analysis

The forty-nine excised spots were digested with trypsin and the resulting peptides analysed using tandem mass spectrometry. Spectra were processed by Peaks 2.4 and Lutefisk97. Resulting sequences were compared to NCBI database using BLAST, to determine the protein of origin (Table 2.7). Forty spots were correlated with described proteins, the other 9 spots could not be matched despite tandem mass spectra from 1-3 peptides could be produced for all of them. From the 40 correlated spots, only 4 produced ambiguous identifications pointing to more than one protein. Thirty-five assigned proteins were identified by homology of sequenced peptides to fish species (16 identifications from *Danio rerio*, 13 from *Tetraodon nigroviridis*, 3 from *Pseudopleuronectes americanus*, and 1 from *Oreochromis nilotilus*, *Takifugu rubripes* and *Fundulus heteroclitus,* respectively), while the missing identifications were assigned from other vertebrate species (2 identification from Mus *musculus*, 2 from *Pan trogolodytes and* 1 *from Homo sapiens*).

Peaks 2.4 provided more confident sequences than Lutefisk97. From 188 sequenced peptides, 104 were predicted more accurately by Peaks, while the other 84 were closely coincident between both *de novo* softwares. Even so, predictions of Lutefisk97 in some spots were of great utility to validate a candidate proposed after one Peaks sequence was analysed (spots 2126, 2499, 2685, 2778, 2908), or were fundamental for protein identification (spot 2909). Coverage of the identified proteins with the sequenced peptides used to assign the protein is detailed in Annex II.1.

Mr and *pI* values of each identified spot were calculated using Image Master Platinum 5.0 tools and the obtained result compared with the *Mr* and *pI* values given by Expasy tools. Deviation between both values, calculated as (Experimental value -Theoretical value) / (Experimental value + Theoretical value) for *Mr* value and as (Experimental value -Theoretical value) for *pI,* were observed for several spots (Annex II.2 - II.4). The significance of these variations will be discussed individually further down in combination with the number of peptides used for spot identification.

Table 2.7.- *De novo* peptide sequencing for protein identification in the analysis of spermatogenesis stages. *nESI-MS/MS*: Peptide sequences obtained from *de novo* sequencing of nESI-MS/MS data from trypsin digested spots (table 4) are displayed in two columns depending on the software used (Peaks 2.4 or Lutefisk 97). For Peaks characters, colours indicate probability (%) of the corresponding residue to be correct. (Red = 99-80%; Blue= 79-60%; Cyan= 59-40%; Black=<40%). Brackets in Lutefisk 97 column contain the mass in Da not assigned to any sequence. Rank-Score for Lutefisk97 indicates position of the candidate sequence within any individual de novo sequencing search and the probability of this sequence to be correct (values from 1 to 0, where 1 is maximum probability). *PROTEIN ID*: NCBI access number and name of the protein that was identified with each sequence using BLAST search for short nearly exact sequences (Sequence position inside the protein for each peptide in Annex II.1).

nESI-MS/MS					PROTEIN ID	
Spot ID	Peaks 2.4		Lutefisk 97		Acc Number	Name
	Sequence	Score %	Sequence	Rank-Score		
1942	NLGCAGVTVVLVR	47	[227,1]GCGAGVLSVLVR	1 0,970	gi|41053792	Phosphoserine aminotransferase 1
1963	LLNFLLLLSR	36	[226,1]NFPELLSR	1 0,613	gi|47577631	Olfactory receptor Olr653
1966	MGMVDAFDVAR	99	MGMVDAFDVAR	1 0,970	gi|47225177	Serine (or cysteine) proteinase inhibitor
	FDGLLGMAYPR	95	FDGLLGMAYPR	1 0,970	gi|27503926	----
	SYQFVEDFLGK	71	YSKFVEDFLGK	1 0,970	----	----
	GQTNFCLDLFK	35	[185,0]TNFCLDLFK	1 0,970	gi|13385352	Serine (or cysteine) proteinase inhibitor
	NNLVQGVLDNMTR	61	[227,1]NVKGVLDNMTR	1 0,970	----	----
	SSANSHPYRYVNK	3	[260,0]VY[319,2]PHSNAR	3 0,267	gi|68430931	----
	RACVPGLLLLAQHR	24	EPWRALNLHVVLR	2 0,394	----	----
	LNLNTWVESQTGKK	21	[226,2]LNTWVESKTK[185,1]	1 0,595	gi|27503926	Serine (or cysteine) proteinase inhibitor
	TTFSGMSPANDLVEANVVHK	67	TTFSGMS[168,1]NNNVLSNVVHK	1 0,631	gi|47225177	Serine (or cysteine) proteinase inhibitor
	LTCAPSGDTGTSLLTVLNWR	99	[213,1]MTPSGTDGTSLVDVLYHR	1 0,922	gi|45382395	----
	VKCADEFPNMNDELMEWKK	40	----	----	----	----
2006	LVLTLVGELPPKDR	79	[324,3]TLVGEPLVKD[154,1]	1 0,444	----	----
	CDMEDGPNVSGWNWK	93	[258,0]WTEVMLSGVSGNTR	1 0,565	----	----

Table 2.7 (continuation).- *De novo* peptide sequencing for protein identification in the analysis of spermatogenesis stages.

nESI-MS/MS					PROTEIN ID	
Spot ID	Peaks 2.4		Lutefisk 97		Acc Number	Name
	Sequence	Score %	Sequence	Rank-Score		
2055	LANYAFEYAR	72	ALNYAFEYAR	1 0,404	gi|47225844	Isocitrate dehydrogenase 3 (NAD+) α
	NLETACFDTLR	88	ARETACFDTLR	1 0,970	gi|47225845	Isocitrate dehydrogenase 3 (NAD+) α
	TPYTDVNLVTLR	99	[197,4]YTDVNLVT[269,0]	1 0,705	gi|47225845	Isocitrate dehydrogenase 3 (NAD+) α
	DWRTLLYYLGAHKMMMTK	22	----	----	----	----
	WMRTHGYGGGSGGFGSASSNMWEER	37	----	----	----	----
2126	DPVVGNPANTNCLLNR	1	YFVGDPALTNCLLAAK	2 0,702	gi|37362242	Malate dehydrogenase 1
	NNLPTFDGWRR	39	[228,0]LPTATVGS[274,0]K	1 0,604	----	----
	QCNSGYTGSMPR	15	[228,0]WALLVGSMPR	4 0,970	gi|37362242	Malate dehydrogenase 1
	DPDGLSLNDFSR	5	LVDGLSLFGDATK	3 0,495	gi|37362242	Malate dehydrogenase 1
2174	HPAPTAGVSFEYDDPYYK	96	----	----	gi|47221930	Polymerase (RNA) II (DNA directed) polypeptide C
2176	TSFFQALVATTK	32	[188,0]FFKALGLCVA	1 0,604	gi|63650325	Acidic ribosomal phosphoprotein P0
	VVNAPCDVTVCHLTGLLAAR	99	WKLSNLLKARTVPDCAHR	1 0,281	gi|63650325	Acidic ribosomal phosphoprotein P0
2243	FVCTGGSAWR	53	[246,0]CTGTNWR	1 0,769	----	----
	ESLDGMFQPR	40	SELDGMFKPR	2 0,288	----	----
	VQVCVTLLDR	51	[226,1]VCVTLLDR	1 0,628	gi|20071298	Uridine phosphorylase 2
	TTYPNLCAGTDR	99	[201,0]YPGGNCAGTNR	1 0,515	gi|6678515	Uridine phosphorylase 2
	RGDLDQGLAEELLK	40	LVDLDKGNAEKLLK	1 0,730	gi|47225480	Uridine phosphorylase 2
	FLFGWGPRGSGWGNTR	99	LYLGWGSLLTGGEGDTR	1 0,628		----
2275	VVSPWNAEDVK	56	KRPWNAEDAR	2 0,505	gi|47210341	Pyruvate dehydrogenase E1-beta
	LLEDNSVPLQK	28	[225,2]EDNSVPKLK	4 0,450	gi|47210341	Pyruvate dehydrogenase E1-beta
	QAGVDHPLSLPR	21	PTGVVE[234,1]DVA[168,1]	1 0,215	----	----
	EGLECEVLNLR	1	NAT[142,0]CEVLNLR	1 0,642	gi|47210341	Pyruvate dehydrogenase E1-beta
	LMEGPAFNYLDAPVTR	2	LMKGPAFNYLDAVEPK	1 0,812	gi|47210341	Pyruvate dehydrogenase E1-beta
	MMLLGEEVAQYDQYK	44	[210,2]VKNYKAVEEGLNDK	2 0,768	gi|47210341	Pyruvate dehydrogenase E1-beta
	YTYMASGLQTVPLVFR	99	[264,1]GVH[158,0]DKRV[210,2]VFR	1 0,601	gi|47210341	Pyruvate dehydrogenase E1-beta
	DSTDNPNDNSGLERDER	99	----	----	----	----
	YEMSQSEMGFTGLAVGSAWWR	37	[214,1]FANASGVALGTFGMKSNP[253,2]R	1 0,691	gi|47210341	Pyruvate dehydrogenase E1-beta

Table 2.7 (continuation).- *De novo* peptide sequencing for protein identification.

nESI-MS/MS						PROTEIN ID	
Spot ID	Peaks 2.4		Lutefisk 97			Acc Number	Name
	Sequence	Score %	Sequence	Rank	Score		
2339	YEALAFAER	49	[292,1]ALAFAER	1	0,724	gi|31982273	Hydroxysteroid (17-beta) dehydrogenase 4
	TQFADLAGHGR	37	PKKAALVSFGR	1	0,570	----	----
	NNVVVMPAGLLR	72	ARVVVDLAGLLR	1	0,802	----	----
	LLGLGLSQSLALEGR	50	A[212,1]LGLSNTLALEGR	1	0,970	gi|31982273	Hydroxysteroid (17-beta) dehydrogenase 4
	SGMNHEVPELHEHR	38	[276,1]NHELTDTNCHR	1	0,291	----	----
	SSMSTSDLDGEDLLRK	99	[173,8]MSTSDLDGEDLL[128,0]R	2	0,960	gi|47220435	----
2436	NSPLQTQHR	15	[202,0]PLSYDER	1	0,532	----	----
	MATLLMQLLR	74	MATPKMLELR	2	0,731	gi|20071768	----
	FAKRDGAEYEK	56	----		----	----	----
2499	SSLELMQLLR	99	[174,0]LELMKPER	1	0,888	----	----
	EAAENSLVAYK	11	[200,0]AENSLVAYK	1	0,872	gi|60416167	14-3-3 protein
	SMAAYKDALSR	17	SMARDKYVDK	1	0,970	----	----
	YGAALGKPPADR	99	----		----	----	----
	YLAEVAVDADR	99	YLAEVAVDADR		----	gi|27368038	14-3-3 protein B
	LYAEFAAGKTR	36	YLAEFAAGKTR	1	0,970	gi|60416167	14-3-3 protein
	ARAGMDMELTVEER	10	----		----	----	----
	GSHALNFSVFHEYLK	53	WPALLFSVFHEYLK	1	0,394	gi|27368037	14-3-3 protein B
	DDNLAMNELPSTHPLR	99				gi|60416167	14-3-3 protein
	MSEDDALAQMPTLSEESYK	56	347,1]DNALAKLDTLSEESYK	1	0,703	gi|44890386	14-3-3- protein activation protein
2521	WVVGFCDER	99	WVVGFCGDER	4	0,970	gi|47220021	6-phosphogluconolactonase
	VTMTFVVPNSAR	99	VTMTFPVVNS[227,1]	1	0,779	gi|47220021	6-phosphogluconolactonase
	SSAAMMARLHEVR	25	[319,1]GEFSSALMAAR	2	0,542	gi|66267654	----

Table 2.7 (continuation).- *De novo* peptide sequencing for protein identification.

nESI-MS/MS						PROTEIN ID	
Spot ID	Peaks 2.4		Lutefisk 97			Acc Number	Name
	Sequence	Score %	Sequence	Rank	Score		
2578	ADVANFPLADGPR	89	SVVANFPLADGPR	3	0,924	gi|56554783	Carbonic anhydrase
	CHANFPLADGPR	62	----		----	gi|56554783	Carbonic anhydrase
	EWGLDRSACHK	24	----		----	----	----
	TSPRLSLSDLNKR	6	----		----	----	----
	QGCHANGNADADGPR	10	[184,1]LALANFPLAD[154,1]R	1	0,341	----	----
	GPGCHANFPLWPGR	13	----		----	----	----
	SLLFSADGEAECCMVSGYWWMNRK	1	[200,0]LFSADWYGSGRMVVHAKNEAFRR	1	0,820	gi|56554783	Carbonic anhydrase
	RWFSRVCQCCHNDDYYMSQWK	99	[199,1]NFSADWAENRVCSADSPSGWCRR	1	0,327	----	----
	WWWDRMFAYQQNWFDEVHTPMLEDFDGPLSYWK	42	----		----	----	----
2587	QLAEEKGCGGFLR	26	[Q/L]AEEKGCGGFLR	2	0,970	----	----
	FPCMSDAYDR	99	FPCMSDAYDR	1	0,970	gi|45387733	Purine-nucleoside phosphorylase
	WVYCMLAGPTYETLAECR	98	WVYCMLAGPTYETLAECR	3	0,904	gi|45387733	Purine-nucleoside phosphorylase
	LMVVLGRNVGMSTVHWDRR	93	DALYLGHLVGMAVVS[256,2]VVVK	1	0,249	gi|45387733	Purine-nucleoside phosphorylase
	YGYELHVGYVCK	30	YGYELVPDMLCK	1	0,636	gi|55640605	Proteasome subunit alpha
	LYKVEYAFK	62	LYKVEYAFK	1	0,970	gi|55640605	Proteasome subunit alpha
	TGPLEVLTLPLVGTYR	90	-----		----	----	----
	YSENQTEPVLEYYR	26	SYENKTE[P/V]LEYYR	2	0,717	gi|47085881	----
2591	LLDAFDSLK	93	LLDAFD[200,0]K	1	0,970	----	----
	EPVSVSPASAMVK	45	226,1]VSVSARTTVR	3	0,334	----	----
	ADVANFPLADGPR	2	SVVANFPLAD[154,1]R	1	0,970	gi|56554783	Carbonic anhydrase
	LPCHANNQDADGPR	20	-----		----	----	----
	FAPPHADRTMECCMNHANGCLWKK	98	[201,0]NFSSPWAHTKSEASSNYTNASFPAK	1	0,415	----	----
	FFNDLVPGEASDQPQVLDMMK	47	[408,6]DLVPGEASDYAGLKMA[336,2]	1	0,560	----	----
2603	MDCTQVGFCGGFTPNNSCR	45	RV[251,1]KVGFCGGFTPNTPYR	2	0,496	gi|55251370	Methionine sulfoxide reductase A
	RRWGYGKVWKKALSLAAGNSKTVRMKGLVEWR	99	----		----	----	----

Table 2.7 (continuation).- *De novo* peptide sequencing for protein identification.

nESI-MS/MS						PROTEIN ID	
Spot ID	Peaks 2.4		Lutefisk 97			Acc Number	Name
	Sequence	Score %	Sequence	Rank-Score			
2650	TLGNLDLVVAR	75	LTEVLDNLV[154,1]	1	0,672	----	----
	EFEGLTFYEK	10	KFEGLTFYEK	1	0,358	gi|1165134	Glutathione S-transferase
	LLLDNPAEQALMYKR	46	PEMPNPDKRLMYKR	1	0,970	gi|1165134	Glutathione S-transferase
	DGFLWVTSFVDPAVVFR	51	[251,2][253,2]DVTVFS[210,2]A[200,0]FR	1	0,324	gi|1165134	Glutathione S-transferase
2667	FLDETANMSADDR	99	FLDETANMSWDR	2	0,970	gi|24413939	Ubiquitin C-terminal hydrolase
	FNLNTAMELNPEMAKR	99	FLLDTAMELNAATLLSR	4	0,970	gi|34393056	Ubiquitin C-terminal hydrolase
	FSAVAAAMR	99	FSAVALCR 3 0,970	3	0,970	gi|21361091	Ubiquitin C-terminal esterase
2685	GPLLLGDVFPNPFVDGYRR	99	[267,2]LLGDVFPNFEADTTLGR	1	0,970	----	Glutathione peroxidase
	LSLLYPATTGR	85	[199,1]LLYPATWK	2	0,229	gi|47227982	Glutathione peroxidase
	FDTPVCMAELACNR	79	[261,3]TPVCTTELAC[270,0]	1	0,454	----	Glutathione peroxidase
2686	TLDSLKLTAQK	29	----		----	----	----
	TYDLGDVFPGGPFVTAYRR	99	[144,0]D[184,1]CDCEDGGPFVDGNM[230,0]	4	0,550	----	----
	VDMDCGSQADTLFWCNFNRK	80	[214,1]MDCNSKESALFMKSNFSV[212,1]	1	0,50	----	----
2696	CAAEPSLLNVSNHMK	28	-----		----	----	----
	VLQLVLFFK	55	VLKLVLFFK	2	0,959	----	----
	FLLNLKGFETDTEFGQLRRR	37	DPCDPTGKKYDTEFGKLV[241,2]K	1	0,970	----	----
2717	AASFAVTFARCR	23	[229,0]FANFTVCLR	1	0,970	----	----
	FMNFDLSAGSFVGFRR	94	NYVYDLSGASFVGM[172,0]R	3	0,943	----	----
	WGAGTLPLGSTNK	65	FLTSGLPLTKPK	1	0,970	----	----
2723	SSVVRPDLLGNK	99	[260,0]GLLDPRVVR	4	0,970	----	----
	FAQFYECVTVCPASWTPK	76	TDKWSAPCVTVCPSKKTPK	1	0,970	gi|62204368	Peroxiredoxin 3
	DYGVLLEGGPLALR	50	[278,1]GVLLEGGPLALR	1	0,970	gi|62204368	Peroxiredoxin 3
	LSNFLNELDSGFR	53	[199,1]NFLDKLFGDSR	1	0,396	gi|66910263	Translin
	MEHWTAGDRLVKFR	18	-------		----	----	----
	ELLTVLQSVHQPSGFK	20	KLLTVLKSVHKN[274,0]K	1	0,655	gi|66910263	Translin
	MLRLSSLEHGEMSARLR	81	MLRNSSLVGARLRW[199,1]K	1	0,303	----	----
	FAQFVETHGEVCPASWTPK	52	[346,1]FVETHGEVC[168,1]SWTPK	1	0,868	gi|62204368	Peroxiredoxin 3

Table 2.7 (continuation).- *De novo* peptide sequencing for protein identification.

nESI-MS/MS						PROTEIN ID	
Spot ID	Peaks 2.4		Lutefisk 97			Acc Number	Name
	Sequence	Score %	Sequence	Rank-Score			
2738	VDFLSAAER	31	[VD]FLRY[195,1]	2	0,463	gi|51468069	Proteasome subunit beta
	QKSSAMLQPLLDNKLGFK	28	F[196,2]SAMLKPLLDNKL[332,2]	1	0,839	gi|51468069	Proteasome subunit beta
	VQYSFDPVGSYKR	22	VKYSFDPVGSYKR	1	0,967	gi|51468069	Proteasome subunit beta
	FWCPRSTPNGSHFK	99	-----		----	----	----
2759	DPELKVTAEADVLR	36	[228,0]NCAEATVKLYC	1	0,377	gi|74096419	Apolipoprotein A-IV4
	GQGRQSVSDMKDQLGPYTEDLR	14	[400,1]MTYPGLGADKMDSVS[128,0][382,2]	1	0,771	gi|74096419	Apolipoprotein A-IV4
2778	VNNSTLLGASGDYYVNGMYK	77	P[255,2]KFLGAKMHTGLLTSDPP	3	0,736	gi|47213154	Proteasome beta 4 subunit
	LTTPMVTGTSVLRK	8	[214,1]TPMVTGTSVLRK	1	0,970	gi|47213154	Proteasome beta 4 subunit
	NNLSKQEALDLVER	70	VKLSKKEALDLVER	1	0,970	gi|47213154	Proteasome beta 4 subunit
	RELLGPLSSETNWDLAR	82	RELLGPLSSENTWDLAR	1	0,970	gi|47213154	Proteasome beta 4 subunit
	SSALSDLAADMLGSYGDRR	99	SSALSDLAADMLGSYGSLAR	1	0,970	gi|47213154	Proteasome beta 4 subunit
	VNNSTLLGASGDYADYKHLK	39	[171,0]NETLLGASGDPSAGRGDHLK	1	0,431	gi|47213154	Proteasome beta 4 subunit
	WWMEAPTVATGFGAYLAQGQRR	61	[201,0][257,1]GKALYKFGTAVTPAVA[288,1]R	1	0,839	gi|47213154	Proteasome beta 4 subunit
2784	YGLLVHVPR	53	YGLLDGTL[201,2]	1	0,419	----	----
	GDEPVLSFYEVR	99	ATKPVLSFYEVR	1	0,766	----	----
2820	LRRVMGWMSCK	27	[170,1]G[198,1]VAPEWVGLK	1	0,214	----	----
	HNMFCLTAYVRR	24	----			----	----
	RYFFAYMWSKQHHR	14	[372,2]YLMEHLLAFFSGR	1	0,444	----	----
2837	CPQVVLSFYEER	30	CPKVVLSFYEER	1	0,950	gi|4530297	Heterochromatin-specific nonhistone protein
2877	SSQVCDYVDSYRVENNNMLQQLR	3	[174,0]KL[200,0]TNEGNVETEVNPVYLKKLR	2	0,498	gi|50370069	Histidyl-tRNA synthetase
2897	WTHCFLFWASVLAVEK	97	[216,0]MGKGRAWFVRGSAVTR	1	0,483	gi|37681759	Cofilin
	LNLVDEAEEPEKGKVGSTLCWYYWKK	99	VKLDDLAKENLKGKVGSVNHLEAEN[294,1]K	1	0,791	----	----
	YALYDATYETK	99	FSLYDATYE[TK]	1	0,970	gi|37681759	Cofilin
2898	YALYDATYETK	99	SFLYDAKLPHF	1	0,580	gi|41946867	Cofilin 2

Table 2.7 (continuation).- *De novo* peptide sequencing for protein identification.

nESI-MS/MS						PROTEIN ID	
Spot ID	Peaks 2.4		Lutefisk 97			Acc Number	Name
	Sequence	Score %	Sequence	Rank	Score		
2908	LELTTMGDR	8	[242,1]LTTMGDR	1	0,568	gi|47217449	Myosin regulatory light chain 2
	NGFNYAEFTR	1	NGFNYAEFTR	1	0,970	gi|47217449	Myosin regulatory light chain 2
	LNGTDLNNVLR	99	LNGTDPEDVLR	1	0,970	gi|47217449	Myosin regulatory light chain 2
	EAFNMLDQNR	50	SLFNMLDKNR	1	0,970	gi|47217449	Myosin regulatory light chain 2
	NGNVVCQDVLR	67	----		----	----	----
	FTDEEVDELFR	99	FTDEEVDELFR	1	0,970	gi|47217449	Myosin regulatory light chain 2
	ATSNVFAMFDQSKLKEFK	31	[188,0][185,0]VFAMFDKSKLKEFK	1	0,970	gi|47217449	Myosin regulatory light chain 2
2909	MWVRLNAGLHLER	11	[316,1]VGVLTYDLLER	1	0,922	gi|47218822	Unnamed protein product
2918	SNFNYVEFTR	7	[201,0]FNYVEFTR	2	0,970	gi|33991794	Myosin light chain
	FTDEEVDELFR	99	248,1]PFEVDELFR	1	0,942	gi|33991794	Myosin light chain
	SGNLVFAMFDKSQLQEFK	1	YEEKLKSEDFMA[196,2]EFK	4	0,394	gi|33991794	Myosin light chain
	NAFACFDEEGTGSLKEDYLR	12	[185,0]FACFDEEGTGSLKED[276,1]R	1	0,970	----	----
2912	LAVGVVEKSR	76	SPVGVVKKSR	1	0,589	----	----
	SLASGSGLVYQTR	47	[199,1]ASGSGLVYKTR	1	0,697	----	----
	YKPGWGSLQSGWGNTR	32	[274,0]DGWGSLLTGWGDKK	1	0,676	----	----
2972	YGLYDATYETK	38	YGLYDATYETK	1	0,970	gi|41946867	Cofilina2
	NNNVLLSLELGPK	5	T[202,0]HLLSLEGK[210,2]	3	0,577	gi|41946867	Cofilina2
3013	LLKMGTVALTK	13	[225,2]EMGSL[217,0][196,2]	3	0,450	gi|37681953|	Transgelin 2
	MQEQLSQFLSAAEK	6	[259,1]EKLSKFLSAAEK	1	0,970	gi|37681953|	Transgelin 2
3022	FPTLSGSMDLADK	41	[244,0]TLSGSFVLEGK	1	0,423	----	----
	DVQCGTVYFEKGTVTQAVPK	29	KWVKFAYFEKGTVTKA[196,2]K	2	0,307	----	----
3089	GDFCLDVGK	61	[171,1]FCLDV[185,0]	1	0,673	gi|47211278	Nucleoside diphosphate kinase
	MLHASEDLLK	49	MLHASEDKLL	1	0,970	gi|47211278	Nucleoside diphosphate kinase
	TFLALQPDRKR	26	[248,1]LPDPKLAWR	2	0,553	----	----
	YFLLPKMNERK	7	[285,1]RCCG[196,2]LEY	1	0,480	----	----
	MLGETNPANSEPSALR	9	[243,1]WLKSDAPNTEGPK	1	0,478	gi|47211278	Nucleoside diphosphate kinase
	DFHNSSLNLRLSSWPGR	48	MNT[168,1]SSLRLMMRDHAR	1	0,655	----	----

Table 2.7 (continuation).- *De novo* peptide sequencing for protein identification.

nESI-MS/MS						PROTEIN ID	
Spot ID	Peaks 2.4		Lutefisk 97			Acc Number	Name
	Sequence	Score %	Sequence	Rank-Score			
3122	LSFGKCGDVMR	99	LSFGKCGDVMR	1	0,970	gi|55250139	Myosin light chain alkali
	MTEEEVETLLAHGWDQGCLNYRWQR	99	[307,2][225,2]SVKTLLEHEDANGGTDLWDFEGR	4	0,492	gi|37362252	Myosin light chain alkali
3159	LSFGQCGDVMR	82	----		----	gi|51261923	Myosin alkali light chain 6
	FFELLTGRLEFK	98	----		----	----	----
	TVFLLFDK	49	[200,0]FLLFDK	1	0,391	gi|37362252	Myosin light chain alkali
	DTFYCCCPAAGKPGVANVCAYDKWMR	5	----		----	----	----
	WGGSMEDFVEGLR	16	[243,1]GSMEDFVE[170,1]R	2	0,561	gi|37362252	Myosin light chain alkali
3233	AYEMADYLR	99	AYEMWYLR	1	0,970	gi|45501160	Profilin 2
	ESFFTNGLTLGSK	96	[216,0]FFTNGLTLGSK	2	0,720	gi|45501160	Profilin 2
	AAGGMPTDEEQATGLER	58	----		----	gi|47228591	Cytochrome C oxidase subunit Vb
3649	DVEPMVEGETAK	24	[214,1]EPMMSW[154,1]R	1	0,281	----	----
	LDDMVNGALESLR	1	[228,0]DMVNGALESLR	1	0,970	----	----
	GGQAASLDDVENPLGYK	25	[242,0]AASLDDVENPLGYK	1	0,970	gi|47215998	Serin protease 35
	TAYTQAQSVNAEKLKSLR	60	374,2]KLKEANVSKAKMMR	1	0,898	gi|52430350	Apolioprotein A1
	QVSPVTDSVVTTLAEATRGKK	25	[510,0]TDSVVTTLAEATAE[269,1]	2	0,888	gi|57157761	Apolipoprotein A-I
	SMSEKYDDNADWPWMWYK	32	----		----	----	----
3675	MNRTMNGKKPEK	65	----		----	----	----
3676	SRAGTLPLGSTNK	48	[260,0][245,0]LPHSTNK	1	0,791	----	----
	AASFANFTVCLR	4	[228,0]FANFTGLMAR	5	0,547	gi|68365664	Profilin family, member 4
3690	LFQVEYALERR	40	[260,0]KALAYEVKLK	1	0,663	gi|37681911	Proteasome subunit, alpha
	SGRVNLELATVVRR	92	[300,1]VNLELATVVRR	3	0,780	----	Proteasome subunit, alpha

2.2.5 Comparison of sequenced peptides and identified proteins with *S. senegalensis* ESTs

As described in materials and methods (see pages 67-68), *de novo* peptide sequences, genomic ESTs and proteins in NCBI were compared searching for similarities. A protein subdatabase was created with the protein matches derived from the screening of databases with the EST sequences. In parallel, ESTs and peptide sequences were also compared. The sets of ESTs presenting good relationship with one or more peptides from the same spot was sent for a common search in the protein subdatabase in order to cross-validate tentative assignations. On the other hand, the sets of *de novo* peptide sequences originating from the same gel spot that could not be assigned initially to the tentatively identified protein were submitted to a refined search comparing these sequences with those in the corresponding EST set.

Twenty-one out of forty-nine spots present at least one peptide which could be related to an EST that matched with the same protein as the original peptide. From them, eleven spots presented between 2 and 6 peptides that confirm in the same way the protein assignation, while two spots (2918 and 3649) produced new peptide assignations that could not be matched in the comparison between MS/MS peptide and protein database

In the case of three spots with more than three assigned peptides (2908, 3089 and 3159), all the sequences previously assigned matched with an EST corresponding to the same gene/protein made in the peptides against protein database. Contrarily, for eight spots with more than three assigned peptides (2055, 2243, 2578, 2667, 2685, 2723, 2738, 3233), none of these peptides found a match with an EST related to the same gene/protein (Table 2.8; see discussion in page 108).

Table 2.8.- Coincidences between MS/MS peptide sequences from *S. senegalensis* and ESTs from *S. senegalensis.* For each spot, 3 different comparisons were made between peptide sequences, ESTs and sequences in the NCBI protein database: peptides against ESTs; ESTs against NCBI protein database; and peptides against NCBI protein database. Proteins resulting from each process were compared and matches between peptide and EST annotated. *Prot ID*: Protein identified from the MS/MS-derived peptides sequences. *Pep seq*: Number of MS/MS peptide sequenced for a certain spot. *Seq related to Prot ID:* Sequences of a spot used to identify the protein. *EST related to Prot ID*: ESTs matching with the protein identified with MS/MS peptides.

Spot ID	Prot ID	Pep Seq	Seq related to Prot ID	EST related to Prot ID
3649	Apolipoprotein A1	4	2	4
2918	Myosin light chain	4	3	4
2176	Acidic ribosomal phosphoprotein P0	2	2	2
2759	Apolipoprotein A-IV4	3	3	3
2837	Heterochromatin-specific nonhistone protein	1	1	1
2898	Cofilin 2	1	1	1
2908	Myosin regulatory light chain 2	7	6	6
3089	Nucleoside diphosphate kinase	6	3	3
3122	Myosin light chain alkali	2	2	2
3159	Myosin alkali light chain 6	5	3	3
2778	Proteasome beta 4 subunit	7	7	6
1966	Serine (or cysteine) proteinase inhibitor	11	7	4
2499	14-3-3 protein (Tyrosine 3-monooxygenase)	10	6	3
2521	6-phosphogluconolactonase	3	2	1
2897	Cofilin	3	2	1
2972	Cofilin2	2	2	1
3013	Transgelin 2	2	2	1
2126	Malate dehydrogenase 1	4	3	1
2650	Glutathione S-transferase	4	3	1
2587	Purine-nucleoside phosphorylase	8	3	1
2275	Pyruvate dehydrogenase E1-beta subunit	9	7	1
1942	Phosphoserine aminotransferase 1	1	1	0
1963	Olfactory receptor Olr653	1	1	0
2006	No ID	2	0	0
2055	Isocitrate dehydrogenase 3 (NAD+) alpha	5	3	0
2174	Polymerase (RNA) II (DNA directed) polypeptide C	1	1	0
2239	Hydroxysteroid (17-beta) dehydrogenase 4	6	2	0
2243	Uridine phosphorylase 1	6	3	0
2436	No ID	3	1	0

Table 2.8 (continuation).- Coincidences between MS/MS peptide sequences from *S. senegalensis* and EST from *S. senegalensis.*

Spot ID	Prot ID	Pep Seq	Seq related to Prot ID	EST related to Prot ID
2578	Carbonic anhydrase	9	3	0
2591	Carbonic anhydrase	6	1	0
2603	Methionine sulfoxide reductase A	2	1	0
2667	Ubiquitin C-terminal hydrolase	3	3	0
2685	Glutathione peroxidase	3	3	0
2723	Peroxiredoxin 3 or Translin	8	5	0
2738	Proteasome subunit beta	4	3	0
2877	Histidyl-tRNA synthetase	1	1	0
2909	gi47218822 Unnamed protein product	1	1	0
3233	Profilin 2 or Cytochrome c oxidase subunit Vb	3	3	0
3690	Proteasome subunit, alpha	2	1	0

2.3 Discussion

The testes from animals involved in this study were classified depending on the relative abundance of germ cells types as described before (García 05). Wild animals captured in spring 2004 presented three of the five possible stages of spermatogenesis described by García-López *et al*. (mid, late, and functional maturation stages). The three stages of spermatogenesis were characterized by different amounts of spermatozoa in the medullar efferent ducts, with its maximum in the functional maturation stage. The distribution of testicular developmental stage in the studied animals (3 animals in mid, 3 animals in late, 3 animals in functional maturation) correlates with the distribution of animals described by García-López and co-workers. They found that from 35 individuals caught from November 2003 to July 2004, those captured between February and May, 6 were at mid spermatogenesis stage, 3 were at late spermatogenesis stage and 7 at functional maturation stage. Only one animal was found in the recovery stage, and no fish was found to be in the early spermatogenesis stage.

Table 2.9.- Number of *S. senegalensis* males sampled at each stage of testicular development by month of collection (adapted from García 05). The months where the individuals for the current study were caught are shadowed.

Testicular developmental stages						
	Early	Mid	Late	Functional maturation	Recovery	Total
November 03	3	2	--	--	--	5
January 04	--	3	2	--	--	5
February 04	--	4	1	--	--	5
March 04	--	2	2	--	--	4
April 04	--	--	--	3	1	4
May 04	--	--	--	4	--	4
June 04	--	--	--	--	5	5
July 04	2	--	--	--	1	3
	5	11	5	7	7	35

Captive males produce sperm all along the year, with a maximum of production occurring between February and April, and a minor peak (around 50% of maximum activity) in summer (Anguis 05). F1 animals at IRTA facilities were sacrificed in April, month that corresponds to the period with the highest sperm production along the year, and classified in the late and functional maturation stages (García 05). The observed spermatogenesis stages in these animals are then consistent with the observations made before by Anguis *et al*. (Table 2.9; Anguis 05).

The 2-D gel analysis was performed on 18x24 cm polyacrylamide supports, with a number of spots per gel between 769 and 1148. From the analyses of spots on 2-D gels (see also chapter 3) and from the shotgun approach (see chapter 1), about 2000 peptide tags were sequenced *de novo*. Combined annotation from peptide tags and genomic ESTs obtained inside the Pleurogene project constitutes the first insight on the Senegalese sole genome.

As mentioned before, the genome of *S. senegalensis* is not described, and thus the number of genes is unknown. Description of fish model organisms (i.e. *Danio rerio*, *Takifugu rubripes* or *Tetraodon nigroviridis*) predicts a number of genes between 24000 and 29000 (Chen 05; www.ensembl.org). Predictions of proteome length based on genome for *Takifugu rubripes* postulate the presence of about 33,700 non-redundant proteins including alternative predictions for the same gene loci but not post-translational modifications (Aparicio 02). Assuming the predictions for fugu fish, the number of detected spots in this work corresponds to 3% of the testis proteome from *S. senegalensis*. For 2-DE studies performed in similar conditions on *D. rerio* (Tay 06, Link 06a-b), the number of spots detected (between 1000 and 1600, depending on the study) represent around 4-5% of the predicted number of genes.

However, this parameter should be corrected by other factors. For instance, the genes expressed in a certain tissue are less than those for the complete genome of one species and, therefore increasing this predicted value. Moreover, the spots in 2-D gels are not univocally related to one gene, because of alternative splicing and PTMs. This in turn will reduce the predicted value for this parameter.

2.3.1 Gel Reproducibility

Due to the spermatogenesis cycle of the Senegalese sole, it was convenient to coordinate specimen sampling in two different years, and therefore, the testis samples of this study were processed in different periods during the year. The first batch was processed in October 2004. This included F0 mid spermatogenesis, late spermatogenesis and functional maturation groups. The second batch of gels was performed in March 2005, and included the F1 functional maturation group. The last batch was performed in June 2005 and the F1 late spermatogenesis group was analysed. The reliability and robustness of the analytical procedures along the time extension of the project was thus critical as gels performed in different batches must be compared.

In addition to this, the Pleurogene project is a collaborative effort that involves research centres in Spain and Canada. Thus, any technical protocols developed in this framework had to take into account that the samples analysed were obtained with the implication of several partners and that the results must be reproducible and shareable by other groups.

Major concerns were related with image reproducibility both in terms of spot distribution (*Mr*/*pI* stability) and intensity (%Vol variation). Reproducibility and robustness along the experiments were checked using six spots distributed through the gel (*Mr* range: 60-17 kDa; *pI* range: 3,7-8,5). The CV of the *Mr* mean values for spots placed in the 60 kDa area (1821 and 1814) were 4,7 and 6,3 respectively, while for the other spots it was lower than 0,2. The CV of the *pI* mean values were never higher than 0,01. These measures showed that IEF system was highly reproducible in the ranges studied. On the other hand the SDS-PAGE separation presented reproducibility with less than 1% of variation under 40 kDa, but it increases up to 5-6% above this mobility limit.

Main reproducibility issues were however found related with spot volumes. The mean CV values for the normalized volume of 488 spots common to all gels were 54, 42, 55, 36 and 38% for F0M, F0L, F0Mat, F1Mat and F1L, respectively. These variations are principally produced during the silver staining process and sample preparation, especially in protein quantification and IPG holder loading (Görg 04, Quero 04). In consequence, changes in spot volumes lower than 30-40% in the comparisons between

different stages can not be confidently assigned to biological changes, but to experimental variability. To diminish false positives, in this study, only variations equal or over two-fold were considered. Exceptionally, statistically significant changes ($P < 0,05$) between 2-fold and 1,6-fold were also considered, when neighbouring spots presented significative variations over 2-fold. This allowed unmasking other spots with the same protein identification and related abundance variations.

After the analytical conditions described in Materials and methods were set, results were found consistent and reproducible over the time, allowing comparisons of gels obtained in different periods using routine procedures for image analysis. Moreover, this approach has been also evaluated in several proteomic studies, resulting always that the technique was consistently reproducible and reliable for comparative studies (Higginbotham 91, Heinke 98, Tsuji 99, Vasseur 99, López 01, Quero 04).

2.3.2 Expression analysis

Forty-nine spots were determined as differential in at least one of the comparisons performed. Few spots were exclusive of a given individual comparison, indicating that the majority of the described spots could play a role in the whole process of spermatogenesis. Changes observed were mainly in the range from ±2 to ±5-fold variations. About 20% of the spots showed changes between ±5 and ±10, and 12% over ±10-fold change (Table 2.10).

The identification of stage-specific differential spots could proportion tentative biomarkers to define the corresponding spermatogenic stage. From the F1L vs. F1Mat comparison, two stage-specific spots were detected and identified as carbonic anhydrase. Also, a specific spot corresponding to a protein involved in the steroid pathway was identified from the F0Mat vs. F1Mat comparison. Protein identification of uni spots from other comparisons are related to structural and antioxidant functions, metabolic pathways, or protein folding processes (Table 2.11). Functional implications in spermatogenesis of these proteins are discussed below.

Conversely, the presence of common differential spots between two comparisons could indicate biological similarities between the studied transitions, especially when those common spots vary in the same sense (Table 2.12). For instance, the transformation from F0M to F0L stages shares 5 spots changing in the same sense with the transformation from F1L to F1Mat. Although histologically F0 and F1 animals are classified identically, the presence of coincident spots between these comparisons could indicate that the molecular changes needed to transform testis from F0M to F0L are similar to those needed to transform testis from F1L to F1Mat. Then, F1L state would be more similar to F0M than to F0L, and F1Mat closer to F0L than to F0Mat, indicating a less mature state than the observed in the histological analysis. This fact correlates with the experimental data, which showed F1Mat animals producing sperm without all the signs of maturity.

Table 2.10.- Number of differential spots observed in the different spermatogenic stages and classification based on their observed expression changes (Δ). Specific spots indicate the number of spots whose variation is considered only significant in the corresponding comparison (see Table 2.11 for spot identification).

	Differential Spots	Specific spots	Spots with		
			$5 \geq \Delta > 2$	$10 \geq \Delta > 5$	$\Delta > 10$
F0M-F0L	11	--	7	2	2
F0L-F0 Mat	15	2	10	3	2
F0M-F0Mat	7	--	4	2	1
F1L-F1Mat	18	2	13	3	2
F0L-F1L	19	4	18	4	2
F0Mat-F1Mat	17	2	12	4	2
Unique Total	49	10	64	18	11

Table 2.11.- Differential spots unique to each experimental comparison in the spermatogenic stages study (see table 2.10)

	Unique spots ID	Protein ID of unique spots
F0L-F0Mat	2898 2909	Cofilin 2 Unnamed protein product gi47218822
F1L-F1Mat	2578 2591	Carbonic anhydrase Carbonic anhydrase
F0L-F1L	1966 2126 2723 2778	Serine (or cysteine) protease inhibitor Malate dehydrogenase Peroxiredoxin 3 or Translin Proteasome beta 4 subunit
F0Mat-F1Mat	2339 2650	Hydroxysteroid (17-β) dehydrogenase 4 Glutathione s-transferase

Table 2.12.- Classification of differential spots based on repetition in comparisons and common sign variation. The total number of differential spots in each comparison is indicated in parenthesis in the header. CS: Total number of Common differential spots between comparisons. SS: Number of spots presenting the same sign variation in both comparisons. F0= wild animals; F1= cultured animals; M= Mid spermatogenic stage; L= Late spermatogenic stage; Mat= functional maturation spermatogenic stage.

	F0M –F0L (11)		F0L-F0Mat (15)		F0M – F0Mat (7)		F1L – F1Mat (18)		F0L – F1 L (24)		F0 Mat – F1 Mat (18)
F0M – F0L (11)											
F0L – F0 Mat (15)	CS	SS									
	6	--									
F0M – F0 Mat (7)	CS	SS	CS	SS							
	2	2	4	3							
F1L – F1 Mat (18)	CS	SS	CS	SS	CS	SS					
	5	5	5	--	2	1					
F0L- F1L (24)	CS	SS	CS	SS	CS	SS	CS	SS			
	6	--	9	8	4	2	13	1			
F0 Mat – F1 Mat (18)	CS	SS	CS	SS	CS	SS	CS	SS	CS	SS	
	7	6	10	--	7	3	9	7	8	2	

2.3.3 Protein identification

More than 80% of the analyzed differential spots (40 out of 49 spots) could be assigned to a protein by MS/MS. Moreover, quite a few of these identifications were confirmed by combining proteomic and EST information.

Two different de novo sequencing softwares and several types of BLAST searches (pblast, blastx, tblastn) were used during the protein identification analysis. The development and optimization of several bioinformatic tools for protein identification was primordial to achieve the objectives of the current investigations. Nowadays, as long as the experimental MS/MS raw data is prime-quality, sequencing softwares play a critical role in determining the number of relevant results finally obtained, and thus sequencing softwares are nowadays in the edge of bioinformatic development (Xu 06).

Despite the amount of data generated in the process described here to identify protein from 2-D spots is not as demanding as the LC-MS/MS data processing, the identification process of proteins from species without sequenced genome is still a high time-consuming work. Unfortunately, *de novo* sequencing softwares available for the study (Peaks 2.4 and Lutefisk 97) were not designed to integrated data from different sources (i.e. BLAST analysis, de novo data from other softwares) and this situation complicates the task of producing good quality results.

In this work, it was resolved to use several identification approaches to cross-validate the candidate sequences. Initial comparison of the two *de novo* sequencing softwares available showed that Peaks gave generally better results than Lutefisk97, as already observed elsewhere (Pevtsov 06, DiMaggio 07). In consequence Lutefisk was used as a confirmation tool for the main data flow produced from Peaks, although in several cases both tools were combined to obtain the final result.

Following the analytical protocol designed for this work, and after a tentative protein was identified, the analysis of the differences between theoretical and experimental values of *Mr* and *pI* was used as a source for additional clues on its identity (figure 2.12). Differences over ±0,2 and ±2 for *Mr* and *pI*, respectively were taken as the threshold values to determine possible erroneous identifications.

Identification of 26 out of 40 differential spots was supported by the correlation under ±0,2 and ±2 between theoretical and experimental *Mr* and *pI* values, respectively. In addition, the number of peptide assignations, the quality of the *de novo* sequences and the coincident aminoacid in the BLAST matches reinforced these assignments.

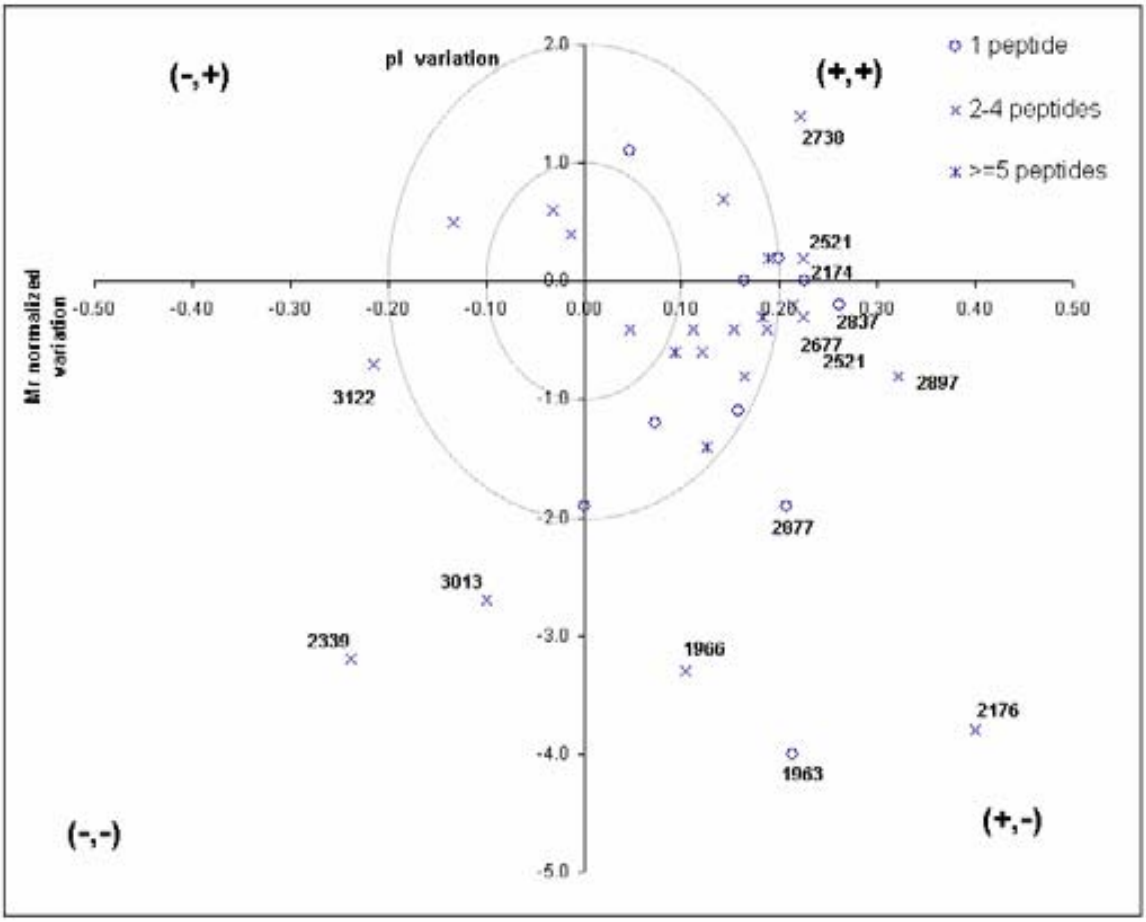

Figure 2.12.- Distribution of spots identified in the spermatogenesis stages comparison depending on the difference between experimental and theoretical values of *Mr* and *pI*. Spots with *Mr* and *pI* variations greater than ±0,2 and ±2 are identified. Normalized *Mr* values are calculated as (Experimental value -Theoretical value) / (Experimental value + Theoretical value). Pairs of plus and minus symbols in brackets indicates that the experimental value is higher **(+)** or lower than the theoretical value **(-)** for Mr and pI, respectively. Depending on the number of peptides used for protein identification, spots are displayed as “o” when 1 peptide was assigned, “x” between 2 and 4, or “⁑” when 5 or more.

For other 9 spots, theoretical and experimental *pI* and/or *Mr* were over the reference values, although the number of assigned sequences (≥2 peptides) or the number of aminoacid identities (≥9 coincidences) in the BLAST alignments supported the assignment. These variations could suggest the presence of PTM (Δ*Mr* and Δ*pI*), a significant modification in the number of charged aminoacids in *S. senegalensis* sequence in respect with the specie for which the protein has been identified (Δ*pI*; *Tetraodon nigroviridis*, *Danio rerio*, *Pan troglodytes* and *Mus musculus*) or the identification of a fragment instead of the full-length protein (Δ*Mr*). The latter case can be supported by inspecting the position in the protein sequence of the identified peptides. For the remaining 5 spots, high Δ*Mr* and/or Δ*pI* differences with only one peptide assignation could be indicative of an incorrect identification, and in this case a careful reanalysis of the original MS/MS sequence and BLAST data was performed. Only assignation for spot 1963 was then rejected.

In summary, 39 out of 40 protein assignations passed the quality control on protein assignment based on the combination of the number of peptides assigned for each spot, BLAST comparison and difference between theoretical and experimental *pI* and *Mr* values.

2.3.4 Use of genomic ESTs for annotation cross-validation

The availability of EST from *S. senegalensis* tissues allowed further validation of tentative peptide sequences. The combination of genomic and proteomic information resulted to be of great value for sequence assignation. For instance, 6 out of 7 peptides from spot 2778 fit perfectly in PGSP0002H09_T7.AB1 EST. Only one peptide did not correspond to any region of the EST. After analyzing the distribution of these peptides in the assigned protein (gi|47213154: [Tetraodon nigroviridis] Proteasome beta 4 subunit), it was noticed that the peptide was situated at the beginning of the protein sequence (figure 2.13).

This fact could indicate the presence of some bias in the EST sequence generated from the polyA mRNA population. The mRNA reversely transcribed to cDNA present from 5' to 3' the coding region, an untranslated region (UTR) of variable length and a polyA region. This reverse transcription was made using polyT as a primer. Then, the resulting

cDNA' should be constituted, from 5' to 3, of a polyT region, an UTR region of variable length and the coding region. Unfortunately, the product length of the reverse transcription does not always cover the complete mRNA sequence with high fidelity and depending on the UTR length, some cDNA will present modified or even truncated coding regions, missing a portion of their 5' sequence. This region corresponds to the N-terminal aminoacids of a protein as expected from the observed disposition of peptides in spot 2778 (figure 2.14). In this way the proteomic approach was complementary to the genomic available data, while the EST sequences confirmed the MS/MS assignations.

>gi|47213154|emb|CAF93844.1| Tetraodon nigroviridis; proteasome beta 4 subunit

GMKLSFWENGPKPGQFYSFPGSRNQTGTSCGPVRHTLNPMVTGTSVLGVKFSGGVIIAADMLG
SYGSLARFRNISRLMKVNDSTILGASGDYADYQYLKRVIEQMVIDEELLGDGHSYSPKAVHSWLT
RVMYNRRSKMNPLWNTVVIGGFYKGESFLGYVDKLGVAYEAPTVATGFGAYLAQPLMREAVEN
KPELSKQEARDLIERCLKVLYYRDARSYNRYEIAIVTEEGVEIISPLSSETNWDIAHMVR

MALDI/nESI (z)	Peaks sequences	Score
2167 (+3)	VNNSTLLGASGDYYVNGMYK	77%
1501 (+1)	LTTPMVTGTSVLRK	8%
1628 (+2)	NNLSKQEALDLVER	70%
1958 (+2)	RELLGPLSSETNWDLAR	82%
1986 (+2)	SSALSDLAADMLGSYGDRR	99%
2497 (+2)	WWMEAPTVATGFGAYLAQGQRR	61%

Figure 2.13.- Peptides described for spot 2778 were aligned over the predicted protein (Proteasome beta 4 subunit). Peptides were aligned with *S. senegalensis* EST, giving a correspondence with PGSP0002H09_T7.AB1. "PMVTGTSVL" is the closer peptide to the N-terminal and the only sequence that does not correspond to a EST region.

The number of identified peptides matching with *S. senegalensis* ESTs (21 out of 40, 53%) is much higher than theoretically expected from the predicted number of genes/proteins for fish species (around 25000 genes and 30000 proteins not including PTM variants; Chen 05). The EST-peptide correlation takes into account 10000 EST and 40 identified proteins. The EST set represents 40% of the total gene number, while proteins are less than 1% of the total predicted proteins. Assuming that every gene finds a match in the general protein set, the theoretical probability of finding a correlation

between groups in this study would be only 16%. These differences can be due to a bias introduced by the experimental procedures in the obtainment of the EST set and the analysis of the proteome. During EST obtention, mRNAs with a high number of copies had a greater chance to be cloned and amplified. More drastically, the 2-DE analyses reveal only the more abundant protein species. In overall, this fact results in the obtainment of EST and protein collections included in the relative small subset of highly expressed molecules, and in consequence, a greater probability of coincidence between them. This situation was also described for the shotgun peptide dataset (see page 57).

Some spots in the EST-peptide-database comparison with several peptides perfectly related to a described protein, did not find any EST relationship (i.e spot 2685). Beside the previous argument of probability and expression, the lack of coincidence could be induced by the transcription problem cited above (the EST does not present a coding region at all, because the UTR is too long). In these cases proteomic information acquires even more relevance, and the complementariety between approaches becomes more evident.

Unfortunately, EST comparison was not able to predict the protein identification for those spots that could not be identified by MS/MS procedures. This is understandable assuming that peptide sequences for this spots are not so reliable, that mRNA for this protein was not captured or that the coding sequence was not transcribed from fish genome. Other similar approaches with *Xenopus laevis* described in literature found similar results (Liska 04).

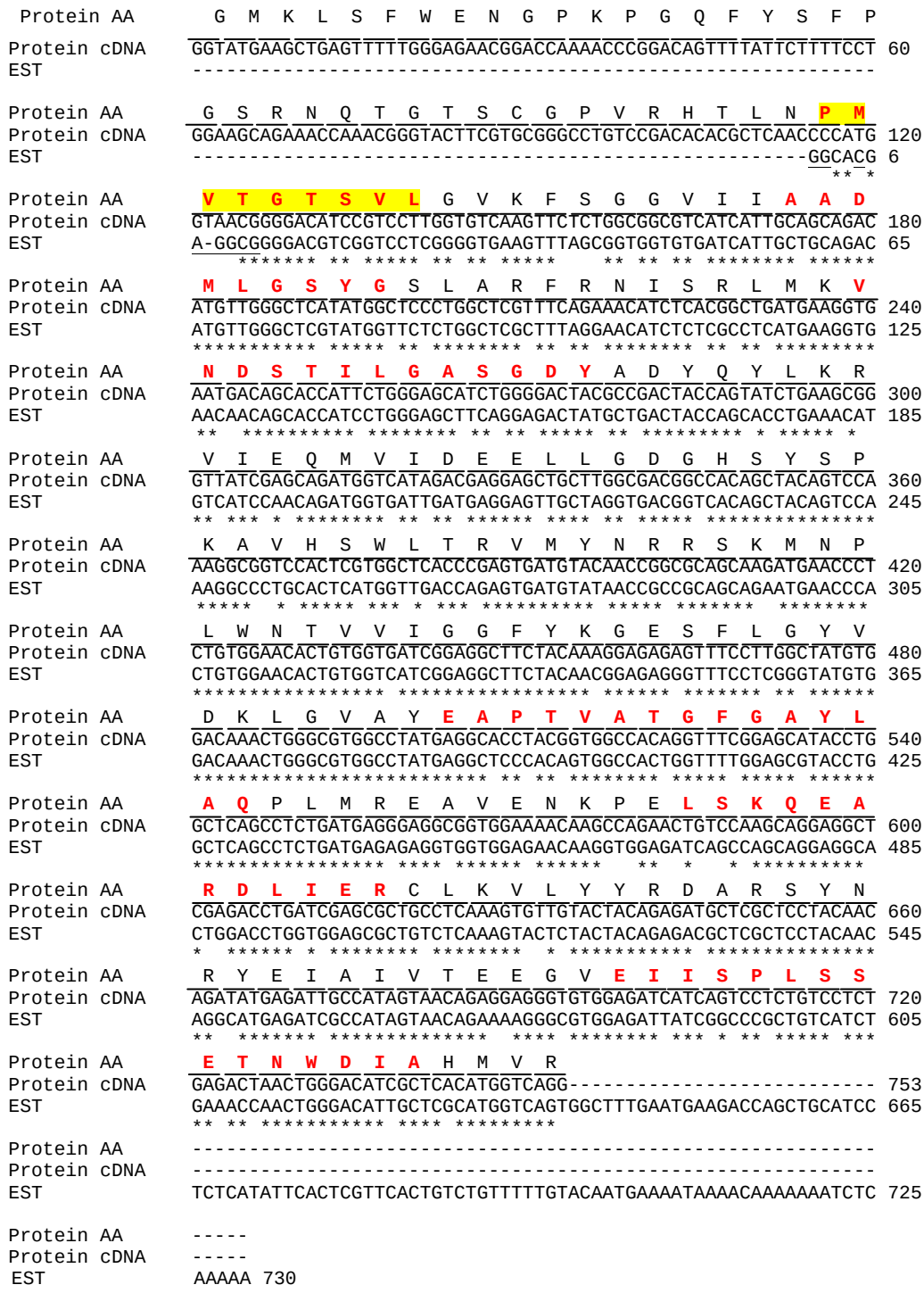

Figure 2.14.- Alignment of EST PGSP0002H09_T7.AB1 with nucleotide and aminoacid sequence of the predicted protein for spot 2778 (gi|47213154: proteasome beta 4 subunit). Peptides sequenced by IT-MS/MS for spot 2778 are in bold. Sequence not found to align between EST and sequenced peptides is highlighted. This peptide is not matching because 4 non-conservative changes are introduced at the end of EST, probably during reverse transcription affecting the “PMVT” aminoacids.

In several cases, one spot was assigned to two different proteins. The set of sequenced peptides for the spot led to the identification of different proteins making difficult to assign univocally one protein identification to that spot. Two main situations could be behind these cases: the use of bad quality spectra and the posibility of protein colocalization in the spot.

Bad quality spectra or spectra with partial, ambiguous data can derive from the analysis of low concentration samples as well as from peptide sequences with unadequate fragmentation characteristics. In the latter case, these spectra can be obtained even from intense spots from where good quality spectra derived from other tryptic peptides produce alternative identifications. In these cases a careful, manual filtering of the data was required in order to select those identifications from the best spectra available.

In other cases, two different assignations could be produced from two different subsets of spectra produced from the same gel spot. Probable causes of this double identification are the colocalization of proteins under the same spot or the contamination by other intense spots in the surroundings. Further complementary analysis such as qualitative Western blot or ELISA should be performed in those cases to determine the protein responsible of the spot variation. In the case of fish species, these confirmatory techniques are not always possible because of the low availability of commercial antibodies, especially for those fish that are not model organisms.

2.3.5 Biological implications of variations in the testis proteome

Transition from mid to late spermatogenesis stages in F0 animals was accompanied by several proteome changes. A significant high variation was found in the acidic ribosomal phophoprotein P0 (spot 2176). Absence or reduction of this protein leads to inactive ribosomes and impaired protein synthesis (Santos 94). The molecular mass difference between theoretical (21 kDa *H. sapiens*, 34 kDa *D. rerio* and *S. cerevisiae*) and experimental values (49 kDa *S. senegalensis*) of spot 2176 is 13 and 38 kDa, respectively. This could indicate that the identified protein is a precursor of functional P0 protein. The profile of this protein along the F0L and F0Mat spermatogenic stages may indicate a maturation of this precursor to produce active P0 protein. Protein synthesis requirements are high in late spermatogenesis, where protamines and transient histone-

replacing proteins are needed to transform spermatids into spermatozoa. On the contrary, this P0 precursor is not processed between F1L and in F1Mat stages and protein synthesis is then impaired, leading to the impossibility to replace histones properly, and possibly causing abnormalities in spermatozoa as often observed in F1 animals.

Another broad change with the same expression profile was observed between the F0M-F0L stages for two spots related to cofilin (2897 and 2972). Spot 2898, that showed significative variations in the F0L-F0Mat comparison, was also related to cofilin. Spots 2897 and 2898 presented the same *Mr* value differing in 0,4 *pI* units, while spot 2972 is placed 3 kDa below 2897. This disposition suggest different post-translational modifications between spots 2897, 2898, and 2972 (figure 2.15). From the available MS experimental data in this study (i.e. MALDI spectra from digested spots, MS/MS spectra of fragmented peptides and situation of the tentative *de novo* sequences inside the homologous assigned protein) it is not possible to confirm which PTM could be associated and which possible cofilin isoform is related to each spot.

In the literature, a prevalent role for cofilin was described in the control of polymerization/depolymerization of actin during spermatogenesis. The actin filaments are involved in the progressive movement of the germ cells from the basal to the luminal compartment of the seminiferous epithelium. In this process, cellular cysts must cross the blood-testis barrier (BTB). Several disassembly and reassembly of cellular junctions occurs during this process: between Sertoli cells (Tight junctions, TJs) and between Sertoli and germ cells (actin-based adherent junctions, AJs) (Cheng 02). These events in spermatogenesis are also associated with extensive turnover of junctions with changes in actin filament organization. This process is mediated by integrins and regulated by cofilin phosphorylation/dephosphorylation, acting as a simple switch for actin assembly and disassembly (Huang 06). Then, variations between cofilin profiles between F0 and F1 group might indicate that isoforms of cofilin are involved in observed sperm abnormalities, possibly by participating in the modulation of sperm actin filaments or by regulating the cell-cell junctions during spermatocyst maturation.

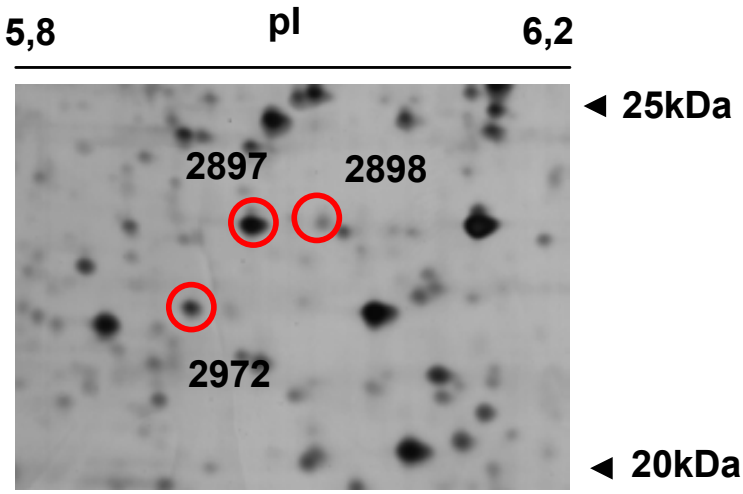

Figure 2.15.- Relative positions in a 2-D gel of spots 2897, 2898, 2972, assigned to isoforms of the cofilin family.

Heterochromatin-specific nonhistone protein (spot 2837) presented great variations not only in the F0 spermatogenesis process but also in F1 animals. This protein is implicated in formation of the XY body during spermatogenesis in mammals. The XY body is essential for heterochromatinization of sex chromosomes and for successful spermatogenesis. Expression of this protein changes along the spermatogenesis process (Motzkus 99) as observed in F0 animals, but not in F1. This may indicate disturbed functionality of XY body formation and therefore impaired spermatogenesis.

Spots 2908, 2918, 3122 and 3159 were assigned to myosin light chain proteins (MLC). All of them presented a similar protein expression profile, with a maximum of presence in late stage for F0 animals, but a maximum in functional maturation stage for F1 group possibly indicating a delay in the spermatogenesis process for F1 individuals, as pointed earlier in this discussion. The relative disposition of spots in the gel could point to *pI* changes due to PTM between spots 2908 and 2918 (figure 2.16). Unfortunately, thid possibility could not be clarified from the available MS data. However, substantial evidences implicate a role for phosphorylation-dephosphorylation systems in the regulation of MLC in sperm motility. MLC kinases and phosphatases were described to be involved in fowl sperm motility (Ashizawa 95). The modulating role of phosphorylation-dephosphorylation described for MLC in sperm motility may have an important implication in the deficiencies observed in F1 animals.

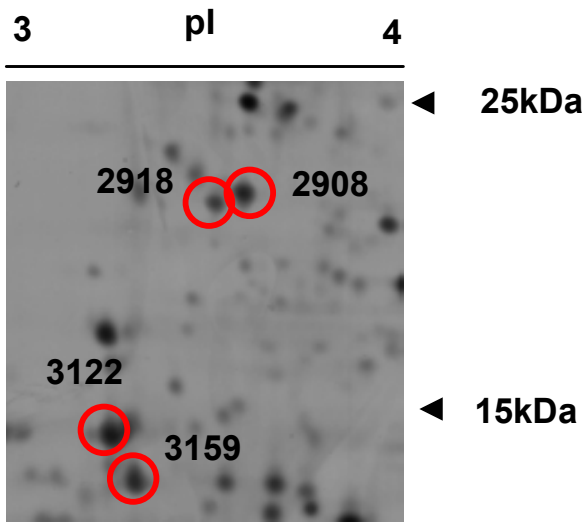

Figure 2.16.- Relative positions of spots 2908, 2918, 3122 and 3159, identified as different isoforms of the myosin light chain family.

Glutathione-S-transferase (spot 2650), glutathione peroxidase (spot 2685), peroxiredoxin 3 (spot 2723) and methionine sulfoxide reductase A (spot 2603) were generally increased in F1 stages respect to the parallel stages in F0 animals. Different roles in spermatogenesis and sperm maturation have been described for these proteins: oxidation of protamine thiols in DNA condensation for stabilizing chromatin by crosslinking protamine disulfides (Pfeifer 01), prevention of protein and DNA damage (Benbahim 02), steroid binding activity (Aravinda 95) and general maintenance of cell redox state, specially by controlling reactive oxygen species (ROS; Rao 00, Drevert 06, Fuji 05, Cabreiro 06). All these fundamental functions should be balanced and, the expression patterns of these 4 proteins showed a variation in F1 animals that may indicate a loss of control of the redox state. This situation can contribute to the abnormalities observed in sperm and the infertility of F1 animals.

The spots assigned to P0 protein, cofilin, MLC and redox proteins are grouped mainly in the subtrees 1 and 3 of the cluster analysis (table 2.6), confirming a common behaviour of these proteins during the studied states.

Spots 2578 and 2591 were identified as carbonic anhydrase (CA). Their expression profile was especially interesting in the F1Mat group where spot 2578 is increased, while spot 2591 decreases respect the other four states. Both spots show identical

electrophoretic mobility, differing only in few *pI* units. This could point to a PTM difference between CA isoforms that may modulate their activity.

CA has been involved in the acquisition of motility of spermatozoa. They acquire this faculty during the passage through the sperm duct. This sperm maturation process involves only physiological but not morphological changes (Miura 03). The pH of both the sperm duct and the spermatozoa cytosol are considered key for sperm motility. The mechanisms regulating pH are not clear, but several elements have been related: CA in spermatozoa membrane (Inaba 03) and epididymis epithelium (Ekstedt 04), 17α,20β–P and cAMP (Miura 03) and the CO_2/ HCO_3^- balance (Inaba 03). The inverse expression profiles of these two spots could indicate that CA regulation in F1 animals is not proper and then sperm motility is impaired due to this PTM regulation deficiency.

The spot 2499, identified as the 14-3-3 protein, changes principally when comparing between F0 and F1 animals the transitions from late to functional maturation stages. Two different isoforms were related to the same spot: β isoform from direct comparison of peptide sequences with NCBI database and δ isoform from comparison of peptide sequences with *S. senegalensis* EST. From the sequenced peptides it is not possible to determine which 14-3-3 protein is differential in this study. Human β, δ and θ isoforms contain 80% of common regions and clustal comparison for β, δ and θ isoforms is not available for any fish species. However, it is clear that the variation observed suggests a biological importance of 14-3-3 proteins during the Senegalese sole spermatogenesis.

As described in the literature, 14-3-3 proteins may be involved in the differentiation of spermatids, principally in the morphogenesis of sperm flagellum (Berruiti 00), and therefore in the acquisition of sperm motility. The process from late to functional maturation includes the transformation from spermatids to spermatozoa (Garcia 05). The variation of 14-3-3 expression profile between F1 and F0 can contribute to explain the abnormalities in form and motility observed in F1 spermatozoa.

The results obtained in the present work shows an absence of spot 3690 in functional maturation stage of F1 fish, while present in F0 fish. Two other spots related to proteasome subunits (2738 and 2778) also showed a different expression pattern in F0 animals and F1 animals. Proteasome components have been connected to spermatogenesis in several studies. One of the key elements of spermatozoa

maturation is the replacement of spermatid histones by protamines to allow a higher package ratio of gamete DNA. The control of this change is under ubiquitin ligases which ubiquitinate histones as they are replaced first by testis-specific transition proteins and then by protamines (Sutovoksky 03, Sassone-Corsi 02). The replaced histones are processed by proteasome after replacement. For example, histones H3 and H2A become ubiquitinated in elongating spermatids, just before the histones are replaced (Agell 88, Chen 98) and knock out of an Ub-conjugating enzyme causes male sterility, with morphological abnormalities in spermatozoids suggesting a failure in nuclear condensation (Roest 96).

As described for spot related to proteasome units, pattern expression for Ubiquitin C-terminal hydrolase (spot 2667) was different between F1 and F0 animals. UCHs are highly expressed in testis. Previous work demonstrated that UCH-L1-deficient mice exhibit progressively decreasing of spermatogonial stem cell proliferation, suggesting that UCH isozymes in the testis function during spermatogenesis (Kwon 03). These observations could be pointing in the same direction described above: sperm maturation is not complete in F1 because histone replacement is not performed effectively as ubiquitin/proteasome pathway is not acting properly.

Spot 2339 was identified as 17-β hydroxysteroid dehydrogenase (17β-HSD). F1 levels of this spot 2339 were always decreased compared with F0 levels. The comparison F1Mat-F0Mat uncovers a 2-fold variation for this protein. This enzyme modulates the biological potency of estrogens and androgens by conversion at position 17: keto-forms are inactive (estrone, Δ4-androstenedione), whereas hydroxy-forms are active and access the steroid receptors (estradiol, testosterone; Mindnich 04). As described in the introduction, testosterone is the precursor of 11-ketotestosterone (11-KT). Testosterone is most effective as a stimulator of hypothalamic and pituitary activity, leading to further testis activation, while 11-KT is most effective as a direct stimulator for spermatogenesis and then considered the main androgen teleost fish (Nagahama 94).

The role of this enzyme in testosterone production and its general decrease in F1 stages may indicate that F1 individuals do not produce enough testosterone, and consequently not enough 11-KT to maintain the signalling needed for complete spermatogenesis. The lack of this hormonal stimulation during spermatogenesis could be the origin of most of the morphological and molecular variations observed for F1 individuals.

The expression pattern of spot 2275, assigned to the E1 β subunit of pyruvate dehydrogenase (PDH), showed a positive 4-fold difference in F1Mat relative to F1L. By contrast, in F0 animals a decrease of near 3 fold was observed for this transition Pyruvate dehydrogenase E1 β subunit is directly related to the testis-specific pyruvate dehydrogenase E1 α subunit (Iannello 92) in the PDH complex as observed in figure 2.17. Regulation of E1 α subunit of the pyruvate dehydrogenase gene has been of special interest because it remains transcriptionally silent in spermatogonia, but is active in spermatocytes (Iannello 97). Assuming that E1 β subunit could reflex E1 α subunit state, PDH activation in F1 animals diverges completely from F0 animals. This difference could lead to an energetic deficiency in spermatozoa causing motility problems.

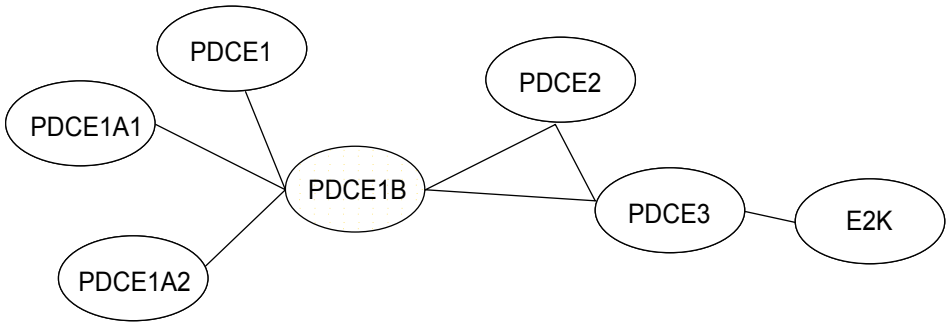

Figure 2.17.- STRING network predictions for spot 2275. Ensemble Danio rerio accession number (ENSDARG00000021346) for the pyruvate dehydrogenase E1 was introduced in STRING (embl.string.de) with the conditions: high confidence 0.900, network depth 2, interactors showed no more than 20. Resulting network based on the identified protein pyruvate dehydrogenase E1 showed relationships between proteins with an overall score superior to 90% of confidence. PDCE1A1: Pyruvate DH Component E1 type A1; PDCE1B: Pyruvate DH Component E1 type B; PDCE1: Pyruvate DH Component E1; PDCE2: Pyruvate DH Component E2; PDCE3: Pyruvate DH Component E3; E2K: α-ketoglutarat DH Component E2.

2.3.6 Relationships between 2-D protein gel analysis and RNA microarray data in F0

Besides the proteomic approach to identify proteins of interest in the spermatogenic process, a microarray analysis of the mRNA of testis from wild *S. senegalensis* was performed. The samples processed were identical to the samples analysed in the proteomic study. Results of this analysis (Castellana and Planas, unpublished data) were then compared with the proteomic experiments.

Two different comparisons were performed in triplicate in an array composed of 5087 oligonucleotids: F0L-F0M and F0Mat-F0L. In the F0L-F0M comparison 20 genes were up-regulated, while 81 down-regulated. In the F0Mat-F0L comparison 25 genes were up-regulated, while 117 down-regulated. One hundred and ten of the sequences in the microarray that were found to be up or down-regulated in any of the comparisons present a related entry with a known gene/protein database.

Seven differential expressed genes (from 243) corresponded with proteins already identified as differential in the proteomic analysis (49 total proteins). Coincident proteins were serine or cysteine proteinase inhibitor (spot 1966), profilin 2 (spot 3233), two genes of proteasome subunits (spots 2738, 2778, 2587, 3690) and two genes of apolipoproteins (spots 2759, 3649). The ubiquitin ligase complex gene was also included in this collection of coincident data because spot 2667 was identified as ubiquitin hydrolase and both proteins are involved in the protein ubiquitination pathway.

The role of two of these gene/protein molecules, proteasome and ubiquitin hydrolase, had been specially adressed in the previous section because their important functions in histone substitution by protamine for proper DNA condensation. However, and despite several isoforms of apolipoproteins have been related with sperm activacion (Akerlof 91, Poussette 93, Leijonhufvud 97), the relevance of the changes observed for this protein was not clear from the proteomics experiments. The main concern was related with the possibility of this changes being derived from the presence of blood in testis samples. Array analyses confirmed that changes in expression of the corresponding gene is actually ocurring during fish spermatogenesis.

Profilin is mainly involved in integrating different signal pathways and transforms the information into actin polymerization/depolimeryzation process. As described for cofilin

(spots 2897, 2898 and 2972) this role is extremely important in cellular sperm maturation and motility.

The low correlation found between mRNA and protein expression values in Senegalese sole testis is already described in literature for other human cancer samples (Huber 03, Chen 02, Orntoft 02, Anderson 97), human pancreas samples (Maziarz 05), murine cell lines (Lian 02, Baik 05) and yeast (Washburn 03, Gygi 99), indicating that protein expression is regulated at other levels than transcription. A higher degree of correspondence is usually found for highly abundant proteins (Celis 00) or for protein pathways considered as a whole (Washburn 03).

Discrepancies between mRNA and protein levels may be attributed to translational regulation, mRNA stability, splicing, post-translational processing regulation, protein degradation, protein turn-over, or a combination of these. The partial analysis of protein isoforms at protein level is also a technical limitation to correlate both expression levels. Negative correlation may reflect negative feedback on the mRNA or the protein or the presence of other regulatory influences not understood currently (Pradet-Balade 01).

All these reasons make hard to predict the overall protein expression based on average mRNA abundance, and, thus, parallel use of DNA microarrays and proteomics provides with a powerful strategy to get new insights into mechanisms by which cells regulates responses to the internal/external environment and to gain a more complete and biologically meaningful picture of the system under study.

In summary, several proteins appear to be implicated in the presence of sperm abnormalities and infertility in F1 Senegalese sole. The major affected processes are the replacement of histones during nuclear condensation, morphogenesis of flagellum, disruption of actin filaments blood-testis barrier, general impaired cell redox and energetic state. All this changes can be caused by the lack of proper hormonal stimulation due to the disruption of the testosterone metabolic pathway.

Chapter 3

Effect of hormone treatments in the testis proteome of cultured *Solea senegalensis.* Study by 2-D DIGE.

In a recent work, Agulleiro *et al*. (2007) demonstrated that the treatment of the Senegalese sole male with gonadotropin releasing hormone agonist (GnRHa) in combination with 11-ketoandrostenedione (OA), a precursor of 11-KT, increases the plasma levels of 11-KT and of the free and sulphated forms of 17,20βP and its metabolites (see Introduction). This combined hormonal treatment accelerated spermatogenesis and markedly increased sperm motility, despite the reduction in the amount of produced milt. Although additional studies are needed to identify the mechanism of action of sex steroids in the testis of the Senegalese sole, this study suggests that GnRHa+OA might be employed as a potential hormonal therapy to ameliorate the reproductive dysfunctions of the captive Senegalese sole male. These data corroborate the role of 11-KT and its precursor testosterone during spermatogenesis in the Senegalese sole as suggested from the experimental observations described in chapter 2.

In collaboration with the group of Dr J. Cerdà, testes from the same animals analyzed in the study described above were evaluated using two complementary expression analysis tools: mRNA microarrays and protein 2-D DIGE gels. Both analyses were performed using the same biological material to provide data without interindividual variations. These analyses have generated information on the variations at the proteome and transcriptome level that could be correlated to the mechanisms of sex steroids and to the physiological changes observed in these animals.

The following chapter is divided in three main parts. The first one is focused on the suitability of 2-D DIGE technology for the study of differentially expressed proteins in the testis of *Solea senegalensis*. As a reference, the F0 samples processed in the previous chapter by 2-DE with conventional procedures are analysed using the DIGE approach. In the second part, once analytical conditions were established, the methodology is then applied to the study of changes of protein levels in testis of the animals treated with hormones in the above-mentioned study. Finally, genomic and proteomic data are correlated.

The whole process of microarray analysis was carried out in the transcriptomic platform of Oryzon Genomics, while the proteomic analyses were performed using the facilities of the CSIC/UAB Proteomics Laboratory, as described in Materials and Methods (Chapter 3).

3.1 Materials and Methods

3.1.1 Fish hormone treatments

Adult Senegalese soles, F1 generation of 1-1.5 year-old, were reared from eggs spawned by different stocks of wild fish acclimated to captivity at the facilities of the "CIFPA-El Toruño" (Puerto de Santa María, Cádiz, Spain). Selected fish were transported to the "Centre of Aquaculture-IRTA". During the adaptation period, fish were fed *ad libitum* once a day with commercial pellets (Proaqua, Spain) and placed in 1,500 l circular tanks (density 0.6-0.8 kg m^{-2}) connected to a recirculated water system for the control of temperature, and maintained at constant photoperiod (13L:11D).

Approximately five months before the hormone treatments were initiated, groups of males (0.79 ±0.03 kg in weight) were maintained under a controlled temperature regime. This regime consisted of a progressive decrease of the temperature from 19.5ºC to 8.5ºC, and a further progressive increase up to 19.5-20ºC, so that fish were maintained below 10ºC for approximately 3 weeks. After this treatment, and when the temperature of the tanks was stable at 19.5-20ºC for approximately two weeks in March, fish were treated with a single Ethylene-Vinyl Acetate implant (Mylonas 98) containing saline (control) or 50 µg kg^{-1} [D-Ala6, Pro9, Net] GnRHa with or without another implant containing 7 mg kg^{-1} OA (Sigma). The males were distributed between six tanks (two tanks per treatment; three fish per tank).

3.1.2 Biological samples

Testis samples from animals in the F0 functional maturation (F0Mat) group were prepared as described in chapter 2, and used as a reference of spermatogenesis stage for wild-caught fish. Testes from 3 individuals of each group of hormonal treatment (control saline, GnRHa and GnRHa+OA) were obtained after 4 weeks of treatment. Fish were sacrificed by stunning and decapitation, and the testes were dissected and weighed, and the GSI was calculated. Testes were divided for further genomic,

proteomic and histological analyses. Samples were frozen in liquid nitrogen and kept at –80 ºC until processed. Transport of these samples was always done in dry ice.

3.1.3 Histological analysis

A piece of each testis was fixed in modified Bouin solution (75% picric acid, 25% formaline) for two hours, then dehydrated, embedded in paraplast (Sigma), sectioned at 5 µm and stained with eosin/hematoxilin or methylene blue/azure II/basic fuchsin. The occurrence of seminiferous lobules, as well as of germinal and somatic cells, in the cortex of the testis was evaluated by microscopic examination by using a Leica DMLB light microscope. Sertoli cells, spermatogonia A, spermatogonia B, spermatocytes I, spermatocytes II, and spermatids were counted in each section. For spermatozoa, the number of cells per seminiferous tubule was also counted on at least 5 different tubules in each section.

3.1.4 Determination of sperm density and motility

The amount of milt produced, the sperm density and the sperm motility duration were determined directly from the testis after fish sacrifice at the end of the hormone treatment, to avoid stressing the animal. The sperm was collected from the whole dorsal testis that was two half sectioned and gently pressed; the volume of milt was then measured by using a micropipette. With this method, milt free of urine could be obtained, and thus its total amount could be measured more accurately. The sperm density was determined on 50- to 100-fold diluted milt samples using a haemocytometer and a Leica DMLB light microscope. The dilution was performed in sperm buffer (150 mM NaCl, 15.2 mM KCl, 1.3 mM $CaCl_2$, 1.6 mM $MgCl_2$, buffered with 5 mM $NaHCO_3$ at pH 8.2). To measure the sperm motility duration, milt samples were diluted 10-fold in filtered seawater and immediately monitored at 200x magnification under the microscope.

The sperm motility duration was defined as the time interval from activation to the cessation of all spermatozoa movement (Lim 04). The morphology of the spermatozoa was examined on a sample of milt diluted 1,000-fold with sperm buffer, and the diameter

and length of the head and tail, respectively, were measured by using the image analysis software AnalySIS (SIS Gmbh).

3.1.5 Protein extraction

Protein for 2-D DIGE purposes was obtained from 3 testes samples of each F0 histological group described in chapter 2 (F0M, F0L and, F0Mat) and from 3 testes samples of each hormone treatment group (Control, GnRHa, GnRHa+OA). For each of them, 50 mg of tissue were disrupted mechanically in 400 μl of TNE buffer (50 mM Tris-HCl pH 7,6; 150 mM NaCl; 2mM EDTA pH 8,0; 1 mM Na_3VO_4; 1 μM Leupeptin; 2 μM Pepstatin; 0.1 μM Aprotinin), then sonicated in water bath at 4ºC for 10 min and NP40, PMSF and DTT were added to achieve 1% v/v, 1 mM and 2 mM, respectively. Afterwards 100 μl from the resulting sample were processed using the 2-D Clean Up kit (GE Healthcare) and the precipitated proteins dissolved with 100 μl of 2-D DIGE labelling buffer (7M urea, 2M thiourea, 4% w/v CHAPS, 30 mM Tris-HCl pH 8,5) at 4ºC during at least 1 hour. Protein from each dissolved sample was quantified using the RcDc kit (Bio-Rad).

3.1.6 Two-dimensional DIGE

Three different 2-D DIGE experiments were performed using the samples described above. First, the labelling process was tested in a self-to-self (S2S) experiment with a pool composed by the F0M, F0L and F0Mat samples. Second, F0M, F0L and F0Mat pools were prepared in a similar way to chapter 2. Finally, testis samples from the hormone treatment experiment and the F0Mat state were analysed together.

In the S2S experiment one pool representing the F0 groups (F0M, F0L and F0Mat) was used to test Cy-labelling. For each gel, three aliquots of 50 μg of protein from the test sample was mixed with 1 μl of a solution of 400 pmols/μl of Cy2 in dimethylformamide (DMF), 1 μl of 400 pmols of Cy3 in DMF, and 1 μl of 400 pmols of Cy5 in DMF, respectively. Samples were prepared to run two identical DIGE gels. Tubes were incubated at 4ºC for 30 minutes in darkness. Then 1 μl of 10 mM lysine in water was added to each tube and incubated at 4ºC in darkness for 10 more minutes. Test

samples labelled with Cy2, Cy3 and Cy5 were mixed. An equal volume of *2x IEF* buffer (7M urea, 2M thiourea, 130 mM DTT, 1% v/v ampholites 3-10 pI (GE Healthcare), bromophenol blue 0,25% w/v) as the resulting mixture was added. Then, a volume of *1x IEF* buffer (7M urea, 2M thiourea, 65 mM DTT, 0,5% v/v ampholites 3-10 pI (GE Healthcare), bromophenol blue 0,12% w/v) necessary to achieve 350 μl was added. Finally HED (DeStreak, GE Healthcare) was added up to 1,2%.

A volume corresponding to 150 μg of protein was loaded into IPGstrips (3-10 L, 18 cm. GE Healthcare). These IPGstrips were processed in an IPGphor II, equilibrated as described in chapter 2, and then loaded over a 12% polyacrylamide gel casted in low fluorescence plates.

Samples were run through the polyacrylamide gels in an Ettan Dalt VI electrophoresis unit (GE Healthcare) at 20ºC (Hetofrig CB refrigerator, Heto) under standard overnight conditions (16:30h at 1 W/gel). Gels were then stored at 4ºC until scanning. Fluorescence images of the gels were acquired on the Typhoon 9400 scanner (GE Healthcare) in the facilities of the Proteomic Laboratory at the Hospital Vall d'Hebron. Cy2, Cy3 and Cy5 images were scanned at 488 nm/520 nm, 532 nm/580 nm and 633 nm/670 nm excitation/emission wavelengths, respectively, and at a 100 μm resolution. Gels were silver stained as described before (Moertz 01) and images acquired in a GS-800 Calibrated Densitometer (Bio-Rad).

For the second experiment, the F0 pools (F0M, F0L and F0 Mat) used in the S2S experiment were analysed under an alternative experimental design. Each pool was labelled separately with Cy3 and Cy5 following the ratio 50 μg protein:400 pmols Cy as described in the S2S experiment. In parallel, aliquots from each pools were mixed together to form the Internal Standard (IS). Enough IS sample (150 μg) for three gels was labelled with Cy2 (labelling ratio 50 μg protein: 400 pmols Cy) as described above. Samples labelled with Cy2, Cy3 and Cy5 belonging to the same gel were mixed (table 3.1) and processed as described for the S2S experiment. IEF, SDS-PAGE, Typhoon gel scanning, silver staining and image acquisition were performed as described for the S2S experiment.

Table 3.1.- Distribution of DIGE evaluation samples in the gels of this experiment.

Gel ID	**Cy 2**	**Cy 3**	**Cy 5**
1	St Int	F0M r1	F0L r1
2	St Int	F0Mat r1	F0M r2
3	St Int	F0L r2	F0Mat r2

For the hormone treatment experiment, the analysed samples were the F0Mat testis and the testis samples of each hormone treatment group (Control, GnRHa, GnRHa+OA). Samples from each group were pooled and resulting pools were labelled separately with Cy3 and Cy5 once or twice (table 3.2) following the ratio 50 μg protein:400 pmols Cy as described in the S2S experiment. Pools were mixed proportionally to form the Internal Standard (IS). Enough IS sample (300 μg) for six gels was labelled with Cy2 (labelling ratio 50 μg protein: 400 pmols Cy) as described above. Samples labelled with Cy2, Cy3 and Cy5 belonging to the same gel were mixed (table 3.2) and processed as described for the S2S experiment. IEF was performed on 24 cm IPGstrips (3-10 L, GE Healthcare). The IEF conditions, SDS-PAGE, Typhoon gel scanning, silver staining and image acquisition were performed as described for the S2S experiment.

Table 3.2.- Distribution of hormone treatment samples in the DIGE gels.

Gel ID	**Cy 2**	**Cy 3**	**Cy 5**
1	St Int	F1 Control r1	F1 GnRHa r1
2	St Int	F1 GnRHa+OA r1	F0Mat r1
3	St Int	F0Mat r2	F1 Control r2
4	St Int	F1 GnRHa r2	F1 GnRHa+OA r2
5	St Int	F0Mat r3	F1 GnRHa r3
6	St Int	F1 Control r3	F1 GnRHa+OA r3

3.1.7 Differential expression analysis and clustering

Fluorescent images were analysed using the Decyder 6.0 software (GE Healthcare). This software package includes two main tools: the Differential In-gel Analysis (DIA) and the Biological Variation Analysis (BVA) modules. The three experiments (S2S, DIGE evaluation and hormone treatment) were studied separately. In the DIA module spots were detected using the following settings of slope (S), volume (Vol), and peak height (PH) for the three different experiments:

1.- S2S:	S>2,5, Vol< 2,5e+4 and 145<PH< 37900
2.- DIGE evaluation:	S>1,8, Vol< 3,8e+4 and 275<PH< 35900
3.- Hormone treatment:	S>1,8, Vol< 4,3e+4 and 360<PH< 38800

In the BVA module, matching was performed using all the fluorescent images included in each experiment. Matching was further refined manually to ensure good quality results. The expression data generated for the S2S experiment was extracted with the XML module and analysed with Excel to determine possible bias derived from different fluorescence or reactivity of the Cy2, Cy3 or Cy5 dyes.

For the DIGE evaluation and the hormone treatment experiments several comparisons were carried out using the BVA module to determine spots with different relative levels (table 3.3). Normalized volume (%Vol) of spots was compared to determine these differences. This value corresponds to the volume of a certain spot in an image divided by the summatory of the volumes of all the spots detected in the same image. The difference between two groups of spots is expressed like in chapter 2 (see page 63).

Determination of the significance of the differences on %Vol between two groups was performed using the p-value (*P*) of the Student's t-test option provided in the Decyder 6.0 package. This *P* represents the probability of obtaining the observed data if the two compared groups have the same protein abundance. If *P* between two groups is 0,01, the probability of obtaining the observed difference in protein abundance by stochastic variation is 1%. Only differences with $P \leq 0.05$ (i.e. 95% of probability) were assumed to be statiscally significant. The value displayed in tables is the probability to obtain the observed difference not because of stochastic variations [(1-*P*)*100].

A hierarchical clustering was performed as described in chapter 2, with normalized volume data for spots present in all gels from the hormone experiment referred to F0Mat values.

Table 3.3.- Comparisons performed in the BVA module of Decyder for the DIGE evaluation and the hormone experiments.

EXPERIMENT		*DIGE evaluation*		*Hormone treatment*
Comparison	1	Mid vs. Late	1	F0 Mat vs. F1 Control
	2	Late vs. Mat	2	F0 Mat vs. F1 GnRHa
	3	Mid vs. Mat	3	F0 Mat vs. F1 GnRHa+OA
	--	-------	4	F1 Control vs. F1 GnRHa
	--	-------	5	F1 Control vs. F1 GnRHa+OA
	--	-------	6	F1 GnRHa vs. F1 GnRHa+OA

3.1.8 Protein identification

Protein identification, bioinformatic analysis of MS/MS spectra and comparison of sequenced peptides and identified proteins with *S. senegalensis* ESTs were carried out following the same procedures described in chapter 2.

3.1.9 Microarray analysis of testis transcriptome in hormone-treated fish.

The mRNA from 3 testis samples for each hormone treatment group (Control, GnRHa, GnRHa+OA) was extracted using a RNeasy kit (Qiagen) following supplier instructions. Concentration of total RNA was then measured using a Nano-drop 1000 spectrophotometer (Nanodrop). RNA purity was calculated from the 260/280 nm and 260/230 nm absorbance ratios. RNA integrity was measured using 200 pg of total RNA in a RNA 6000 Pico LabChip with a Bioanalyzer 2001 (Agilent). Preparation of cDNA from mRNA was performed using the Message Amp kit II-96 for RNA (Ambion), following supplier instructions. The resulting double strand cDNA sequences were labelled with the incorporation of Cy3 or Cy5 nucleotides (Cy3/Cy5-CTP Perkin Elmer) during an *in vitro* transcription to cRNA. Labelled cRNA was purified and its quality

checked in the Nanodrop 1000 spectrophotometer and the Bioanalyzer 2001. Samples from individuals in the same histological state were analyzed in triplicate in a different array each time. Arrays were DNA 11K-chips (Agilent) composed of the 10,000 *S. senegalensis* ESTs generated inside the Pleurogene project as described in chapter 2. The GnRHa state (Cy3) was compared with the Control state (Cy5) in one triplicate, and with the GnRHa+OA state in the other triplicate. DNA-cRNA hybridizations were detected in the DNA microarray scanner (Agilent) using a 10 μm resolution and 30% of photomultiplier range for red (Cy3: 532 nm/580 nm) and green (Cy5: 633 nm/670 nm) channels. Data from microarray scans were then obtained using the Feature Extraction software (Agilent). Statistical analysis of results was made using Polyphemus, a software developed at Oryzon Genomics. This software first filters the data with values under background mean plus 3 times its standard deviation. In a second step, Polyphemus normalizes data to balance possible experimental variability and fluorescence levels of sample compared in each array. Normalization is performed using the local regression model LOWES to correct the non linear intensities and increase the quality of the analysis. This correction is performed thanks to the addition of fluorescent standard at several intensities in each hybridization assay. Finally, comparisons between states are performed and array spots with variations higher than three standard deviations and $P \leq 0{,}01$ are taken into account to elaborate the biological meaning of the results.

3.2 Results

3.2.1 Effect of hormone treatments on spermatogenesis

The effect of the GnRHa and GnRHa+OA treatments on spermatogenesis was evaluated by histological examination of the testis cortex. This region is where the developing germ cells are located, and holds the seminiferous lobules, opposed to the medullar region, which contains the efferent duct system that collects and stores the sperm (figure 3.1; García 05). Fish from all experimental groups showed production of sperm on day 28 of treatment, although differences in the occurrence of Leydig cells and in the progression of spermatogenesis were observed. The spermatogenic process appeared to be stimulated in both treated groups with respect to controls, since the percentage of spermatogonia B, spermatocytes I and spermatids per seminiferous tubule in the testis of GnRHa-treated fish were higher than those in the saline-treated fish. According to the stimulatory effect of GnRHa, the number of spematozoa per seminiferous tubule was higher in males treated with GnRHa than in control males. However, fish treated with GnRHa+OA showed the same amount of spermatozoa per seminiferous tubules as controls, but presenting the most advanced stage of spermatogenesis of both treatments.

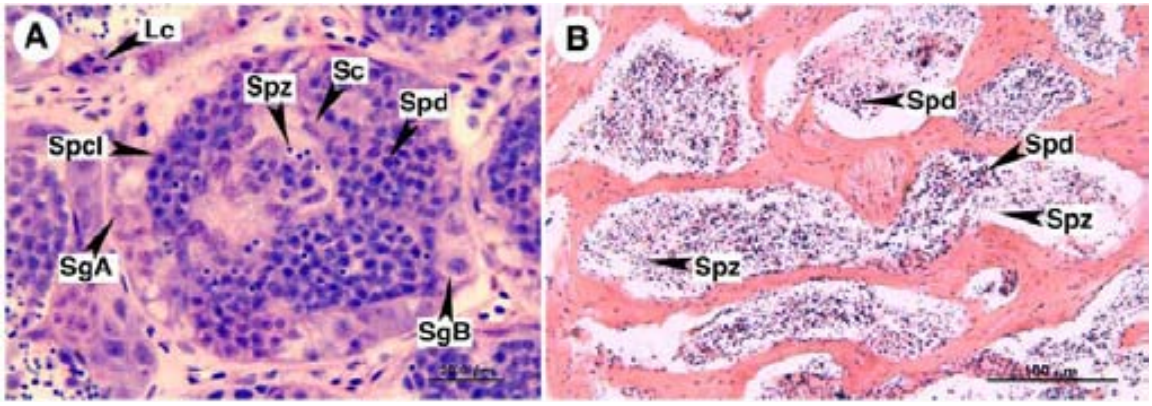

Figure 3.1.- Photomicrographs of histological sections of Senegalese sole testis stained with methylene blue/azure II/basic fuchsin (A) or hematoxilin and eosin (B). (A) Section of the cortical area of the testis showing a seminiferous lobule containing spermatogonia A (Spg A), spermatogonia B (Spg B), spermatocytes I (Spc I), spermatids (Spd) and spermatozoa (Spz). Sertoli (Sc) and Leydig cells (Lc) adjacent to the lobules are also indicated. (B) Section of the medullar area of the testis in which efferent tubules filled with Spd and Spz can be observed.

3.2.2 Determination of GSI, sperm density and motility

Following the fish sacrifice and the removal of the testis from each male at the end of the experiment, the GSI and the production of milt by each group was evaluated (figure 3.2, Annex III.1). The analysis revealed that the GSI values remained similar before and after the experiment. Regarding to milt production, the treatment with GnRHa alone increased significantly the volume produced with respect to the control males. Since there were no differences in the density of the sperm between the different treatments, the production of spermatozoa by this group appeared to be increased, in agreement with the histological results. In contrast, males implanted with GnRHa+OA present volumes of milt in the testis not significantly different from controls. However, determination of spermatozoa motility after its activation in seawater revealed that GnRHa+OA-treated males produced spermatozoa that were approximately twice more motile than those produced by the control and GnRHa-treated males, while there were no differences in the diameter and length of the head and tail, respectively, of the spermatozoa produced by the different groups.

3.2.3 Two-dimensional DIGE: self-to-self analysis

Two gels were performed with a pool sample representing the three F0 groups (figure 3.3). This pool sample was labelled separately with Cy2, Cy3 and Cy5, mixed and processed in a 2-D gel. For each spot, the normalized volumes of the signals from the different fluorochrome emitters were measured. A mean value of the normalized volume (%Vol) for each spot-emitter was calculated from these two gels. Finally, a linear regression analysis was used to determine the analytical bias. The r factor for the three comparisons (Cy2/Cy3, Cy3/Cy5 and Cy2/Cy5) was ≥ 0,99, indicating a good correlation between normalized %Vol of the spots labelled with Cy2, 3 and 5 (figure 3.4). Similar studies for silver stained gels are already available in the literature, resulting in correlation values between 0,98 and 0,96 (Quero 04, López 01).

Therefore, the set-up labelling procedure was able to label the same sample in rather identical grades with the three different cyanines. Observed variations in further expression analysis should not be produced by the labelling procedure.

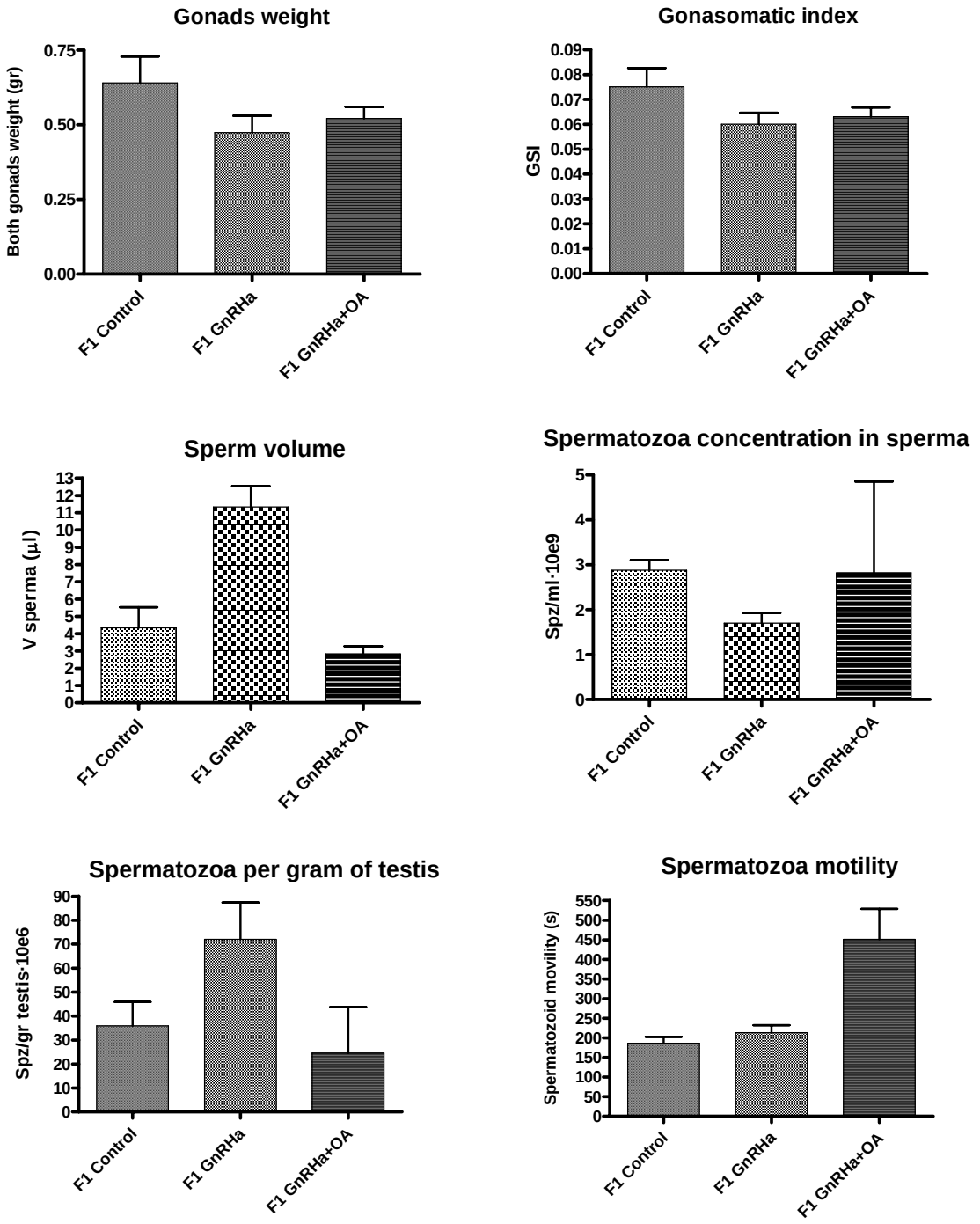

Figure 3.2.- Effect of GnRHa (50 µg kg-1) with or without OA (7 mg kg-1) on gonadosomatic index (GSI), spermatozoa (Spz) production, milt production and sperm motility duration in the Senegalese sole.

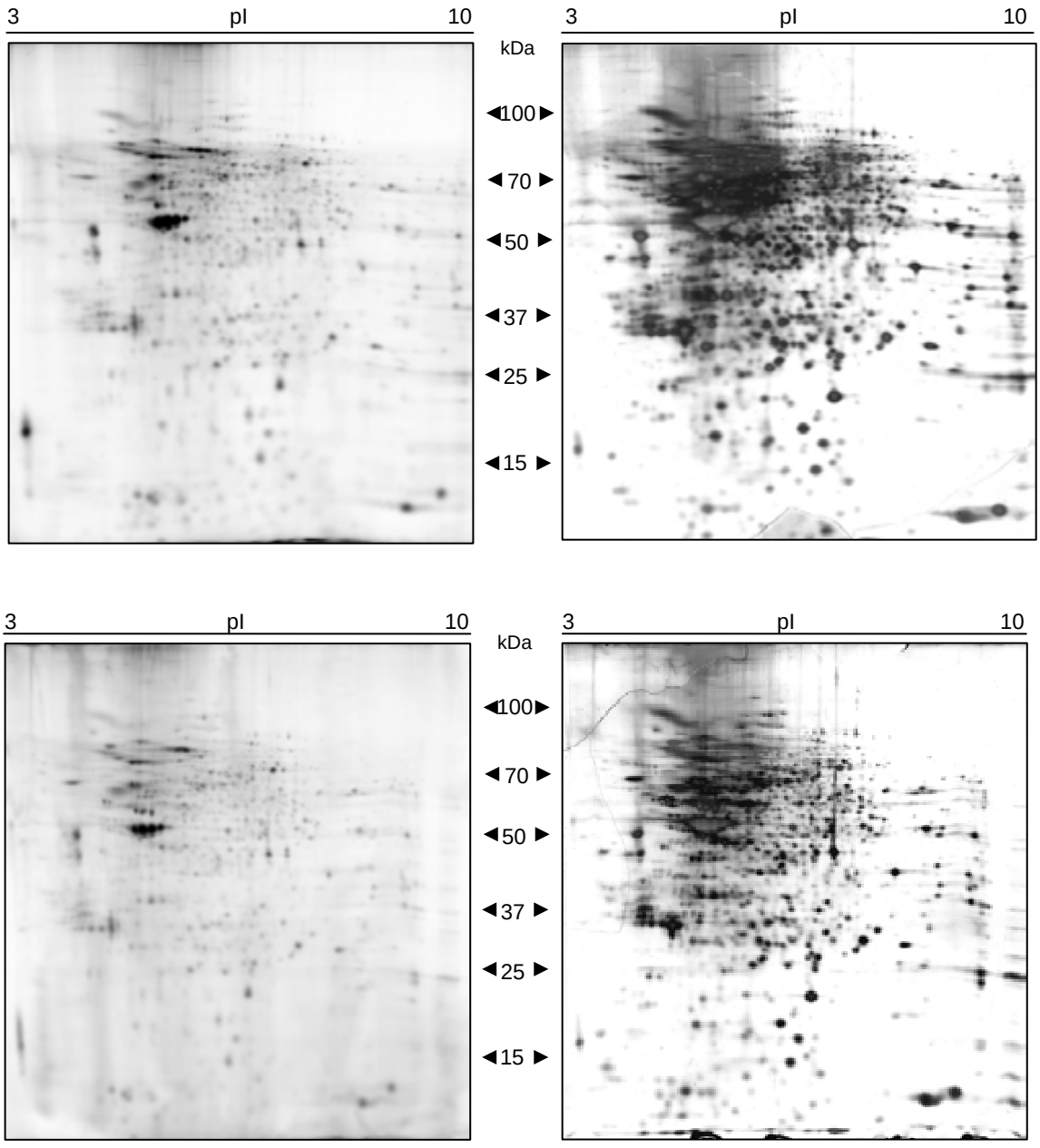

Figure 3.3.- Gels analysed in the S2S experiment (*pI* range 3-10 L and *Mr* range 150-10 kDa). In the left side, the total fluorescence image (Cy2+Cy3+Cy5) acquired in the Typhoon scanner (GE Healthcare). In the right side, image of the silver stained gel obtained in the GS800 densitometer (BioRad).

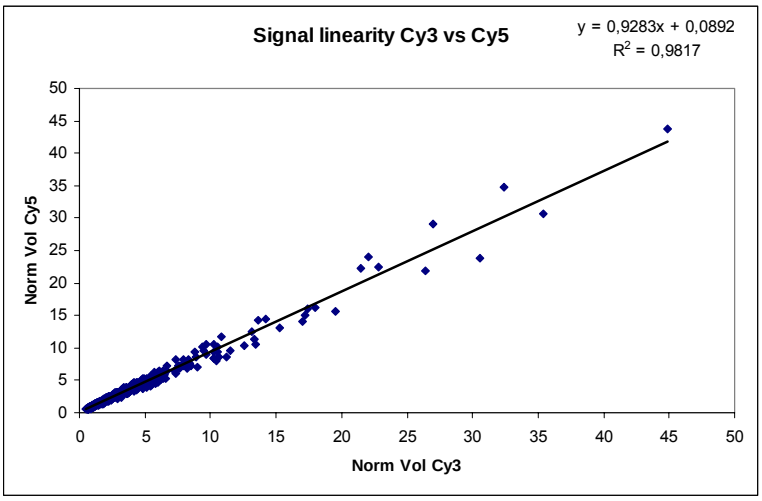

Figure 3.4.- Determination of labelling linearity. The figure compares the normalized volume of spots from the same protein sample of Senegalese sole testis labelled with Cy3 and Cy5. For the other comparisons the regression curve is y=1,1x-0,24 and r=0,99 (Cy2-Cy3) and y=1,0x-0,15 and r=0,99 (Cy2-Cy5).

3.2.4 Two-dimensional DIGE: evaluation experiment

Three gels were performed with the sample distribution described in table 3.1. The number of spots detected was 1555, 1782 and 1597 for gel 1, gel 2 and gel 3, respectively (figure 3.5). The number of spots matched between all three gels was 1183. Expression differences between samples were determined using the Decyder 6.0 statistical package. Three comparisons were performed between states, resulting in 15 spots with differential levels in at least one comparison with a minimum variation of ±1,4 and a confidence ≥95% (table 3.4, figure 3.6). Eleven proteins were unambiguously identified using *de novo* sequencing of tryptic peptides and BLAST analysis of candidate sequences. In one case the spot was assigned to 2 different proteins, another spot identification was not possible although three peptides were sequenced, and two spots were analysed without results because of the low amount of material present in the sample (table 3.5).

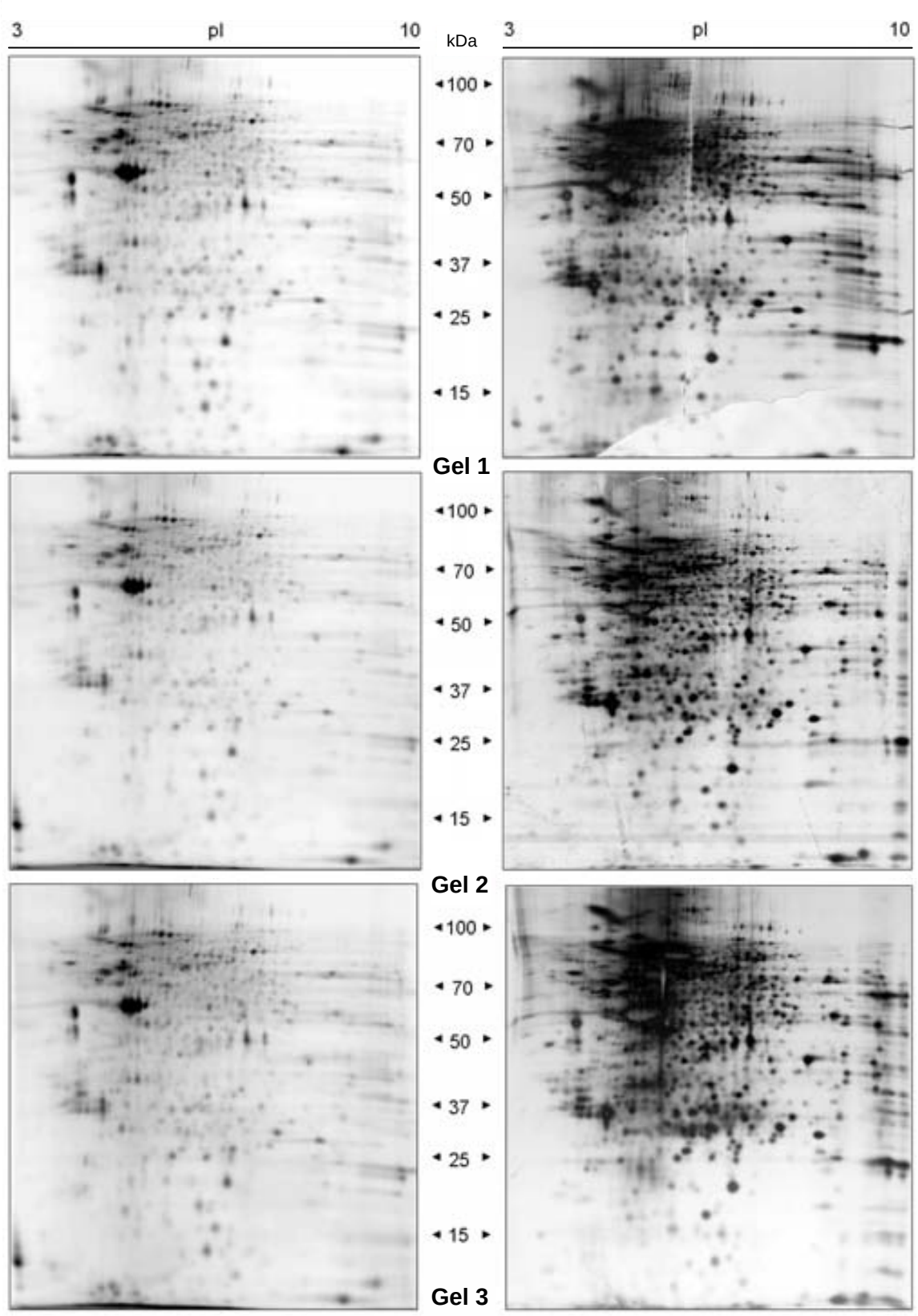

Figure 3.5.- Gels analysed in the DIGE evaluation experiment (*pI* range 3-10 L and *Mr* range 150-10 kDa). In the left side, the total fluorescence image (Cy2+Cy3+Cy5) acquired in the Typhoon scanner (GE Healthcare). In the right side, image of the silver stained gel obtained in the GS800 densitometer (BioRad).

Resulting proteins were compared with the list of proteins from the experiment in chapter 2 with silver stained gels. Differential proteins identified as carbonic anhydrase (1403-DIGE) and as a mixture of carbonic anhydrase and apolipoprotein AI (1400-DIGE) were also characterized in the 2-DE expression analysis in chapter 2 (spots 2578-silver and 3649-silver, respectively). Protein profile between studied states (F0 Mid, F0 Late and F0 Functional maturation) in spot 1403-DIGE was very similar to the expression profile in spot 2578-silver. The profile of variations among the three states is slightly different for the pair of spots 1400-DIGE:3649-silver (figure 3.7). This difference between abundance profiles was probably a consequence of the mixture of proteins underneath this spot in the DIGE analysis.

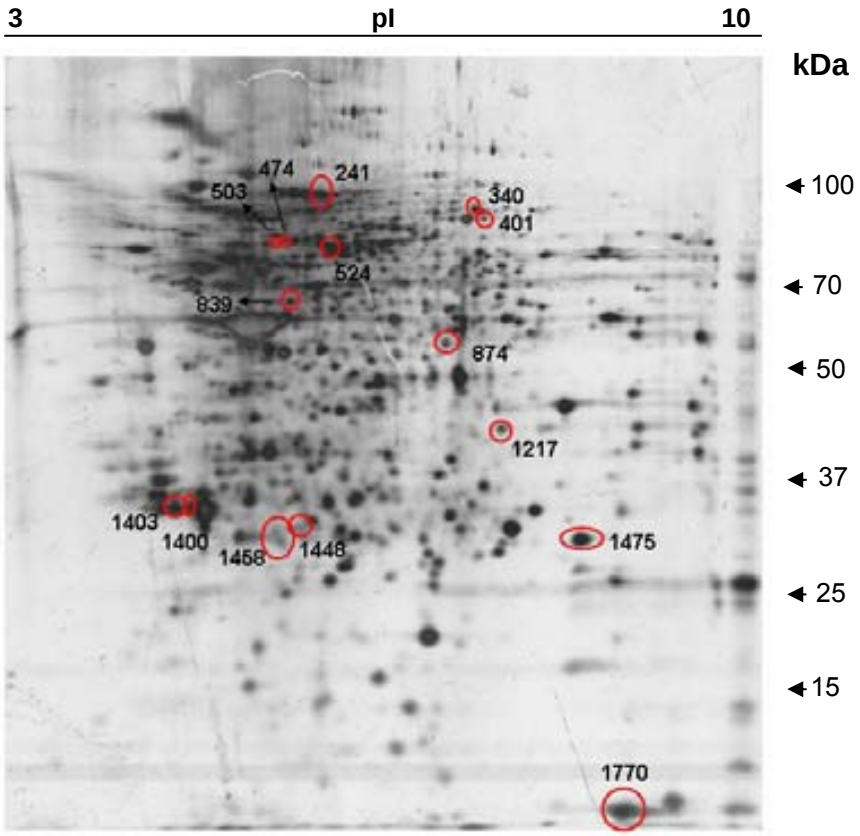

Figure 3.6.- Differentially expressed spots in the DIGE evaluation experiment excised from gel 2. Gel range: *pI* 3-10L, *Mr* 150-10 kDa.

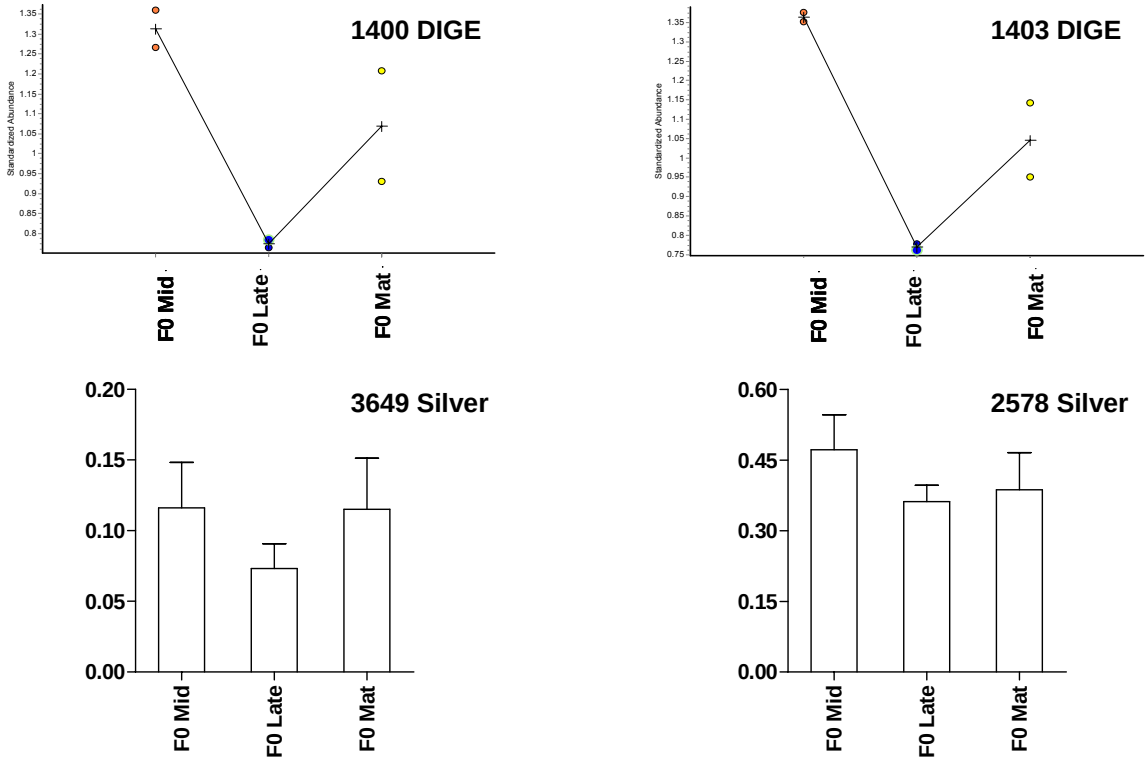

Figure 3.7.- Protein profile of coincident spots between 2-D DIGE and 2-D Silver-stained gels in the differential expression analysis of F0 Mid, F0 Late and F0 Functional maturation spermatogenesis stages in *S. senegalensis* (1403-DIGE with 2578-silver; 1400-DIGE with 3649-silver).

Table 3.4.- Expression changes for the differential spots detected by 2-D DIGE in the analysis of sole testis. *p*>: probability in percentage of obtaining the observed difference not because of stochastic variation (only probabilities >95% are described) Δ: variation values. Variation was calculated as vali/valj where vali=max (val1, val2) and valj=min (val1, val2). Variation is indicated as a positive value in case of overexpression and as a negative value in case of subexpression.

Spot ID	Acc Num	Prot ID	Comparison					
			L/M		Mat/L		Mat/M	
			p > (%)	Δ	p > (%)	Δ	p > (%)	Δ
241	gi|6959826	Transferrin	98,1	-1,42	----	1,04	97,9	-1,36
340	gi|47223919	Complement C3	99,59	-1,53	98,8	1,47	----	-1,04
401	gi|31872040	Transketolasa	98,5	1,45	99,23	-1,72	----	-1,18
474	gi|37681753	Chaperonin containing TCP1	96,4	1,41	----	-1,30	----	1,08
503	gi|41053915	Ubiquitin specific protease 14	----	1,05	94,8	-1,48	97	-1,41
524		No ID	97,7	-1,28	99,9	1,42	----	1,11
839	gi|47210587	GDP-dissociation inhibitor	----	1,22	97,7	-1,41	----	-1,16
874	gi|22671694	Aldolase C	----	-1,43		1,00	99,86	-1,42
1217	gi|47221006	Calponin C	91,7	-1,26	96,5	1,41	----	1,12
1400	gi|56554783/ gi|60417202	Carbonic anhydrase/ Apoliprotein AI	99,5	-1,7	----	1,38	----	-1,23
1403	gi|56554783	Carbonic anhydrase	99,95	-1,77	----	1,36	----	-1,30
1448	gi|55251222	Peroxiredoxin 6	----	1,20	96,2	-1,57	----	-1,31
1458		No ID	98,9	1,20	99,6	-1,4	98,8	-1,17
1475		No ID	----	-1,25	----	-1,24	99,66	-1,56
1770	gi|22002420	Alpha type globin	99,46	-1,6	98,3	1,69	----	1,06

Table 3.5.- Protein identification by *de novo* sequencing of the 2-D DIGE differential spots detected in the analysis of sole testis (see table 3.4). *nESI-MS/MS*: Peptide sequences obtained from *de novo* sequencing of nESI-MS/MS data from trypsin digested spots (table 4) are displayed in two columns depending on the software used (Peaks 2.4 or Lutefisk 97). For Peaks characters, colours indicate probability (%) of the corresponding residue to be correct. (Red = 99-80%; Blue= 79-60%; Cyan= 59-40%; Black=<40%). Brackets in Lutefisk 97 column contain the mass in Da not assigned to any sequence. Rank-Score for Lutefisk97 indicates position of the candidate sequence within any individual de novo sequencing search and the probability of this sequence to be correct (values from 1 to 0, where 1 is maximum probability). *PROTEIN ID*: NCBI access number and name of the protein that was identified with each sequence using BLAST search for short nearly exact sequences.

nESI-MS/MS					PROTEIN ID	
Spot ID	Peaks 2.4		Lutefisk 97		NCBI	Name
	Sequence	Score %	Sequence	Rank-Score		
241	(CamC)DGYNGAFR	68	[276.1]GYNGAFR	1 0.289	gi|6959826	Transferrin
	YLNLVQSLK	53	YLNLVKSLK	2 0.970		
	SAGFPLNAVGR	47	[158.0]GWNLPMGR	1 0.929		
	LLNWQGSDVSR	44	LLNWKGSDVSR	1 0.970		
	SSPAGPV(CamC)SAFEK	79	[174.0]PAGPVCSKFAK	1 0.582		
	QPWAQNLLADDYR	36	[225.2]WAKNLLADDYR	1 0.970		
	DSGL(CamC)EL(CamC)TGD(CamC)SK	59	SDGLCELCTGDCSK	1 0.923	gi|6959826	Transferrin
	RF(CamC)AFNPAAGVLDVR	99	[273.1]DLVGAAPNFACER	1 0.970		
	EDQTAMT(CamC)NLAKVAPHAVEAR	49	[158.0]TMRETCNPSKVPAHAV[200.0]R	1 0.392	gi|6959826	Transferrin
	ELSLLLNSLNAVENFNLFG(CamC)R	26	[228.0]YYNNSLNAVENFNLF[217.0]R	1 0.532	gi|6136041	Transferrin
340	(CamC)GLRAAASK	71	AYDDHRR	1 0.435		
	M(CamC)VYLQAQFPDR	26	MCVYLKAKFS[281.2]	4 0.605	gi|47223919	Complement C3
401	(CamC)MTKENGELVDRDFVK	99	MLFKENDANGRAF[271.1]R	1 0.348		
	SPPT(CamC)TLFYPSDRMWR	69	[202.0]VGERLFYPSDRSTER	1 0.488	gi|31872040	Transketolase

Table 3.5 (continuation).- *De novo* peptide sequencing for protein identification in the set up of DIGE approach for the analysis of sole testis proteome.

nESI-MS/MS						PROTEIN ID	
Spot ID	Peaks 2.4		Lutefisk 97			NCBI	Name
	Sequence	Score %	Sequence	Rank-	Score		
474	WVGGPELELLALATNR	97	WVGGPELELLALATNR	3	0.970	gi|37681753	Chaperonin containing TCP1
	FQNGWGSAGLSGWGDKK	24	FKNGWGSLMDLRNTR	1	0.762		
	ALETFPFDPNNTESLHK	94	[313.0]TFPFDPNNTE[210.2]VR	1	0.739	gi|37681753	Chaperonin containing TCP1
	NTYPSSNSSYGSNGSYGSGWRR	14	[403.2]GLSGYSGGGSGYSSNSGT[386.1]	1	0.209		
503	LPAYLTVQMVR	50	LPAYAKLKMVR	1	0.435	gi|41053915	Ubiquitin specific protease 14
	DDRQETGVKPDR	75	[198.1]LFANTGVK[211.1]R	3	0.504		
	SSTNGWGSLQSGWYHK	50	[226.1]YGWGTVKSGRAMVR	1	0.539		
524	DNKARLYPR	50	DFMHATAE[210.2]	1	0.257		
	T(CamC)QDPANGDQNK	29	[261.1]KDYFDRSR	1	0.428		
	TTLVNAASMDANVLR	50					
839	MLMYPYTR	97	MLLLTKVTR	1	0.923		
	TTESSASGTREGK	23	[202.0]MSSAEPGVFGK	1	0.342		
	LQL(CamC)DSPYAPDR	28	KLLCDPSYALVR	1	0.933	gi|47210587	GDP-dissociation inhibitor
	MTGSDFDFGEMER	49	MTGSDFDEFGMATL	1	0.970	gi|47210587	GDP-dissociation inhibitor
	DMTVSDLYEPTDR	74	[246.0]TVSDLYEPTDR	1	0.730	gi|47210587	GDP-dissociation inhibitor
	TDDYLDQP(CamC)LDTLNR	88	[331.1]YLDKPCLDTLNR	1	0.970	gi|47210587	GDP-dissociation inhibitor
	SPYLYPLYGLGELPKFKR	24	[232.0]NNYPLYGLGELHYEAR	2	0.719	gi|47210587	GDP-dissociation inhibitor
874	QLLFTADKR	17	[258.0]PFTANER	1	0.339	gi|22671694	Aldolase C
	SPQASALNAWR	17	[184.1]VVSALNAWR	2	0.470		Aldolase C
	GSHQYPALTPEQK	51					Aldolase C
	MMGPTPSELALLENANVLAR	32	[279.1]HTPSELALLENANVLAR	3	0.970		Aldolase C
	RVPLAGTDGETTTQGLDGLSER	38	N[158.0]S[202.0]NLGKTTTEGDTGA[291.0]R	1	0.608		Aldolase C
1217	AAELGGKPPR	99	[188.0]TTYGLPR	1	0.755		
	AAVAFGLTGEVK	75	SGPAFGLSAEVK	1	0.970	gi|47221006	Calponin 1
	MFHDPVDKSTLSLQMDER	14	[260.0]RNPVDAGSTLSLKM[244.0]R	1	0.805		

Table 3.5 (continuation).- *De novo* peptide sequencing for protein identification in the set up of DIGE approach for the analysis of sole testis proteome.

nESI-MS/MS					PROTEIN ID	
Spot ID	Peaks 2.4		Lutefisk 97		NCBI	Name
	Sequence	Score %	Sequence	Rank-Score		
1400	LLDAFDSLK	98%	LLDAFDSLK	1 0.970		
	WVANFPLADGPR	73%	SVVANFPLADGPR	1 0.970	gi|56554783	Carbonic anhydrase
	LDDMVNQLESLR	50%	[228.0]DMVNGALESLR	1 0.970		
	KWW(CamC)EHSPLDLVHHMFYHGVLYWR	17%	[469.3]SKMGNKASLYPPNTKPSKFNVGHPK	1 0.329		
	NNGKADVPAP(CamC)KHVR	99%	[171.0]NKADVPAPCKHVR	1 0.756		
	DPTASLDDVENPLGYK	67%	241.2]AASNDDVELPLGYK	4 0.642		
	GRTPVTDSVVTTLAEATAELR	17%	[201.0]LPVTDWVTTLAEATAELR	1 0.970	gi|60417202	Apolipoprotein AI precursor
	YVYDLVPWASDYE(CamC)LDMMK	49%				
1403	WVANFPLADGPR	82%	SVVANFPLADGPR	1 0.970	gi|56554783	Carbonic anhydrase
	G(CamC)YYLVPWATT(CamC)PPPNDVYK	30%	[408.2]NLHRCTTALLGVLD[253.2]R	1 0.258		
	RDMEEAEEE(CamC)(CamC)MMDNYRQTFRK				gi|56554783	Carbonic anhydrase
	YDWRG(CamC)DDLLLGYREHETMDDNDSSTLTDGH(CamC)WYK				gi|56554783	Carbonic anhydrase
1448	SSSDLELR	27	NFDLELR	1 0.372		
	YLYGKGAR	52	YLYKGGAR	5 0.634		
	LSLLYGDPWK	31	[199.1]LLYPATTGR	1 0.661		Peroxiredoxin 6
	MHLLGDVFPNPFVDGYRR	99	[267.2]LLGDVFPNFEADTTLGR	2 0.970	gi|55251222	Peroxiredoxin 6
1770	LQVDYDPPK	38	LKVDNNPFK	1 0.970		
	FLQNVALALSEK	99	FLKNVALALSKE	1 0.970	gi|22002420	Alpha type globin
	MMTPEVKVSVDK	84	DFTPEVKVSVDK	3 0.970		
	SSGLAEAGLLDSHQK	99%	[184.1]LNSDLLGAEALGR	1 0.970		
	LLSHSLQLVLAMYYPK	74	LLSHSLKLVLAMYYPK	2 0.970		
	ALWAVEGLDDLKLNLSR	20	[184.1]WAVEGLDDLKLNLSR	1 0.970		
	YTFSHWSDLSPTSEVKK	54%	TYFSHWSDLSPTSEKVK	1 0.970	gi|22002420	Alpha type globin

3.2.5 Two-dimensional DIGE and clustering: hormone treatments analysis.

Six gels were performed with the sample distribution described in table 3.2. The number of spots detected was 1596, 1564, 1586, 1453, 1475 and 1412, from gel 1 to 6, respectively (figures 3.8 and 3.9). The number of spots matched between all six gels was 1014. Expression differences between samples were determined using the statistical package in Decyder 6.0. Six comparisons were performed between states and fifty-nine spots were selected. Only the 691 spots present in all images were taken into account. These spots were differently expressed in at least one comparison with a minimum average variation of ±1,7 and a confidence value ≥ 95% (figures 3.10 and 3.11; table 3.6). Spots were classified by similarity on their protein levels profile, similar to chapter 2 (page 83).

Less than 40 out of the 691 spots (5%) present in all images of the hormone treatment analysis showed variations over ±2 in the comparisons performed between the analyzed states. This percentage increased to 12% when minimum variation was ±1,6. These figures indicate the range of spots with differential levels expected to be observed using a DIGE approach when studying the testis proteome of *S. senegalensis* under the studied hormone treatments.

For 2-DE analysis in chapter 2, about 65 out of the 489 spots (13%) present in all gels showed variations over ±3. This percentage increased to 20% when minimum variation changes to ±2,5. Comparing the values obtained for 2-DE and DIGE experiments, spots changing ±1,6 times represents around the 50% of the total spots, for only 12% in the DIGE approach. Therefore, using DIGE better than a silver-based protein detection method allowed observing smaller variations in gel-based differential expression analysis.

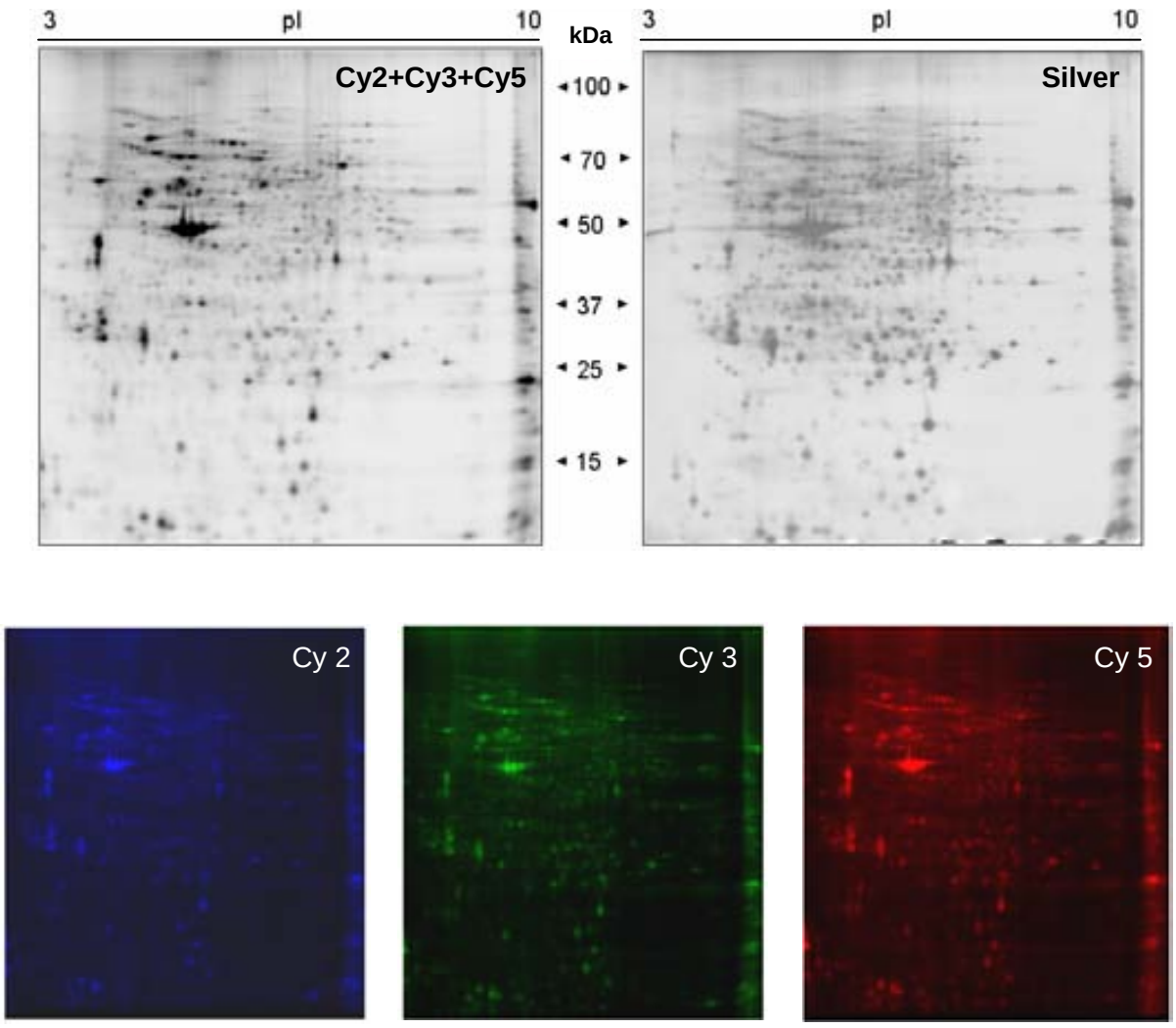

Figure 3.8.- Fluorescent images and silver stained image of gel 1 in the hormone treatment study (*pI* 3-10 L ; *Mr* 150-10 kDa acquired on a Typhoon 9400 scanner. Cy2, Cy3 and Cy5 images were scanned at 488nm/520 nm, 532 nm /580 nm and 633 nm/670 nm excitation/emission wavelengths respectively, at a 100-μm resolution.

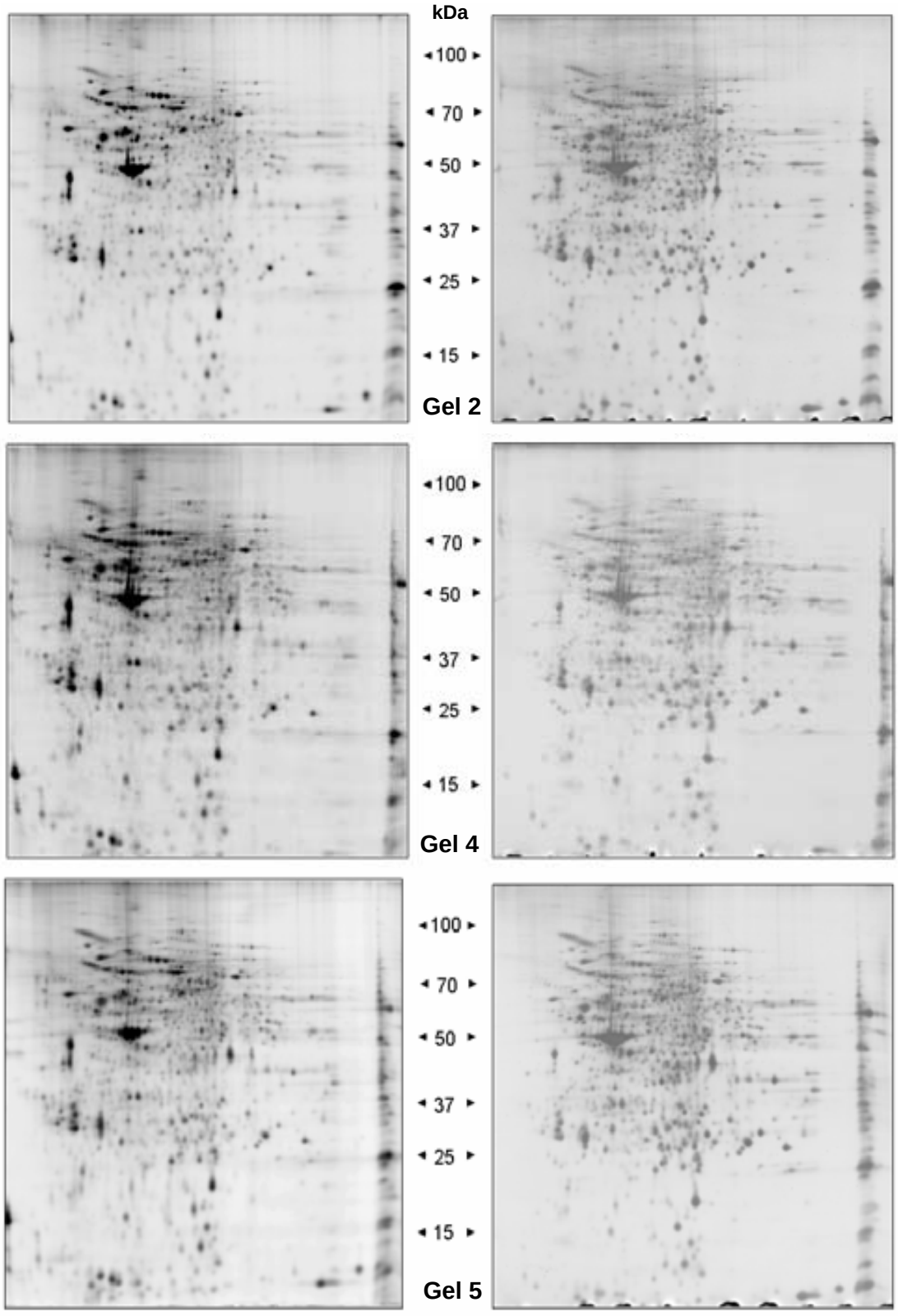

Figure 3.9.- Gels 2, 4 and 5 analysed as part of the hormone effect studies (pI 3-10 L; Mr 150-10 kDa). In the left side, the total fluorescence image, and in the right side the image of the silver stained gel obtained in the GS-800 densitometer.

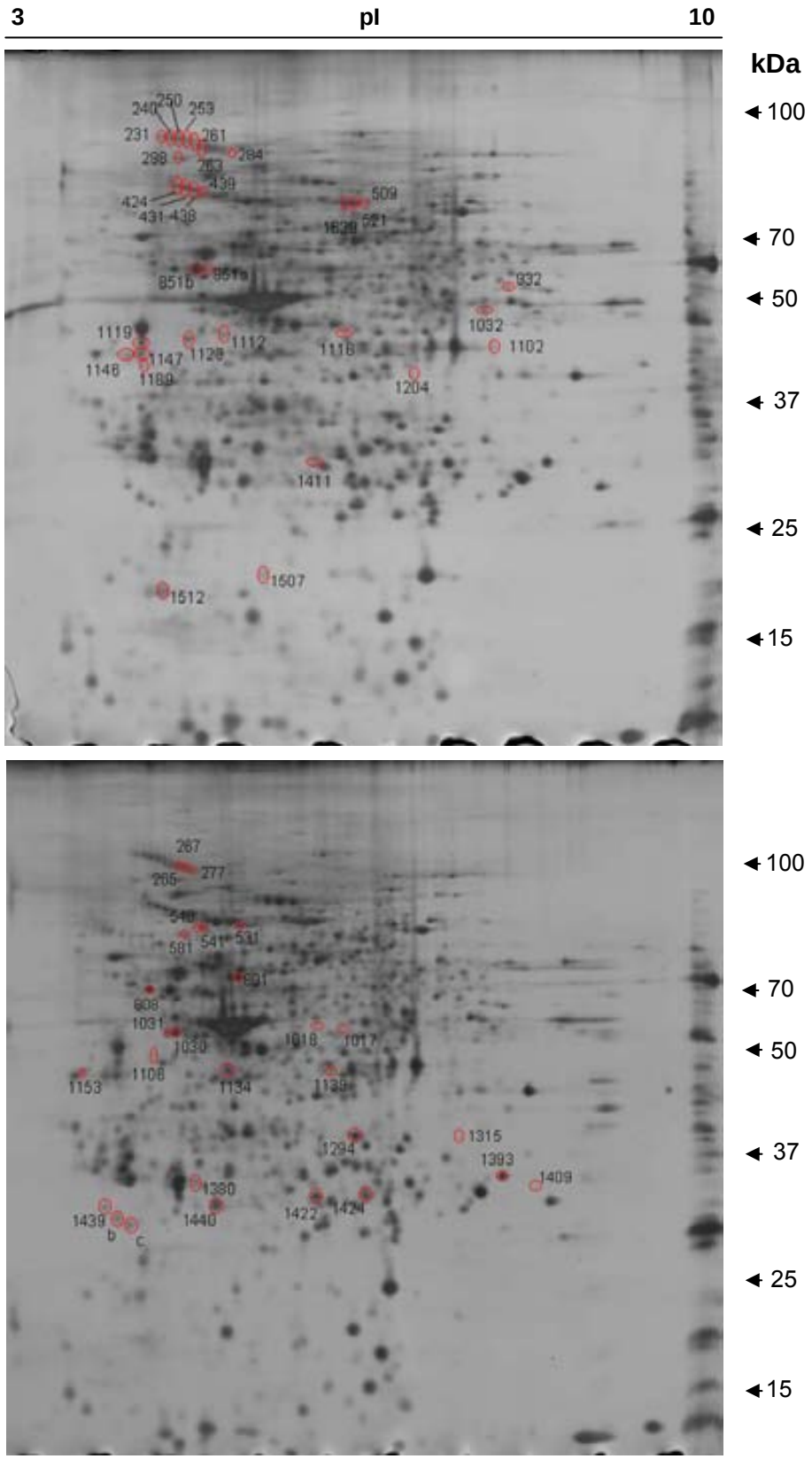

Figure 3.10.- Differentially expressed spots in the hormone treatment study excised from gel 1 (up) and 2 (down). Gel range: *pI* 3-10L, *Mr* 150-10 kDa.

Table 3.6.- Protein level changes for the spots submitted to identification in the analysis of hormone effect over testis proteome. p>: probability in percentage of obtaining the observed difference not because of stochastic variation (only cases with probabilities >95% are shown) Δ: variation values. Variation was calculated as vali/valj where vali=max (val1, val2) and valj=min (val1, val2). Variation is indicated as a positive value in case of overexpression and as a negative value in case of subexpression.

Spot ID	NCBI	Prot ID	Comparison											
			F0Mat-F1C		F0Mat-F1GnRHa		F0Mat-F1GnRHa+OA		F1C-F1GnRHa		F1C-F1GnRHa+OA		F1GnRHa-F1GnRHa+OA	
			p > (%)	Δ	p > (%)	Δ	p > (%)	Δ	p > (%)	Δ	p > (%)	Δ	p > (%)	Δ
231		No ID	99,99	-1,66	99,9	-1,48	99,99	-3,27	----	1,12	99,99	-1,96	99,99	-2,21
240	gi|47224921	Alpha-2-macroglobulin-1	99,99	-2	99,9	-1,45	99,99	-2,53	99,7	1,38	97,5	-1,27	99,9	-1,74
250	gi|47224921	Alpha-2-macroglobulin-1	99,99	-2,27	99,99	-1,48	99,99	-2,22	99,99	1,53	----	1,02	99,99	-1,5
253	gi|47224921	Alpha-2-macroglobulin-1	99,99	-2,72	99,99	-1,71	99,99	-2,14	99,9	1,59	99,3	1,27	99,7	-1,25
261	gi|47224921	Alpha-2-macroglobulin-1	99,99	-2,8	99,99	-1,9	99,99	-2,15	98,7	1,48	97,5	1,3	----	-1,13
263	gi|47224921	Alpha-2-macroglobulin-1	99,40	-1,50	99,8	-1,82	99,8	-2,5	95,1	-1,21	99,0	-1,67	----	-1,37
265	gi|47224921	Alpha-2-macroglobulin-1	----	-1,1	----	1,25	99,5	-1,66	98,4	1,37	99,6	-1,52	99,9	-2,08
267	gi|47224921	Alpha-2-macroglobulin-1	----	1,04	98,0	1,58	99,99	-1,79	97,6	1,52	99,99	-1,85	99,9	-2,82
277	gi|47224921	Alpha-2-macroglobulin-1	95,0	-1,14	98,9	1,31	99,99	-1,9	99,9	1,5	99,99	-1,66	99,99	-2,5
284	gi|47224921	Alpha-2-macroglobulin-1	97,2	-1,91	----	-1,34	99,1	-2,34	98,4	1,42	95,5	-1,23	99,9	-1,75
298	gi|31323728	Chaperone protein GP96	99,9	1,55	96,1	-1,39	97,5	-1,51	99,6	-2,15	99,6	-2,34	----	-1,09
424	gi|74096001	Hemopexin	99,98	-1,98	----	-1,02	99,99	-1,64	99,99	1,94	98,9	1,21	99,99	-1,61
431	gi|74096001	Hemopexin	99,98	-2,15	----	-1,16	99,9	-1,67	99,99	1,85	99,5	1,29	99,9	-1,44
438	gi|74096001	Hemopexin	99,99	-2,07	99,6	-1,28	99,99	-1,57	99,99	1,61	99,9	1,32	99,9	-1,22
439		No ID	99,96	-1,96	98,9	-1,39	99,7	-1,56	99,8	1,4	99,4	1,25	87,0	-1,12
509		No ID	96,1	-2,14	----	-1,61	97,1	-2,11	----	1,33	----	1,02	76,0	-1,31
531	gi|74096001	Hemopexin	99,95	-1,40	99,8	-1,41	99,7	1,23	----	-1,01	99,99	1,72	99,99	1,73
540	gi|59710087	Keratin	95,4	-1,13	95,5	1,3	99,8	2,28	98,9	1,46	99,9	2,56	98,5	1,75
541	gi|59710087	Keratin	----	-1,01	----	1,21	99,99	3,19	98,2	1,23	99,99	3,23	99,99	2,63

Table 3.6 (continuation).- Protein level changes for the spots submitted to identification in the analysis of hormone effect over testis proteome.

Spot ID	NCBI	Prot ID	Comparison											
			F0Mat-F1C		F0Mat-F1GnRHa		F0Mat-F1GnRHa+OA		F1C-F1GnRHa		F1C-F1GnRHa+OA		F1GnRHa-F1GnRHa+OA	
			p > (%)	Δ	p > (%)	Δ	p > (%)	Δ	p > (%)	Δ	p > (%)	Δ	p > (%)	Δ
581	gi|59710087	Keratin	99,93	-1,41	----	-1,11	99,9	1,62	97,6	1,27	99,99	2,29	99,8	1,81
801	gi|37362196	Cytosolic non-specific dipeptidase	----	1,00	99,4	-1,32	99,9	1,38	99,8	-1,33	99,99	1,38	99,99	1,83
808		No ID	99,3	-1,54	96,2	-1,21	98,8	1,29	94,8	1,28	99,9	2	99,7	1,56
851a	gi|47218629	ATP synthase β-subunit	99,8	-1,84	99,7	-1,67	99,3	-1,59	----	1,1	----	1,16	----	1,06
851b	gi|47218629	ATP synthase β-subunit	----	-1,08	97,3	-1,18	----	-1,08	95,1	-1,09	----	1,01	98,0	1,1
932		No ID	----	1,11	99,6	-1,44	99,9	-1,85	99,8	-1,59	99,99	-2,04	96,1	-1,28
1017	gi|61403546	3-hydroxyisobutyryl-Coenzyme A hydrolase	----	-1,09	99,0	1,39	99,7	-1,91	98,8	1,52	99,1	-1,74	99,9	-2,65
1018		No ID	----	-1,89	----	1,13	----	1,09	96,3	2,13	97,2	2,06	12,0	-1,03
1030	gi|47212109	Keratin 18	99,5	-1,25	----	-1,1	99,99	1,72	95,0	1,14	99,99	2,15	99,99	1,89
1031	gi|47212109	Keratin 18	99,9	-1,41	95,6	-1,12	99,9	1,48	99,9	1,26	99,99	2,08	99,99	1,66
1032	gi|54035446	Proteasome 26S subunit ATPase 6	99,9	1,53	----	-1,23	98,2	-1,4	99,6	-1,88	99,9	-2,15	64,0	-1,14
1102	gi|56718619	Glyceraldehyde 3-phosphate dehydrogenase	99,89	-2,97	99,5	-2,67	99,8	-2,72	----	1,11	----	1,09	2,0	-1,02
1106	gi|37682099	Keratin 8	99,0	-3,41	99,9	-2,88	99,99	-4,08	----	1,19	----	-1,2	86,0	-1,42
1112		No ID	99,96	-2,23	99,0	-1,52	99,6	-1,55	98,9	1,47	99,6	1,44	13,0	-1,02
1116		No ID	----	1,00	98,3	-1,76	99,7	-1,83	98,1	-1,75	99,7	-1,82	9,0	-1,04
1119	gi|28557116	Tropomyosin	98,9	-1,18	99,99	1,84	99,9	1,49	99,99	2,17	99,99	1,76	99,6	-1,23
1123	gi|47213546	Keratin S8 type I	99,99	-3,29	99,99	-1,77	99,99	-2,07	99,99	1,85	99,99	1,59	99,9	-1,17
1134	gi|47216949	Annexin A3	----	-1,02	----	1,15	99,99	-1,6	----	1,17	99,99	-1,57	99,9	-1,84
1139	gi|74310597|	NADH dehydrogenase 5	97,6	1,63	98,3	1,73	----	-1,15	95,8	1,06	99,9	-1,87	99,9	-1,99
1146	gi|66792936	Tropomyosin 4 isoform 1	99,99	-1,53	99,99	1,29	----	1,03	99,99	1,97	99,99	1,58	99,9	-1,25
1147	gi|74136103	Tropomyosin 2	99,98	-1,74	99,7	1,26	----	1,07	99,99	2,2	99,99	1,86	98,9	-1,18
1153		No ID	----	-1,26	----	-1,32	99,3	2,05	----	-1,05	99,9	2,58	99,99	2,7

Table 3.6 (continuation).- Protein level changes for the spots submitted to identification in the analysis of hormone effect over testis proteome.

Spot ID	NCBI	Prot ID	Comparison											
			F0Mat-F1C		F0Mat-F1GnRHa		F0Mat-F1GnRHa+OA		F1C-F1GnRHa		F1C-F1GnRHa+OA		F1GnRHa-F1GnRHa+OA	
			p > (%)	Δ	p > (%)	Δ	p > (%)	Δ	p > (%)	Δ	p > (%)	Δ	p > (%)	Δ
1189	gi|41054657	HEAT-like repeat containing 1	98,9	-1,17	99,9	1,57	99,8	1,27	99,9	1,83	99,9	1,49	96,9	-1,23
1204	gi|68372040	similar to oxidative-stress responsive 1	99,98	-2,05	99,9	-1,59	99,6	-1,72	96,9	1,28	----	1,19	57,0	-1,08
1294	gi|94482754	3-hydroxyisobutyrate dehydrogenase	99,8	1,52	99,7	1,3	98,3	-1,25	----	-1,17	99,9	-1,9	99,9	-1,63
1315		No ID	99,99	-2,59	----	-1,04	96,2	-1,21	99,99	2,48	99,9	2,14	91,1	-1,16
1380		No ID	98,7	-2,57	----	-2,04	97,3	-2,05	----	1,26	----	1,25	3,0	-1
1393	gi|47227808	Short-chain dehydrogenase/reductase	99,1	1,52	----	1,09	98,4	-1,44	99,9	-1,39	99,99	-2,19	99,99	-1,57
1409	gi|51858534	LRP16 protein	----	2,79	----	1,12	99,4	-1,54	----	-2,5	96,7	-4,3	99,99	-1,72
1411	gi|37362126	Glutathione S-transferase	99,9	1,63	98,4	-1,29	96,7	-1,22	99,99	-2,1	99,99	-1,99	67,0	1,05
1422	gi|56789119	Peroxiredoxin 6	97,0	1,14	99,9	1,33	99,99	2,03	99,8	1,17	99,99	1,78	99,99	1,52
1424	gi|47193903	Peroxiredoxin 6	----	-1,02	99,99	-1,34	99,99	-2,89	99,99	-1,31	99,99	-2,83	99,99	-2,16
1439	gi|57157763	Apolipoprotein A-IV1	99,63	2,49	99,6	2,55	99,9	3,21	33,0	1,02	99,9	1,29	99,3	1,26
1439 b	gi|68400425	Proteasome subunit beta type 5	99,8	1,58	99,99	1,78	99,8	1,54	96,6	1,13	37,0	-1,02	98,3	-1,15
1439 c		No ID	99,2	1,57	97,0	1,37	99,5	1,72	96,9	-1,15	----	1,1	99,1	1,26
1440	gi|37722017	Ubiquitin C-terminal hydrolase	99,9	1,58	96,0	1,15	97,6	-1,18	99,99	-1,38	99,99	-1,87	99,99	-1,36
1507	gi|51858515 gi|67772036 gi|47939430	Ferritin subunits (H, M, L)	99,99	-7,69	99,99	-8,88	99,9	-6,34	----	-1,15	----	1,21	----	1,4
1512	gi|37779086 or gi|33991794	Putative transient receptor protein 2 or Myosin light chain	99,99	1,62	99,99	2,69	99,99	2,36	99,99	1,67	99,99	1,46	97,6	-1,14
1639		No ID	97,10	-2,48	----	-1,69	----	-2,25	----	1,46	----	1,1	----	-1,33

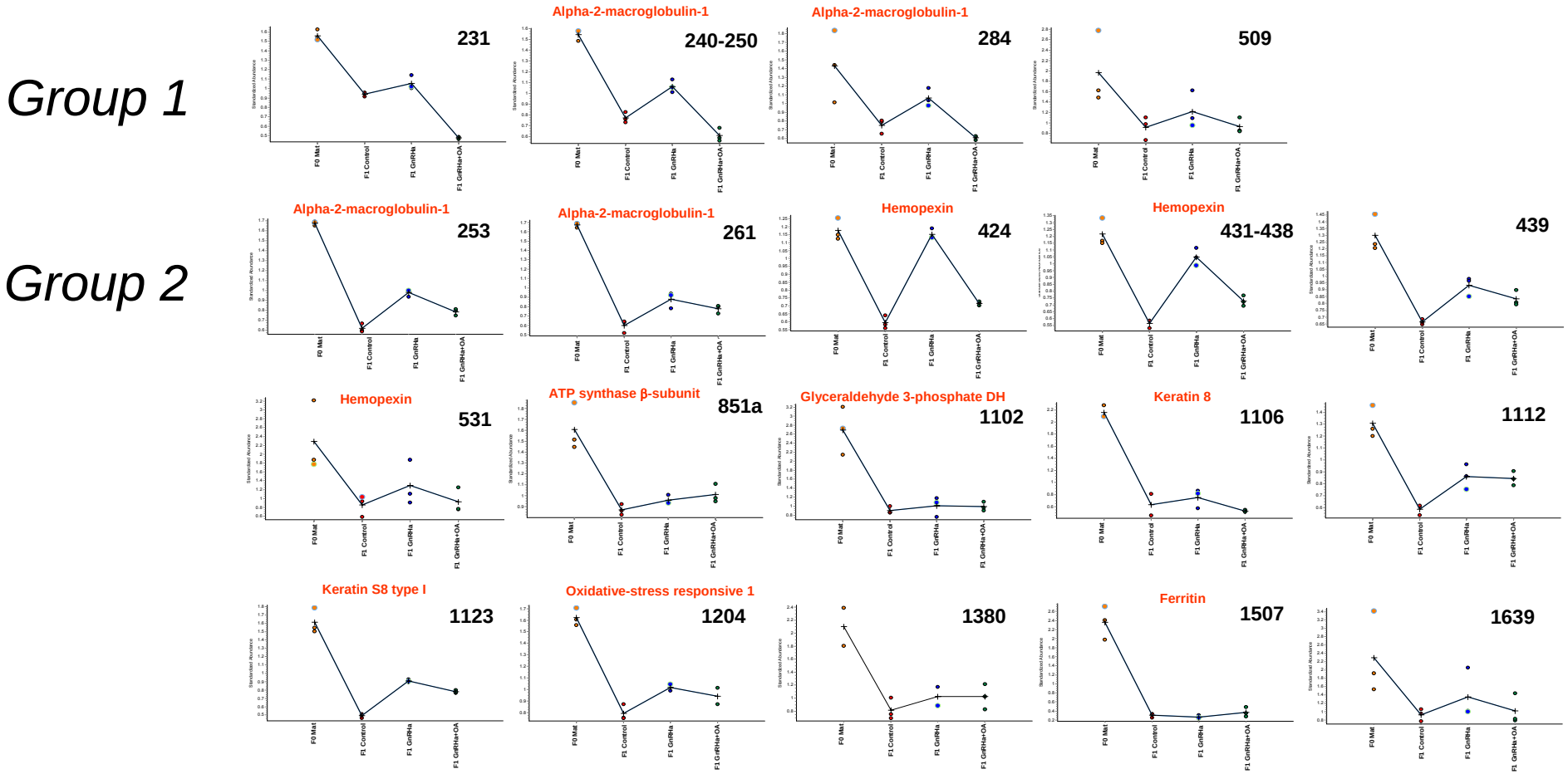

Figure 3.11.- Protein level profiles of the spots selected after differential expression analysis for the hormone treatment study. In each graphic the mean %Vol in each studied state with its individual measures and the identification of this protein are displayed, when available. Graphics are classified in nine groups depending on the protein level profile resulting from connecting mean %Vol values in each of the four studied states (F0Mat, F1 Control, F1 GnRHa and F1 GnRHa+OA).

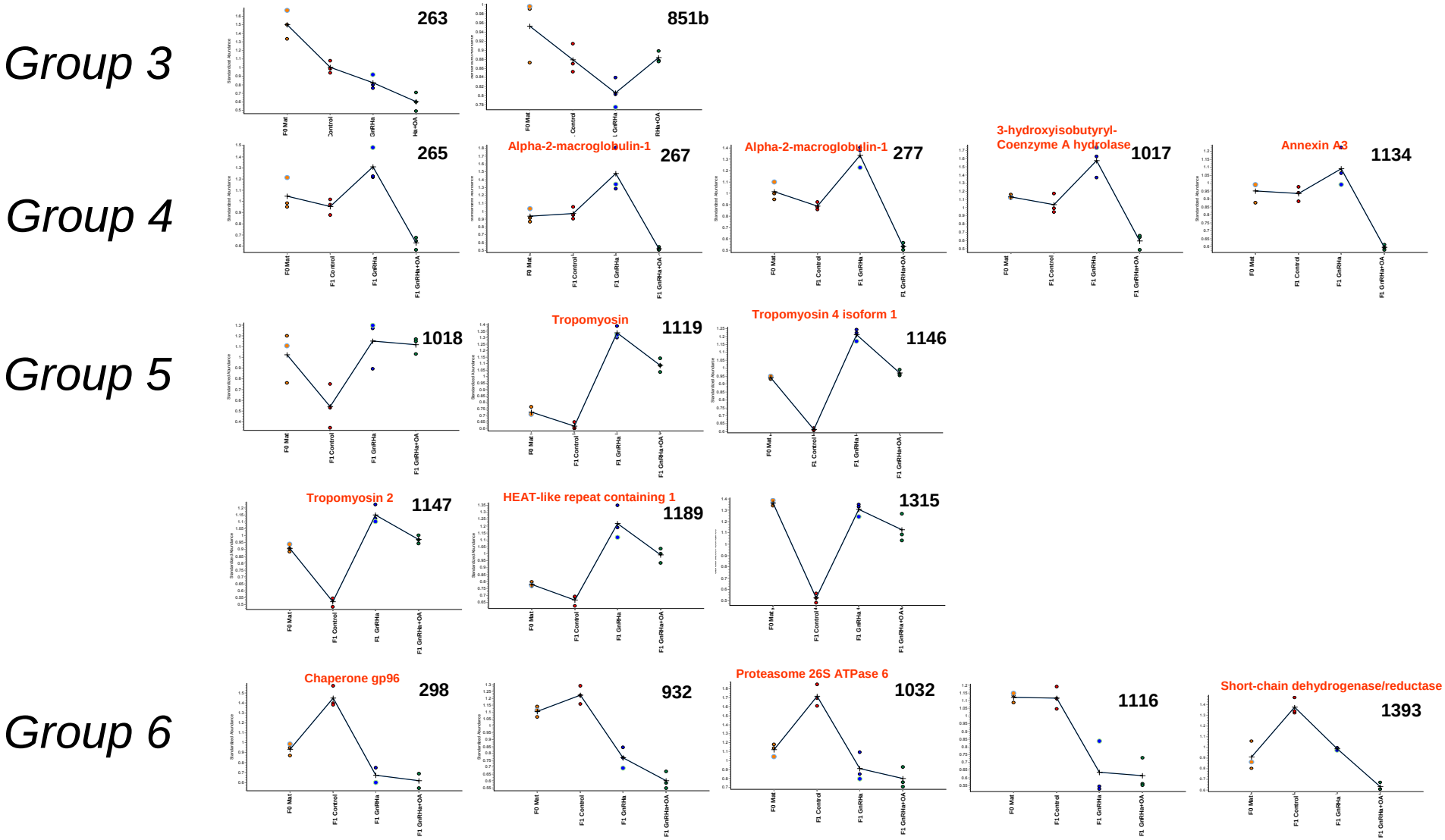

Figure 3.11 (continuation)

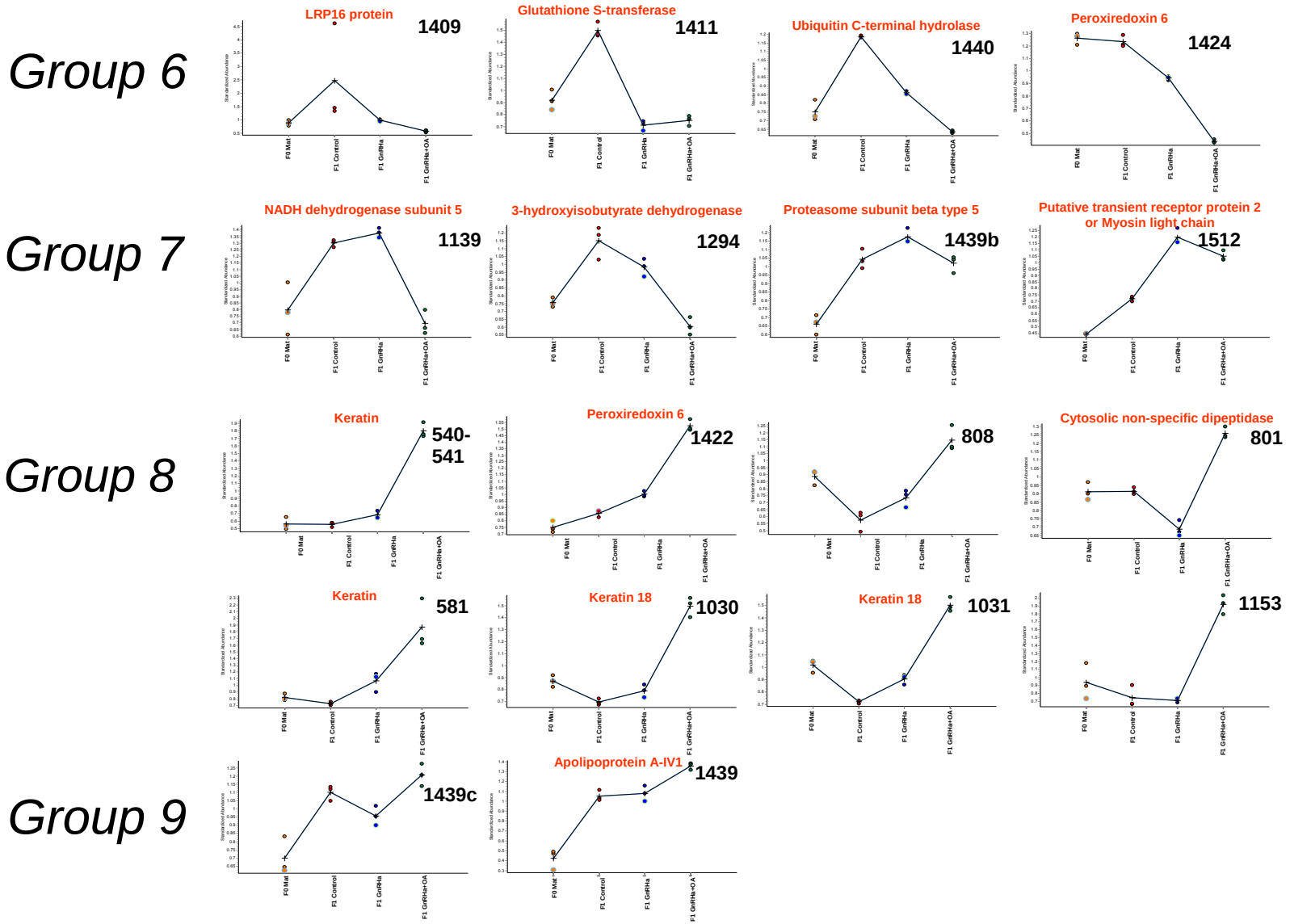

Figure 3.11 (continuation)

Normalized volume data of spots present in all images along the gels on the hormone experiment was referred to F0Mat state values. Clustering of these data from hormone treatment was performed with Cluster 3.0 and visualized with Java TreeView 1.0.7, unveiling five main subtrees of spots (figure 3.12).

The classification of spots in both manual and informatic clustering showed similar patterns of spot distribution (see colour legend in table 3.7), except for group 2 of figure 3.11. This was splitted in three different subtrees, unveiling more profiles in this group than that determined by manual classification. As in chapter 2 (see page 86), this type of protein level profile classification was used as a main guide when discussing biological function of spots with similar protein abundance patterns.

Table 3.7.- MS/MS analyzed spots from 2-D DIGE gels present in expression data clustering subtrees from the hormone treatment experiment. Spots were highlighted to display the classification group in figure 3.11. *Legend* = : Groups 6+9+7; : Groups 8+3+5; : Groups 1+4; : Group 2.

Subtree	Spots	Protein ID
1	326, 1116, 851a, 261, 1507, 801, 1153, 531, 1031, 1030	Alpha-2-macroglobulin-1, No ID, ATP synthase β-subunit, Alpha-2-macroglobulin-1, Ferritin, No ID, Cytosolic non-specific dipeptidase, No ID, Hemopexin, Keratin 18, Keratin 18
2	581, 808, 439, 1112, 1018, 1315, 1189, 1147, 1146, 1119, 424, 1512, 540, 541, 1422	Keratin, No ID, No ID, No ID, No ID, No ID, HEAT-like repeat containing 1, Tropomyosin 2, Tropomyosin 4 isoform 1, Tropomyosin, Hemopexin, Putative transient receptor protein 2 or Myosin light chain, Keratin, Keratin, Peroxiredoxin 6.
3	250, 253, 1102, 431, 1123, 1639, 267, 277, 1134, 265, 240, 284, 1204, 1017, 231	Alpha-2-macroglobulin-1, Alpha-2-macroglobulin-1, Glyceraldehyde 3-phosphate dehydrogenase, Hemopexin, Keratin S8 type I, No ID, Alpha-2-macroglobulin-1, Alpha-2-macroglobulin-1, Annexin A3, Alpha-2-macroglobulin-1, Alpha-2-macroglobulin-1, Alpha-2-macroglobulin-1, similar to oxidative-stress responsive 1, 3-hydroxyisobutyryl-Coenzyme A hydrolase, Alpha-2-macroglobulin-1.
4	1409, 1032, 1411, 298, 932, 1424, 1393	LRP16 protein, Proteasome 26S subunit ATPase 6, Glutathione S-transferase, Chaperone protein GP96, No ID, Peroxiredoxin 6, Short-chain dehydrogenase/reductase.
5	1439, 1440, 1139, 1294	Apolipoprotein A-IV1, Ubiquitin C-terminal hydrolase, NADH dehydrogenase 5, 3-hydroxyisobutyrate dehydrogenase.

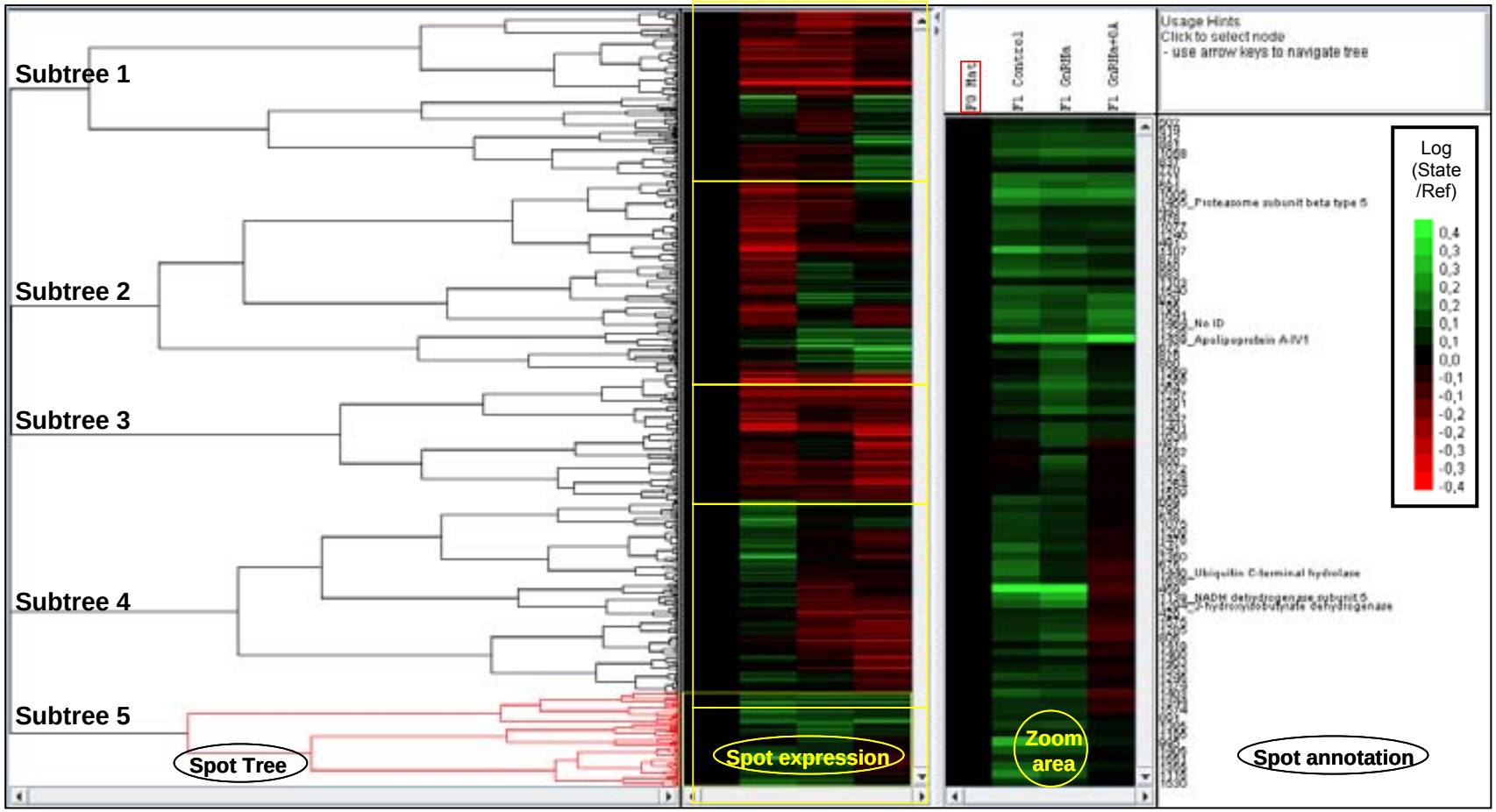

Figure 3.12.- Dendrogram of the spots present in all gel images from the hormone treatment study. Six subtrees are visible from the “Spot tree“ panel. Relative spot expression to F0Mat state (red squared) is displayed in the “Spot expression” panel, where Subtrees are divided by yellow lines. The “Zoom area” and “Spot annotation” panel are focused on the subtree 5. Spot belonging to this subtree are displayed with ID when available. Colour code: green= overexpression; red= underexpression; black= no change.

3.2.6 Mass spectrometry and bioinformatic analysis

The fifty-nine excised spots were digested with trypsin and the resulting peptides analysed using tandem mass spectrometry. Spectra were processed with Peaks 2.4 and Lutefisk97. Following the procedures optimized for the analysis of the MS data in chapter 2, Peaks 2.4 was used as the main *de novo* sequencing engine while candidates coming from Lutefisk were used as confirmatory. Only when Peaks provided no candidates, Lutefisk sequences were used instead. A final number of 355 tentative sequences were compared to NCBI database using BLAST to determine the protein of origin (table 3.8). Forty-eight spots were correlated with described proteins, while 7 spots were sequenced (1-7 sequenced peptides), but no protein was identified. No sequence was possible from the other three spots, probably because of the low amount of material. The assigned proteins were identified by homology of sequenced peptides to fish species like *Danio rerio* (19 spots), *Tetraodon nigroviridis* (12 spots), *Takifugu rubripes* (8 spots), *Oncorhynchus mykiss* (1 spot), *Micropterus salmonoides* (1 spot), *Pleuronecetes platessa* (1 spot), *Siniperca chuats* (1 spot) or *Pagrus major* (1 spot), and to other species like *Xenopus sp.* (2 spots) and *Cylindrophis ruffus* (1 spot). The coverage of the identified proteins with the sequenced peptides used to assign the protein is detailed in Annex III.2.

The *Mr* and *pI* values of each identified spot were calculated using Decyder tools and compared with the *Mr* and *pI* values given by Expasy tools for every identified protein. Deviation between both experimental and theorical values was calculated as (Experimental value -Theoretical value) / (Experimental value + Theoretical value) for *Mr*, while for *pI* was calculated as Experimental value -Theoretical value (Annex III.3). In the corresponding graphic distributions of these values, it was observed that most of the predicted *pI* values from database sequences were greater than those from experimental data. This trend was also observed for the proteins identified during the 2-DE comparison of cultured and wild fish in chapter 2. Contrarily, predicted and theoretical *Mr* was randomly distributed in this experiment and no general tendency could be observed.

.

Table 3.8.- *De novo* peptide sequencing for protein identification in the analysis of hormone effect over testis proteome. nESI-MS/MS: Peptide sequences obtained from *de novo* sequencing of nESI-MS/MS data from trypsin digested spots (table 4) are displayed in two columns depending on the software used (Peaks 2.4 or Lutefisk 97). For Peaks characters, colours indicate the probability (%) for the corresponding residue to be correct. (Red = 99-80%; Blue= 79-60%; Cyan= 59-40%; Black=<40%). Brackets in Lutefisk 97 column contain the mass in Da not assigned to any sequence. Rank-Score for Lutefisk 97 indicates position of the candidate sequence within any individual de novo sequencing search and the probability of this sequence to be correct (values from 1 to 0, where 1 is maximum probability). PROTEIN ID: NCBI access number and name of the protein that was identified with each sequence using BLAST search for short nearly exact sequences (Sequence position inside the protein for each peptide in Annex III.2).

nESI-MS/MS					PROTEIN ID	
Spot ID	Peaks 2.4		Lutefisk 97		NCBI	Name
	Sequence	Score	Sequence	Rank-Score		
240	LLQLSYSLNSEAR	32%	EPKLSYSLNSEAR	2 0.975	gi|47224921	Alpha-2-macroglobulin-1
	MDVLLQDQNLVVK	43%	[246.0]VLLKGNTYFSK	1 0.990		
	WDYQVLLTVGDEK	24%	[188.0]LYKVLLTVGDEK	4 0.864		
	VYDVLELEDANDNR	48%	MP[248.1]LELEDAN[248.1]H	1 0.620		
	QVDVQDQTVTEWVSFK	4%	[227.1]DHWETVTKDKVPAR	1 0.990		
	MQHSL(CamC)GLSALDKWEPK	21%	[185.0]PNSLCGLSALDKSVLLK	1 0.990	gi|47224921	Alpha-2-macroglobulin-1
	Q(CamC)EHLDLTADVEEEYHR	33%	FM[276.1]LDLTADVEEE[158.0]GLK	1 0.767		
250	QPELSYSLNSEAR	12%	LLKLSYTVDSKAR	1 0.523	gi|47224921	Alpha-2-macroglobulin-1
	EDTLLQGWLNVVK	26%	FVVLWNGKLVNAR	1 0.904		
	DWYQVLLTVGDEK	22%	[218.1]GDMAVLLTVGDEK	1 0.990		
	MMDVLEELDANNDR	29%	MMDVLEELDANNDR	1 0.836		
	QVDVQDQTVTEWVHPK	4%	[227.1]DVKDKTVTEWV[234.1]K	1 0.990		
	WWSH(CamC)GLSALDQWEPK	22%	[202.0]GHSLCGLSALDKSVLLK	1 0.990	gi|47224921	Alpha-2-macroglobulin-1
	QMGTHLDLTADVEEEYHR	36%	[212.1]DFEEEVDATLDLVD[194.1]K	1 0.716		

Table 3.8 (continuation).- *De novo* peptide sequencing for protein identification in the analysis hormone effect over testis proteome.

nESI-MS/MS					PROTEIN ID	
Spot ID	Peaks 2.4		Lutefisk 97		NCBI	Name
	Sequence	Score	Sequence	Rank-Score		
253	DYLMNMMK	12%	LSS[269.2]PL[260.0]	1 0.241		
	NQPGHSMMLPK	2%				
	QPELSYSLNSEVK	12%	LLKLSYTVNSERA	1 0.642	gi|47224921	Alpha-2-macroglobulin-1
	VFVLLQGNTYFSK	16%	FVVLLKGNTYFSK	1 0.990		
	WDYQVLLTVGDEK	17%	[218.1]GDTTVLLTVGDEK	1 0.990		
	VYDVLELEDANDNR	20%	[264.1]LVLENKDANDNR	1 0.664		
	MRAPTAEDLGYWGLVR	19%	F[211.1]PTAEDLGYSV[251.1][174.0]	1 0.612	gi|47224921	Alpha-2-macroglobulin-1
	VQDVQDQTVTEWVHPK	10%	[227.1]DVKDKTVTEGEV[234.1]K	1 0.990		
	MQHSL(CamC)GLSALDKWEPK	16%	[184.1][212.1]SLCGLSALDKSVLLK	1 0.893	gi|47224921	Alpha-2-macroglobulin-1
261	LLQLSYSLNSEAR	28%	[241.2]LLSYSLNSEVK	2 0.782	gi|47224898	Alpha-2-macroglobulin-1
	NMTLLKDKNLVVK	28%	[246.0]VLLKGNTYFSK	1 0.990		
	DWYQVLLTVGDEK	36%	MGLYKVLLTVGDEK	1 0.985		
	FDDVLELEDANDNR	7%	[264.1]LVLELEDANDNR	1 0.336		
	MNFQENGELVDRFWR	34%	VF[256.2]YLVLEGNEKFLN	1 0.374		
	FLLWKALGPALGSVDGHDK	8%	FLL[168.1]KNMEYEK[228.0]RR	1 0.130		
263	LLQLSYSLNSEVK	19%	LLKLSYSLNSEVK	1 0.945	gi|47224898	Alpha-2-macroglobulin-1
	VFVLLQGNTYFSK	22%	FVVLLLMRYFSK	1 0.990		
	GDEYKVLLTVGDEK	48%	[214.1]SYKVLLTVGDEK	1 0.906		
	VYDVLELEDANDNR	47%	[264.1]LVLELEDANNDR	1 0.522		
	QVDVQDQTVTEWVHPK	15%	[227.1]DVKDKTVTEGEV[234.1]K	1 0.834		
	MQHSL(CamC)GLSALDQWEPK	29%	[184.1][212.1]SLCGLSALDKSVLLK	1 0.990	gi|47224921	Alpha-2-macroglobulin-1
	QMGTHLDLTADVEEEYHR	57%	[259.1]GTGEEEVDATLDLHT[170.1]K	1 0.952		
265	EPQLSYSLNSEVK	13%	LLKLSYCGPSEAR	1 0.722	gi|47224898	Alpha-2-macroglobulin-1
	FVVLLQDELNVVK	28%	FVVLLEDRYFSK	1 0.990		
	RHNGQVLLTVGDEK	52%	[301.1]YKVLLTRDTR	1 0.688		
	QVDVQDQTVTEWVHPK	4%	[227.1]DVRSKTVTELKNEY	1 0.673		
	(CamC)HWAHEYSNNRLKDRR	9%				

Table 3.8 (continuation).- *De novo* peptide sequencing for protein identification in the analysis hormone effect over testis proteome.

nESI-MS/MS					PROTEIN ID	
Spot ID	Peaks 2.4		Lutefisk 97		NCBI	Name
	Sequence	Score	Sequence	Rank-Score		
267	MPS(CamC)LSFR	97%	MPSCLSFR	1 0.745	gi|47224921	Alpha-2-macroglobulin-1
	DYL(CamC)AFTR	25%	LSRVTPL[260.0]	1 0.129		
	AQSFLFLDPK	23%	AKSFLFLDPK	1 0.877	gi|55667245	Alpha-2-macroglobulin precursor
	RFFLTSPPQR	38%	MGNHGSTLFNVA	1 0.223	gi|47224921	Alpha-2-macroglobulin-1
	SQEKLTPALLEK	15%	NTEKLT[168.1]LLEK	1 0.745		
	MYTTVPVVAKMNR	24%	MYTTVVPVAKMNR	1 0.270		
	NMVDLKDQLNVVK	20%	FVVLLEDKLNVVK	5 0.986		
	MRAPTAEDLGYWGLVR	69%	LCLGLAEDLGYW[170.1]VR	1 0.760	gi|47224921	Alpha-2-macroglobulin-1
	QVDVQDQTVTEPTSHPK	48%	EV[213.1]EDKTVTEL[323.1][211.1]	1 0.288		
277	NYL(CamC)AFTR	28%	LSSG[194.1]DLFL	1 0.286		
	MGNFLTSPPQR	49%	[255.2]LKSTLFKR	1 0.062	gi|47224921	Alpha-2-macroglobulin-1
	YMDWPVVAKMNR	26%	[294.1]DSV[208.1]SAKH[264.1]	1 0.236		
	MRAPTAEDLGYWGLVR	45%	LSASPTAEDLGYWGLVR	3 0.740	gi|47224921	Alpha-2-macroglobulin-1
	DW(CamC)LLAVRLTLRWPLWQK	37%	[557.2]LSVRLKL[967.3]	1 0.224		
284	TWVHVFTR	21%	LSS[168.1]TPNMK	1 0.288		
	NKFSVWENK	5%	LEFSKNSGNR	1 0.909		
	DYMSV(CamC)GTHRRK	10%				
	MRAPTAEDLGYWGLVR	40%	EAASPTAEDLGYSVD[154.1]R	1 0.579	gi|47224921	Alpha-2-macroglobulin-1
	QRQNNLAFSATEEALKSYWR	5%	[411.9]NNLAFSATEEALKST[404.2]	1 0.722		
298	F(CamC)QLPDTK	53%	FCKLPDTE	2 0.111		
	VAFDEYGSK	12%	VAFDEYGSK	1 0.606		
	LSLFVVNRPR	25%	[200.0]LFVV[199.1]APR	1 0.811		
	RVDSDLDPLNVSR	31%	RVDSDDL[210.2]NVSR	2 0.452	gi|31323728	Chaperone protein GP96
	M(CamC)SFLNFDESAAWER	17%				
	MNFQENGELVDLNDFR	80%	FPFEEEVLEMCHFLN	1 0.694		
	FMFTDEWMAANEELWR	25%	[226.1]SLTNEDAMAANEELTLK	1 0.850		
	YEHP(CamC)ALVASQYGWSGNPYR	10%	[266.1]Y[257.1]ALVASKYGWS[225.2][234.1]K	1 0.470	gi|31323728	Chaperone protein GP96

Table 3.8 (continuation).- *De novo* peptide sequencing for protein identification in the analysis hormone effect over testis proteome.

nESI-MS/MS						PROTEIN ID	
Spot ID	Peaks 2.4		Lutefisk 97			NCBI	Name
	Sequence	Score	Sequence	Rank-	Score		
424	WQDLFGFHK	18%	VSGADLFGCDH	1	0.898	gi|74096001	Hemopexin
	LVNSEQLPALFK	20%					
	W(CamC)WDWLFFK	82%	ADCWDWLFFK	1	0.990		
	KLTHPVLMEGYPK	30%	KDVHPVLMEGYPK	1	0.990		
	LVVGNHYYTFESLK	69%	VLRNHYYTFESLK	1	0.990	gi|74096001	Hemopexin
431	WQDLFGFHK	10%	VSGADLFGCDH	1	0.902	gi|74096001	Hemopexin
	LVNSEQPLALFK	20%					
	W(CamC)WDWLFFK	89%	ADCWDSVLFFK	1	0.990		
	QDVHLMLVLE(CamC)R	22%	VGSVHLMLVLGYPK	1	0.896		
	VLVGNHYYTFESLK	63%	VLVGNHYYTFESLK	1	0.979	gi|74096001	Hemopexin
438	LVNSEQLPALFK	66%	VLNSEKPLALFK	1	0.990		
	QNYHRHV(CamC)QR	3%					
	KDVHLMLVLE(CamC)R	14%	KDVHPVLMEGYPK	1	0.952		
	VLVGNHYYTFESLK	50%	VLVGNHYYTFESLK	1	0.990	gi|74096001	Hemopexin
509	QANTVLATGNYR	8%					
	NSAWEVSANLDK						
	WNLLLNSEWR	41%	SRGLLLNSEWR	1	0.598		
531	ERHPELD(CamC)K	11.4%	DLGHPFKLTR	1	0.530		
	DEWTLTRNR	31.4%					
	W(CamC)TADSVLFFK	19%	WCTADSVLFFK	1	0.990	gi|74095891	Hemopexin
	MLHYTSSTHPYK	14.1%	TAA[199.1]CSETYHPK	1	0.478		
	FGHGPAKLSNEVFK	11.8%	[204.1]HGPAKLRADSFK	4	0.712	gi|74095891	Hemopexin
	HYPHLPADMWRR	7.4%	KDGPHLD[227.1]AM[212.1]R	1	0.484		
	MNQLPKDVTMWNLLK	20.2%	[259.1]NLWMTVDKPLNNK	1	0.440		
	NMFQENGELVDLNMMR	15.8%	[259.1]NLWMTVDKPLNNK	1	0.440		

Table 3.8 (continuation).- *De novo* peptide sequencing for protein identification in the analysis hormone effect over testis proteome.

nESI-MS/MS					PROTEIN ID	
Spot ID	Peaks 2.4		Lutefisk 97		NCBI	Name
	Sequence	Score	Sequence	Rank-Score		
540	FSEMKAGTAGR	8%	[292.6]KSNKTA[213.0]	1 0.110		
	TPNYVAVTAKR	50%	AN[188.0]SGGAVT[228.0]K	1 0.353		
	TPSYLTGYQRK	48%	TPSYLTGYAGRK	1 0.600		
	VKDMVTVVAEVR	4%	[227.1]DMVSPDAEVR	2 0.990	gi|59710087	Keratin
	FW(CamC)GGSSQAVKFNK	23%	[174.0]YGGVGSSGAAVGAFNK	1 0.781		
	TQSMNYSAYGLES(CamC)R	27%	[269.2]GLERSYMVN[301.1]K	1 0.27	gi|59710087	Keratin
	(CamC)TWWGSQLSGWGNTR	30%	[274.0]DGWGSLNTGWGNEK	1 0.655		
	LQYETEL(CamC)ELKSQLK	7%	KLYETELCELAGSKLK	1 0.872		
	TWPPLNLELDYFHFGR	16%	SLLA[210.2]NLELDPTLKVLR	1 0.828		
541	QPEEQTT(CamC)R	17.3%				
	FS(CamC)GVGSSKAVETMR	30.8%	[174.0]YGGVGSSKAV[198.1]YR	3 0.587		
	RHENGEL(CamC)PFHYR	36.9%				
	QTSMNYSAYGLES(CamC)R	44.2%	[229.3]SMNYSMCLES[188.0]K	1 0.266	gi|59710087	Keratin
581	TPSYLTGYKRK	54%	TPSYLTGSE[231.0]K	1 0.499		
	ARDMVSLVAQQK	8%	[227.1]DMDALVAEVR	1 0.990	gi|39645432	Keratin
	DTWVVEMDNSR	43%	ESWVVEMDNSR	1 0.990	gi|39645433	Keratin
	MPGLSDELDFLR	37%	MPGLSDELDFLR	1 0.804	gi|59710087	Keratin
	AEHGRGSSGAAVQNFK	11%	[174.0]YGGVGSSGAAVKNFK	1 0.841	gi|59710087	Keratin
	LALDPLESTYR	96%	LALDLELATYR	1 0.990		
	QTSMNYSAYGLES(CamC)R	69%	KTSMNYSAYGLESA[245.0]	1 0.572		
	MRAPTAEDLGYSVGLVR	52%	DRSPTAEDLGYSVGLVR	1 0.734		
	FLKS(CamC)ELQ(CamC)NQSQLK	7%	KLYETELCELKS[241.2]K	1 0.890		
	RRAALPVGELDQMNDYR	40%	[200.0]LRPAALELDKKNA[210.2]R	1 0.435		

Table 3.8 (continuation).- *De novo* peptide sequencing for protein identification in the analysis hormone effect over testis proteome.

nESI-MS/MS						PROTEIN ID	
Spot ID	Peaks 2.4		Lutefisk 97			NCBIr	Name
	Sequence	Score	Sequence	Rank	Score		
801	DYNENFSR	35%					
	NLTVEMVDLGK	1%	LKSVEMVDL[184.9]	1	0.286	gi|76362269	Cytosolic non-specific dipeptidase
	AEFREDVVLR	4%	EAFRPAMKRK	1	0.554		
	VVEEQVLSHLEK	25%	VVEEKVLSHLEK	1	0.990	gi|37362196	Cytosolic non-specific dipeptidase
	FLQSRMAGRSKLK	14%	[259.1]KSRKMNEKLK	1	0.782		
	MMDDNRSLYVKR	47%	[262.1]DDNADGLYVKR	1	0.990		
	EWQPVTLTFG(CamC)RLR	15%	K[184.1]MPVTLTFKAMRR	1	0.610	gi|37362196	Cytosolic non-specific dipeptidase
	FWAEHA(CamC)MYWKTR	10%	EDSE[185.0][154.1]ARTGPVAGTR	1	0.164		
	N(CamC)WSLHGELKFSEAQK	28%	YPSLSLHGLEGAFTDAKK	1	0.828		
	WDH(CamC)EVQSVSAWPERK	25%				gi|37362196	Cytosolic non-specific dipeptidase
	MDVHYVTGFVLPGVVWWR	64%	[246.0]VHYASVFVPLGVV[198.1][202.0]K	1	0.501		
808	FMHNAMEELMHK	11%	[258.0]GDVAMEELG[211.1]K	1	0.746		
	WFWTVSVHTYYR	79%					
	MRQTSNQTGGDSEKLLKR	33%	[188.0]VKLGAGNCGGTKNS[213.1]ER	1	0.601		
	FMHAAAKAADDDKKNVWR	2%	[215.0]LSAAAKAADDDKKNVWR	1	0.699		
851a	LYTVAAFLR	7.2%	[262.1]DVAAFLR	1	0.418		
	RWRGLYYYYLGY(CamC)R	35.6%					
851b	LTAMDGTEGLVR	18.3%	TLAMDGTEGLVR	1	0.990	gi|47218629	ATP synthase β-subunit
	MLLVNGEGNGPER	16.6%	LMNVLGEPLDER	1	0.990	gi|47218629	ATP synthase β-subunit
	FTQAGSEVSALLGR	38.8%	FTKAGFVRALLGR	1	0.792	gi|47218629	ATP synthase β-subunit
	WPTGLTVAEYFR	95.2%	[170.1]LTGLTVAYEFR	1	0.746	gi|47218629	ATP synthase β-subunit
	FAAHMELLNNVAK	18.9%	[226.1]FLEALLNNVAK	3	0.508	gi|47218629	ATP synthase β-subunit
	MDHNENMAYNVHK	14%					
	LVLEVAQHLWRWK	37.5%	NVKLVAKHLWNTVR	1	0.864	gi|47218629	ATP synthase β-subunit
	MLDPNLVGAEHYDLAR	23.6%	LMDPNLVGAEHYDLVK	1	0.984	gi|47218629	ATP synthase β-subunit
	RWRGLYYYYLGY(CamC)R	24.1%					
	GLTVEAYFR	57.5%				gi|47218629	ATP synthase β-subunit

Table 3.8 (continuation).- *De novo* peptide sequencing for protein identification in the analysis hormone effect over testis proteome.

nESI-MS/MS					PROTEIN ID	
Spot ID	Peaks 2.4		Lutefisk 97		NCBI	Name
	Sequence	Score	Sequence	Rank-Score		
932	LSHWVEFK	70%	LSSPATLNKD	1 0.531		
	NKEQFLDLR	27%	MRDPELRDM	1 0.277		
	MMNWLQVYDSR	6%	YLCDSKLWNMN	1 0.360		
	(CamC)PDPENLYLAAV(CamC)LK	68%	[257.1]D[226.1]NLYLAAVSWK	1 0.595		
1017	WYARL(CamC)NR	26%				
	LGLFLALTGFR	1%	[242.1][188.0]LALTGFR	4 0.636	gi|61403546	3-hydroxyisobutyryl-Coenzyme A hydrolase
	LNAALNLPMVR	26%	ARAALNLPMVR	1 0.907		
	RDSLAQDFFR	39%	VGDSLAKDFFR	2 0.835	gi|89268269	3-hydroxyisobutyryl-Coenzyme A hydrolase
	EEYLLNNALGSYR	84%	[258.0]YLLNNALGSYR	1 0.864	gi|61403546	3-hydroxyisobutyryl-Coenzyme A hydrolase
	NYLHDSVTSLVPWK	33%				
1018	FQTW(CamC)HFVYR	10%	[276.1]HPKKLWNMN	1 0.341		
	QWKKLKFLPMR	2%				
1030	(CamC)VQVSLEAPK	21.2%			gi|47212109	Keratin 18
	EYPLLDDRLK	22%	YEPLLDDRLK	1 0.832		
	NHENEVMELR	92%	NHENEVMELR	1 0.866	gi|47212109	Keratin 18
	KGDLAQLMEDMR	87.5%	[250.2]YAKLMEDMR	2 0.918	gi|47212109	Keratin 18
	WYYAKGMYEL(CamC)HR	37.5%				
	Y(CamC)FLELELASQQSLK	20.3%	[241.2]KTLELELASKKSLK	1 0.990	gi|47212109	Keratin 18
	LNWYSSSLYGKNF(CamC)R	16.8%	[188.9]PKYSSSLYGGAGGY[300.1]	1 0.291		
	NMFQENGELVDYYYR	23.2%	NMFKENGELVDECELN	1 0.805		
	(CamC)HEQQTQEYEVLLNMK	7.8%	FMNLLVEYKKTKK[253.2]R	1 0.554	gi|47212109	Keratin 18

Table 3.8 (continuation).- *De novo* peptide sequencing for protein identification in the analysis hormone effect over testis proteome.

nESI-MS/MS					PROTEIN ID	
Spot ID	Peaks 2.4		Lutefisk 97		NCBI	Name
	Sequence	Score	Sequence	Rank-Score		
1031	Q(CamC)SHFKR	40%	[174.0]KFHSNR	1 0.990		
	MMLQLNWR	8%	DFLKLDNAR	1 0.990		
	YEPLHHSHNK	39%				
	QGDLAQLMEDMR	23%	ANDLAKLMEDMR	1 0.990	gi|47212109	Keratin 18
	MGSRSL(CamC)PKSGNDK	71%	[333.3]VSLKCPSGWGN	1 0.457		
	KLRWELELASQQAEK	12%	S[154.1]KTLELELASKK[199.1]E	1 0.901	gi|47212109	Keratin 18
	LNWYSSSLYGGANF(CamC)R	12%	TSPKYSSSLYNAGGYGDK	1 0.766		
1032	Q(CamC)QFFTYFK	20%				
	NV(CamC)TEAGLFALR	62%	NVCTEKLFALR	1 0.969	gi|54035446	Proteasome 26S subunit ATPase 6
	LGASKLD(CamC)NFLK	20%	VAASAGLDCNFLK	1 0.980	gi|54035446	Proteasome 26S subunit ATPase 6
	WPSWRLGFVPR	20%				
	FKPQGSLTFYVR	5%				
	NFYEYEQFWNK	11%				
	RMDVFHFK(CamC)VLR	57%				
	EVLELPLTNPELFKR	10%	VD[278.1]RHFK[259.1]LR	1 0.266	gi|54035446	Proteasome 26S subunit ATPase 6
	WWLG(CamC)GLSTGYGAALNTAK	20%	[258.0]LNGCGLSTGYKALNTAK	1 0.631		
1102	VPVADVWVDLT(CamC)R	89%	VPVADVSVVDLTCR	1 0.865	gi|56718619	Glyceraldehyde 3-phosphate dehydrogenase
	VFLRAVFARAWRR	14%				
	RAL(CamC)YDDAGFGYHSR	18%				
	YRKWGSQLSGWWNK	27%	FKAECRLLSGWGNRT	1 0.689		
	W(CamC)APSSLRAGLWSLLNR	10%	[245.0]TWRLRARLSSPATLN	1 0.756		
	MWFKENGELSPLDYRK	8%				
	CamC)NLFQENGELVDLYLKK	11%	CNLFKENGELVDEFLKK	1 0.565		
	YYEPSPDAPMFVMRA(CamC)VK	26%			gi|56718619	Glyceraldehyde 3-phosphate dehydrogenase

Table 3.8 (continuation).- *De novo* peptide sequencing for protein identification in the analysis hormone effect over testis proteome.

nESI-MS/MS						PROTEIN ID	
Spot ID	Peaks 2.4		Lutefisk 97			NCBI	Name
	Sequence	Score	Sequence	Rank-	Score		
1106	QNSLTDELNFLR	26%	[242.1]SLTDELNFLR	1	0.990	gi|37682099	Keratin 8
	RRMMSSLLSSFTYK	24%					
	FAKLAYMAVGNSGPNSK	15%					
	F(CamC)HELDNNLEKLSSYK	35%	V[244.0]TELDNNLEKLSSYK	1	0.883		
1116	GFYSTVVMKDFK	11%	A[250.2]SFVVMCTAW	1	0.397		
	WWNVSMNMTFYK	13%					
	FLVGGLNAP(CamC)KWSPR	8%	[260.0]VNLN[184.1]LTEGGVNK	1	0.371		
	EMVGVANNWNLLWR	30%	[260.0]VGGLE[154.1]MRGEPSR	1	0.406		
1119	EP(CamC)VASLNR	1%	[200.0]ADVASLNR	1	0.653	gi|28557116	Tropomyosin
	LDQENALDR	14%	LDKENALDR	1	0.455	gi|28557116	Tropomyosin
	MELQELKLK	2%	EMLKKNKLK	1	0.990	gi|28557116	Tropomyosin
	VLLLEGDLER	23%	[212.1]LLEGDLER	1	0.854	gi|28557116	Tropomyosin
	LQLVEEELDR	35%	LKLVEEELDR	1	0.990	gi|28557116	Tropomyosin
	FVEEFQTAEEK	18%	VFEEFKTAEEK	1	0.990	gi|28557116	Tropomyosin
	QDVFEEFKTAEEK	5%	DKVFEEFKTAEEK	1	0.990	gi|28557116	Tropomyosin
1123	ESSQVKNDR	6%	ATMKTSLL[198.1]	1	0.288		
	QNQELATYR	22%	LEKELATYR	1	0.990		
	FNMGSWAEPK	7%					
	QSVEADLANLR	29%	KSVEADLANLR	1	0.990	gi|47213546	Keratin S8 type I
	RDEQQGYDYK	28%	ASLEKKGYDYK	1	0.990		
	QWEANGGANHDR	19%	RSLERTLATYR	1	0.954		
	RSNEQEHELPK	3%					
	EKWWGRVVRR	23%	PSLEADLNALRR	1	0.491		
	MPALSTETLKTTK	27%	[228.0]ALSTTELKTTK	1	0.902		
	QANETEEATAPLGSNSK	41%	SLLETEESRPLGSGGSK	1	0.953		
	WWNTLNVEVDASPKQRWK	24%	[257.1]ARDTNVEVDAS[225.2]KDLNK	1	0.627	gi|47213546	Keratin S8 type I

Table 3.8 (continuation).- *De novo* peptide sequencing for protein identification in the analysis hormone effect over testis proteome.

nESI-MS/MS					PROTEIN ID	
Spot ID	Peaks 2.4		Lutefisk 97		NCBI	Name
	Sequence	Score	Sequence	Rank-Score		
1134	NVFRLQVR	13%	[213.1]LNGCTVR	1 0.426		
	NTATGLMDLR	27%	ESLDLMDLR	1 0.634		
	SPSEAYKAETGK	32%	[184.1]SEAYKAE[158.0]K	1 0.592	gi|47216949	Annexin A3
	EELFDVTMLTLR	76%	[258.0]LFDCGNLTLR	1 0.987		
	QMQE(CamC)TLTELFSDK	23%	K[158.0]TECTLTELFSSR	1 0.888	gi|47216949	Annexin A3
	MNFQENGELVDLRFTK	17%	NM[275.0]ENGELVDL[158.0]FKV	1 0.442		
	RRATRDVKAGA(CamC)WYHYR	41%				
	FF(CamC)LLYSQLESEVSGDYVMPR	42%	[305.1]PFMYSKLESEVSGDYG[270.1]R	1 0.713	gi|47216949	Annexin A3
1139	VTGLFEL(CamC)R	8%	[200.0]GLSNFNKD	1 0.745		
	AQVLWALESYGR	27%	[198.2]VLWALESY[213.0]	1 0.286	gi|74310597|	NADH dehydrogenase subunit 5
	LRLTAYSWY(CamC)GR	50%	[174.0]PDPAYSWATLHN	1 0.976		
	MP(CamC)TEDEFAEDQPR	26%				
	RDW(CamC)GGPAAVV(CamC)KRR	5%				
1146	FKKTGLTEKK	25%	[200.0]VDFLTKEK	1 0.893		
	LQLVEEELDR	34%	LKLVEEELDR	1 0.990	gi|66792936	Tropomyosin 4 isoform 1
	KLYAVHTALQK	5%	RSASAELVAVNR	1 0.468		
	RFRNAWPWR	9%	KAGDTVAPKEDNR	1 0.376		
	QQDAEEGVAALNR	9%			gi|66792936	Tropomyosin 4 isoform 1
	FLWEAHENDYDK	31%	V[188.0]DELDKFSEALK	1 0.988		
	FLAAELFENSERR	14%	LVVLEGELEKAEER	1 0.981		
	LVVLEGELEKAEER	3%	[258.0]LVKLELDRAKER	1 0.677		
	EQLVLEELDRAEKR	23%	[274.0]DLEEELKNGKDKLK	1 0.655	gi|66792936	Tropomyosin 4 isoform 1
	QWFLHGMYEY(CamC)DK	12%				
	FLELEEKSRNVEWVR	6%	[245.0]FKENGELVEEKFVK	1 0.687		

Table 3.8 (continuation).- *De novo* peptide sequencing for protein identification in the analysis hormone effect over testis proteome.

nESI-MS/MS					PROTEIN ID	
Spot ID	Peaks 2.4		Lutefisk 97		NCBI	Name
	Sequence	Score	Sequence	Rank-Score		
1147	SGDLEEQNK	27%	SGDLEEELK	1 0.990		
	NNKENALDR	31%	LDKENALDR	1 0.822	gi|74136103	Tropomyosin 2
	LVLLEGDLER	85%	LVLLEGDLER	1 0.990	gi|74136103	Tropomyosin 2
	QLLVEEELDR	33%	LKLVEEELDR	1 0.990	gi|74136103	Tropomyosin 2
	FKLGLLKAHKK	15%	[222.9]EEELLGLKK	1 0.465	gi|74136103	Tropomyosin 2
	LQEEELLGLKK	17%	LKEEELLGLKK	1 0.990	gi|74136103	Tropomyosin 2
	VDDDLEENLAQAK	21%	[214.1]MVLEENLAKAK	1 0.990	gi|74136103	Tropomyosin 2
	REDELDQYSESLK	95%	VWDELDKYSESLK	1 0.990	gi|74136103	Tropomyosin 2
	QMLEEELGANVTNLNK	28%	FEPKEELGANVTNLNK	1 0.990	gi|74136103	Tropomyosin 2
1153	F(CamC)HASYETQYVSHA(CamC)K	11%	[245.0]T[168.1]WTRARLS[255.2][172.0]R	1 0.248		
1189	DDQMALVASLNR	32%	DGWEWVASLNR	1 0.990		
	WLLDDTLPLFER	56%	WLLDDTL[210.2]FER	1 0.919	gi|41054657	HEAT-like (PBS lyase) repeat containing 1
	MH(CamC)WPAQDAGDFYLKLWR	8%	[245.0]NNKEYMDGADEYFL[212.1]K	1 0.433		
	EWWRLLVLSQAVNN(CamC)WYK	43%	[297.2]M[227.1]NDTALVLVNPS[196.2][243.1]K	1 0.388		
	WWKWVLALGGLDQ(CamC)SYWPK	30%	N[257.1]EDAVLALGLGDKCSSA[260.0]R	1 0.473	gi|41054657	HEAT-like (PBS lyase) repeat containing 1
1204	FEAFFPASHAKK	8%	FEAFFPFFAEK	1 0.414		
	FGATGFLKNLTEK	24%	[174.0]TSAFLELLTTR	1 0.990		
	VMRVEKLVDSDAR	31%	[230.0]GVVEKLVDDSAR	1 0.990		
	FNANGSFLYEHLR	22%	FEGLGSFLYEYDK	1 0.973		
	APPNFSYN(CamC)MREK	34%	PA[211.1]FSMASPGPALEK	1 0.438		
	FNVPESELLEVLWK	23%	[174.0]SVPESLLEEVLASR	1 0.990	gi|68372040	Similar to oxidative-stress responsive 1

Table 3.8 (continuation).- *De novo* peptide sequencing for protein identification in the analysis hormone effect over testis proteome.

nESI-MS/MS					PROTEIN ID	
Spot ID	Peaks 2.4		Lutefisk 97		NCBI	Name
	Sequence	Score	Sequence	Rank-Score		
1294	DFSWFKFLR	17%	DFSSVFKFLR	1 0.990		
	MPGLAQNTATDTK	17%	DLGLAKNTATDTK	1 0.990	gi|94482754	3-hydroxyisobutyrate dehydrogenase
	MNPVLEHAQYFR	81%	[245.0]KNEWFLVPLN	1 0.227		
	DWPLSSLAHKLYR	37%	[188.0]LPLSSLAHKLYR	1 0.730	gi|94482754	3-hydroxyisobutyrate dehydrogenase
	NFVHDSSTLDPEQR	11%	MPRLVCMLDPAVSR	1 0.531		
	MMLVTSLEHQDLDK	46%	[260.0]TLTSLEHKDLSR	1 0.777		
	FSTPVLATDVFRE(CamC)R	19%	[236.2]VKRFVDTALVWVK	1 0.485		
	FWDPLLHYRNSGWK	19%				
	EWPWNALVVDSF(CamC)(CamC)K	95%	[216.0][154.1]DLNALVVDSS[210.2]VAK	1 0.920		
	MNLFMDAPVTGRKWRR	43%	[358.1]FMDAPVTNVGAADRR	1 0.990	gi|94482754	3-hydroxyisobutyrate dehydrogenase
1315	TPGWLTYLFHR	29%	[198.1]LFLYTLPLGR	1 0.707		
1380	KNF(CamC)FMMPEK	10%	[242.1]FMMFCPEK	2 0.357		
	VEFVVNGALESLR	48%	AKSGMVNGALESLR	3 0.407		
1393	YAVTALTEGLR	99%	[234.1]VTALTWLR	1 0.990	gi|47227808	Short-chain dehydrogenase/reductase
	VKLTDMSPPSHK	13%				
	VALVTGASVGLGAATAR	62%	PWVTGASVGLGAATAR	1 0.990	gi|47227808	Short-chain dehydrogenase/reductase
	TPPSADVHMDVHSK	55%	VVSPADVHFVSS[277.1]	1 0.623		
	WGDDVNVLALPVHRK	23%	[265.2]CNFVLALSLCTR	1 0.637	gi|47227808	Short-chain dehydrogenase/reductase
	VTSLSPGLVETEFAFR	99%	VTSLSPGLVETEFAFR	1 0.823	gi|47937924	Short-chain dehydrogenase/reductase
	EAAE(CamC)KSAGYSGTLLPYK	28%	[247.0]FYMSAGYS[158.0]LLPYK	1 0.449		
	MQESNEEELLSMFRDK	16%	[275.0]LSGGEEELLSMFSALK	1 0.895	gi|47227808	Short-chain dehydrogenase/reductase
	E(CamC)LQLNNAGLAHTDKLTPR	6%	VGDMKLNNAGLAHSL[225.2]LSW	1 0.278		
1409	YYGSHMGHFFTK	15%				
	MWYWTPSN(CamC)(CamC)K	4%				
	T(CamC)MEKDGGANGRNRGYR	6%				
	WAFP(CamC)LSTGLYGYHWK	61%	WAFPCLSTGLYGY[323.1]K	1 0.710	gi|51858534	LRP16 protein
	YHLEYRHESPSLAEHK	17%				

Table 3.8 (continuation).- *De novo* peptide sequencing for protein identification in the analysis hormone effect over testis proteome.

nESI-MS/MS					PROTEIN ID	
Spot ID	Peaks 2.4		Lutefisk 97		NCBI	Name
	Sequence	Score	Sequence	Rank-Score		
1411	YYTLLQERH(CamC)K	62%	YYTLLTRR[184.1]LK	1 0.677		
	MP(CamC)TEDHGGQPLLNR	48%				
	SS(CamC)MMLRKALMYQR	47%	[226.1]LDNPDKRLMYKR	1 0.990	gi|37362126	Glutathione S-transferase
	RYWDVTVFH(CamC)ASLFR	60%	[174.0]FLADVTVFPTVSALFR	1 0.647		
	(CamC)(CamC)RHVRGDMKWWFR	20%				
	R(CamC)WWWFGHAARRRR	6%				
	RWWWVAFRKLTMWR	20%				
	LFHLYYSWYVPEEER	46%	MHELYYSDAYV[226.1]EER	1 0.258	gi|64236	Glutathione S-transferase
	WWWR(CamC)WHGTY(CamC)WR	9%	[241.2]DMACLFWLRTSGWR	1 0.213		
1422	T(CamC)PLVTSK	17%				
	LSLLYREGLK	37%				
	VLDSLKLTAQK	22%	VLDSLKLTAKK	1 0.990	gi|56789119	Peroxiredoxin 6
	N(CamC)RLDVPRVR	36%	[170.1]FLLD[196.2]GVVR	1 0.709		
	LGFG(CamC)DY(CamC)LFK	99%	LGFGCDYCLFK	1 0.990		
	TMMMGDVFPGGPFVDGLYAK	15%	S[293.2]LGDVFPNFEADTTLGR	1 0.918		
	(CamC)A(CamC)NRDFPAKFVDGLFVK	33%	[232.0]CLGDVFPNFEARCNGR	1 0.990		
	MWEEWDSEAAAHPY(CamC)WDRK	2%				
1424	NFDELLR	99%	NFDELLR	1 0.990	gi|47193903	Peroxiredoxin 6
	LGVGFVLLR	99%	LGVGFVLLR	1 0.990		
	DVVLGLLPR	98%	[214.1]VLAVLPR	1 0.990		
	LSLLYPATWK	68%	LSLLYPDGWK	1 0.919	gi|47193903	Peroxiredoxin 6
	VLDSLQLTAKK	44%	VLDSLKLTAKK	1 0.990	gi|47193903	Peroxiredoxin 6
	RLPEGEQFFAHR	34%				
	YVTPV(CamC)MAELAMNGK	96%	DFTPVCTTELACAAK	1 0.838	gi|37748290	Peroxiredoxin 6
	RLLLGDVFPNPFVDGLFSK	37%	[267.2]LLGDVFPNPFVDGLN[249.3]	1 0.407	gi|37748290	Peroxiredoxin 6

Table 3.8 (continuation).- *De novo* peptide sequencing for protein identification in the analysis hormone effect over testis proteome.

nESI-MS/MS						PROTEIN ID	
Spot ID	Peaks 2.4		Lutefisk 97			NCBI	Name
	Sequence	Score	Sequence		Rank-Score		
1439	LFEQKNKVLKTK	1%					
	DGWVD(CamC)VNKYVVALR	20%	MARVVYGAGGVMDKALR	1	0.699	gi|57157763	Apolipoprotein A-IV1
	QWAPLSKDFMTKFNR	28%	KWAPLSKDFMTKFNR	1	0.990		
	KWAPLSQDFFTQFNR	11%	[158.0]RA[210.2]SKDFFTKFNR	1	0.848		
	MQWVEAQMTPYTKEMR	3%	[320.0][225.2]AGAKMT[260.0]TKEMR	1	0.491	gi|57157763	Apolipoprotein A-IV1
1439b	ALQSSDMVGGASTMVALR	34%	[184.1]GASSDMVNAGYVVALR	1	0.580		
	WQAPLSQDFMTYEPR	47%	[215.0]VA[210.2]SKDFMTK[289.0]K	1	0.673	gi|68400425	Proteasome subunit beta type 5
	GQVT(CamC)KAQMTHS(CamC)YAMR	49%	[188.0][226.1]MKAKMT[260.0][269.2][220.1]R	1	0.245		
	VEVWGENMQPYALYYSK	72%	[270.1]GWWNMKEMATRV[170.1]K	1	0.616		
	YDSAA(CamC)DVLTLND(CamC)WRK	21%	[276.1]NFEDYYPTMCNLSR	1	0.208		
1439c	GHPDTLAMLR	61%					
	ALLDPLESTYR	99%	[184.1]LDLELATYR	1	0.592		
	AEDLQFASFLDK	21%					
	MAALTQQLK(CamC)KK	6%	[220.1]RWLKKTLAAN	1	0.960		
	FQTWLQSDFDR	25%					
	ETPHAVGT(CamC)TYYR	15%					
	MMNHSSLGGLSSNLSWHK	35%					

Table 3.8 (continuation).- *De novo* peptide sequencing for protein identification in the analysis hormone effect over testis proteome.

nESI-MS/MS					PROTEIN ID	
Spot ID	Peaks 2.4		Lutefisk 97		NCBI	Name
	Sequence	Score	Sequence	Rank-Score		
1440	FSAVAL(CamC)R	99%	FSAVALCR	1 0.990	gi|37722017	Ubiquitin C-terminal hydrolase
	TTFNSDRDK	45%	TTFNRNF[184.1]	1 0.488		
	MRYSLVWESK	73%				
	QQKVGNLAEDSK	16%	KKKVGNLAEDSK	1 0.990		
	AKPGELSQFLNNR	46%				
	LFDETANFSADDR	67%	FLDETANFSADDR	1 0.944	gi|47211292	Ubiquitin C-terminal hydrolase
	VDVNGQLYEFDGR	52%	[213.1]VPGRYLKGN[224.1]A	1 0.331	gi|37722017	Ubiquitin C-terminal hydrolase
	FSADMMHGNARDASK	15%				
	FGQVAVTAGKAPVAVANK	31%	FLALGVESHATVAVKGK	1 0.901		
	KDALPVSEATDVYWR	22%	[242.1]ALCWHSMNF[213.1]K	1 0.299		
	T(CamC)LRQWLETTMFHR	15%	[232.0]VFVNVHRTEAS[170.1][172.0]R	1 0.233		
	LGLFFNVNGQLYEYRR	49%				
	(CamC)NLFKENGELVDQVVYR	47%	CNLYLDPSEL[215.0]KFLKK	1 0.374		
	YS(CamC)NS(CamC)GTLALLHAVANDWR	91%	[361.2]NNAVAHLLALTGCSP[253.2]R	1 0.712	gi|47211292	Ubiquitin C-terminal hydrolase
	MAKFMAVAVLALLHAVANNKSK	23%	[230.0]PTLH[168.1]TLALLHAVANN[215.0]K	1 0.315	gi|47211292	Ubiquitin C-terminal hydrolase
1507	LLSFKNNR	40%	LLSFKNNR	1 0.990	gi|67772036	Ferritin middle subunit
	MAEYLFSR	95%			gi|51858515	Ferritin heavy polypeptide
	LGDYLGTLTR	80%	LGDYLGTLTR	1 0.990	gi|47939430	Ferritin lower subunit
	RGNKALVELHK	37%	NVNKALLD[250.2]K	1 0.628		
	N(CamC)LTWTRTLVR	36%	[220.1]RWLKKTLAAN	1 0.990		
	DLTANPELPLPER	5%	DDVALPGA[210.2]AL[184.1]K	1 0.285		
	FWNELLT(CamC)GWNK	55%	FWLGSFLYEYNE	1 0.581		
1512	GNFNYAEFTR	9%	[171.0]FNYAEFTR	1 0.990	gi|37779086 or gi|33991794	Putative transient receptor protein 2 or Myosin light chain
	ARGTDMLPVLR	81%	LDGTDPEDVLR	1 0.778		
	EAFNMLDQNR	45%	[200.0]FNMLDKNR	1 0.889		
	FTDEEVDELFR	99%	FTDEEVDELFR	1 0.990		

3.2.7 Comparison of sequenced peptides and identified proteins with *S. senegalensis* ESTs

The same procedure described in chapter 2 was carried out with sequences from differential spots resulting from the hormone treatment experiment. Twenty-three out of fifty-nine spots produced from one to seven peptides that could be related to an EST that matches with the same protein as the original peptide (table 3.9). Nine of these spots discover new peptide assignations (17 new correlations) that could not be matched in the comparison between peptide and protein database.

3.2.8 Relationships between 2-D protein gel analysis and mRNA microarray data of testis from fish treated with hormones

A transcriptomic approach was performed in parallel to proteomic analysis using the same testis tissue from F1 *S. senegalensis* in both cases. Two different comparisons were performed in triplicate in an array composed of 5087 oligonucleotides: F1 GnRHa vs. F1 Control and F1 GnRHa vs. F1 GnRHa+OA. In the F1 GnRHa-Control comparison 32 genes were found up-regulated, while 38 were down-regulated. In the F1 GnRHa-GnRHa+OA comparison 11 genes were up-regulated, while 34 down-regulated (see; Annex III.6 for detailed results). No gene identification was found to be coincident with any of the protein described in the proteomic analysis (total proteins: 48). About half of the sequences in the microarrays that were found to be up or down-regulated in any of the comparisons (61 among 115) present a related entry with a known gene/protein database. However, none of those genes could be directly correlated with any protein. Only in the case of the gene PRP19, which is described to posses ubiquitin ligase activity, could be related to the protein assigned to the spot 1440 (ubiquitin C-terminal hydrolase). This gene is down regulated 1,86 times (p> 99%) in the GnRHa+OA state in comparison with the GnRHa state. In the proteomic analysis the spot is 1,36 times (p>99%) less present in the GnRHa+OA state than in the GnRHa state. However, for the comparison between F1 Control and F1 GnRHa, the genomic and proteomic data are in the opposite sense (gene up-regulated 1,5 times in GnRHa (p>99,9%), lower protein levels 1,4 times in GnRHa (p> 99,9%), probably indicating that gen and protein, although functionally related, are not under direct relationship.

Table 3.9.- Coincidences between MS/MS-derived peptide sequences from differential spots and EST from *S. senegalensis.* For each spot, 3 different comparisons were made between peptide sequences, ESTs and protein data in the NCBI database: peptides against ESTs; ESTs against database sequences; and peptides against database sequences. Proteins resulting from each process are compared and peptide-EST matches annotated. *Prot ID:* Protein identified from the MS/MS peptides. *Pep seq:* Number of MS/MS peptides sequenced for a certain spot. *Seq related to Prot ID:* Sequences from a spot used to identify the protein. *EST related to Prot ID:* Number of EST that matches with the protein identified with MS/MS peptides.

Spot ID	Prot ID	Pep Seq	Seq related to Prot ID	EST related to Prot ID
1123	Keratin S8 type I	11	2	6
1439	Apolipoprotein A-IV1	5	2	4
1507	Ferritin subunits (H, M, L)	7	3	5
1146	Tropomyosin 4 isoform 1	11	3	4
1512	Putative transient receptor protein 2 or Myosin light chain	4	4	4
1422	Peroxiredoxin 6	8	1	1
1102	Glyceraldehyde 3-phosphate dehydrogenase	8	2	2
284	Alpha-2-macroglobulin-1	5	1	1
1147	Tropomyosin 2	9	8	7
801	Cytosolic non-specific dipeptidase	11	4	3
581	Keratin	10	4	3
1030	Keratin 18	9	5	3
1119	Tropomyosin	7	7	4
1411	Glutathione S-transferase	9	2	1
1031	Keratin 18	7	2	1
298	Chaperone protein GP96	8	2	1
277	Alpha-2-macroglobulin-1	5	2	1
267	Alpha-2-macroglobulin-1	9	4	2
1424	Peroxiredoxin 6	8	5	2
1134	Annexin A3	8	3	1
1032	Proteasome 26S subunit ATPase 6	9	3	1
253	Alpha-2-macroglobulin-1	9	3	1
851b	ATP synthase β-subunit	10	8	2
1439b	Proteasome subunit beta type 5	5	1	0
1440	Ubiquitin C-terminal hydrolase	15	5	0
1409	LRP16 protein	5	1	0
1393	Short-chain dehydrogenase/reductase	9	5	0
1294	3-hydroxyisobutyrate dehydrogenase	10	3	0
1204	similar to oxidative-stress responsive 1	6	1	0
1189	HEAT-like repeat containing 1	5	2	0
1139	NADH dehydrogenase 5	5	1	0

Table 3.9 (continuation).- Coincidences between MS/MS peptide sequences and EST from *S. senegalensis*

Spot ID	Prot ID	Pep Seq	Seq related to Prot ID	EST related to Prot ID
1106	Keratin 8	4	1	0
1017	3-hydroxyisobutyryl-Coenzyme A hydrolase	6	3	0
932	Interferon induced protein 56	4	1	0
541	Keratin	4	1	0
540	Keratin	9	2	0
531	Hemopexin	8	2	0
521	Rho guanine nucleotide exchange factor	1	1	0
438	Hemopexin	4	1	0
431	Hemopexin	5	2	0
424	Hemopexin	5	2	0
265	Alpha-2-macroglobulin-1	5	1	0
263	Alpha-2-macroglobulin-1	7	2	0
261	Alpha-2-macroglobulin-1	6	1	0
250	Alpha-2-macroglobulin-1	7	2	0
240	Alpha-2-macroglobulin-1	7	2	0

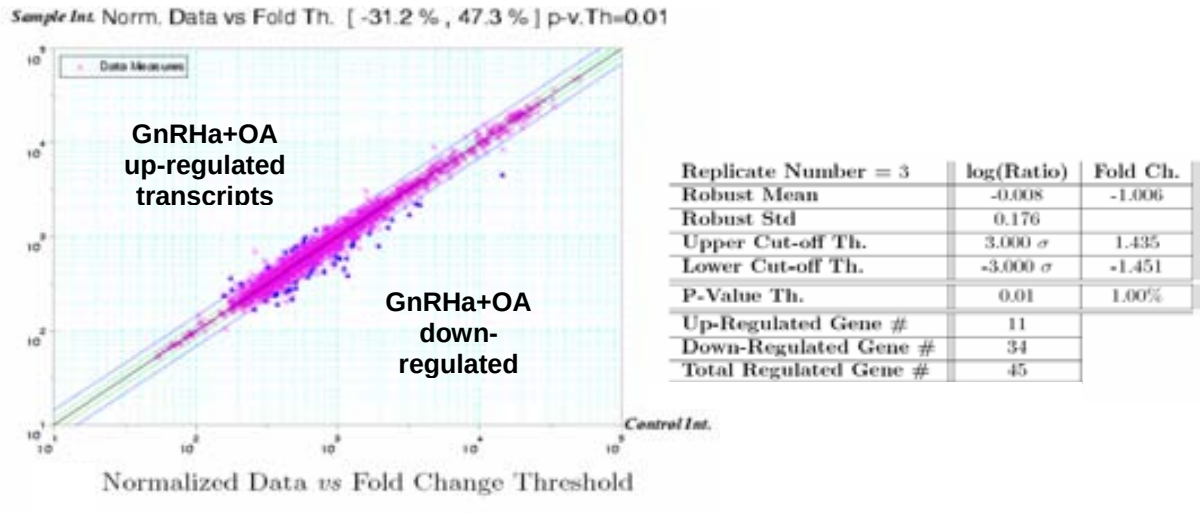

Figure 3.13.- DNA microarray hybridization results for the comparison between GnRHa (Cy3 Control) and GnRHa+OA (Cy5 Sample). Normalized intensities of the triplicate of each transcript for Cy3 and Cy5 are plotted in panel (a). The cut-off threshold to determine transcripts that are up or down-regulated is ±3 σ (points outside the blue line). A fold change value of +1.2 reflects a 20% up-regulation, while -1.4 means a 40% of down-regulation. The *P* threshold is set at 0,01, meaning that probability of an observed variation is not because of an stochastic event is 99%.

3.3 Discussion

3.3.1 Effect of hormone treatments on sperm and testis physiological features

The effects of hormone treatment on the measured physiological parameters were notable, especially in the amount of milt produced and the number and motility of spermatozoa. Among all these parameters, spermatozoa motility seems to be the most critical aspect to achieve successful fecundation in fish species (Coward 02). The GnRHa+OA treatment increased spermatozoa motility more than two times. When GnRHa was applied to animals the production of milt was doubled respect to controls, but when OA was present the amount of milt produced was decreased to control levels. These data indicate that GnRHa+OA treatment possibly generates less but more capable spermatozoa, and therefore the fertility of these animals could be higher than that from control or GnRHa treated fish.

The study from Agulleiro *et al* (2007) described that males treated with GnRHa+OA had a much stronger and sustained increase of 11-KT plasma levels than males treated with GnRHa alone. Also, males treated with GnRHa+OA showed more Leydig cells and a higher proportion of spermatozoa per seminiferous lobule in the testis with respect to males treated with only GnRHa. These data clearly indicated that GnRHa+OA effectively accelerated spermatogenesis, and such acceleration of spermatogenesis was possibly associated with the production of more capacitated sperm, thereby increasing its motility.

In studies on spermatogenesis in other fish species, it was described the key role in sperm motility of the gonadotropin-induced 17α,20β-P hormone, by increasing the pH of sperm duct. However, 11-KT and testosterone do not show any direct effect on the acquisition of sperm motility in fish (Miura 92, Nagahama 94). In the present study we found that sperm motility was increased in presence of OA, a precursor of 11-KT. Therefore, it is most likely that sperm motility in the Senegalese sole is increased by enhancing the plasma levels of 11-KT, which might induce the synthesis of maturation-induction steroids in the testis (Agulleiro 07).

3.3.2 Evaluating DIGE for expression changes in testis proteome

In the previous chapter, a 2-DE approach along with silver staining was used to characterize several expression changes during spermatogenesis stages in testis from wild and cultured individuals of *S. senegalensis.* In this chapter 2-D DIGE conditions were optimized to evaluate the expression changes in testis by using, for comparison, the same type of samples already analyzed by silver staining. The S2S and DIGE evaluation experiments aimed to determine whether DIGE approach was valuable for the analysis of testis proteome, and to set up the conditions to analyze variations in the hormone treatment experiment. Moreover, comparing both 2-DE methodologies could give an idea about how complemetary these two methodologies are.

The S2S experiment showed a good linearity among the different labelled samples, validating the CyDye labelling procedure for the solea testis extracts. Some deviation from linearity was observed for spots with normalized volumes higher than 20. In the final setup, spots with volumes above this limit were discarded from the comparison in the spot detection step in the DIA module. As most of the spots (over 95%) presented values of normalized volumes under 20, elimination of outsiders produced less noisy results with a minimal loss of information.

As a second part of the set up of the DIGE technology, results from comparable experimental designs for silver 2-DE and DIGE were analysed. In order to perform this comparison, testis sample from the same animals classified in chapter 2 as F0M, F0L and F0Mat were processed under DIGE compatible protocols. Fifteen differential spots were processed using the same protocol than in chapter 2. Procedures described there for mass spectrometry, bioinformatic and BLAST comparison generate results of the same quality in terms of MS/MS spectra quality, *de novo* sequencing scores for Peaks and Lutefisk, and BLAST scores. Proportionally, the number of identified proteins was very similar (DIGE: 12 out of 15 -80%; Silver: 40 out of 49 -82%).

Two spots were found coincident between the DIGE and the silver staining analyses. One of the reasons explaining the different spot datasets found with each methodology could lie on the chemical fundaments of protein detection of each experiment. CyDyes are covalently attached to the epsilon amino group of lysine of proteins via an amide linkage. The proportion of cyanine to protein is set in order to label only 1-2% of lysines

present in the sample. This substeochiometric labelling lead to a situation where lysine-rich proteins will have a higher probability of being labelled and thus detected than proteins with less lysines. In accordance, an empirical reduction of about 20% of the total number of spots was found in a DIGE image in comparison to silver stained image of the same gel when compared. In overall, besides silver staining can be considered a more universal staining method than DIGE, both methods show different specificities, originating collections of proteome components that can differ significantly. Selection of any of the two methods must be considered thus for each case in terms of throughput and the need for visualizing the maximum possible number of spots.

In the present case, the use of both approaches has extended the number of characterized proteins that could be involved in molecular processes related to spermatogenesis.

3.3.3 DIGE of testis proteome after hormone treatment

After evaluating the suitability of the DIGE system for studying the proteome of *S. senegalensis* testis, the analysis of samples from the hormone treatment experiment was performed. The complete set of comparisons produced 59 unique differential spots. Few of these spots were exclusive for each comparison, indicating that the majority of them are involved in the physiological processes affected by the different hormone treatments. Variations of these spots were mainly between ±1,5 to ±5-fold, with only few cases with variations over ±5.

3.3.4 Combining *Mr*, *pI* and sequencing information to validate protein identification

Proteins were identified as previously described (see pages 65-67). Regarding to *de novo* sequencing softwares, also in this case, Peaks was more efective in producing *de novo* sequences with a good BLAST matching than Lutefisk (see 2.3.3).

As discussed in chapter 2, comparison of experimental and theoretical *Mr* and *pI* values for the identified proteins provided additional information on possible modifications/fragments from the database canonical sequence and also helped to

validate the tentative assignations (see graphics in Annex III.4 and III.5). In cases when high differences between experimental and theoretical values were observed, the number of MS/MS peptides assigned to the identified proteins become then very useful to increase confidence in correct protein assignation to a certain spot.

Table 3.10.- Classification of differential spots in hormone experiment based on comparison and variation. Unique spots indicate the number of spots whose variation is considered significant only in that comparison. Spots in each classification are divided in two groups depending on their change ratio.

	Differential spots over ±1,5 fold change	Unique spots over ±2 fold change	Spots with	
			5≥ Δ >2	10≥ Δ >5
F0Mat-F1C	35	5	17	1
F0Mat-F1GnRHa	18	0	5	1
F0Mat-F1GnRHa+OA	41	2	18	1
F1C-F1GnRHa	23	3	7	0
F1C-F1GnRHa+OA	33	7	14	0
F1GnRHa-F1GnRHa+OA	25	4	7	0
Unique Total	59	20	58	1

As explained in chapter 2 (section 2.3.3), differences over ±0,2 and ±2 between theoretical and experimental values of *Mr* and *pI*, respectively, were taken as the threshold values to determine possible erroneous identifications (figure 3.14). About half of the tentatively identified proteins showing differential levels after hormone treatment (22 out of 46), were under these limits. Moreover, their identifications were fully supported by 2 to 7 sequenced peptides and more than 7 aminoacid coincidences in BLAST comparison. For spots over these references values, the number of assigned sequences (≥2 peptides) or the number of aminoacid identities (≥9 coincidences) in the BLAST alignments supported the assignment. Explanation for these differences in *Mr* and/or *pI* values is available in chapter 2 and in table 3.11. Only four spots presented ΔMr and ΔpI values over the arbitrary reference and could only be supported by one peptide or a number of aminoacid coincidences under 7 in the BLAST analysis. These

spots were not taken into account for further biological interpretations of hormone treatments in S*. senegalensis* testis proteome.

Forty and forty-six protein assignations in chapters 2 and 3, respectively, fulfilled the described criteria for confirming protein assignation in the current work. Only the assignation of 3 proteins with high values of ΔMr and/or ΔpI and just one supportive sequenced peptide were deleted from following discussions about biological meaning of the observed variations. Both in chapter 2 and 3, the explained parameters proportioned an extra quality control in protein identification that may be of interest for other gel-based proteomic studies on species without sequenced genome like *S. senegalensis.*

Data in chapter 2 indicated that tryptic peptides would match to the corresponding EST with more probability when they are placed closer to the C-terminus of the corresponding protein. This fact has been confirmed after EST analysis from peptides in the hormone treatment experiment (figure 3.15). Moreover, the observation of the matching ratio from proteins with higher and lower *Mr* suggest that, with a fixed number of sequenced peptides assigned to a protein, peptides from high *Mr* proteins present less probability to match EST than peptides from low *Mr* protein. The explanation of this observation is also based in the procedure of ESTs obtainment. In this case, the longer the protein is, the less probable is to catch a sequencing region on the EST intersecting one of the available peptide sequences. This will be in agreement with the fact that for a protein like ATP synthase β-subunit (spot 851b; *Mr* 56) with 8 sequenced peptides assigned, only to 2 peptides were found matching an EST, while in the case of tropomyosin (spot 1147; *Mr* 41) also with 8 assigned peptides match an EST with 7 peptides.

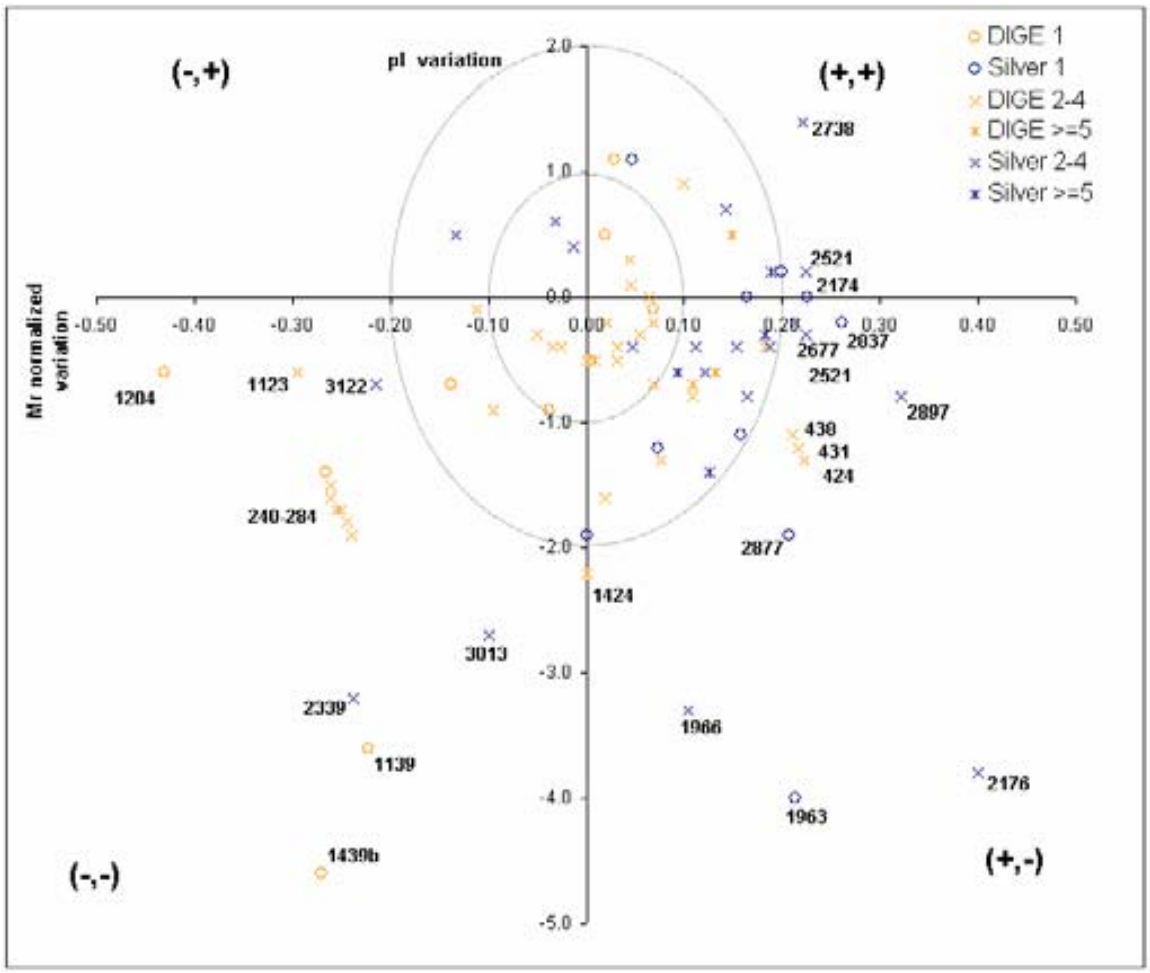

Figure 3.14.-Distribution of spots identified in the spermatogenesis stages (Silver) and the hormone treatment experiment (DIGE) depending on the difference between experimental and theoretical values of *Mr* and *pI*. Spots with values greater than ±0,2 and ±2 for Mr and pI respectively are identified. Normalized value is calculated as (Experimental value-Theoretical value) / (Experimental value + Theoretical value). **(+, +)** indicates experimental value is higher both for *Mr* and *pI*. See figure 2.12 in page 107 for legend of plus and minus pairs and table 3.11 for spot identifications.

Table 3.11.- Spots identified in the spermatogenesis stages comparison (Silver) and the hormone experiment (DIGE) with differences between experimental and theoretical values of *Mr* and *pI* greater than 0,2 and 2, respectively (figure 3.14). Exp= Experiment where the spots was differential. S= Silver: Spermatogenesis stages comparison. D= DIGE: Hormone treatment experiment; Peptides Seq/ID= Number of MS/MS sequenced peptides and peptides yielding protein identification; *Mr*/*pI* region= in figure 3.14, quadrant where the spot is placed (see figure 2.12 in page 107 for description of plus-minus pairs); Tentative explanation= Possible reasons for differences between experimental and theoretical values of *Mr* and *pI.*

Exp	Spot ID	Prot ID	Peptides Seq/ID	Mr/pI Region	Tentative explanation
D	1123	Keratin S8 type I	11/2	-/-	Fragment or homology difference
D	240-284	Alpha-2-macroglobulin-1	7/2	-/-	Precursor
S	2339	Hydroxysteroid (17-beta) dehydrogenase 4	6/2	-/-	Homology difference
S	3013	Transgelin 2	2/2	-/-	Homology difference
S	3122	Myosin light chain alkali	2/2	-/-	Fragment or homology difference
D	1204	Oxidative-stress resp 1	6/1	-/-	Fragment or homology difference
D	1439b	Proteasome β type 5	5/1	-/-	Error in protein assignation
D	1139	NADH dehydrogenase 5	5/1	-/-	Error in protein assignation
D	1424	Peroxiredoxin 6	8/5	0/-	Phosphorylation
D	424-431-438	Hemopexin	5/2	+/-	Precursor
S	1966	Serine (or cysteine) proteinase inhibitor	11/3	+/-	Homology difference
S	2667	Ubiquitin C-terminal hydrolase	3/3	+/-	Precursor
S	2897	Cofilin	3/2	+/-	Precursor
S	2176	Acidic ribosomal phosphoprotein P0	2/2	+/-	Homology difference
S	1963	Olfactory receptor Olr653	1/1	+/-	Error in protein assignation
S	2174	Polymerase (RNA) II (DNA directed) polypeptide C	1/1	+/-	Precursor or homology difference
S	2837	Heterochromatin-specific nonhistone protein	1/1	+/-	Precursor or homology difference
S	2877	Histidyl-tRNA synthetase	1/1	+/-	Homology difference
S	2738	Proteasome subunit beta	4/3	+/+	Precursor or PTM
S	2521	6-phosphogluconolactonase	3/2	+/+	Precursor or PTM

>gi|47218629|emb|CAG04958.1| ATP synthase β-subunit [Tetraodon nigroviridis]

MLGAVGRCCTGALQALKPGVQPLKALVGSPAVLARRDYVAPAAAAATANGRIVAVIGAVVDVQF
DEGLPPILNALEVAGRDSRLVLEVAQHLGENTVRTIAMDGTEGLVRGQKVLDTGAPIRIPVGPET
LGRIMNVIGEPIDERGPITTKQTAPIHAEAPEFTDMSVEQEILVTGIKVVDLLAPYAKGGKIGLFGG
AGVGKTVLIMELINNVAKAHGGYSVFAGVGERTREGNDLYHEMIESGVINLKDTTSKVALVYGQ
MNEPPGARARVALTGLTVAEYFRDQEGQDVLLFIDNIFRFTQAGSEVSALLGRIPSAVGYQPTLA
TDMGTMQERITTTKKGSITSVQAIYVPADDLTDPAPATTFAHLDATTVLSRAIAELGIYPAVDPLDS
TSRIMDPNIVGAEHYDVARGVQKILQDYKSLQDIIAILGMDELSEEDKLTVARARKIQRFLSQPFQ
VAEVFTGHLGKLVPLKETIKGFQSILAGEYDALPEQAFYMVGPIEEVVQKAKKLVEEQS

>gi|54035446| 26S protease regulatory subunit S10B [Danio rerio]

MAENREKGLQDYRKKLLEHKEIDGRLKELREQLKELTKQYEKSENDLKALQSVGQIVGEVLKQLT
EEKFIVKATNGPRYVVGCRRQLDKSKLKPGTRVALDMTTLTIMRYLPREVDPLVYNMSHEDPGS
VSYSEIGGLSEQIRELREVIELPLTNPELFQRVGIIPPKGCLLYGPPGTGKTLLARAVASQLDCNFL
KVVSSSIVDKYIGESARLIREMFNYARDHQPCIIFMDEIDAIGGRRFSEGTSADREIQRTLMELLNQ
MDGFDTLHRVKMIMATNRPDTLDPALLRPGRLDRKIHIELPNEQARLDILKIHSGPITKHGDIDYEA
IVKLSDGFNGADLRNVCTEAGMFAIRAHEYVTQEDFMKAVRKVADSKKLESKLDYKPV

>gi|37748290|gb|AAH59671.1| Peroxiredoxin 6 [Danio rerio]

MPGILLGDVFPNFEADTTIGKIKFHEFLGNSWGILFSHPRDFTPVCTTELARAAKLHEEFKKRDVK
MIALSIDSVEDHRKWSEDILAFNQDKACCPMPFPIIADDKRELSVLLGMLDPDERDKDGMPLTAR
CVFVVGPDKRLKLSILYPATTGRNFDEILRVVDSLQLTATKKVATPVDWKPGQEVMVIPSLSDEE
ANKLFPAGFTLKEVPSGKKYIRYTKP

Figure 3.15.- Peptides described for spots 851b, 1032 and 1424 (underlined) were aligned over the predicted protein (ATP synthase β-subunit, 26S protease regulatory subunit S10B, Peroxiredoxin 6, respectively). Peptides giving a correspondence with *S. sengalensis* EST (CL52Contig1, CL516Contig1 and CL1Contig9, respectively) are placed close to the C-terminal aminoacid sequence (underlined). Peptides close to the N-terminal find an EST correspondence with less probability than peptides next to C-terminal.

3.3.5 Biological implications

Spots with significant variations in the protein levels along the different studied states were classified into several groups, based on their protein profiles, in order to unmask proteins changing in the same direction due to hormone treatments. Spots changing exclusively in one comparison more than ±1,9 folds were also selected as tentative markers for a certain state (table 3.12). Literature data and protein database annotations for these spots were analyzed in order to link determined variations in testis proteome with observed physiological and histological features in each studied state.

Table 3.12.- Spot ID and Prot ID of the differential spots unique to each experimental comparison in the hormone experiment.

	Unique spots	Unique spot ID	Protein identification for unique spots
F0 Mat-F1C	5	431	Hemopexin
		438	Hemopexin
		1204	Similar to oxidative-stress responsive 1
		1380	No ID
		1639	No ID
F0 Mat-F1GnRHa	0	----	----
F0 Mat-F1GnRHa+OA	2	250	Alpha-2-macroglobulin-1
		1422	Peroxiredoxin 6
F1C-F1GnRHa	3	1119	Tropomyosin
		1147	Tropomyosin 2
		1411	Glutathione S-transferase
F1C-F1GnRHa+OA	8	581	Keratin
		932	No ID
		1030	Keratin 18
		1031	Keratin 18
		1032	Proteasome 26S subunit ATPase 6
		1393	Short-chain dehydrogenase/reductase
		1409	LRP16 protein
		1440	Ubiquitin C-terminal hydrolase
F1GnRHa-F1GnRHa+OA	4	265	Alpha-2-macroglobulin-1
		267	Alpha-2-macroglobulin-1
		277	Alpha-2-macroglobulin-1
		1017	3-hydroxyisobutyryl-Coenzyme A hydrolase

In the general introduction, it was reported that males in F0Mat state are at maximum spawn stage, producing spermatozoa with high motility, without morphological abnormalities, and with the highest fecundation rate relative to any other stage (Anguis 05). Therefore, for this study, F0Mat stage was considered as the optimum stage of spermatogenesis to be reached in captivity. As the observed morphological and physiological features of testis from F1 Control fish were away from that stage, it could be expected that an effective hormone treatment should bring the situation to a phenotype as close as possible to the F0Mat state.

The physiological data obtained suggest that the GnRHa+OA treatment was the most effective procedure to improve the spermatogenic process, since spermatozoa motility was increased (figure 3.2). In consequence, proteins with relevant variations between F1 Control and F1 GnRHa+OA, and presenting levels similar to the state considered here as optimum (F0Mat) could be of special relevance for male fish fertility.

Proteins with differential abundance level only after GnRHa+OA treatment (table 3.12) present mainly two profile tendencies: the protein abundance is higher in GnRHa+OA than in any other state (for example spots 581, 1030 and 1031; group 8 in figure 3.11) or the protein level in the F0Mat state is lower than in F1 Control and similar to GnRHa+OA (for example spots 1440, 1409, 1393, 1032; group 6 in figure 3.11). Accordingly, these relevant spots were concentrated in two different regions of the dendrogram in the cluster analysis (see table 3.7; subtrees 1-2 and subtrees 4-5, respectively)

These first five spots were all assigned to keratin or tropomyosin related proteins, indicating an important role of GnRHa+OA treatment in structural rearrangements, possibly leading to the observed increment of spermatozoa motility.

From the second set of spots, number 1393 was identified as short chain dehydrogenase/reductase (SCHAD), a protein found in *Danio rerio* and *Tetraodon nigroviridis,* and homologous to members of the 17-β hydroxysteroid dehydrogenase family in other vertebrates. Labrie *et al.* (1997) described the activity of 17-β hydroxysteroid dehydrogenases in human tissues and its importance in sex steroid activity as a control point for its intracellular concentration. This family of enzymes has two major roles: catalyze the conversion of androstenedione into testosterone, and inactivate sex steroids to reduce its activity. Then, increased levels of 1393 in F1 Control

could partially block the effect of testosterone in testis and, by consequence, affect the spermatogenesis process. Therefore, the observed features in F1 Control can partially be caused by an anomalous increased level of an enzyme that is reducing the activity of testorene and its derivates.

In chapter 2 spot 2339, also related to the family of 17-β hydroxysteroid dehydrogenase enzymes, was found to be increased in wild animals with respect to cultured fish, while in this chapter spot 1393 present the opposite variation between wild and cultured fish. This may indicate that, although functionally related, these proteins have different roles in hormone metabolism in *S. senegalensis*. This family of proteins will become then interesting candidates for further research on hormone regulation in both wild and cultured Senegalese sole.

LRP16 protein (spot 1409) presented increased levels in F1 Control, but lower levels in the other three states (F0Mat, F1 GnRHa, F1 GnRHa+OA). LRP16 protein has been described as up-regulated by 17-β-estradiol effect through estrogen receptor in mammals (Zhao 05). Estrogen receptors have been described in fish male reproductive organs, where estrogen action was related to the renewal of spermatogonial stem cells (Miura 99). Considering these observations, increased levels of LRP16 indirectly suggest that estrogen concentrations are also increased in F1 Control state relative to the F0Mat ideal state. The balance between androgen and estrogens is essential for normal sexual development and reproduction (Conley 01). Hormone treatment may normalize this steroid ratio, and then promote a normal spermatogenic process. Future estrogen/androgen measurements in the studied states will be of great interest to determine the effect of this balance on spermatogenesis in *S. senegalensis*.

Spots 1032 and 1440 were assigned, respectively, to proteasome 26S ATPase 6 and ubiquitin C-terminal hydrolase, both involved in protein degradation. Their expression profile indicated an accumulation of this protein in F1 Control fish. Levels after hormone treatment were similar than expression in F0Mat, suggesting that steroid application modified protein catabolic processes towards the desired spermatogenic state. Implications in spermatogenesis of proteasome proteins and ubiquitin hydrolases/lyases were already discussed in chapter 2.

Spot 298 presented an expression profile similar to other spots described until now (group 6 of figure 3.11). Spot 298 was assigned to chaperone gp96 of *Danio rerio*, a protein with a 93% of homology with the mouse tumour rejection antigen gp96. This protein has been localized on precursor germ cells but not on spermatozoa in the seminiferous tubules of mouse testes (Asquith 05). In this study, chaperone gp96 was highly abundant in F1 Control testis, but less abundant in the other three states, indicating a major presence of germ cells than mature spermatozoa in F1 Control state. This fact is coincident with the observations on histological preparation in Agullerio *et al*. (2007). All together indicates that spermatogenesis in F1 Control presented a lower number of mature spermatozoa than in the other three states, while after hormone treatment it acquires similar levels to the F0Mat state. The monitorization of this protein during spermatogenesis could be of interest as a biomarker of the maturation grade of testis in *S. senegalensis*.

Summarising, the biological functions described for the proteins showing similar levels in F0Mat and F1GnRHa+OA but differing in F1 Control and F1 GnRHa suggest that testosterone effect is reduced in testis of F1 Control fish. This which can cause an altered estrogen/androgen balance that will end in impaired spermatogenesis, as demonstrated by the observed low spermatozoa motility and by the underexpression of a mature spermatozoa biomarker for spermatozoids maturity (gp96). Other processes like protein exchange of histones and protamines, and structural proteins could be also involved in the increase of motility in the phenotype observed for F1GnRHa+OA fish relative to F1 Control animals.

The GnRHa treatment influenced sperm volume but not the number of spermatozoa produced (figure 3.2). Differential spots in testis of these animals could be related to these processes, especially when they were expressed at the same level than F0Mat fish but different in F1 Control or F1 GnRHa+OA states. Some of the spots assigned to hemopexin (424, 431 and 438) and α-2-macroglobulin-1 (240, 250, 265 and 284) fit this expression profile.

Alpha-2-macroglobulin-1 is a non-specific inhibitor of proteases produced in testis by Sertoli cells, where it probably inhibits proteases from degenerating late spermatids, like acrosin (Cheng 90). A lack of this activity leads to disruptions in the blood-testis barrier, abnormal spermatozoa development and finally to infertility (Metayer 02). Then, the

increment in the number of spermatozoa produced by GnRHa can be mediated by the presence of this protease inhibitor. Interestingly, the protein level of some isoforms of α-2-macroglobulin-1 was higher in GnRHa-treated fish than other cultured states, probably indicating that PTM regulation is also playing a role in modulating the final α-2-macroglobulin-1 activity.

Hemopexin spots showed protein levels in the GnRHa fish similar to those in F0Mat animals. Hemopexin is a heme-binding protein which prevents oxidative stress caused by free Fe species (Tolosano 02). Possible damage caused by oxidative stress on spermatogenesis was already described in chapter 2. The presence of similar levels of hemopexin in GnRHa and F0 Mat states could indicate similar protective conditions against oxidative stress. This protective environment favours then the spermatogenic process, and thus more spermatozoa could be produced in the GnRHa treatment with respect to F1 Control and GnRHa+OA states.

The spots assigned to hemopexin and α-2-macroglobulin-1 are mainly grouped in the subtree 3 of the cluster analysis (table 3.7), confirming a common expression pattern of these proteins with protective functions on spermatozoa. This combinated protective effect could explain the increase on the number of spermatozoa after GnRH treatment.

Spot 1507 was assigned to ferritin, a protein that has been described to store ionic Fe in Sertoli and Leydig cells, thus providing this element to the developing gametes during spermatogenesis (Wise 03). Protein levels in F1 states are almost two times less than in males at F0Mat state. In mammals a decreased of intracellular ferritin is related to a decrease of available Fe. Therefore, the low levels of ferritin in the testis of F1 males might indicate a lack of available ionic Fe to gametes. The low availability of this element was reported to affect adversely reproduction in other animals in captivity (Hidiroglou 79).

3.3.6 Complementing proteomic data with transcriptomic analysis

In chapter 2, few protein changes matching with the transcriptome analysis were observed. This observation was however not unusual as judged from other combined proteomic and genomic studies published (see references in 2.3.6). In the hormone

experiment, direct correspondences at protein and mRNA level were not found. As discussed in chapter 2, the lack of correspondence between mRNA and protein level can be caused by several reasons: translational regulation, mRNA stability, splicing, post-translational processing regulation, and partial analysis of protein isoforms, protein degradation or a combination of these facts.

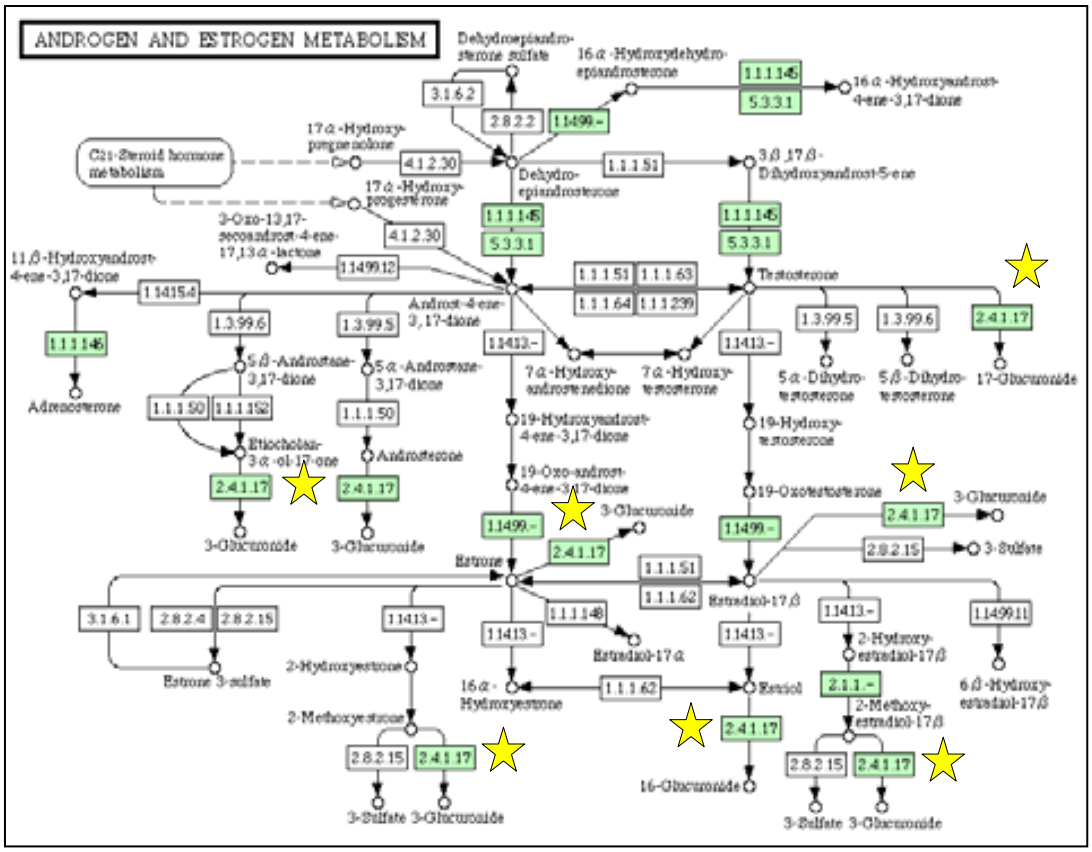

Figure 3.16.- Implication of UDP-glucuronate β-D-glucuronosyltransferase (E.C. 2.4.1.17) in androgen and estrogen metabolism in *Danio rerio* (KEGG pathway dre00150). Enzyme 2.4.1.17 is involved in elimination of testosterone, androsterone, etiocholan-3 α-ol-17-one, estrone, estradiol-17 β, estriol, and 2-methoxyestrone.

The extent of correspondence between mRNA and protein variations increases when complete protein pathways are considered (Washburn 03). In this study, three elements involved in the sex steroid pathway (proteins: SCHAD and LPRP16; gene: UDP-glucuronate β-D-glucuronosyltransferase) were found as differential in proteomic and

genomic analysis of testis under hormone treatment. The degree of correlation between both approaches is similar to that described for yeast by Washburn *et al*. (2003), who found five correlations at the pathway level, for instance at the purine or the aromatic amino acid biosynthetic pathways.

The biological meaning of expression changes of UDP-glucuronate β-D-glucuronosyltransferase should be related with its implication in the pathway of steroid hormone elimination and in general detoxification (figure 3.16). The increment in hormone treated states possibly indicates that the application of hormonal implants is increasing the concentration of sex steroids. Probably, the hormone doses administered to fish males were above the physiological levels, and therefore the fish responded by activating the enzymes involved in hormone elimination.

In conclusion hormone treatments in males under captivity of the Senegalese sole led to improvements in the number (GnRHa) and motility (GnRHa+OA) of spermatozoa. These physiological progressions in spermatogenesis after hormone treatment were related to the variation in the abundance of proteins involved in iron metabolism and in protective functions on spermatozoa (GnRHa), and in testosterone catabolism, response to estrogens and the exchange of histones and protamines (GnRHa+OA). Moreover, the protein chaperone gp96 was proposed as possible biomarker for determining spermatogenesis maturity in *S. senegalensis*.

Confidence on these protein identifications, performed through *de novo* sequencing of MS/MS fragmented peptides and BLAST, was increased with further comparisons with genomic EST from *S. senegalensis* and with the combined analysis of theorical and experimental *Mr* and *pI* values along with MS/MS fragmented peptides.

In overall, these results constitute an original contribution for the flatfish aquaculture field and proportion a new insight in the molecular mechanisms involved in the spermatogenesis of the Senegalese sole.

Chapter 4

Database for 2-D LC MS/MS and 2-D gel-experiments of *Solea senegalensis*.

The high-throughput experiments involved in modern “omic” technologies such as genomics, transcriptomics, proteomics or metabolomics, generate vast amounts of complex data. Projects dealing with any of these “omic” approaches should be then prepared to deal with large amounts of data both at the processing stages as well as during daily data retrieving and consultign (Wilke 03).

The Pleurogene project aims to integrate all the data from DNA microarrays, histological preparations and proteome experiments performed within the project in an interactive bioinformatic platform known as Pleuromold. This platform is derived from a previous interactive database designed at Oryzon Genomics (OG), focused on the integration of mRNA expression analyses and tissue histological preparations in *Oryza sativa* (Mercadé in preparation). This type of integrative platforms, known as e-mold, recreates an organism *in silico* enabling the integration of structural and molecular information. Pleuromold was designed as a visual computer-based atlas where mRNA/protein expression data is organized in function of the studied tissue. Precise sample features of the target species like developmental stage or histological structure are strongly considered to make the e-mold organization.

In collaboration with Jaume Mercadé from the OG Bioinformatic unit, data from 2-D LC MS/MS (Chapter 1) and 2-D gel experiments (Chapters 2 and 3) were organized in a database built into the framework of an e-mold designed at OG and, then integrated in Pleuromold. In this way, information produced in the previous three chapters will be available for other scientific groups interested in flatfish reproduction. Moreover, the integration of genomic and proteomic data in an e-mold environment will provide a wider vision of the *Solea senegalensis* reproduction and a better understanding of the flatfish biology.

4.1 Material and methods

4.1.1 Biological data

2-D LC MS/MS. The list of nearly 1300 peptides characterized in chapter 1, including all parameters described for each entry, was considered for storing and consulting in the database. This list was introduced with a brief method description of the 2-D LC MS/MS system, and the bioinformatic treatment performed to the MS/MS spectra.

Histological preparations. Representative histological images of testis tissue corresponding to the different spermatogenesis stages studied in chapter 2 (F0 Mid, F0 Late, F0 Mat, F1 Late, F1 Mat) and in chapter 3 (F0 Mat, F1 Control, F1 GnRHa, F1 GnRHa+OA) were included in the database. These images were introduced with a brief description of the histological preparation and indications to interpret biological structures present in the images.

2-D gel experiments. Low resolution (300 dpi) gel images acquired on a GS-800 Calibrated Densitometer (Bio-Rad) after silver staining were stored in the database. This collection was accompanied by general experimental information and included 30 gel images related with spermatogenesis stages (Chapter 2) and 6 more images related to hormone treatment (Chapter 3). For each differential spots on chapter 2 and 3 (49 spots and 59 spots, respectively), an information package was prepared containing the gel image localization, the graphic of the normalized expression values in the studied states, the statistical values of confidence in variation when proceed, the MALDI spectrum of the digested spot, the n-ESI MS/MS of the sequenced peptides, the Peaks 2.4 and Lutefisk 97 candidates for each sequenced peptides, the protein assignation of each spot and the protein coverage of the sequenced peptides over the assigned protein.

4.1.2 Protein module database organization

2-D LC MS/MS. Peptide sequences were introduced in a tabulated text format. Each entry included the sample identification (testis or larva) and the experimental source

(2-D LC salt step), the accession number to NCBI and Unigene human protein databases, the identification data obtained from BLAST comparison (score and e-value), the peptide mass (Da) and charge of the MS/MS fragmented ion, the calculated peptide charge at pH 3, and the Peaks 2.4 and Lutefisk 97 peptide sequence and score.

2-D gel experiments.- Information was organized taking into account the source experiment. Accordingly, a main “Experiment“ field , identified with the key “id-exp”, was created. This field holds several attributes including the “exp_type” that identifies the study (spermatogenesis and hormone treatment studies indicated as "Silver" or "DIGE", respectively) and a short experimental description of the experiments that could be accessed through a “description” key.

Information related to the studied states of each experiment was included in the field “State”. This field includes the name of the studied states (id_state), the “id_exp” where each state is studied, an image of a 2-D gel from this state, and a testis histological preparation of the mentioned state.

Data belonging to univocal identification of the spot inside the database was provided in the “Spot” field by “id_spot”. This key term was formed with the name of the experiment “id_exp” plus the “spot_name” (the number of the spot in each 2D experiment). For instance in spot 2897 in the spermatogenesis stage experiment will be known as Silver_2897. Under the “Spot” field it was also found the situation of the spot in a 2-D gel (spot_map), the MALDI MS spectrum from after digesting the spot (Maldi), the protein related to this spot (prot_id), and the histogram with the normalized volumes of this spot in the states studied in the present experiment (histogram).

Sequence information from n-ESI MS/MS analysis and *de novo* sequencing was divided in three fields. “Peptide”: Each sequenced peptide is named with an “id_peptide” composed with the “id_spot” and its m/z value and charge. The fragmentation spectrum is also presented. “Peaks”: For each sequenced peptide (id_peptide) the five candidates are shown when available. “Lutefisk”: For each sequenced peptide (id_peptide) the five candidates are shown when available. For both “Peaks” and “Lutefisk”, general sequencing parameters are displayed.

Final peptide sequences chosen to relate spots with identified proteins are found under the “Sequence” field. Each sequence is identified by the “id_peptide”, the “prot_id” and the “id_exp” keys. Information on the protein identified for each spot was located in the “Protein“ field. This information included the protein name, the specie of homology where protein was identified, the sequence coverage of the sequenced peptides for the identified protein (sequence), the theoretical molecular mass and isoelectric point and a short definition on biological aspects of the protein.

All these fields and terms were related inside the database structure as described in figure 4.1, providing that each element inside the database is always univocally identified to avoid conflicts during the query module.

4.1.3 Application architecture and implementation

The present application was implemented in a client server architecture to allow many users working simultaneously and accessing the data in concurrent and remote mode. Function in this client server architecture was divided in two parts: the server, who manages the data storage and delivery, and the client, responsible of presenting the server to the users and allowing them to perform operations on it.

A relational database was designed to capture all the relationships between experimental data and to obtain fast and accurate retrieval. To ensure robustness and reliability, open source MySQL 5.0 (www.mysql.com) was selected as the Database Management system (DBMS).

A standalone client was implemented in Java (www.sun.com). Standalone applications are more difficult to implement and deploy than other possibilities, but allow a friendly interaction to the future user. On the other hand, Java selection takes full advantage of graphical user interface (GUI) building libraries such as Swing. The possibility to employ powerful 2D graphical imaging libraries such as Java Advanced Imaging (JAI), and to provide portability to any operative system (OS) were also key points to determine this selection. Java Database Connectivity (jdbc) application programming interface (API) and driver were used in order to connect the client to the server.

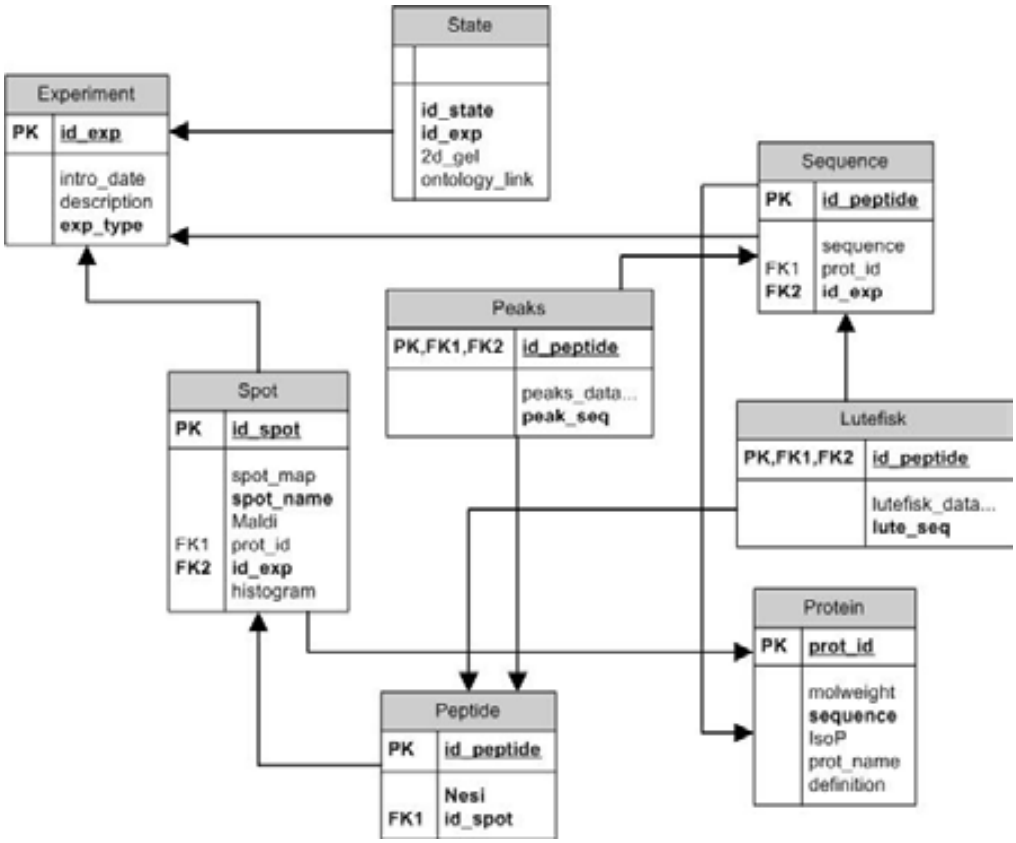

Figure 4.1.- Database structure for 2-D gels based experiments in the protein module. Information is placed under eight fields "Experiment", "State", "Spot", "Peptide", "Peaks", "Lutefisk", "Sequence" and "Protein". Each field contains both data and field-linking terms. For instance, "Spot" contains own terms like "histograms" or "Maldi", and foreign keys to "Experiment" (id_exp) or "Protein" (prot_id). Relationships between fields are depicted by arrows. Arrows indicate relationship between fields. "Experiment" field→*Terms*: id_exp= Identification of the 2D experiment; intro_date= date when information is introduced in the DB; description= experimental methodology; exp_type= protein detection method. "State" field→ Terms: id_state= experimental group studied; 2d_gel=2-D gel image; ontology_link=image of tissue preparation. "Spot" field→ Terms: id_spot =identification of the spot in the database; spot_map=gel image localizing spot; spot_name= spot number in the database; Maldi=MALDI MS spectrum; prot_id= protein identification in the DB; histogram=spot normalized expression volumes. "Peptide" field→ Terms: id_peptide=peptide identification in the DB; Nesi=nESI MS/MS spectrum. "Peaks" field→ Terms: peaks_seq=peptide candidates from Peaks2.4; peaks_data=*de novo* sequencing conditions for Peaks. "Lutefisk" field→ Terms: lute_seq= peptide candidates from Lutefisk; lutefisk_data= *de novo* sequencing conditions for Lutefisk. "Sequence" field → Terms: sequence= peptide sequence used to identify spot related protein. "Protein" field → molweight=molecular weight of the identified protein; IsoP=isoelectric point of the protein; prot_name=name of the protein in NCBI protein DB; definition=biological functions related to the assigned protein.

4.2 Results

4.2.1 Pleuromold interfaces

The Pleuromold interface is organized in three main parts: first a browsable tree that contains an ontology of cell types, tissues and organs at distinct developmental stages of the organism in study; second an atlas of interactive pictures coherent with those terms included in the ontology; and third, two interactive lists to work with the experimental data and a regions worklist. Behind the GUI, data is also organized in three distinct and independent modules. Thus, it is possible to work in three different query modes: expression data coming from microarray technology experiments, expression data obtained from *in situ* hybridizations, and expression data from proteomic experiments. The querying mode appears defined in the upper part of the main frame (figure 4.1). Further explanations about modules and query modes are focused only on those related to protein.

The GUI design allows the user to navigate intuitively through the organism data both by using the tissue ontology tree or the picture atlas. Besides providing spatial and developmental contextualization useful for analysis, the ontology tree and the atlas contextualize the information displayed in the tool to the user. For those users unfamiliar with the organism, the picture atlas includes graphical maps showing all those regions and subregions included in the database that can be highlighted on demand. In a higher degree of interactivity, the user can also ask the application to highlight only the regions below the mouse pointer so they become evident one at a time, as the mouse pointer moves over them (figure 4.2).

The information from proteomic experiments were displayed in two ways depending on the primal experiment:

2-D LC MS/MS. Proteins identified from peptides sequenced in chapter 1 are distributed depending on the original sample (testis or larva). Each protein list is then available under the testis or larva entry in Pleuromold. Peptides originally sequenced in the shotgun experiment can also be consulted for each protein in the list (figure 4.3).

2-DE: In the case of testis, proteins could be originated from shotgun or 2-D gel experiments. A general list of those proteins is displayed under testis description in Pleuromold with the prefixes Exp1-[SHOTGUN] for 2-D LCMS/MS proteins, Exp 2-[2D gel] for spermatogenesis stage study, and Exp 3-[2D gel] for hormone treatment experiment. From this list, proteins are related to the original spot information in each 2-D gel experiment. It is possible to consult the biological variation among the states in each experiment, 2-D gel position, related MALDI-TOF, n-ESI MS/MS, peptide *de novo* sequence and alignment of these peptides on the assigned protein ID (figures 4.4-4.7).

4.2.2 Pleuromold queries

Pleuromold allows for full acces to the data stored in the database. The basic querying unit is the protein. Thus, by selecting a protein present in the work list, the user can make questions such as regions containing proteomic experiments or regions where the selected proteins were identified. Immediately, those regions appear listed in the region work list, providing the user with a protein expression profile based on the ontology. The same question can be performed to any region and the query retrieves all the present proteins expressed in that region. These proteins appear redundantly in case where the same protein was found in distinct experiments for the same region. This redundancy allows the statement of the certainty of the expression and the independent retrieval of information from each experiment.

Besides the simple queries described above, Pleuromold permits more refined questions about protein presence using logical operations, both on proteins and regions selected on the worklists. For instance, the user can perform a query about differential proteins present in one region, but not in another, just by selecting the two regions of interest. In the current implementation of the program the query operation is not commutative, so to retrieve the proteins specific to the second region the user should perform the same operation but interchanging the operands. An analogous query can be performed by selecting proteins pairs in the work list. In this case, the user can ask for regions where a given protein was specifically found relative to the other. Pleuromold users can also perform sum and intersection operations on data. For instance, a possible sum question could be proteins present in region 1 or in region 2, and for an intersection question proteins that are present in both region 1 and 2 at the same time.

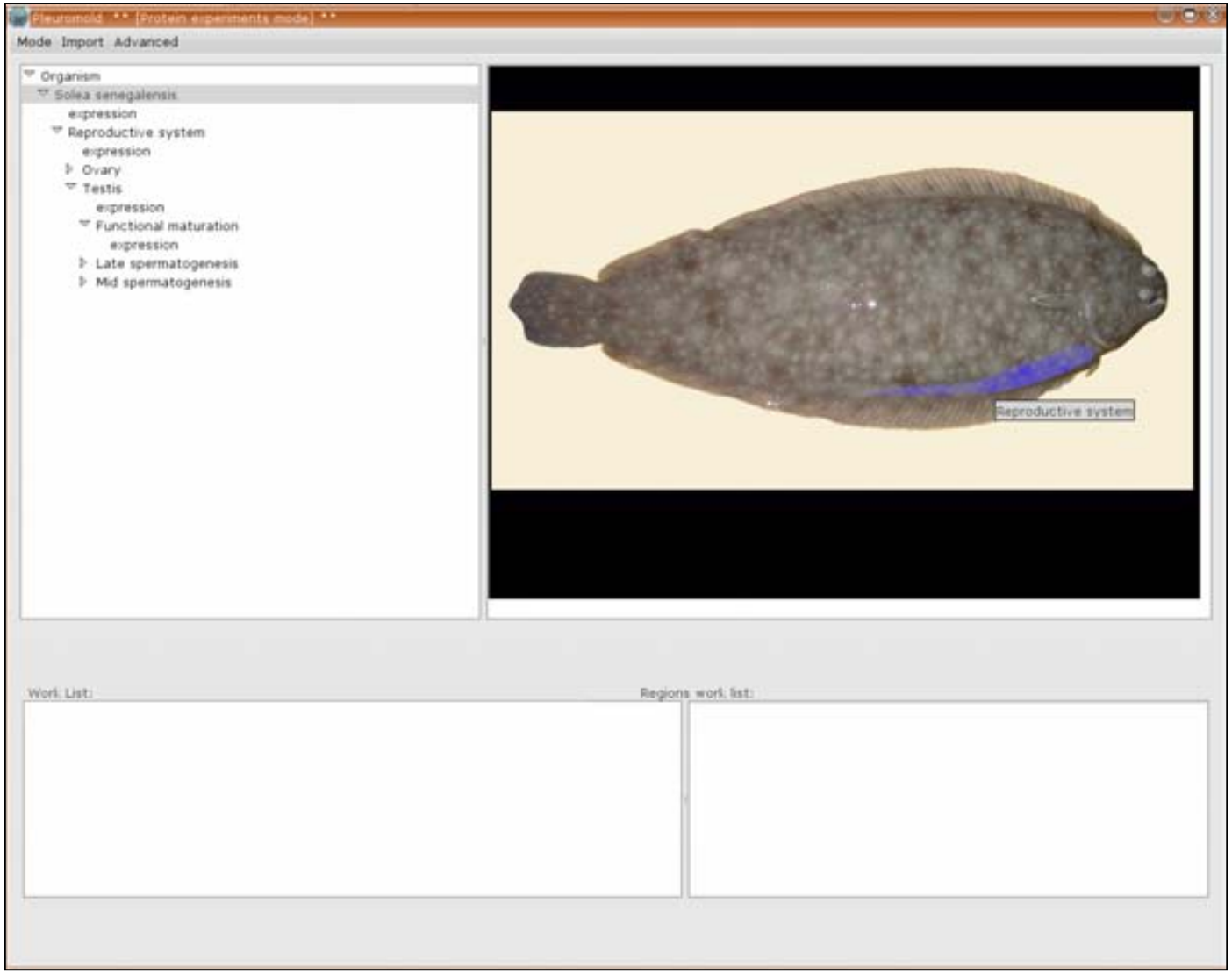

Figure 4.2.- Pleuromold graphic interface (protein module) showing the tissue ontology tree (left), the visual atlas (right) and the interactive worklist regions (down). In the initial screen the complete dorsal part of *S. senegalensis* body is displayed with the gonadal region highlighted. When this region is selected descriptions performed on testis are presented as described in the next figure.

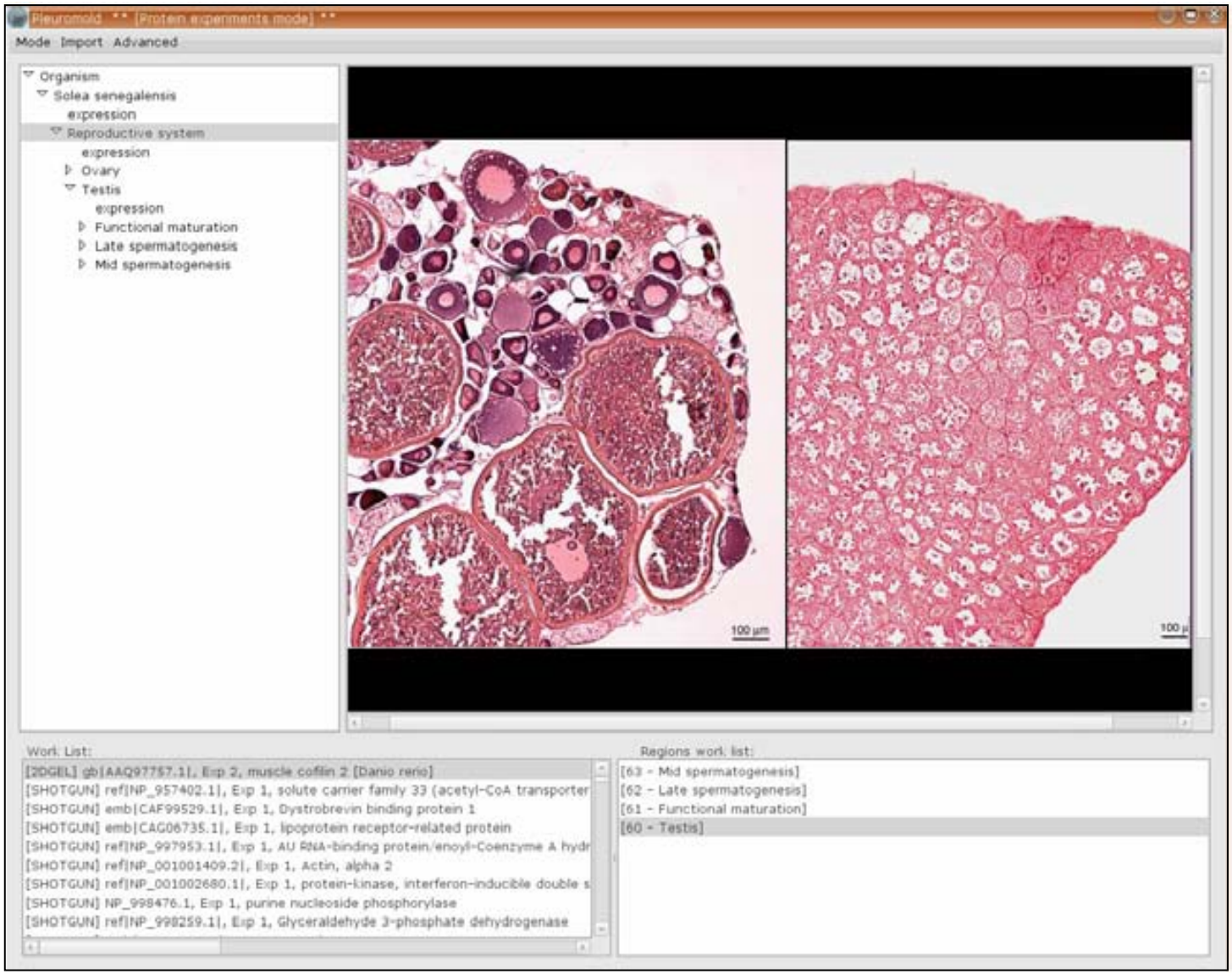

Figure 4.3.- Pleuromold graphic interface for 2-D LC MS/MS experiment in testis. The protein list for shotgun experiment with testis sample is found under expression experiments of reproductive system in *S. senegalensis*. This protein list includes all the proteins expressed in testis and described either by shotgun (Exp1) or 2-DE gel approach (Exp 2 for Silver, Exp 3 for DIGE). A testis histological preparation (right) is also displayed next to an ovary preparation (left).

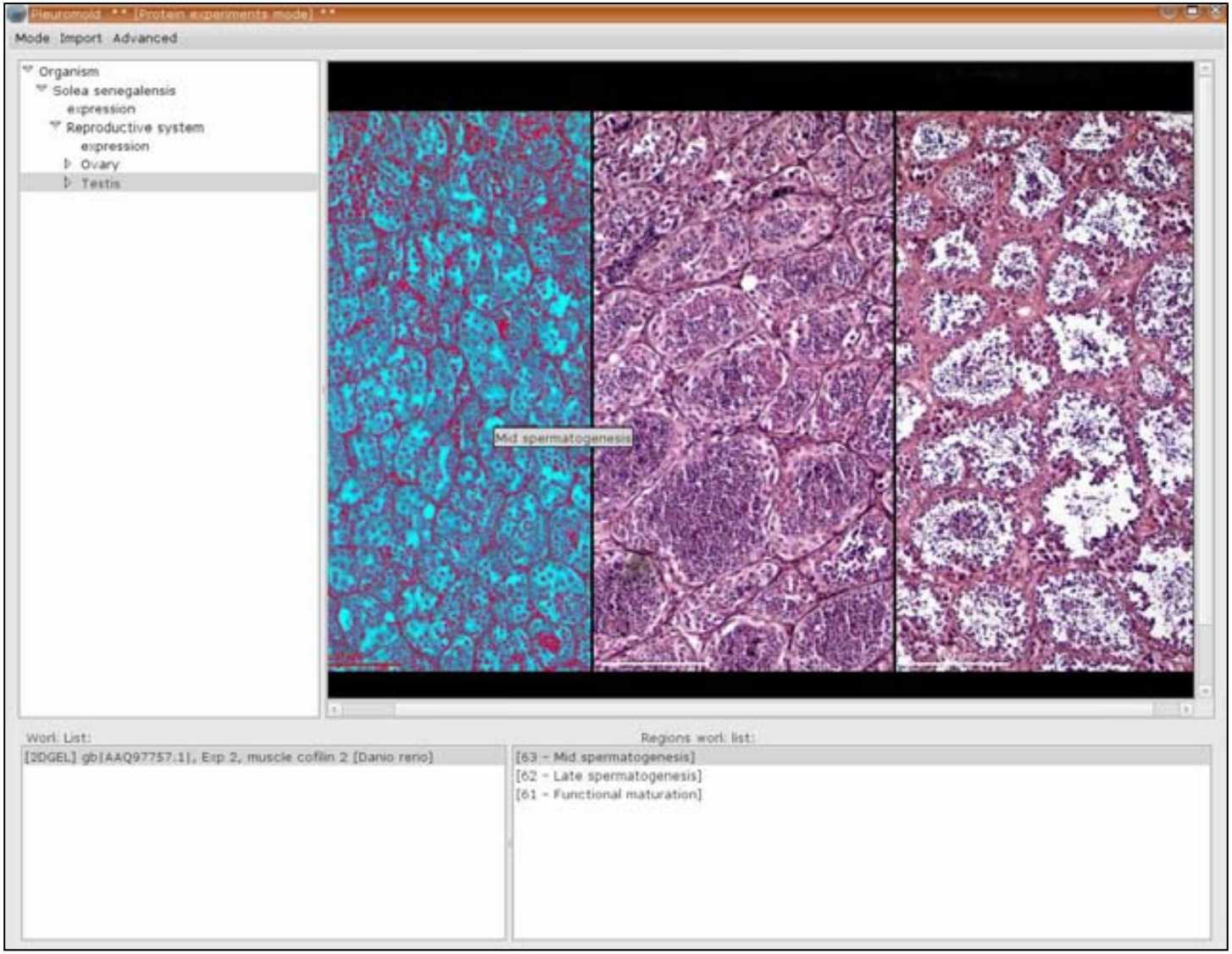

Figure 4.4.- Pleuromold graphic interface (protein module) for 2-D gel experiment in testis (I). From the general protein list in figure 4.2, protein cofilin 2 from Danio rerio (NCBI accession number gbIAAQ97757.1) related to spot Silver_2897 was selected. Histological preparations of the spermatogenesis stages studied in chapter 2 are displayed. In this figure mid spermatogenesis stage is selected.

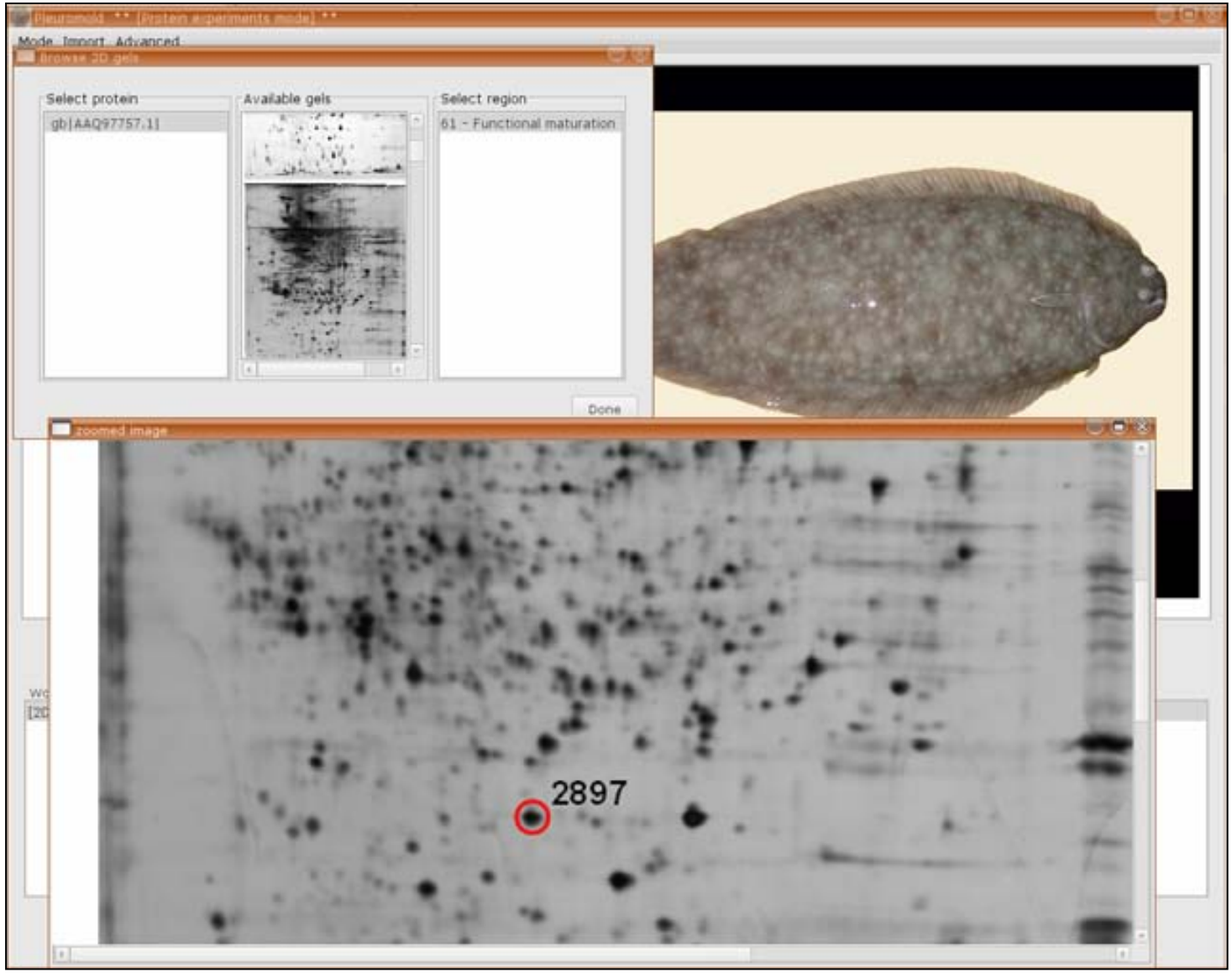

Figure 4.5.- Pleuromold graphic interface (protein module) for 2-D gel experiment in testis (II). Gels available for spot Silver_2897 assigned to protein cofilin 2 (NCBI gbIAAQ97757.1) are displayed in the “Browse 2D gels” window (in this case from F0 Functional maturation). From this window gels can be selected and also position for spot is available. Mass spectrometry information is accessible from this point as described in the next figure.

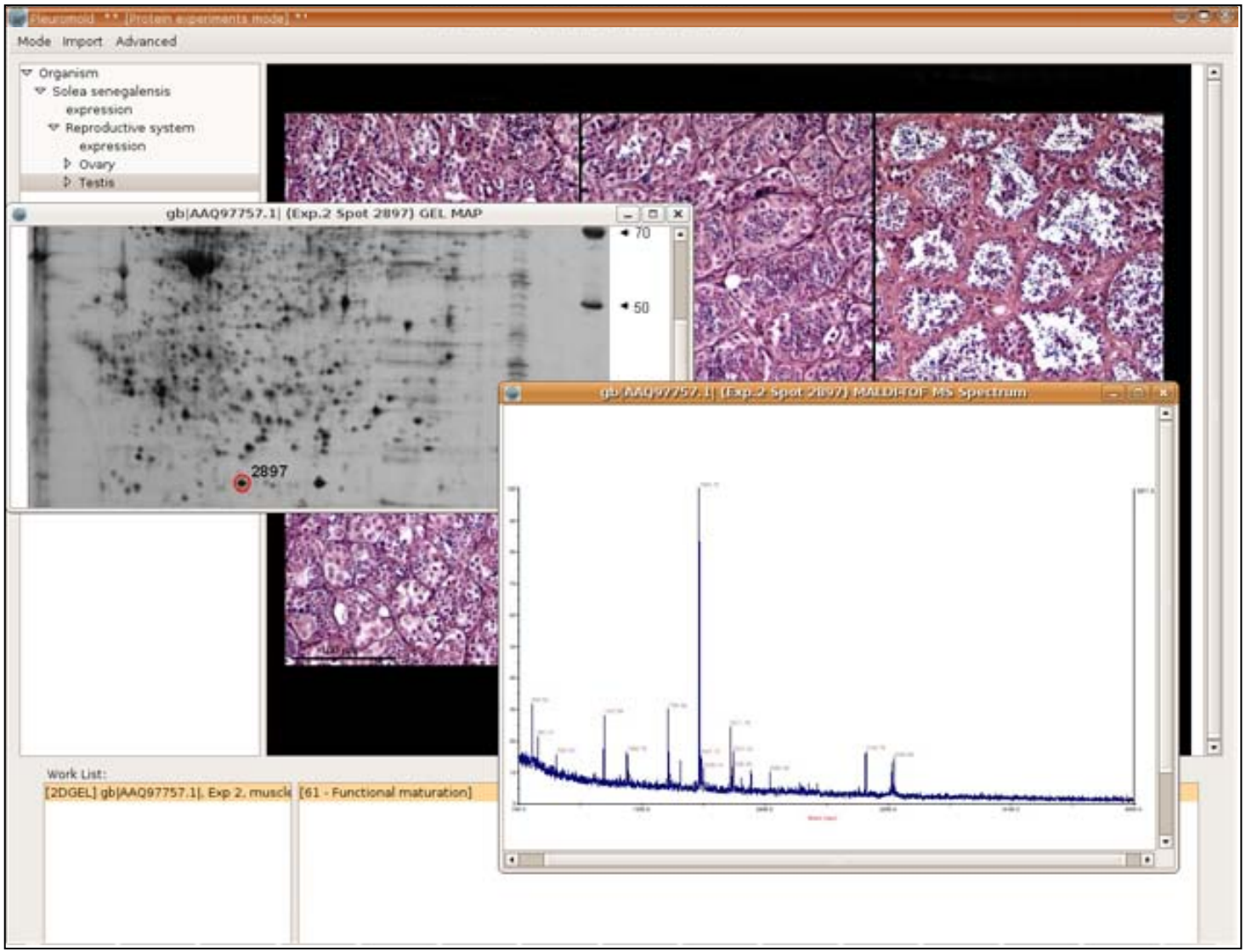

Figure 4.6.- Pleuromold graphic interface (protein module) for 2-D gel experiment in testis (III). MS information available for spot Silver_2897 assigned to protein cofilin 2 (NCBI gbIAAQ97757.1) is displayed. The information includes MALDI-TOF spectrum of digested spot and fragmentation spectra of some digested peptides. From this point is possible to consult *de novo* sequence candidates and protein identification from these sequences.

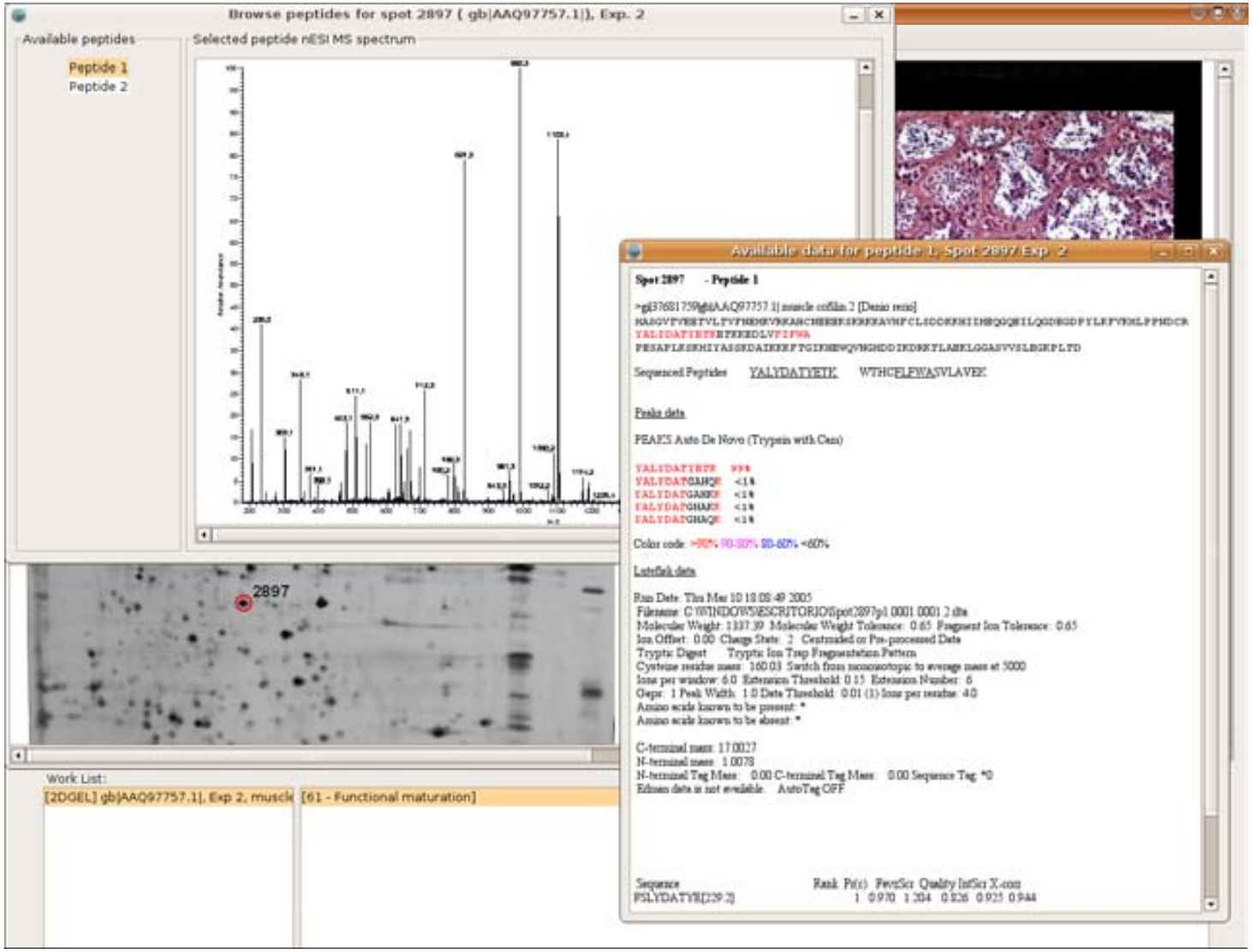

Figure 4.7.- Pleuromold graphic interface (protein module) for 2-D gel experiment in testis (IV). De novo sequences and protein ID information available for spot Silver_2897 assigned to protein cofilin 2 (NCBI gbIAAQ97757.1) is displayed. The information includes Peaks and Lutefisk candidates and the sequences used to assign protein ID to the mentioned spot.

4.3 Discussion

The information generated to describe *S. senegalensis* testis and larva at molecular level during the Pleurogene project aims to yield new tools and basic knowledge on the fish physiology, which could be of interest for optimizing flatfish culture and commercialization. In this respect, Pleuromold provides a user-friendly storage and consulting platform for the data generated inside the mentioned project.

Nowadays, three different types of public web-based databases have been designed according to the available information. The first one integrates data principally from already existing databases of proteins (NCBI, Uniprot, PDB) and genes (Ensemble, GenBank; Hinrichs 06, Jones 06, Goesmann 05). These sorts of databases provide of a common space for consulting existing gene/protein information. Other more specific databases provide of organism (mouse embryonic development, Williams 96) or specific tissue images (brain, Gustafson 07; dermopathology, Feit 05; breast histopathology, Lundin 07) obtained using mainly photographs, histological techniques, tissue microarrays or magnetic resonance imaging from the group publishing the database or from already available data in different public collections. Images are then linked to constitute an atlas, with different related information available during navigation. Finally, the third type combines tissue image with tissue-related genomic data (Lein 07), similar to what is described above for Pleuromold. Additional to data from DNA microarrays, Pleuromold design assumes the inclusion of results from proteomic analysis and *in situ* hibridations in the visual atlas of *S. senegalensis.* Moreover, Pleuromold users can define the items to be displayed in the tissue ontology tree and participate in the creation of the final tool. Data is also inserted directly after user decision, providing a customer-tailored analysis instrument. This structure provides a general description of the biological interest rather than only an image or gene/protein description alone, since the gene or protein data is always contextualized in a biological ontology tree. Moreover, the information displayed in Pleuromold was entirely obtained within the Pleurogene project, as little previous information was available for genes, proteins or tissue from the Senegalese sole. All the data then was generated with the purpose to fit an e-mold platform. The result is a bioinformatic visual tissue atlas with genomic and proteomic data available to perform consultancies at molecular level. Thus, Pleuromold is an essential tool for designing further functional analysis on *S. senegalensis* and homologous flatfish species.

Conclusions

Chapter 1

1.- More than one thousand and two hundred proteins from testis and larva of *Solea senegalensis* were described for the first time. This dataset was obtained in an on-line 2-D LC-MS/MS system followed by *de novo* peptide sequencing method and homology-driven protein identification.

Chapters 2 and 3

2.- The procedure to identify proteins from 2-D gels by tandem mass spectrometry, *de novo* peptide sequencing, and homology-driven identification led to three hundred and fifty-five tentative peptide sequences corresponding to near one hundred proteins of *Solea senegalensis* testis.

3.- The proteomic and genomic analysis of testis in several spermatogenic stages from wild and F1 cultured *Solea senegalensis* unravelled differences in proteins related to the metabolism of testosterone, the histone replacement by protamines, the cell redox balance and the flagellum morphogenesis in sperm. Disorders in these processes would be involved in the detected impairment in sperm quality of F1 fish.

4.- The improvement of spermatozoa motility after the GnRHa+OA treatment on *Solea senegalensis* males correlated with a variation in the level of proteins related to androgen/estrogen balance.

5.- The increased number of spermatozoa observed in GnRHa-treated males of *Solea senegalensis* coincided with variations in the abundance of proteins concerning to protection against oxidative stress and extracellular proteases.

6.- The chaperone gp96 was proposed as a biomarker of maturation in spermatogenesis of *Solea senegalensis*.

Chapter 4

7.- An integrative bioinformatics platform was specifically designed and developed to store and consult in a general organism environment the information obtained by proteomic techniques to describe the proteome of testis and larva from *Solea senegalensis*.

References

Abian, J., Oosterkamp, A. J., Gelpí, E. (1999). "Comparison of conventional, narrow-bore and capillary liquid chromatography/mass spectrometry for electrospray ionization mass spectrometry: practical considerations." Journal of Mass Spectrometry **34**(4): 244-254.

Aebersold, R., Mann, M. (2003). "Mass spectrometry-based proteomics." Nature. **13**(422): 198-207.

Agell, N., Mezquita, C. (1988). "Cellular content of ubiquitin and formation of ubiquitin conjugates during chicken spermatogenesis." The Biochemical Journal **250**: 883-889.

Agulleiro, M. J., Anguis, V., Cañavate, J.P., Martínez-Rodríguez, G., Mylonas, C.C., Cerdà, J. (2006). "Induction of spawning of captive-reared Senegal sole (*Solea senegalensis*) using different administration methods for gonadotropin-releasing hormone agonist." Aquaculture **257**: 511-524.

Agulleiro, M. J., Scott, A.P., Duncan, N., Mylonas, C.C., Cerdà, J. (2007). "Treatment of GnRHa-implanted Senegalese sole (*Solea senegalensis*) with 11-ketoandrostenedione stimulates spermatogenesis and increases sperm motility." Comparative Biochemistry and Physiology, Part A **In press**.

Åkerlof, E., Jornvall, H., Slotte, H. (1991). "Identification of apolipoprotein A1 and immunoglobulins as components of a serum complex that mediates activation of sperm motility." Biochemistry **30**: 8986-8990.

Alban, A., David, S.O., Bjorkesten, L., Andersson, C., Sloge, E., Lewis, S., Currie, I. (2003). "A novel experimental design for comparative two-dimensional gel analysis: two-dimensional difference gel electrophoresis incorporating a pooled internal standard." Proteomics **3**(1): 36-44.

Alpert, A. J., Andrews, P.C. (1988). "Cation-exchange chromatography of peptides on poly(2-sulfoethyl aspartamide)-silica." Journal of Chromatography **443**: 85-96.

Altschul, S. F., Gish, W., Miller, W., Myers, E.W., Lipman, D.J. (1990). "Basic local alignment search tool." Journal of Molecular Biology **215**: 403-410.

Anderson, L., Seilhamer, J. (1997). "A comparison of selected mRNA and protein abundances in human liver." Electrophoresis **18**(3-4): 533-537.

Anguis, V., Cañavate, J.P. (2005). "Spawning of captive Senegal sole (*Solea senegalensis*) under a naturally fluctuating temperature regime." Aquaculture **243**: 133-145.

Aparicio, S., Chapman, J., *et al.* (2002). "Whole-Genome Shotgun Assembly and Analysis of the Genome of Fugu rubripes." Science **297**: 1301-1310.

Aravinda, S., Gopalakrishnan, B., Dey, C.S., Totey, S.M., Pawshe, C.H., Salunke, D., Kaur, K., Shaha, C. (1995). "A testicular protein important for fertility has glutathione S-transferase activity and is localized extracellularly in the seminiferous tubules." Journal of Biological Chemistry **270**(26): 15675-15685.

Ashizawa, K., Wishart, G.J., Hashimoto, K., Tsuzuki, Y. (1995). "Dephosphorylation of a 30-kDa protein of fowl spermatozoa by the addition of myosin light chain kinase substrate peptide inhibits the flagellar motility." Biochemical and Biophysical Research Communications **215**(2): 706-712.

Baik, J. Y., Lee, M.S., An, S.R., Yoon, S.K., Joo, E.J., Kim, Y.H., Park, H.W., Lee, G.M. (2006). "Initial Transcriptome and Proteome Analyses of Low Culture Temperature-Induced Expression in CHO Cells Producing Erythropoietin." Biotechnology and Bioengineering. **93**(2): 361-371.

Baynes, S. M., Howell, B.R., Beard, T.W., Hallam, J.D. (1994). "A description of spawning behaviour of captive dover sole, Solea solea (L.)." Neth. J. Sea Res. **32**: 271-275.

Baynes, S. M., Scott, A.P. (1995). "Seasonal variations of parameters of milt production and in plasma concentration of sex steroids of male rainbow trout (*Salmo gaidneri*)." General and Comparative Endocrinology **57**: 150-160.
Benbrahim-Tallaa, L., Tabone, E., Tosser-Klopp, G., Hatey, F., Benahmed, M. (2002). "Glutathione S-Transferase Alpha Expressed in Porcine Sertoli Cells Is under the Control of Follicle-Stimulating Hormone and Testosterone." Biology of Reproduction **66**: 1734-1742.

Berlinsky, D. L., King, W.V., Smith, T.I.J., Hamilton II, R.D., Holloway Jr., J., Sullivan, C.V. (1996). "Induced ovulation of Southern flounder *Paralichthys lethostigma* using gonadotropin releasing hormone analogue implants." Journal of the world aquaculture society **27**: 143-152.

Berlinsky, D. L., William, K., Hodson, R.G., Sullivan, C.V. (1997). "Hormone induced spawning of summer flounder *Paralichthys dentatus*." Journal of the world aquaculture society **28**: 79-86.

Berruti, G. (2000). "A Novel Rap1/B-Raf/14-3-3 u Protein Complex Is Formed in Vivo during the Morphogenetic Differentiation of Postmeiotic Male Germ Cells." Experimental Cell Research **257**: 172–179.

Billard, R. H. (1983). "Spermiogenesis in the rainbow trout (Salmo gairdneri). An ultrastructural study." Cell and tissue research **233**(2): 265-284.

Bjellqvist, B., Ek, K., Righetti, P. G., Gianazza, E. *et al.* (1982). "Isoelectric focusing in immobilized pH gradients: principle, methodology and some applications." Journal of Biochemical and Biophysical Methods **6**: 317-339.

Blom, K. F. (1997). "Strategies and Data Precision Requirements for the Mass Spectrometric Determination of Structures from Combinatorial Mixtures." Analytical Chemistry **69**(21): 4354-4362.

Blom, N., Gammeltoft, S., Brunak, S. (1999). "Sequence and Structure-based Prediction of Eukaryotic Protein Phosphorylation Sites." Journal of Molecular Biology **294**: 1351-1362.

Booy, A. T., Haddow, J.D., Ohlund, L. B., Hardie, D.B., Olafson, R.W. (2005). "Application of Isotope Coded Affinity Tag (ICAT) Analysis for the Identification of Differentially Expressed Proteins Following Infection of Atlantic Salmon (Salmo salar) with Infectious Hematopoietic Necrosis Virus (IHNV) or Renibacterium salmoninarum (BKD)." Journal of Proteome Research **4**(325-334).

Borg, B., Antonopoulou, E., Anderson, E., Carlberg, T., Mayer, I. (1993). "Effectiveness of several androgens in stimulating kidney hypertrophy, a secondary sexual character, in castrated male three-spined sticklebacks, *Gasterosteus aculeatus.*" Canadian journal of zoology **71**: 2327-2329.

Cabreiro, F., Picot, C.R., Friguet, B., Petropoulos, I. (2006). "Methionine sulfoxide reductases: relevance to aging and protection against oxidative stress." Annals of the New York Academy of Sciences. **1067**: 37-44.

Cañavate, J. P., Fernández-Díaz, C. (1999). "Influence of co-feeding larvae with live and inert diets on weaning the sole Solea senegalensis onto commercial dry feeds." Aquaculture **174**: 255–263.

Carrascal, M. (2005). Estudio de la vía de presentación de péptidos por moléculas de MHC de clase II mediante estrategias proteómicas. Barcelona, University of Barcelona.

Carrascal, M., Abián, J. (2003). Capillary separations. HPLC of Peptides and Proteins: Methods and Protocols., Humana Press Inc. **251:** 143-164.

Carrascal, M., Carujo, S., Bachs, O., Abian, J. (2002). "Identification of p21Cip binding proteins by gel electrophoresis and capillary liquid chromatography microelectrospray tandem mass spectrometry." Proteomics **2**: 455-468.

Carrera, M., Cañas, B., Piñeiro, C., Vázquez, J., Gallardo, J.M. (2006). "Identification of commercial hake and grenadier species by proteomic analysis of the parvalbumin fraction." Proteomics **6**(19): 5278-5287.

Celis, J. E., Kruhoffer, M., Gromova, I., Frederiksen, C., Ostergaard, M., Thykjaer, T., Gromov, P., Yu, J., Palsdottir, H., Magnusson, N., Orntoft, T.F. (2000). "Gene expression profiling: monitoring transcription and translation products using DNA microarrays and proteomics." FEBS Letters **480**(1): 2-16.

Cerdà, J., *et al*. (In preparation). "Development and application of an oligo-based microaaray for a commercial marine flatfish, the Senegalese sole (*Solea senegalensis*): integration into the bioinformatic platform Soleamold."

Chen, G., Gharib, T., Huang, C., Taylor, J., *et al*. (2002). "Discordant Protein and mRNA Expression in Lung Adenocarcinomas." Molecular and cellular proteomics **1**(4): 304-313.

Chen, H. Y., Sun, J.M., Zhang, Y., Davie, J.R., Meistrich, M.L. (1998). "Ubiquitination of histone H3 in elongating spermatids of rat testes." Journal of Biological Chemistry **273**: 13165-13269.

Chen, P. Y., Manninga, H., Slanchev, K., Chien, M., Russo, J.J., Ju, J., Sheridan, R., John, B., Marks, D.S., Gaidatzis, D., Sander, C., Mihaela Zavolan, M., Tuschl, T. (2005). "The developmental miRNA profiles of zebrafish as determined by small RNA cloning." Genes and Development **19**: 1288-1293.

Cheng, C. Y., Grima, J., Stahler, M.S., Guglielmotti, A., Silvestrini, B., Bardin, C.W. (1990). "Sertoli cell synthesizes and secretes a protease inhibitor, a-2-macroglobulin." Biochemistry **29**(4): 1063-1068.

Cheng, C. Y., Mruk, D. D. (2002). "Cell Junction Dynamics in the Testis: Sertoli-Germ Cell Interactions and Male Contraceptive Development." Physiological Reviews **82**: 825-874.

Choe, L. H., Aggarwal, K., Franck, Z., Lee, K.H. (2005). "A comparison of the consistency of proteome quantitation using two-dimensional electrophoresis and shotgun isobaric tagging in Escherichia coli cells." Electrophoresis **26**(12): 2437-2449.

Clearwater, S. J., Crim, L.W. (1998). "Gonadotropin releasing hormone-analogue treatment increases sperm motility seminal plasma pH and sperm production in yellowtail flounder *Pleuronectes ferrugineus.*" Fish physiology and biochemistry. **19**: 349-357.

Conley, A., Hinshelwood, M. (2001). "Mammalian aromatases." Reproduction **121**: 685-695.

Cottrell, J. S. (1994). "Protein identification by peptide mass fingerprinting." Peptide research **7**(3): 115-124.

Coward, K., Bromage, N.R., Hibbitt, O., Parrington, J. (2002). "Gamete physiology, fertilization and egg activation in teleost fish." Reviews in Fish Biology and Fisheries . **12**: 33–58.

Davis, M. T., Beierle, J., Bures, E.T., McGinley, M.D., Mort, J., Robinson J.H.,Spahr C.S. , Yu W., Luethy, R. ,Patterson, S.D. (2001). "Automated LC–LC–MS–MS platform using binary ion-exchange and gradient reversed-phase chromatography for improved proteomic analyses." Journal of Chromatography B **752**: 281-291.

Davis, M. T., Beierle, J., Bures, E.T., McGinley, M.D., Mort, J., Robinson, J.H., Spahr, C.S., Yu, W., Luethy, R., Patterson, S.D. (2001). "Automated LC-LC-MS-MS platform using binary ion-exchange and gradient reversed-phase chromatography for improved proteomic analyses." Journal of Chromatography B **752**: 281-291.

Dennis, G., Sherman, B.T., Hosack,D.A., Yang, J., Gao, W., Lane, H.C., Lempicki R.A. (2003). "DAVID: Database for Annotation, Visualization, and Integrated Discovery." Genome Biology **4**(9): R60.

DiMaggio, P. A. J., Floudas C.A. (2007). "De Novo Peptide Identification via Tandem Mass Spectrometry and Integer Linear Optimization." Analytical Chemistry **79**: 1433-1446.

Dinis, M. T. (1992). "Aspects of the potential of *Solea senegalensis* Kaup for aquaculture: larval rearing and weaning to artificial diets." Aquacult. Fish. Manag. **23**: 515-520.

Dinis, M. T., Ribeiro, L., Soares, F., Sarasquete, C. (1999). "A review on the cultivation potential o*f Solea senegalensis* in Spain and in Portugal." Aquaculture **176**: 27-38.

Dodds, E. D., H. J. An, et al. (2006). "Enhanced peptide mass fingerprinting through high mass accuracy: Exclusion of non-peptide signals based on residual mass." Journal of Proteome Research **5**(5): 1195-1203.

Drake, P., Arias, A.M., Rodríguez, R.B. (1984). "Cultivo extensivo de peces marinos en los esteros de las salinas de San Fernando (Cádiz).Características de la producción de peces." Inf. Téc. Inv. Pesq **116**: 23.

Drevet, J. R. (2006). "The antioxidant glutathione peroxidase family and spermatozoa: A complex story." Molecular and Cellular Endocrinology **250**: 70-79.

Ekstedt, E., Holm,. L, Ridderstråle, Y. (2004). "Carbonic anhydrase in mouse testis and epididymis; transfer of isozyme IV to spermatozoa during passage." Journal of Molecular Histology **35**: 167-173.

Ekström, S., Malmström, J., Wallman, L., Löfgren, M., Nilsson, J., Laurell, T., Marko-Varga, G. (2002). "On-chip microextraction for proteomic sample preparation of in-gel digests." Proteomics **2**: 413-421.

Essader, A. S., , Cargile, B.J., Bundy, J.L., Stephenson, J.L. Jr. (2005). "A comparison of immobilized pH gradient isoelectric focusing and strong-cation-exchange chromatography as a first dimension in shotgun proteomics." Proteomics. **5**(1): 24-34.

Ethier, J. F., Findlay, J.K. (2001). "Roles of activin and its signal transduction mechanisms in reproductive tissues." Reproduction **121**(5): 667-675.

Feit, J., Kempf, W., Jedlickova, H., Burg, G. (2005). "Hypertext atlas of dermatopathology with expert system for epithelial tumors of the skin." Journal of Cutaneous Pathology **32**: 433–437.

Fenn, J. B., Mann, M., Meng, C.K., Wong, S.F., Whitehouse, C.M. (1989). "Electrospray ionization for mass spectrometry of large biomolecules." Science **246**: 64-71.

Finnskog, D., Ressine, A., Laurell, T., Marko-Varga, G. (2004). "Integrated Protein Microchip Assay with Dual Fluorescent- and MALDI Read-Out." Jourtnal of proteome research **3**: 988-994.

Fishelson, L., Delarea, Y., Gon, O. (2006). "Testis structure, spermatogenesis, spermatocytogenesis, and sperm structure in cardinal fish (Apogonidae, Perciformes)." Anatomy and embriology **211**: 31-46.

Fröhlich, T., Arnold G.J. (2006). "Proteome research based on modern liquid chromatography – tandem mass spectrometry: separation, identification and quantification." Journal of Neural Transmission. **113**: 973-994.

Fuji, J., Iuchi, Y., Matsuki, S., Ishii,T. (2003). "Cooperative function of antioxidant and redox systems against oxidative stress in male reproductive tissues." Asian Journal of Andrology **5**: 231-242.

Fukai, T., J. Kuroda, et al. (2000). "Accurate mass measurement of low molecular weight compounds by matrix-assisted laser desorption/ionization time-of-flight mass spectrometry." Journal of the American Society for Mass Spectrometry **11**(5): 458-463.

García-López, A., Fernández-Pasquier, V., Couto, E., Canario, A.V.M, Sarasquete, C., Martínez-Rodríguez, G. (2006). "Testicular development and plasma sex steroid levels in cultured male Senegalese sole *Solea senegalensis* Kaup." General and Comparative Endocrinology **147**: 343-351.

García-López, A., Martínez-Rodríguez, G., Sarasquete, C. (2005). "Male reproductive system in Senegalese sole *Solea senegalensis* (Kaup):Anatomy, histology and histochemistry." Histology and Histopathology **20**: 1179-1189.

Gaspari, M., Verhoeckx, K.C.M., Verheij, R., van der Greef, J. (2006). "Integration of Two-Dimensional LC-MS with Multivariate Statistics for Comparative Analysis of Proteomic Samples." Analytical Chemistry **78**: 2286-2296.

Gibson, R. N. (2005). Flatfishes. Biology and Exploitation.

Goesmann, A., Linke, B., Bartels, D., Dondrup, M., Krause, L., Neuweger, H., Oehm, S., Paczian, T., Wilke, A., Meyer, F. (2005). "BRIGEP—the BRIDGE-based genome–transcriptome–proteome browser." Nucleic Acids Research **33**: W710–W716.

Goos, H. J. T., Consten, D. (2002). "Stress adaptation, cortisol and pubertal development in the male common carp, *Cyprinus carpio.*" Molecular and cellular endrocrinology **197**(105-116).

Görg, A., Weiss, W.,Dunn, M.J. (2004). "Current two-dimensional electrophoresis technology for proteomics." Proteomics **4**: 3665-3685.

Graham, K. L., Robinson, W.H., Steinman, L., Utz, P.J . (2004). "High-throughput methods for measuring autoantibodies in systemic lupus erythematosus and other autoimmune diseases." Autoimmunity **37**(4): 269-272.

Grier, J. H. (1975). "Aspects of germinal cyst and sperm development in *Poecilia latipinna* (Teleostei: Poeciliidae)." Journal of Morphology **146**(2): 229-49.

Grier, J. H. (1993). Comparative organization of Sertoli cells including the Sertoli cell barrier. The Sertoli Cell. G. M. D. Russell L.D.**:** 703-709.

Gustafson, C., Bug, W.J., Nissanov, J. (2007). "NeuroTerrain – a client-server system for browsing 3D biomedical image data sets." BMC Bioinformatics **8**(40).

Gygi, S. P., Rist, B., Griffin, T.J., Eng, J., Aebersold, R. (2002). "Proteome analysis of low-abundance proteins using multidimensional chromatography and isotope-coded affinity tags." Journal of Proteome Research **1**(1): 47-54.

Gygi, S. P., Rochon, Y., Franza, B.R., Aebersold, R. (1999). "Correlation between Protein and mRNA Abundance in Yeast." Molecular and cellular biology **19**(3): 1720-1730.

Haab, B. B. (2003). "Methods and applications of antibody microarrays in cancer research." Proteomics **3**: 2116-2122.

Hanash, S. M., Bobek, M.P., Rickman, D.S., Williams, T., Rouillard, J.M., Kuick, R., Puravs, E. (2002). "Integrating cancer genomics and proteomics in the post-genome era." Proteomics **2**: 69-75.

Harmin, S. A., Crim, L.W. (1993). "Influence of gonadotropic hormone releasing hormone analog (GnRH-A) on plasma sex steroids profiles and milt production in male winter flounder, *Pseudopleuronectes americanus* (Walbaum)." Fish physiology and biochemistry. **10**: 399-407.

Heinke, M. Y., Wheeler, C.H., Chang, D., Einstein, R., Drake-Holland, A., Dunn, M.J., dos Remedios, C.G. (1998). "Protein changes observed in pacing-induced heart failure using two-dimensional electrophoresis." Electrophoresis **19**: 2021-2030.

Hernandez, P., Müller, M., Appel, R.D. (2006). "Automated protein identification by tandem mass spectrometry: issues and strategies." Mass Spectrometry Reviews **25**: 235-254.

Hidiroglou, M. (1979). "Trace element deficiencies and fertility in ruminants: a review." Journal of Dairy Science **62**(8): 1195-1206.

Higginbotham, J. W., Smith, J.S., Smith, O.S. (1991). "Quantitative analysis of two-dimensional protein profiles of inbred lines of maize (*Zea mays L*)." Electrophoresis **12**(425-431).

Hinrichs, A. S., Karolchik, D., *et al.* (2006). "The UCSC Genome Browser Database: update 2006." Nucleic Acids Research **34**: D590-D598.

Hogstrand, C., Balesaria, S., Glover, C.N. (2002). "Application of genomics and proteomics for study of the integrated response to zinc exposure in a non-model fish species, the rainbow trout." Comparative Biochemistry and Physiology Part B **133**: 523-535.

Huang, T. Y., DerMardirossian, C., Bokoch GM (2006). "Cofilin phosphatases and regulation of actin dynamics." Current Opinion in Cell Biology **18**: 26-31.

Huber, M., Bahr, I., Kratzschmar, J.R.,Becker, A., Muller, E., Donner, P., Pohlenz, H., Scheneider, M.R., Sommer, A. (2003). "Comparison of Proteomic and Genomic Analyses of the Human Breast Cancer Cell Line T47D and the Antiestrogen-resistant Derivative T47D-r." Molecular and cellular proteomics **3**: 44-55.

Iannello, R. C., Dahl, H.H. (1992). "Transcriptional expression of a testis-specific variant of the mouse pyruvate dehydrogenase E1 alpha subunit." Biology of Reproduction **47**(1): 48-58.

Iannello, R. C., Young, J., Sumarsoni, S., Tymms, M.J., Dahl, H.M.,Gould, J., Hedger, M., Kola, I. (1997). "Regulation of Pdha-2 Expression Is Mediated by Proximal Promoter Sequences and CpG Methylation." Molecular and cellular biology **17**(2): 612-619.

Inaba, K., Dreanno,C., Cosson J. (2003). "Control of Flatfish Sperm Motility by CO_2 and Carbonic Anhydrase." Cell Motility and the Cytoskeleton **55**: 174-187.

Jaillon, O., Aury, J-M., *et al*. (2004). "Genome duplication in the teleost fish *Tetraodon nigroviridis* reveals the early vertebrate proto-karyotype." Nature **431**(21 OCTOBER 2004): 946-957.

Jones, J., Cote, R.G., *et al.* (2006). "PRIDE: a public repository of protein and peptide identifications for the proteomics community." Nucleic Acids Research **34**: D659–D663.

Joos, T. O., Schrenk, M., Hopfl, P., Kroger, K., Chowdhury, U., Stoll, D., Schorner, D., Durr, M., Herick, K., Rupp, S., Sohn, K., Hammerle, H. (2000). "A microarray enzyme-linked immunosorbent assay for autoimmune diagnostics." Electrophoresis. **21**(13): 2641-2650.

Karas, M., Hillenkamp, F. (1988). "Laser desorption ionization of proteins with molecular masses exceeding 10,000 daltons." Analytical chemistry **60**: 2299-2301.
Kaur, P. and P. B. O'Connor (2006). "Algorithms for automatic interpretation of high resolution mass spectra." Journal of the American Society for Mass Spectrometry **17**(3): 459-468.

Kimmel, C. B., Miller, C.T., Moens, C.B. (2001). "Specification and morphogenesis of the zebrafish larval head skeleton." Developmental biology **233**(2): 239-257.

Knight, M. I., Chambers, P.J. (2003). "Problems associated with determining protein concentrations." Molecular Biotechnology **23**: 19-28.

Knoll-Gellida, A., Andre, M., Gattegno, T., Forgue, J., Admon, A., Babin, P.J. (2006). "Molecular phenotype of zebrafish ovarian follicle by serial analysis of gene expression and proteomic profiling, and comparison with the transcriptomes of other animals." BMC Genomics **7**(46).

Koller, A., Washburn, M.P., Lange, B.M., Andon, N.L., Deciu, C., Haynes, P.A., Hays, L., Schieltz, D., Ulaszek, R., Wei, J., Wolters, D., Yates, J.R. 3rd. (2002). "Proteomic survey of metabolic pathways in rice." PNAS **99**(18): 11969-74.

Kwon, J., Kikuchi, T., Setsuie, R., Ishii, Y., Kyuwa, S., Yoshikawa, Y. (2003). "Characterization of the testis in congenitally ubiquitin carboxy-terminal hydrolase-1 (Uch-L1) defective (gad) mice." Experimental animals **52**(1): 1-9.

Labrie, F., Luu-The, V., Lin, S., Labrie, C., Simard, J., Breton, R., Brlanger, A. (1997). "The key role of 17b-hydroxysteroid dehydrogenases in sex steroid biology." Steroids **62**: 148-158.

Leijonhufvud, P., Åkerlo, E., Pousette, A. (1997). "Structure of sperm activating protein." Molecular Human Reproduction **3**(3): 249–253.

Lein, E. S., Hawrylycz, M.J., *et. al.* (2007). "Genome-wide atlas of gene expression in the adult mouse brain." Nature **445**: 168-176.

Leitner, A., Lindner, W. (2006). "Chemistry meets proteomics: The use of chemical tagging reactions for MS-based proteomics." Proteomics **6**: 5418–5434.

Lian, Z., Kluger, Y., Greenbaum, D.S., Tuck, D., Gerstein, M., Berliner, N., Weissman, S.M., Newburger, P.E. (2002). "Genomic and proteomic analysis of the myeloid differentiation program: global analysis of gene expression during induced differentiation in the MPRO cell line." Blood **100**(9): 3209-3220.

Lim, H. K., Pankhurst, N.W., Fitzgibbon, Q.P. (2004). "Effects of slow release gonadotropin releasing hormone analog on milt characteristics and plasma levels of gonadal steroids in Greenback flounder, Rhombosolea tapirina." Aquaculture **240**: 505-516.

Link, V., Carvalho, L., Castanon, I., Stockinger, P., Shevchenko, A., Heisenberg, C.P. (2006 a). "Identification of regulators of germ layer morphogenesis using proteomics in zebrafish." Journal of Cell Science **119**(10): 2073-2083.

Link, V., Shevchenko, A., Heisenberg, C.P. (2006 b). "Proteomics of early zebrafish embryos." BMC Developmental Biology **6**(1).

Liska, A. J., Popov, A.V., Sunyaev, S., Peg Coughlin, P., Habermann, B., Shevchenko A., Bork P., Karsenti, E., Shevchenko, A. (2004). "Homology-based functional proteomics by mass spectrometry: Application to the Xenopus microtubule-associated proteome." Proteomics **4**: 2707–2721.

López, J. L. (2007). "Applications of proteomics in marine ecology." Marine Ecology Progress Series **332**: 275-279.

López, J. L., Mosquera, E., Fuentes, J., Marina, A., Vázquez, J., Alvarez, G. (2001). "Two-dimensional gel electrophoresis of *Mytilus galloprovincialis*: differences in protein expression between intertidal and cultured mussels." Marine Ecology Progress Series **224**: 149-156.

Love, D. R., Pichler, F.B., Dodd, A., Copp, B.R., Greenwood, D.R. (2004). "Technology for high-throughput screens: the present and future using zebrafish." Current Opinion in Biotechnolgy **15**: 564-571.

Lundin, M., Lundin, J., Helin, H., Isola, J. (2004). "A digital atlas of breast histopathology: an application of web based virtual microscopy." Journal of Clinical Pathology **54**: 1288–1291.

MacCoss, M. J. (2005). "Computational analysis of shotgun proteomics data." Current Opinion in Chemical Biology **9**: 88-94.

MacCoss, M. J., McDonald, W.H., Saraf, A., Sadygov, R., Clark, J.M., Tasto, J.J., Gould, K.L., Wolters, D., Washburn, M., Weiss, A., Clark, J.I., Yates, J.R. 3rd. (2002). "Shotgun identification of protein modifications from protein complexes and lens tissue." PNAS **99**(12): 7900-7905.

Mann, M. (1995). "Useful tables of possible and probable peptide masses." 43rd ASMS Conference on Mass Spectrometry and Allied Topics, Atlanta, GA.

Marengo, E., Robotti, E,, Antonucci, F., Cecconi, D., Campostrini, N., Righetti, P.G. (2005). "Numerical approaches for quantitative analysis of two-dimensional maps: a review of commercial software and home-made systems." Proteomics **5**(3): 654-666.

Marouga, R., David, S., Hawkins, E. (2005). "The development of the DIGE system: 2D fluorescence difference gel analysis technology." Analytical and Bioanalytical Chemistry **382**: 669-678.

Martin, S. A., Vilhelmsson, O., Medale, F., Watt, P., Kaushik, S., Houlihan, D.F. (2003). "Proteomic sensitivity to dietary manipulations in rainbow trout." Biochimica et Biophysica Acta **165**(1-2): 17-29.

Martínez, I., Tone Jakobsen, F. (2004). "Application of proteome analysis to seafood authentication." Proteomics **4**(2): 347-354.

Martin-Robichaud, D. J., Powell, J., Wade, J. (2000). "Gonadotropin-releasing hormone affects sperm production of Atlantic halibut (*Hippoglossus hippoglossus*)." Bulletin of the Aquaculture Association of Canada **4**: 45-48.

Maux, D., Enjalbal, C., Martínez, J., Aubagnac, J.L. (2002). "New example of proline-induced fragmentation in electropray ionization mass spectrometry of peptides." Rapid communications in mass spectrometry **16**: 1470-1475.

Mayer, I., Borg, B., Schulz, R. (1990a). "Conversion of 11-ketoandrostenedione to 11-ketotestosterone by blood cells of six fish species." General and Comparative Endocrinology **77**: 70-74.

Mayer, I., Borg, B., Schulz, R. (1990b). "Seasonal changes in and effect of castration/androgen replacement on the plasma levels of five androgens in the male three-spined stickleback, *Gasterosteus aculeatus L.*" General and Comparative Endocrinology **79**: 23-30.

Maziarz, M., Chung, C., Drucker, D., Emili, A. (2005). "Integrating Global Proteomic and Genomic Expression Profiles Generated from Islet b Cells." Molecular and cellular proteomics **4**(4): 458-474.

Mercadé, J., *et al*. (In preparation).

Métayer, S., Dacheux, F., Dacheux, J., Gatti, J. (2002). "Comparison, Characterization, and Identification of Proteases and Protease Inhibitors in Epididymal Fluids of Domestic Mammals. Matrix Metalloproteinases Are Major Fluid Gelatinases." Biology of Reproduction **66**: 1219-1229.

Miller, I., Crawford, J., Gianazza, E. (2006). "Protein stains for proteomic applications: Which, when, why?" Proteomics **6**: 5385–5408.

Miller, J. C., Zhou, H., Kwekel, J., Cavallo, R., Burke, J., Butler, E.B., Teh, B.S., Haab, B.B. (2003). "Antibody microarray profiling of human prostate cancer sera: antibody screening and identification of potential biomarkers." Proteomics **3**(56-63).

Mindnich, R., Moller, G., Adamski. J. (2004). "The role of 17 beta-hydroxysteroid dehydrogenases." Molecular and Cellular Endocrinology **218**: 7-20.

Miura, T., Miura, C., Ohta, T., Nader, M.R., Todo, T.,Yamauchi,K. (1999). "Estradiol-17b stimulates the renewal of spermatogonial stem cells in males." Biochemical and Biophysical Research Communications **264**: 230-234.

Miura, T., Miura, C.I. (2003). "Molecular control mechanisms of fish spermatogenesis." Fish Physiology and Biochemistry **28**: 181-186.

Miura, T., Yamauchi, K., Takahashi, H. Nagahama, Y. (1992). "The role of hormones in the acquisition of sperm motility in salmonid fish." Journal of experimental zoology **261**: 359-363.

Miura, T., Yamauchi, K., Takahashi, H., Nagahama, Y. (1991). "Hormonal induction of all stages of spermatogenesis in vitro in the male Japanese eel (*Anguilla japonica*)." PNAS **88**: 5774-5778.

Moertz, E., Krogh, T. N., Vorum, H., Görg, A. (2001). "Improved silver staining protocols for high sensitivity protein identification using matrix-asisted laser desorption/ionization-time of flight analysis." Proteomics **1**: 1359-1363.

Monti, G., De Napoli, L., Mainolfi, P., Barone, R., Guida, M., Marino, G., Amoresano, A. (2005). "Monitoring Food Quality by Microfluidic Electrophoresis, Gas Chromatography, and Mass Spectrometry Techniques: Effects of Aquaculture on the Sea Bass (*Dicentrarchus labrax*)." Analitycal Chemistry **77**: 2587-2594.

Moon, S. H., Lim, H.K., Kwon, J.Y., Lee, J.K., Chang, YJ. (2003). "Increased plasma 17-hydroxyprogesterone and milt production in response to gonadotropin-releasing hormone agonist in captive male starry flounder, *Platichthys stellatus.*" Aquaculture **218**: 703-716.

Motzkusa, D., Singhb, P.B., Hoyer-Fendera, S. (1999). "M31, a murine homolog of Drosophila HP1, is concentrated in the XY body during spermatogenesis." Cytogenetics and Cell Genetics **86**: 83-88.

Mylonas, C. C., Woods III,L.C., Thomas, P., Zohar, Y. (1998). "Endocrine Profiles of Female Striped Bass (*Morone saxatilis*) in Captivity, during Postvitellogenesis and Induction of Final Oocyte Maturation via Controlled-Release GnRHa-Delivery Systems." General and Comparative Endocrinology **110**: 276-289.

Nagahama, Y. (1994). "Endocrine regulation of gametogenesis in fish." Int. J. Dev. Biol. **38**: 217-229.

O'Farrell, P. Z., Goodman, H. M., O'Farrell, P. H. (1977). "High resolution two-dimensional electrophoresis of basic as well as acidic proteins." Cell **12**: 1133-1141.

Old, W. M., Meyer-Arendt, K., Aveline-Wolf, L., Pierce, K.G., Mendoza, A., Sevinsky, J.R., Resing, K.A., Ahn, N.G. (2005). "Comparison of label-free methods for quantifying human proteins by shotgun proteomics." Molecular and cellular proteomics **4**(10): 1487-14802.

Ong, S., Mann, M. (2005). "Mass spectrometry-based proteomics turns quantitative." Nature Chemical Biology **1**(5): 252-262.

Ørntoft, T., Thykjaer, T., Waldman, F., Wolf, H., Celis, J. (2002). "Genome-wide Study of Gene Copy Numbers, Transcripts, and Protein Levels in Pairs of Non-invasive and Invasive Human Transitional Cell Carcinomas." Molecular and cellular proteomics **1**(1): 37-45.

Pankhurst, N. W., Poortenaar, C.W. (2000). "Milt characteristics and plasma levels of gonadal steroids in greenback flounder *Rhombosolea tapirina* following treatment with exogenous hormones." Mar. Freshw. Behav. Physiol **33**: 141-159.

Patel, K., Dunn, M.J., Gunther, S., Postel, W., Gorg, A. (1988). "Dual-label autoradiographic analysis of human skin fibroblast and myoblast proteins by two-dimensional polyacrylamide gel electrophoresis using immobilised pH gradients in the first dimension." Electrophoresis. **9**(9): 547-554.

Peng, J., Schwartz, D., Elias, J.E., Thoreen, C.C., Cheng, D., Marsischky, G., Roelofs, J., Finley, D., Gygi, S.P. (2003). "A proteomics approach to understanding protein ubiquitination." Nature biotechnology **21**(8): 921-926.

Pevtsov, S., Fedulova, I., Mirzaei, H., Buck, C., Zhang, X. (2006). "Performance Evaluation of Existing De Novo Sequencing Algorithms." Journal of Proteome Research **5**: 3018-3028.

Pfeifer, H., Conrad, M., Roethlein, D., Kyriakopoulos, A., Brielmeier, M., Bornkamm, G.W., Behne, D. (2001). "Identification of a specific sperm nuclei selenoenzyme necessary for protamine thiol crosslinking during sperm maturation." The FASEB Journal **15**: 1236-1239.

Piñeiro, C., Barros-Velázquez, J., Vázquez, J., Figueras, A., Gallardo, J.M. (2003). "Proteomics as a Tool for the Investigation of Seafood and Other Marine Products." Journal of Proteome Research **2**: 127-135.

Pousette, Å., Leijonhufvud, P.K.G., Åkerlof, E. (1993). "Purification, structure and partial characterization of the major sperm activating protein complex in human serum." Scandinavian Journal of Clinical and laboratory Investigation **53**: 39-44.

Pradet-Balade, B., Boulme, F., Beug, H., Mullner, E.W., Garcia-Sanz, J.A. (2001). "Translation control: bridging the gap between genomics and proteomics?" Trends in Biochemical Sciences **26**(4): 225-229.

Provan, F., Bjornstad, A., Pampanin, D.M., Lyng, E., Fontanillas, R., Andersen, O.K., Koppe, W., Bamber, S. (2006). "Mass spectrometric profiling – A diagnostic tool in fish?" Marine Environmental Research **62**: S105-S108.

Pudney, J. (1995). "Spermatogenesis in nonmammalian vertebrates." Microscope research and technique **32**: 459-497.

Quero, C., Colome, N., Prieto, M.R., Carrascal, M., Posada, M., Gelpi, E., Abian, J. (2004). "Determination of protein markers in human serum: Analysis of protein expression in toxic oil syndrome studies." Proteomics **4**(2): 303-315.

Rabilloud, T., Vuillard, L., Gilly, C., Lawrence, J. J. (1994). "Silver staining of proteins in polyacrylamide gels: a general overview." Cellular and Molecular Biology **40**: 57–75.

Rao, A. V., Shaha, C. (2000). "Role of glutathione S-transferases in oxidative stress-induced male germ cell apoptosis." Free Radical Biology and Medicine **29**: 1015-1027.

Reinders, J., Lewandrowski, U., Moebius, J., Wagner, Y., Sickmann, A,. (2004). "Challenges in mass spectrometry-based proteomics." Proteomics **4**: 3686–3703.

Rexroad, C. E., Y. Lee,Y., Keele, J.W., Karamycheva, S., G. Brown, G., Koop, B., Gahr S.A., Paltia, Y., Quackenbushc, J. (2003). "Sequence analysis of a rainbow trout cDNA library and creation of a gene index." Cytogenetic and Genome Research **102**: 347–354.

Rice, P., Longden, I. Bleasby, A. (2000). "EMBOSS: The European Molecular Biology Open Software Suite." Trends in Genetics **16**(6): 276-277.

Rijnsdorp, A. D., Witthames, P.R. (2005). Ecology of reproduction. Flatfishes. Biology and exploitation. G. R.N.**:** 68-87.

Rime, H., Guitton, N., Pineau, C., Bonnet, E., Bobe, J., Jalabert, B. (2004). "Post-ovulatory ageing and egg quality: A proteomic analysis of rainbow trout coelomic fluid." Reproductive Biology and Endocrinology **2**(26).

Rodríguez, A., Pascual, E. (1982). "Primeros ensayos sobre la utilización de la hipófisis del atún (Thunnus thynnus) en la maduración y puesta de Solea senegalensis y Sparus aurata." Inv. Pesq. **97**: 1-11.

Rodríguez, C., Quero, C., Dominguez, A., Trigo, M., Posada de la Paz, M., Gelpi, E., Abian, J. (2006). "Proteotyping of human haptoglobin by MALDI-TOF profiling: Phenotype distribution in a population of toxic oil syndrome patients." Proteomics **Suppl 1**: S272-81.

Rodríguez, R. B. (1984). Biología y cultivo de *Solea senegalensis* Kaup 1858 en el Golfo de Càdiz. Sevilla, Universidad de Sevilla.

Roepstorff, P., Fohlmann, J. (1984). "Proposal for a common nomenclature for sequence ions in mass spectra of peptides." Biomedical mass spectrometry **11**: 601.

Roest, H. P., van Klaveren, J., de Wit. J., van Gurp, C.G., Koken, M.H., Vermey, M., van Roijen, J.H., Hoogerbrugge, J.W., Vreeburg, J.T., Baarends, W.M., Bootsma, D., Grootegoed, J.A., Hoeijmakers, J.H. (1996). "Inactivation of the HR6B ubiquitin-conjugating DNA repair enzyme in mice causes male sterility associated with chromatin modification." Cell **86**(5): 799-810.

Rottmann, R. W., Shireman, J.V., Chapman, F.A. (1991). "Hormonal Control of Reproduction in Fish for Induced Spawning." Southern Regional Aquaculture Center Publications **424**.

Russell, S., Hayes, M.A., Simko, E., Lumsden, J.S. (2006). "Plasma proteomic analysis of the acute phase response of rainbow trout (Oncorhynchus mykiss) to intraperitoneal inflammation and LPS injection." Developmental and Comparative Immunology **30**: 393-406.

Saldanha, A. J. (2004). "Java Treeview: extensible visualization of microarray data." Bioinformatics **20**(17): 3246-3248.

Santos C., B. J. P. G. (1994). "Ribosomal Protein P0, Contrary to Phosphoproteins P1 and P2, Is Required for Ribosome Activity and Saccharomyces cerevisiae Viability." Journal of Biological Chemistry **269**(22): 15689-15696.

Sassone-Corsi, P. (2002). "Unique chromatin remodeling and transcriptional regulation in spermatogenesis." Science **296**(5576): 2176-2178.

Schulz, R. W., Blum, V. (1991). "Extragonadal 17b-hydroxysteroid dehydrogenase activity in rainbow trout." General and Comparative Endocrinology **82**: 197-205.

Schulz, R. W., Vischer, H.F., Cavaco, J.E.B, Santos, E.M., Tyler, C.R., Goos, H.J.Th., Bogerd, J. (2000). "Gonadotropins, their receptors, and the regulation of testicular functions in fish." Comparative Biochemistry and Physiology Part B **129**: 407-417.

Shaw, M. M., Riederer, B.M. (2003). "Sample preparation for two-dimensional gel electrophoresis." Proteomics **3**: 1408-1417.

Shen, Y., Jacobs, J.M., Camp, D.G., Fang, R., Moore, R.J., Smith, R.D., Xiao, W., Davis, R.W., Tompkins, R.G. (2004). "Ultra-high-efficiency strong cation exchange LC/RPLC/MS/MS for high dynamic range characterization of the human plasma proteome." Analytical chemistry **76**(4): 1134-44.

Shrader, E. A., Henry, T.R., Greeley, M.S. Jr, Bradley, B.P. (2003). "Proteomics in zebrafish exposed to endocrine disrupting chemicals." Ecotoxicology **12**(6): 485-488.

Smith, R. W., Wood, C.M., Cash, P. Diao, L., Part, P. (2005). "Apolipoprotein AI could be a significant determinant of epithelial integrity in rainbow trout gill cell cultures: A study in functional proteomics." Biochimica et Biophysica Acta **1749**: 81-93.

Standing, K. G. (2003). "Peptide and protein de novo sequencing by mass spectrometry." Current opinion in structural biology. **13**: 595-601.

Stentiford, G. D., Viant, M.R., Ward, D.G., Johnson, P.J., Martin, A., Wenbin, W., Cooper, H.J., Lyons, B.P., Feist, S.W. (2005). "Liver Tumors in Wild Flatfish: A Histopathological, Proteomic, and Metabolomic Study." OMICS A Journal of Integrative Biology **3**: 281-299.

Sutovsky, P. (2003). "Ubiquitin-Dependent Proteolysis in Mammalian Spermatogenesis, Fertilization, and Sperm Quality Control: Killing Three Birds With One Stone." Microscopy reserach and technique. **61**: 88-102.

Tanner, S., Shen, Z., Ng, J., Florea, L., Guigó, R., Briggs, S.P., Bafna, V. (2007). "Improving gene annotation using peptide mass spectrometry." Genome Research **17**: 231–239.

Tay, T. L., Lin, Q., Seow, T.K., Tan, K.H., Hew, C.L., Gong, Z. (2006). "Proteomic analysis of protein profiles during early development of the zebrafish, *Danio rerio*." Proteomics **6**: 3176–3188.

Taylor, J. A., Johnson, R.S. (1997). "Sequence database searches via de novo peptide sequencing by tandem mass spectrometry." Rapid communications in mass spectrometry **11**: 1067-1075.

Tolosano, E., Fiorella, A. (2002). "Hemopexin: Structure, Function, and Regulation." DNA and Cell Biology **21**(4): 297-306.

Tsuji, T., Shimohama, S., Kamiya, S., Sazuka, T., Ohara, O. (1999). "Analysis of brain proteins in Alzheimer's disease using high-resolution two-dimensional gel electrophoresis." Journal od Neurology **166**: 100-106.

Tvedt, H. B., Benfey, T.J., Martin-Robichaud, D.J., Power, J. (2001). "The relationship between sperm density, spermatocrit, sperm motility and fertilization success in Atlantic halibut, *Hippoglossus hippoglossus*." Aquaculture **194**: 191-200.

Tyers, M., Mann, M. (2003). "From genomics to proteomics." Nature **13**(422): 193-197.

Vacher, C., Mañanos, E.L., Breton, B., Marmignon, M.H., Saligaut, C. (2000). "Modulation of pituitary dopamine D1 or D2 receptors and secretion of follicle-stimulating hormone and luteinizing hormone during the annual reproductive cycle of female rainbow trout." Journal of neuroendocrinology. **12**: 1219-1226.

Vermeirssen, E. L. M., Mazorra de Quero, C., Shields, R.J., Norberg, B., Kime, D.E., Scott, A.P. (2004). "Fertility and motility of sperm from Atlantic halibut (*Hippoglossus hippoglossus*) in relation to dose and timing of gonadotropin releasing hormone agonist implant." Aquaculture **230**: 547-567.

Vermeirssen, E. L. M., Scott, A.P., Mylonas, C.C., Zohar, Y. (1998). "Gonadotrophin-releasing hormone agonist stimulates milt fluidity and plasma concentrations of 17α, 20β-dihydroxylated and 5β-reduced, 3α-hydroxylated C21 steroids in male plaice (Pleuronectes platessa)." General and comparative endocrinology. **112**: 163-177.

Vasseur, C., Labadie, J., Hebraud, M. (1999). "Differential protein expression by Pseudomonas fragi submitted to various stresses." Electrophoresis **20**(2204-2213).

Vermeirssen, E. L. M., Shields, R., Mazorra de Quero, C., Scott, A.P. (2000). "Gonadotropin-releasing hormone agonist raises plasma concentrations of progestogens and enhances milt fluidity in male Atlantic halibut (*Hippoglossus hippoglossus*)." Fish physiology and biochemistry. **22**: 77-87.

Viner, R., Zhang, T., Miller, K. (2005). "Complementary Analysis of Human CSF Proteins by Nano LC-MALDI and ESI-MS/MS." Thermo Electron application notes **356**.

Vollmer, M., Nägele, E., Moritz, R. (2004). "On-line and Off-line 2-D LC–ESI MS-MS Methods in Proteomic Analysis." Pharmaceutical Discovery **6**: 42-49.

Washburn, M. P., Ulaszek, R., Deciu, C., Schieltz, D.M., Yates, J.R. 3rd. (2002). "Analysis of quantitative proteomic data generated via multidimensional protein identification technology." Analytical chemistry **74**(7): 1650-1657.

Welt, C., Sidis, Y., Keutmann, H., Schneyer, A. (2002). "Activins, inhibins, and follistatins: from endocrinology to signaling. A paradigm for the new millennium." Experimental biology and medicine **227**(9): 724-752.

Weltzien, F. A., Andersson, E., Andersend, O., Shalchian-Tabrizie, K., Norberg, B. (2004). "The brain–pituitary–gonad axis in male teleosts, with special emphasis on flatfish (Pleuronectiformes)." Comparative Biochemistry and Physiology Part A. **137**: 447–477.

Weltzien, F. A., Norberg, B., Swanson, P. (2003). "Isolation and chartacteritzation of FSH and LH from pituitary glands of Atlantic halibut (*Hippoglossus hippoglossus L.*)." Genral and Comparative Endocrinology **131**: 97-105.

Weltzien, F. A., Taranger, G.L., Karlsen, O., Norberg, B. (2002). "Spermatogenesis and related plasma androgen levels in Atlantic halibut (*Hippoglossus hippoglossus L.*)." Comparative Biochemistry and Physiology Part A **132**: 567-575.

Wessel, D., Flugge, U.I. (1984). "A method for the quantitative recovery of protein in dilute solution in the presence of detergents and lipids." Analytical Biochemistry **138**(1): 141-143.

Westermeier, R., Marouga, R. (2005). "Protein Detection Methods in Proteomics Research." Bioscience Reports **25**(1-2): 19-32.

Wilke, A., Ruckert, C., Bartels, D., Dondrup, M., Goesmann, A., Huser, A.T., Kespohl, S., Linke, B., Mahne, M., McHardy, A., Puhler, A., Meyer, F. (2003). "Bioinformatics support for high-throughput proteomics." Journal of Biotechnology **106**: 147-156.

Wilkins, M. R., Pasquali, C., Appel, R.D., Ou, K., Gola,z O., Sanchez, J.C., Yan, J.X., Gooley, A.A., Hughes, G., Humphery-Smith, I., Williams, KL., Hochstrasser, D.F. (1996). "From proteins to proteomes: large scale protein identification by two-dimensional electrophoresis and amino acid analysis." Biotechnology **14**(1): 61-65.

Williams, B. S., Doyle, M.D. (1996). "An Internet Atlas of Mouse Development." Computerized Medical Imaging and Graphics **20**(6): 433-447.

Wise, T., Lunstra, D.D., Rohrer, G.A., Ford, J.J. (2003). "Relationships of testicular iron and ferritin concentrations with testicular weight and sperm production in boars." Journal of Animal Science **81**(2): 503-511.

Wolff, S., Otto, A., Albrecht, D., Zeng, J.S., Buttner, K., Gluckmann, M., Hecker, M., Becher, D. (2006). "Gel-free and gel-based proteomics in Bacillus subtilis: a comparative study." Molecular and cellular proteomics **5**(7): 1183-1192.

Wolters, D. A., Washburn, M.P., Yates, J.R. 3rd. (2001). "An automated multidimensional protein identification technology for shotgun proteomics." Analytical chemistry **73**(23): 5683-5690.

Wysocki, V. H., Tsaprailis, G., Smith, L.L., Breci, L.A. (2000). "Mobile and localized protons: a framework for understanding peptide dissociation." Journal of mass spectrometry **35**(12): 1399-1407.

Xu, C., Ma, B. (2006). "Complexity and scoring function of MS/MS peptide de novo sequencing." Computational systems bioinformatics.: 361-9.

Zhao, Y. L., Han, W.D., Li, Q., Mu, Y.M., Lu, X.C., Yu, L., Song, H.J., Li, X., Lu, J.M., Pan, C.Y. (2005). "Mechanism of transcriptional regulation of LRP16 gene expression by 17-b estradiol in MCF-7 human breast cancer cells." Journal of Molecular Endocrinology **34**: 77-89.

Zhu, B. Y., Mant, C.T., Hodges, R. S. (1991). "Hydrophilic-interaction chromatography of peptides on hydrophilic and strong cation-exchange columns." Journal of Chromatography A **548**: 13-24.

Zhu, H., Bilgin, M., Snyder, M. (2003). "Proteomics." Annual Reviews in Biochemistry **72**: 783–812.

Zubarev, R. A., Hakansson, P., Sundqvist, B. (1996). "Accuracy requirements for peptide characterization by monoisotopic molecular mass measurements." Analytical chemistry **68**: 4060-4064.

Annexes

Annex I.1

Detailed comparison between *Solea senegalensis* testis and larva and *Oncorhynchus mykiss* (Rainbow trout) gene ontology charts for Biological Process, Molecular Function, and Cellular Component classification levels at hierarchical level 1. Proteins from *Solea senegalensis* were obtained from BLAST comparison with experimental peptides. Proteins from larva and testis were analysed separately.

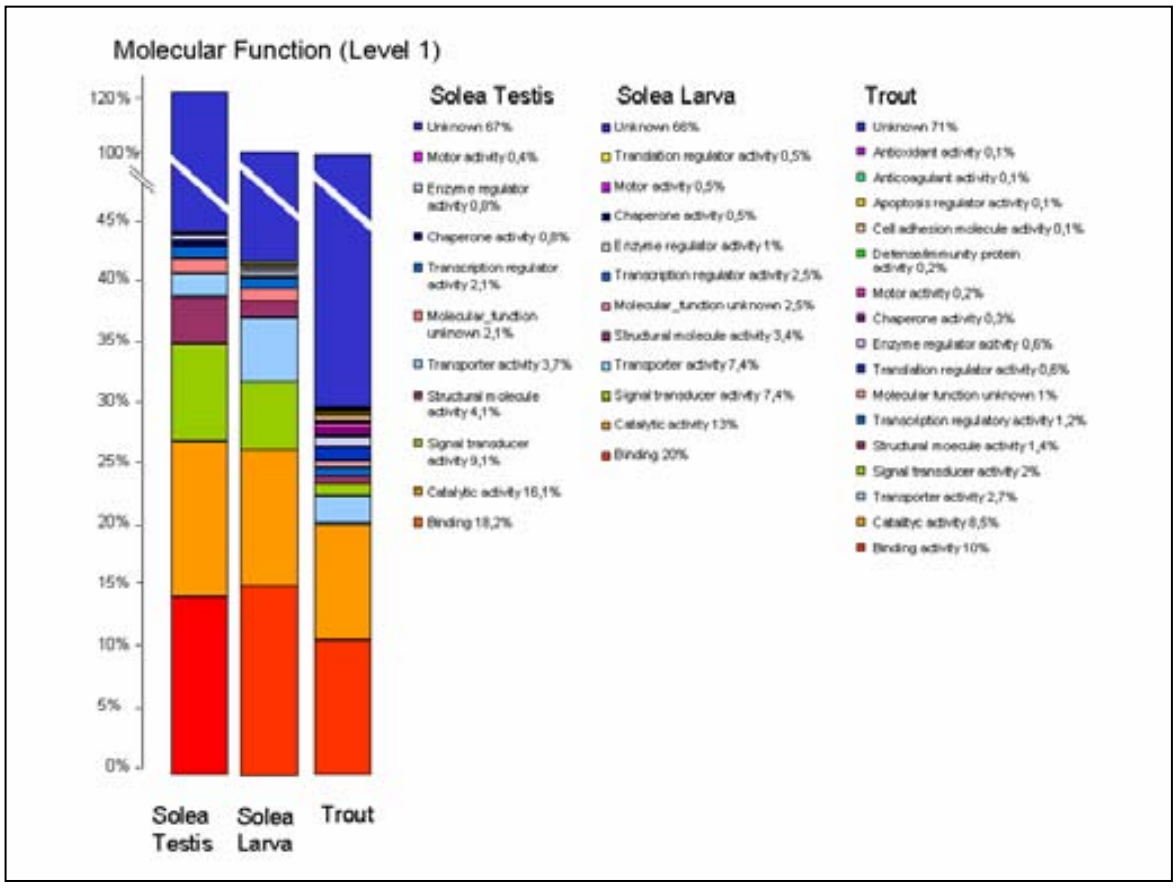

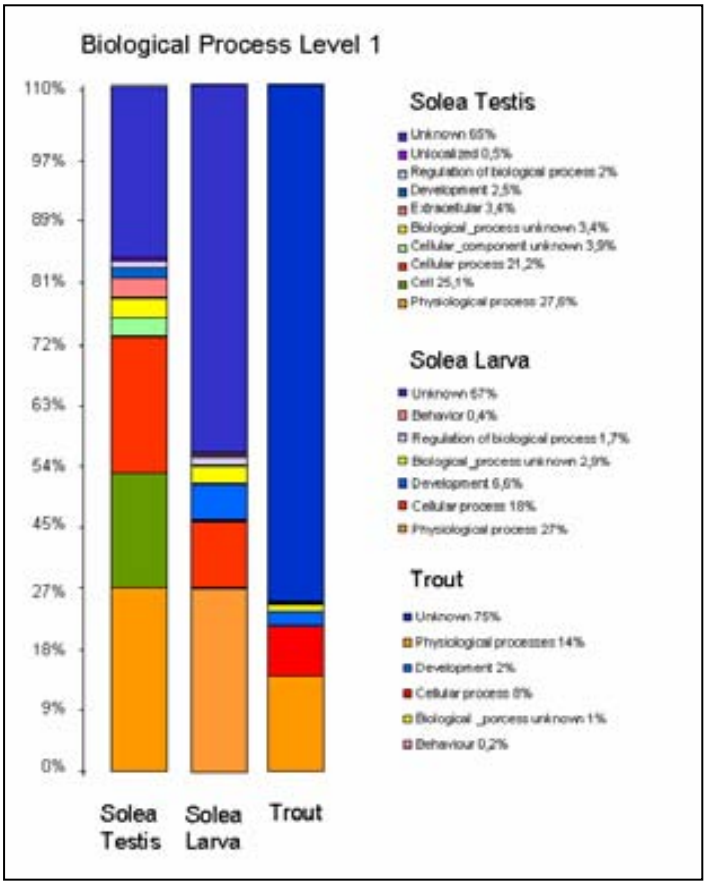
Biological Process Level 1
110%
97%
89%
81%
72%
63%
54%
45%
27%
18%
9%
0%
Solea Testis
Solea Larva
Trout
Solea Testis
Unknown 65%
Unlocalized 0,5%
Regulation of biological process 2%
Development 2,5%
Extracellular 3,4%
Biological_process unknown 3,4%
Cellular_component unknown 3,9%
Cellular process 21,2%
Cell 25,1%
Physiological process 27,6%
Solea Larva
Unknown 67%
Behavior 0,4%
Regulation of biological process 1,7%
Biological_process unknown 2,9%
Development 6,6%
Cellular process 18%
Physiological process 27%
Trout
Unknown 75%
Physiological processes 14%
Development 2%
Cellular process 8%
Biological _porcess unknown 1%
Behaviour 0,2%

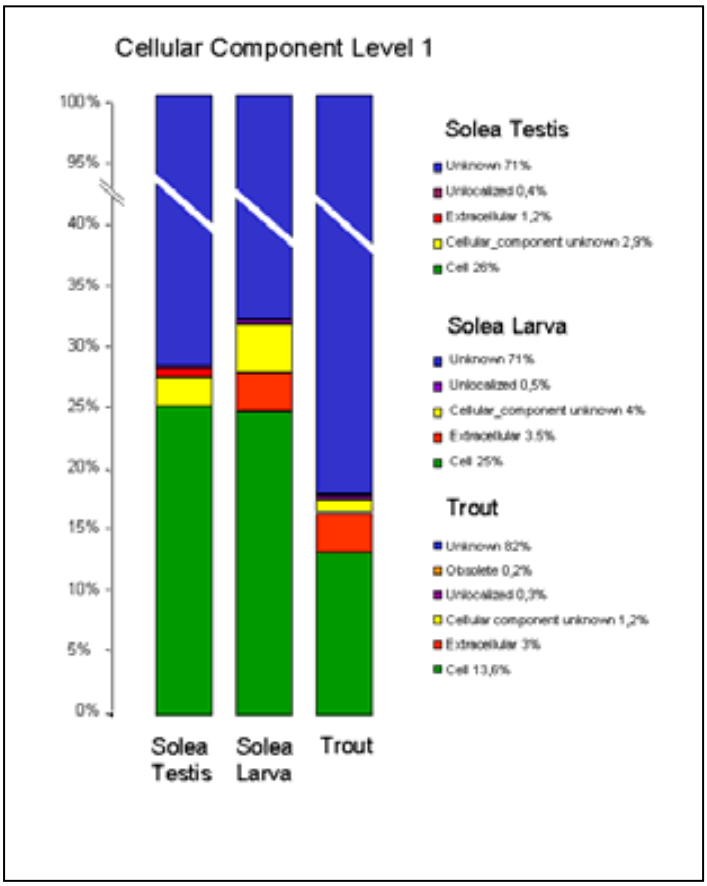
Cellular Component Level 1
100%
95%
40%
35%
30%
25%
20%
15%
10%
5%
0%
Solea Testis
Solea Larva
Trout
Solea Testis
Unknown 71%
Unlocalized 0,4%
Extracellular 1,2%
Cellular_component unknown 2,9%
Cell 26%
Solea Larva
Unknown 71%
Unlocalized 0,5%
Cellular_component unknown 4%
Extracellular 3,5%
Cell 25%
Trout
Unknown 82%
Obsolete 0,2%
Unlocalized 0,3%
Cellular component unknown 1,2%
Extracellular 3%
Cell 13,6%

Annex I.2

Gene ontology charts of the proteins described for *Solea senegalensis.* Proteins were obtained through BLAST search using peptide sequences obtained by 2D LC-MS/MS and adequately filtered. Charts represented up to the level 1 in Molecular Function classification, up to level 2 in Biological Process classification and up to level 3 in Cellular Component.

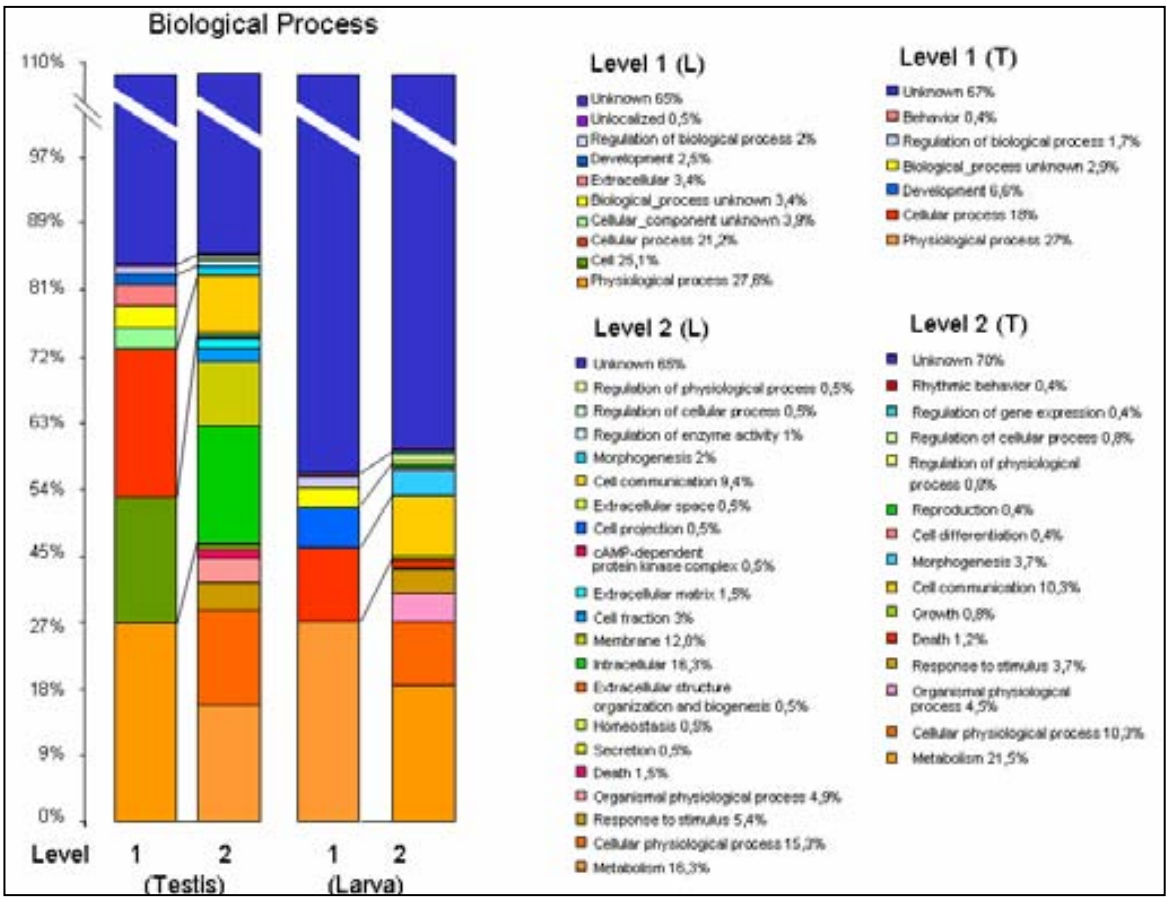

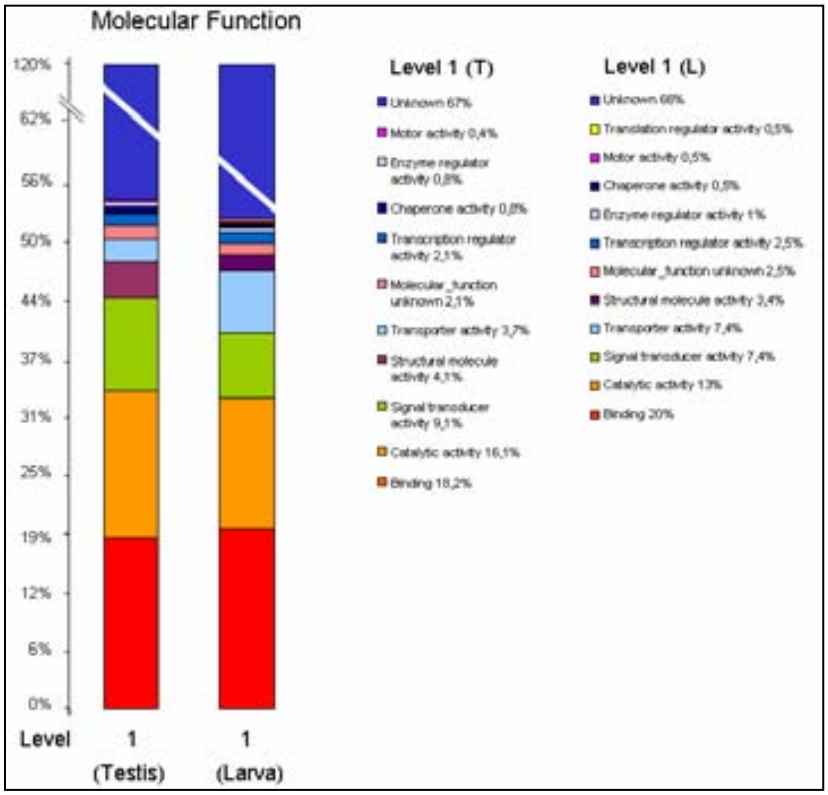
Molecular Function
120%
62%
56%
50%
44%
37%
31%
25%
19%
12%
6%
0%
Level 1 (Testis)
Level 1 (Larva)
Level 1 (T)
Unknown 67%
Motor activity 0,4%
Enzyme regulator activity 0,8%
Chaperone activity 0,8%
Transcription regulator activity 2,1%
Molecular_function unknown 2,1%
Transporter activity 3,7%
Structural molecule activity 4,1%
Signal transducer activity 9,1%
Catalytic activity 16,1%
Binding 18,2%
Level 1 (L)
Unknown 66%
Translation regulator activity 0,5%
Motor activity 0,5%
Chaperone activity 0,5%
Enzyme regulator activity 1%
Transcription regulator activity 2,5%
Molecular_function unknown 2,5%
Structural molecule activity 3,4%
Transporter activity 7,4%
Signal transducer activity 7,4%
Catalytic activity 13%
Binding 20%

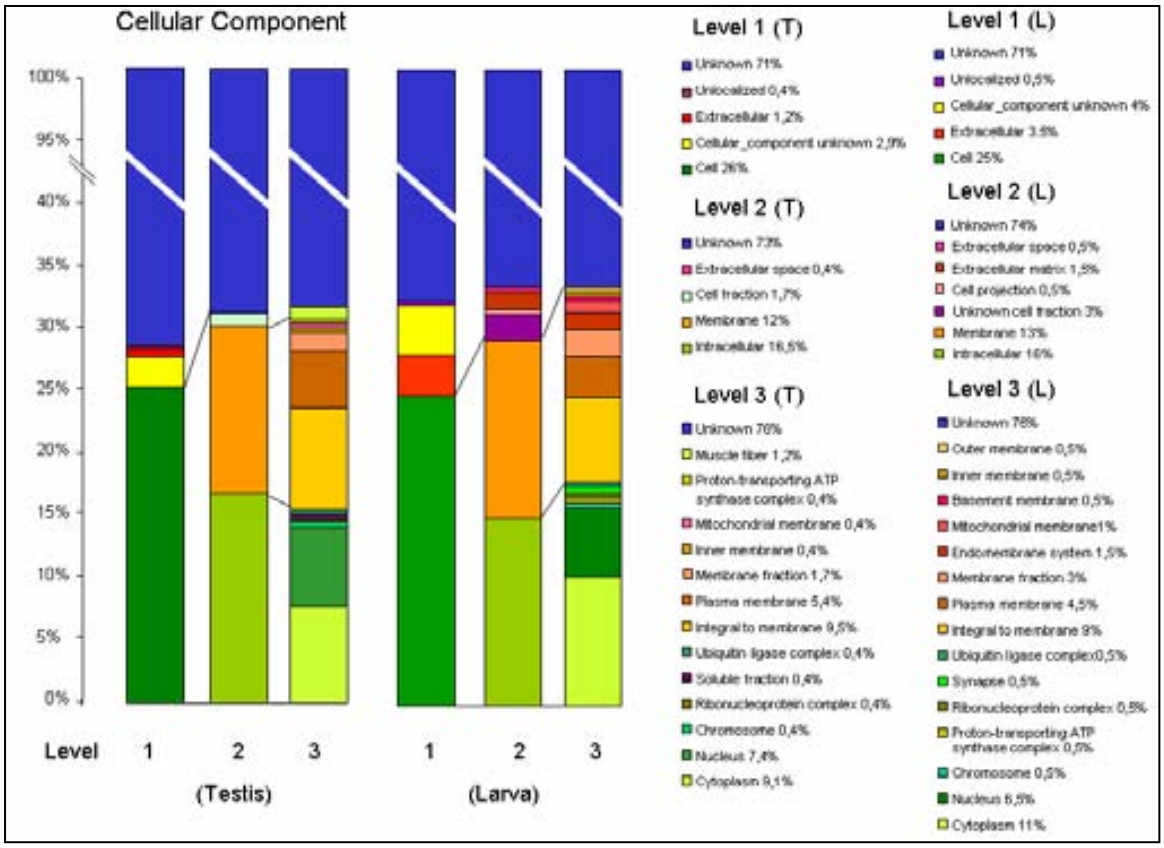
Cellular Component
100%
95%
40%
35%
30%
25%
20%
15%
10%
5%
0%
Level 1 2 3 1 2 3
(Testis)
(Larva)
Level 1 (T)
Unknown 71%
Unlocalized 0,4%
Extracellular 1,2%
Cellular_component unknown 2,9%
Cell 26%
Level 2 (T)
Unknown 73%
Extracellular space 0,4%
Cell fraction 1,7%
Membrane 12%
Intracellular 16,5%
Level 3 (T)
Unknown 76%
Muscle fiber 1,2%
Proton-transporting ATP synthase complex 0,4%
Mitochondrial membrane 0,4%
Inner membrane 0,4%
Membrane fraction 1,7%
Plasma membrane 5,4%
Integral to membrane 9,5%
Ubiquitin ligase complex 0,4%
Soluble fraction 0,4%
Ribonucleoprotein complex 0,4%
Chromosome 0,4%
Nucleus 7,4%
Cytoplasm 9,1%
Level 1 (L)
Unknown 71%
Unlocalized 0,5%
Cellular_component unknown 4%
Extracellular 3,5%
Cell 25%
Level 2 (L)
Unknown 74%
Extracellular space 0,5%
Extracellular matrix 1,5%
Cell projection 0,5%
Unknown cell fraction 3%
Membrane 13%
Intracellular 16%
Level 3 (L)
Unknown 78%
Outer membrane 0,5%
Inner membrane 0,5%
Basement membrane 0,5%
Mitochondrial membrane1%
Endomembrane system 1,5%
Membrane fraction 3%
Plasma membrane 4,5%
Integral to membrane 9%
Ubiquitin ligase complex0,5%
Synapse 0,5%
Ribonucleoprotein complex 0,5%
Proton-transporting ATP synthase complex 0,5%
Chromosome 0,5%
Nucleus 6,5%
Cytoplasm 11%

Annex I.3. - Peptide charge distribution for the *Solea senegalensis* sequenced peptides. The peptide charge distribution of the sole testis and larva peptide sequences described with the MDLC approach is grouped depending on the salt step where they were acquired. Charge was calculated using the iep function of EMBOSS.

	Peptide charge								
[NH4AcO]	1	2	3	4	5	6	7	8	9
0 mM	12	68	48	30	26	11	2	1	0
10 mM	3	20	51	41	43	17	9	7	3
50 mM	2	27	55	56	42	21	2	3	1
100 mM	4	36	48	72	32	21	10	2	0
250 mM	0	20	50	64	29	23	13	4	0
500 mM	1	16	33	38	24	19	7	5	1
500 mM	0	13	33	35	29	8	5	3	0

Annex II.1

The NCBI protein identification and sequence, sequenced peptides and their situation in the homologous protein (red letters) from the identified spots in the spermatogenesis stages study in chapter 2.

Spot 1942 >gi|39795813|gb|AAH64289.1| Phosphoserine aminotransferase 1 [Danio rerio]

MEKKQTVNFGAGPAKLPKSVLLQAQKELQDYSGTGISILEMSHRSSDFTKIINTTENLIRELLNVPENYKILFLQGGG
SGQFSAVPLNLIGLKEERCADYLVTGTWSARAAKEAEKYGKVNVIHPKLDSTKIPDSSTWSLNPSASYVYYCCNET
VHGVEFNFIPDTKGVILVSDMSSNFLSRPVDVSKFGLIFAGAQKNVGCAGVTVVIVREDLIGKALKECPIILDYQVQA
GNNSLYNTPPCFSIYIMGLVLEWIRNNGGADAMERLNKQKSALVYDIINRSNGFYSCPVDAACRSRMNIPFRIGKKE
GDESLEKSFLDGASKLGMISLKGHRSVGGIRASLYNAVTVEDVKILAAYMEDFLRNH

Sequenced Peptides NLGCAGVTVVLVR

Spot 1963 >gi|47577631|ref|NP_001000637.1| olfactory receptor Olr653 [Rattus norvegicus]

MEIRNNVTEFVLLGLTQNLHMQKIVFVVFLVIYVFSVVGNLLILITITNSQLLGAPMYYFLAYLSFIDACYSSVNTPKLIF
DSLHKKKSIKFNGCMTQVFAEHFFGGAEIILLTVMAYDRYVAICKPLHYATIMNRQLCNILVGVSWVGGFLHAGIQM
LFMIGLPFCGPNVIDHFMCDLNPLLALACVDTHILGLFVAANSGFICLLNFLLLLVSYLVILHSLKNHSAEGRRKALST
CVSHITVVVLFFVPGIFVYMRPAATLPIDKAVAIFYTIITPMLNPLIYTLRNAQMKNAIWKLFSTNINSDEK

Sequenced Peptides LLNFLLLLSR

Spot 1966 >gi|47225177|| serine (or cysteine) proteinase inhibitor [Tetraodon nigroviridis].

MASPSPLSKANTSFSLALFRELGDNDRTANIFYSPFSISSALAMVLLGAGGNTATEMSEVLCFTEAEKPKDVEEQQ
QQQQLQQQHHLRLPDFLKKCLKTEGCQDDIHTSFSQLLDELHKKNAPYALSVANRLYGKHYRAELESVDFQSAAE
ASRIHINSWVEKQTEGKIKDLLVQGIVSSDTRLVLVNAIYFKGKWNKQFKEEATRDAQFNVTKNSSKPVKMMHQTS
KFPFTFIPEAKCQILEMPYIGEELSMLIFLPYQMEDSSTGLEKLEKLLTYDKFMEWTRPDMMDSVEVQVGLPRFKLE
EKFNMKNVLVKMGMVEAFDVATSNFSGMSPANDLFLSEVVHKAFVEVNEEGTEAAAATGAIMMLRCARPSERFY
ADHPFLFFIRHNPSMSILFAGRYCSPE

Sequenced Peptides MGMVDAFDVAR TTFSGMSPANDLVEANVVHK

>gi|13385352|ref|NP_080143.1| serine (or cysteine) proteinase inhibitor, clade B (ovalbumin), member 11 [Mus musculus]

MDPITTASTEFCLDVFKELSSNNVGENIFFSPLTTFYALSMLLLGTRGKSAEQMEKVLHYDSFSGVLKAKTKNSSEC
SQVGVMHPDFRALISHINQQNSLSVANRIYGTRSISFHKQYVRCCEKLYQAKLQTVDFELSTEETRKSINAWVKNKT
NGKITNLFAKGTIDPSSVMVLVSAIYFKGQWQNKFQKRETVKAPFHMGVGKSAVVNMMYQTGTFKLAIIKEPEMQV
LELPYANNKLRMIILLPVGTASVSQIEKHLNVKMLREWTNPSNMVEREVDVHIPKFSLSVKYDLNTLLKSLGMRDIFN
VANADLSGMSPDKGLYLSKVVHKSYVDVNEEGTEAAAATGESISVKRLPVTVQFTANCPFLFFIWDESGNILFAGK
FASP

Sequenced Peptides GQTNFCLDLFK

>gi|39795277|gb|AAH63756.1| Serine (or cysteine) proteinase inhibitor, clade B (ovalbumin), member 3A [Mus musculus]

MHLFAEATTKFTLELYRQLRESDNNIFYSPISMMTALAMLQLGAKGNTEKQIEKVLQFNETTKKTTEKSAHCHDEEN
VHEQFQKLMTQLNKSNDAYDLKAANSIYGAKGFPFVQTFLEDIKEYYQANVESLDFEHAAEESEKKINSWVESQTN
GKIKDLFPNGSLNRSTILVLVNAVYFKGQWNHKFDEKHTTEEKFWLNKNTSKPVQMMKQNIEFNFMFLEDVQAKIV
EIPYKGKELSMIVLLPVEINGLKQLEEQLTADKLLEWTRAENMHMTELYLSLPRFKVDEKYDLPIPLEHMGMVDAFD
PQKADFSGMSSTQGLVVSKVLHKSFVEVNEEGTEAAAATGVEVSLTSAQIAEDFCCDHPFLFFIIHRKTNSILFFGRI
SSP

Sequenced Peptides LNLNTWVESQTGKK

Spot 2055 >gi|47225844Isocitrate dehydrogenase 3 (NAD+) [Tetraodon nigroviridis];

MAGRAWRSAASWAFGALRKETPQVRGTNRAIHTVTLIPGDGIGPEISTAVMKIFEAAEAPIQWEERNVTAIQGPGG
KWIIPPDCKESMDRNKIGLKGPLKTPIAAGHPSMNLLLRKTFDLYANVRPCVSIEGYKTPYADVNLVTIRENTEGEYS
GIEHVIVDGVVQSIKLITEEASQRIAEYAFEYARNNQRGSVTAVHKANIMRMSDGLFLRKCREAAEKHKDVKFTEMY
LDTVCLNMVQDPSQFDVLVMPNLYGDILSDLCAGLIGGLGVTPSGNIGANGVAIFESVHGTAPDIAGKDLANPTALL
LSAVMMLRHMGLHNHAKRIETACFDTIRDKQVLTKDLGGNSKCSEFTAAICQRVKDLN

Sequenced Peptides TPYTDVNLVTLR LANYAFEYAR NLETACFDTLR

Spot 2126 >gi|37362242|gb|AAQ91249.1| malate dehydrogenase 1, NAD [Danio rerio]

MAEPIRVLVTGAAGQIAYSLLYSIAKGDVFGKDQPIILVLLDITPMLPVLDGVVMELQDCALPLLREVIPTDKVEVGFK
DLDAAILVGSMPRKEGMERKDLLKANVAIFKTQGEALEKYAKKTVKVLVVGNPANTNCLIASKSAPSIPKENFSCLT
RLDHNRARSQVAMRVGVPSDSVKNVTIWGNHSSTQYPDVHHAIVTRNGKEIAAFDAVNDESWLKGDFISTVQQR
GAAVIKARKLSSAMSAAKAICDHMRDIWFGTPDGEWVSMGIYSSGNSYGVPDDLMYSFPVKIKNKSWKVVDGLSI
NDFSRGKMDATAAELVEERDTALTFLSA

Sequenced Peptides QCNSGYTGSMPR DPVVGNPANTNCLLNR
DPDGLSLNDFSR

Spot 2174 >gi|47221930| [Tetraodon nigroviridis] Polymerase (RNA) II (DNA directed) polypeptide C

MPYANQPTVKITELTDENVKFVIENTDLAVANSIRRVFMSEVPTIAIDWIQIDANSSVLHDEFVAHRVGLIPLTSDDIV
DKLQYSRDCTCDDFCPECSVELTLDVRCTEDQTRHVTSRDLLSNNPRVIPVTSRSRDNDPNDYVEQDDILVVKLR
KGQELRLRAYAKKGFGKEHAKWNPTAGVSFEYDPDNVLRHTVYPRPEEWPKSEYSEIEEDEIQAPFDPNGKPEKF
FYNVESCGSLRPENIVMSALAVLKKKLSDLQTQLSHEIQSDVLTIN

Sequenced Peptides HPAPTAGVSFEYDDPYYK

Spot 2176 >gi|63650325 similar to acidic ribosomal phosphoprotein P0 [Mus musculus]

MPREDRATWKSNYFLKIIQLLDDYPKCFIVGADNVGSKQMQQICMSLRGKAVVLMGKNTMMRKAIGGHLENNPAL
EKLLPHIRRNMGFVFTKEDFTEIRDILLANKVPAAARAGAIAPCEVTVPAQNTGLGPEKTSFFQALGITTKISRGTIEIL
SDVQLIKTGDKVGASEATLLNMLNISPLLLRADHPAGV

Sequenced Peptides VVNAPCDVTVCHLTGLLAAR TSFFQALVATTK

Spot 2243 >gi|47225480|emb|CAG11963.1| [Tetraodon nigroviridis] uridine phosphorylase 2

MDGNVPEPSSSPVCVHNPHLETLKDDILYHFSLGTSTHDLPAIFGDVKFVCVGGSPSRMKAFIEYIAAELNMEDPKS
EYPNICAGTDRYTMYKVGPVLSVSHGVGIPSIAIMLHELIKLLYHARCKDVTIIRLGTSGGIGLEPGTVVVTKQAVDAT
FLPKFEQVILGKTVVRNTDLDQSLAEQLLECSQELNQFETVLGKTMCTMDFYEGQARLDGAFCSYTEEDKQEYLK
ARDAGVCNIEMESSVFATMCKMSGLKAAVVCVTLLNRLKGDQLDSSHHVLQNYQQRPQILVGSYIKKEL

Sequenced Peptides TTYPNLCAGTDR RGDLDQGLAEELLK
VQVCVTLLDR

Spot 2275 >gi|47210341| [Tetraodon nigroviridis] pyruvate dehydrogenase E1-beta subunit

MAMSLVNIIRKGKPVVSALRRRNFHKTVPAAVQVTVRDALNQAMDEELERDERVFLLGEEVAQYDGAYKVSRGLW
KKYGDKRVIDTPISEMGFAGIAVGAAMAGLRPICEFMTFNFSMQAIDQVINSAAKTYYMSAGLQPVPIVFRGPNGAS
AGVAAQHSQCFAAWYAHCPGLKVVSPWNAEDCKGLLKAAIRDDNPVVFLENELMYGVPFDMSEESQSKDFVIPIG
KAKVERAGNHVTLVSHSRYVGHCLDAAAVLAKEGIECEVINLRTIRPMDVGCIEASVMKTNHLLTVEGGWPQFGVG
AEICAQIMEGPAFNYLDAPVSRVTGVDIPMPYAKILEDNSVPQVKDIIFSVKKMLNV

Sequenced Peptides MMLLGEEVAQYDQYK YEMSQSEMGFTGLAVGSAWWR
YTYMASGLQTVPLVFR VVSPWNAEDVK EGLECEVLNLR
LMEGPAFNYLDAPVTR LLEDNSVPLQK

Spot 2339 >gi|55624676| hydroxysteroid (17-beta) dehydrogenase 4 [Pan troglodytes]

MALGRQVLPASGVTLNYISQDSKGAARSALIFLPEIGKSLTLVPPPPFPASSCPAVGVQRLCLFVCVSLQALFMGSP
LRFDGRVVLVTGAGAGLGRAYALAFAERGALVVVNDLGGDFKGVGKGSLAADKVVEEIRRRGGKAVANYDSVEE
GEKVVKTALDAFGRIDVVVNNAGILRDRSFARISDEDWDIIHRVHLRGSFQVTRAAWEHMKKQKYGRIIMTSSASGI
YGNFGQANYSAAKLGLLGLANSLAIEGRKSNIHCNTIAPNAGSRMTQTVMPEDLVEALKPEYVAPLVLWLCHDSCE
ENGGLFEVGAGWIGKLRWERTLGAIVRQKNHPMTPEAVKANWKKICDFENASKPQSIQESTGSIIEVLSKIDSEGG
VSANHTSRATSTATSGFAGAIGQKLPPFSYAYTELEAIMYALGVGASIKDPKDLKFIYEGSSDFSCLPTFGVIIGQKS
MMGGGLAEIPGLSINFAKVLHGEQYLELYKPLPRAGKLKCEAVVADVLDKGSGVVIIMDVYSYSEKELICHNQFSLF
LVGSGGFGGKRTSDKVKVAVAIPNRPPDAVLTDTTSLNQAALYRLSGDWNPLHIDPNFARPIHLPQYVRMYRAIDL
KSGSGKVYQGPAKGAADTTIILSDEDFMEVVLGKLDPQKAFFSGRLKARGNIMLSQKLQMILKDYAKL

Sequenced Peptides YEALAFAER LLGLGLSQSLALEGR

Spot 2436 >gi|20071768|gb|AAH27160.1| Dolichyl-phosphate beta-glucosyltransferase-like [Mus musculus]

MATLLLQLLGLGVALAAAALILVSIVAFITATKMPPCYQHEEEKFFLNAKGQKEALPSIWDSPTKQLSVVVPSYNEEK
RLPVMMDEALNYLEKRQKHDCTFTYEVIVVDDGSEDQTSKVALKYCQKYGSDKVRVITLVRNRGKGGAVRMGVF
SSRGEKILMADADGATKFPDVEKLEKGLSDLQPWPEQMAIACGSRAHLEKESIAQRSYFRTFLMYGFHFLVWFLC
VKGIRDTQCGFKLLTREAAARTFSSLHIERWAFDVELLYIAQCLQIPIAEVAVNWTEIEGSKLVPFWSWLQMGKDLL
FIRLRYLTGAWRLKQTRKAS

Sequenced Peptides MATLLMQLLR

Spot 2499 >gi|44890386|gb|AAH66763.1| Tyrosine 3-monooxygenase/tryptophan 5-monooxygenase activation protein, epsilon polypeptide [Danio rerio] of 14-3-3 protein

MGDREDLVYQAKLAEQAERYDEMVDSMKKVAGMDVELTVEERNLLSVAYKNVIGARRASWRIISSIEQKEENKGG
EDKLKMIREYRQTVENELKSICNDILDVLDKHLIPAANSGESKVFYYKMKGDYHRYLAEFATGNDRKEAAENSLVAY
KAASDIAMTDLQPTHPIRLGLALNFSVFYYEILNSPDRACRLAKAAFDDAIAELDTLSEESYKDSTLIMQLLRDNLTL
WTSDMQGDGEEQNKEALQDVEDENQ

Sequenced Peptides YLAEFAAGKTR GSHALNFSVFHEYLK
EAAENSLVAYK DDNLAMNELPSTHPLR
GSHALNFSVFHEYLK MSEDDALAQMPTLSEESYK

Spot 2521 >gi|47220021|emb|CAG12169.1| [Tetraodon nigroviridis] 6-phosphogluconolactonase

MAGRRVVVFPSSAELGPALASLVASRAEEAIASHGRFTVGLSGGSLVSMLSKELLALPSLDCSKWVVGFCDERLV
PFDDPESTYGLYKSHFFSKVNIPAGGILTIDSSLPVNDCAEDYERKLKEVFPDDDFPVFDLLLLGMGPDGHTCSLFP
DHPLLEETKKIVAPISDSPKPPPQRVTLTFPVVNSARCVAFVSTGGSKAPVLKEVLEGEGHPVYPAARVVPANGEL
FWLVDDPAAASLTIQVERL

Sequenced Peptides WVVGFCDER VTMTFVVPNSAR

Spot 2578 >gi|56554783|gb|AAV97962.1| carbonic anhydrase [Pseudopleuronectes americanus]

MSWGYAADNGPDKWADNFPVANGPRQSPIDILPGEASFDGALKPLSLKYDPSNCLEILNNGHSFQVTFVDDTDSS
TLKDGPISGVYRLKQFHFHWGACDERGSEHTVAGTMYPAELHLVHWNTKYPSFGDAASKPDGLAVVGVFLKIGAE
NANLQKVLDAFSSIQAKGKQTTFAGFDPASLLPGCLDYWTYDGSLTTPPLLESVTWIVCKEPISISAEQMAKFRSLL
FSAEGEAECCMVDNYRPPQPLKGRTVRASFK

Sequenced Peptides ADVANFPLADGPR CHANFPLADGPR
SLLFSADGEAECCMVSGYWWMNRK

Spot 2587 >gi|45387733|ref|NP_991218.1| hypothetical protein zgc:77182 [Danio rerio] Purine-nucleoside phosphorylase

MSTSSECSFSYEEYKETADWLLANTDIRPKVAIICGSGLGGLADLLDNKQVFPYDKIPRFPHSTVQGHKGQLVFGE
LNGKQCVCMQGRFHFYEGYNVATVTYPVRVFFLLGIETLIVTNAAGGLNPKFKVGDIMVIKDHINMPGFAGQNPLC
GHNEERFGVRFPCMSDAYDRDLAQLVRKTAKELGCDSFLQEGVYCMLAGPSYETIAEC
RVLQMLGADAVGMSTVPEVVIARHCGIRVFGLSLITNKVVTDYDSKERANHEEVLETTRMRTEDLQRIVSNVVRKM

Sequenced Peptides FPCMSDAYDR WVYCMLAGPTYETLAECR
LMVVLGRNVGMSTVHWDRR

>gi|55640605|ref|XP_509906.1| PREDICTED: similar to Proteasome subunit alpha type 6 (Proteasome iota chain) [Pan troglodytes]

MSRGSSAGFDRHITIFSPEGRLYQVEYAFKAINQGGLTSVAVRGKDCAVIVTQKKVPDKLLDSSTVTHLFKITENIGC
VMTGMTADSRSQVQRARYEAANWKYKYGYEIPVDMLCKRIADISQVYTQNAEMRPLGCCMILIGIDEEQGPQVYK
CDPAGYYCGFKATAAGVKQTESTSFLEKKVKKKFDWTFEQTVETAITCLSTVLSIDF
KPSEIEVGVVTVENPKFRILTEAEIDAHLVALAERD

Sequenced Peptides LYKVEYAFK YGYELHVGYVCK

Spot 2591 gi|56554783|gb|AAV97962.1|carbonic anhydrase [Pseudopleuronectes americanus]

MSWGYAADNGPDKWADNFPVANGPRQSPIDILPGEASFDGALKPLSLKYDPSNCLEILNNGHSFQVTFVDDTDSS
TLKDGPISGVYRLKQFHFHWGACDERGSEHTVAGTMYPAELHLVHWNTKYPSFGDAASKPDGLAVVGVFLKIGAE
NANLQKVLDAFSSIQAKGKQTTFAGFDPASLLPGCLDYWTYDGSLTTPPLLESVTWIVCKEPISISAEQMAKFRSLL
FSAEGEAECCMVDNYRPPQPLKGRTVRASFK

Sequenced Peptides ADVANFPLADGPR

Spot 2603 >gi|55251370|emb|CAH68999.1| novel protein similar to vertebrate methionine sulfoxide reductase A (MSRA) [Danio rerio]

MVARTSVRLIWRQFIQSRMGEMSSKVQMISPEEALPGREQSIKVSAKHDVNGNRTVPPFPEGLQMVLFGMGCFW
GAERKFWRQKGVYSTQVGYSGGYTPNPTYEEVCTGKTGHTEVVRVVFEPQKIKFSELLKVFWESHNPTQGMRQ
GNDVGTTYRSSIYTNTQEQLEQALQSREEYQKVLTEEGFGAITTEITMAKEFYYAEDYHQQYLSKNPDGYCGLGG
TGVSCPIGLKSKH

Sequenced Peptides MDCTQVGFCGGFTPNNSCR

Spot 2650 >gi|1165134|emb|CAA64496.1| glutathione S-transferase [Pleuronectes platessa]

MAQDMTLLWGSGSCPCWRVMILLEEKNLQGYNHKLLSFDKKEHKSQEVLDINPRGQLPSFKHGDNVVNDSYAAC
FYLESQFKSQGNQLIPDSPAEQALMYQRMFEGLTLYEKLNAVIYYDWFVPEGERHDSALKRNKEALATELKLWEG
YLQKHGKHLAGRSFSLADVTVFPTVATLFRMGLSAESYPQLGQYHALLKERPGIKRSWPPHWLENPKGQDALKDI

Sequenced Peptides LLLDNPAEQALMYKR EFEGLTFYEK
DGFLWVTSFVDPAVVFR

Spot 2667 >gi|24413939|dbj|BAC22191.1| ubiquitin C-terminal hydrolase [Oreochromis niloticus]

MEWTPMEINPEMLNKMMGKLGVGESWRFVDVLGLEGEQLSSVPKPCCALMLLFPLTQQHETFRAQQADKVSGG
SEAYFLKQTAVNSCGTIALLHAVANNKDKMTFDGASALKKFLDETANMSPDDRAKHLEKNQAIFDAHNEIAAQGQC
RPEADKVNFHFIAFVNVNGQLYEFDGKINGPVNHGHTKEESFVMDAAKVCRGFMEREEVRFSAVALCQN

Sequenced Peptides FNLNTAMELNPEMAKR FLDETANMSADDR
FSAVALCR

Spot 2685 >gi|47227982|emb|CAF97611.1| unnamed protein product [Tetraodon nigroviridis] Glutathione peroxidase

MPGLLLGEVFPDFRAETTTGTISFHQFLGDSWAILFSHPGDYTPVCTTELGRAARLSGEFSKRRVKMVALSVNSLE
DHQGWTKVVRETHRAVTAGHMCMCARLSAHQDILAYNGEDGESGELPFPIIADANRELAVALGMLDPEEKDKDG
MPLTARCASVFIIGPDKRLKLSLLYPATTGRNFDEILRVVDSLQLTAAKRVATPADWKPGECVMVPPSMSEEEAAA
MFPEGIYSKELPSGKKYLRYTPQP

Sequenced Peptides GPLLLGDVFPNPFVDGYRR FDTPVCMAELACNR
LSLLYPATTGR

Spot 2723 >gi|62204368|gb|AAH92846.1| Peroxiredoxin 3 [Danio rerio]

MAATIGRLLGASARRAAVCGLKTLVPRNGVSVIRAPQPLACIAAQKACFSISAARWAPAVTQAAPHFKGTAVINGEF
KEISLGDFKGKYLVLFFYPLDFTFVCPTEIVAFSDKANEFHDVNCAVVGVSVDSHFTHLAWTNTPRKSGGLGKIQIP
LLADLTKQVSRDYGVLLEGPGIALRGLFIIDPNGIVRHMSVNDLPVGRSVGETLRLVKAFQFVETHGEVCPASWTPK
SPTIKPTPDGSKEYFEKVN

Sequenced Peptides DYGVLLEGGPLALR FAQFYECVTVCPASWTPK

>gi|66910263|gb|AAH96804.1| Hyp pro LOC321908 [Danio]: Translin; Testisbrain RNA binding protein

MSVTEMFSYIQGFLSADQDIREDIRKVVQGLEQTARGILTVLQSVHQPTGFKDIPSKCLKARELFCTVRNHTGELKT
KFPVEQYYRYHELWRFVLQRLAFLAAFVVYLESEALVTREEVAKILAIEVDREKGFHLDVEDYLAGVLILASELSRLA
VNSVTAGDYGRPLRISNFINELDSGFRLLNLKNDPLRKRYDGLKYDVKKIEEVVYDLSIRGLAKEQEAGEEK

Sequenced Peptides ELLTVLQSVHQPSGFK LSNFLNELDSGFR

Spot 2738 >gi|51468069|ref|NP_001003889.1| proteasome (prosome, macropain) subunit, beta type, 1 [Danio rerio]

MISAQAYGENGKMKEYHYTGPVEHKFSPYAFNGGTVLAVAGEDFAIVASDTRLSEGYSIHSRDSPKCYKLTDTTVL
GCSGFHGDCLTLTKIIEARLKMYKHSNNKSMTSGAIAAMLSTILYGRRFFPYYVYNIIGGLDEEGRGAVYSFDPVGS
YQRDTYKAGGSASAMLQPLLDNQIGFKNMENVEHVPLTQEKAVQLVKDVFISAAERD
VYTGDALKVCIVSKEGIKEEIVPLRKD

Sequenced Peptides VQYSFDPVGSYKR QKSSAMLQPLLDNKLGFK VDFLSAAER

Spot 2759 >gi|74096419|ref|NP_001027893.1| apolipoprotein A-IV4 [Takifugu rubripes]

MKVLVVLALAVFSGCQANLFYADAPKPQLEVLTDAFWDYVAKATQTADDTLQMVRKSQFGQDVSARLTESADMA
SKYAVSIQEQLPPGAQDLITKVTTEADVLRERVTQELSTVRNKLEPYTEDMKAKVQARVEQLKQELAPYADSVDSE
ALRATLMQKSEELKSSLEQSVKDLQAQLGPYTDDLKLKVDGHLQNFQQNLAPMAEKVQTELNQRAQQVKDMAAP
FVDELRDKLDPYAQDLQARLASLYESFVKAG

Sequenced Peptides DPELKVTAEADVLR GQGRQSVSDMKDQLGPYTEDLR

Spot 2778 >gi|47213154|| [Tetraodon nigroviridis proteasome beta 4 subunit;

GMKLSFWENGPKPGQFYSFPGSRNQTGTSCGPVRHTLNPMVTGTSVLGVKFSGGVIIAADMLGSYGSLARFRNIS
RLMKVNDSTILGASGDYADYQYLKRVIEQMVIDEELLGDGHSYSPKAVHSWLTRVMYNRRSKMNPLWNTVVIGGF
YKGESFLGYVDKLGVAYEAPTVATGFGAYLAQPLMREAVENKPELSKQEARDLIERCLKVLYYRDARSYNRYEIAIV
TEEGVEIISPLSSETNWDIAHMVR

Sequenced Peptides LTTPMVTGTSVLRK SSALSDLAADMLGSYGDRR
VNNSTLLGASGDYYVNGMYK WWMEAPTVATGFGAYLAQGQRR
VKLSKKEALDLVER RELLGPLSSETNWDLAR

Spot 2837 >gi|4530297| heterochromatin-specific nonhistone protein [Homo sapiens]

KDKVEYLLKWKGFSDEDNTWEPEENLDCLDLIAEFLQSQKTAHETDKSEGGKHKADSDSEDKGEESKPKGKKEE
SEKPRGFARGLEPERIIGATDSSGEVMFLMKWKNSNEADLVPAKEASVKCPQVVISFYEERLTWHSYPSEDDDKK
NDKN

Sequenced Peptides CPQVVLSFYEER

Spot 2877 >gi|50370069|gb|AAH76141.1| Zgc:92657 [Danio rerio] (histidyl-tRNA synthetase)

MKAIIQRVTRASVTVGEEQISSIGRGLCVLLGISAEDTQKDVDYMVRKILNLRVFEDENGRAWSRSVMDGELEVLCV
SQFTLQCLLKGNKPDYHAAMPAELAQPFYNNMLEQLRETYKPELIKDGQFGAKMQVLIQNDGPVTIQLESPPAPTD
PKLLSKQEKQQQRKEKTRSKGPSDSSREKAAQRSKVDPSASSGAEGDVSSEREP

Sequenced Peptides SSQVCDYVDSYRVENNNMLQQLR

Spot 2897 >gi|37681759|gb|AAQ97757.1| muscle cofilin 2 [Danio rerio]

MASGVTVEETVLTVFNEMKVRKAHCNEEEKSKRKKAVMFCLSDDKKHIIMEQGQEILQGDEGDPYLKFVKMLPPN
DCRYALYDATYETKETKKEDLVFIFWAPESAPLKSKMIYASSKDAIKKKFTGIKHEWQVNGMDDIKDRKTLAEKLGG
ASVVSLEGKPLTD

Sequenced Peptides YALYDATYETK WTHCFLFWASVLAVEK

Spot 2898 >gi|41946867|gb|AAH65947.1| Cofilin 2 (muscle) [Danio rerio]

MASGVTVSDEVIKVFNDMKVRKSSSSDEVKKRKKAVLFCLSDDKKKIIVEEGRQILVGDIGDSVDDPYACFVKLLPL
NDCRYGLYDATYETKESKKEDLVFIFWAPEGAPLKSKMIYASSKDAIKKKFTGIKHEWQVNGLDDIQDRSTLAEKLG
GNVVVSLEGRPL

Sequenced Peptides YALYDATYETK

Spot 2908 >gi|47217449 [Tetraodon nigroviridis] Myosin regulatory light chain 2

MSSKRTKAKTTKKRPQRATSNVFAMFDQSQIQEFK//EAFNMIDQNRDGFVDKEDLHDMLASLGKNPTDEYLEAM
MNEAPGPINFTMFLTMFGEKLNGTDPEDVIRNAFACFDEEGTGFIQEDYLRELLTTMGDR//FTDEEVDELFREAPID
KKNNFNYVEFTRILKHGAKDKDD

Sequenced Peptides ATSNVFAMFDQSKLKEFK EAFNMLDQNR LNGTDPEDVLR
LELTTMGDR FTDEEVDELFR NGFNYAEFTR

Spot 2909 >gi|47218822|emb|CAG02807.1| unnamed protein product [Tetraodon nigroviridis]

MESAEAVAADVSRSRSVTIEISNLTKNYCLINPRVYLESGETYNPPQPTVRPLMTEVCTFSKSSGIPTGSVGVLTYE
LLERRSTMLPETLAIMFSVPYDYSFYNNWFAVGIYETGTKCNEGLYKQMYNEKKQAEHGFVREKANGSGINYVGG
NLDIRATMNPLGKAIMKVEVWDAFFPFSE

Sequenced Peptides VGVLTYDLLER

Spot 2918 >gi|33991794|gb|AAH56526.1| Myosin light chain (19.9 kD) (mlc-4) [Danio rerio] (regulatory Subunit)

MSSKRAKGKITKKRPQRATSNVFAMFDQSQIQEFKEAFNMIDQNRDGFIDKEDLHDMLASLGKNPADDYLEAMMT
EAPGPINFTMFLTMFGEKLNGTDPEEVIRNAFACFDEEGTGFIHEDYLRELLTTMGDRFTDEEVDELFREAPIDKKS
NFNYVEFTRILKHGAKDKDD

Sequenced Peptides SGNLVFAMFDKSQLQEFK NAFACFDEEGTGSLKEDYLR
FTDEEVDELFR SNFNYVEFTR

Spot 2972 >gi|41946867|gb|AAH65947.1| Cofilin 2 (muscle) [Danio rerio].

MASGVTVSDEVIKVFNDMKVRKSSSSDEVKKRKKAVLFCLSDDKKKIIVEEGRQILVGDIGDSVDDPYACFVKLLPL
NDCRYGLYDATYETKESKKEDLVFIFWAPEGAPLKSKMIYASSKDAIKKKFTGIKHEWQVNGLDDIQDRSTLAEKLG
GNVVVSLEGRPL

Sequenced Peptides YGLYDATYETK

Spot 3013 >gi|37681953|gb|AAQ97854.1| transgelin [Danio rerio]

MANKGPSYGLSREVQSKIDKKYDPELEGRLVQWIVSQCGEAIGKPQPGKQGFQQWLKDGCILCELINSLFKDSKP
VKKIQSSSMAFKQMEQISQFLTAAERYGITKSDIFQTVDLWEGKDLAAVQMTLLSLGSLAVTKDDGCYRGDPAWFP
KKSHENRREFSEEQMKEGHSVIGLHMGTNIGASQAGMTGYGRPRQILNNQ

Sequenced Peptides MQEQLSQFLSAAE LLKMGTVALTK

Spot 3089 >gi|47211278|emb|CAF90396.1| unnamed protein product [Tetraodon nigroviridis] nucleoside diphosphate kinase

MSSQLERTFIAVKPDGVQRGIVGEIIKRFEVKGFKLVAMKMVQASEDLLMNHYIDLKDRPFFPQLVKYMSSGPVVA
MVWEGKGVVKTGRVMLGETDPAKSSPGTIRGDFCIDVSKNIIHGSDSVESANKEISLWFQEGELVDYT

Sequenced Peptides MLHASEDLLK MLGETNPANSEPSALR GDFCLDVGK

Spot 3122 gi|51261923|gb|AAH79951.1| Myosin alkali light chain 6, smooth muscle form [Xenopus tropicalis]

MCDYSDDQIADYKESFQLFDRVGDGKILFGQCGDVMRALGQNPTNAEVMKVLGNPKPEDMNIKTLDFEQFLPMM
QTVAKNRDVPGLEDIIEGLRVFDKEGNGTVMGSELRHVLVSLGEKMTDDEVETLLSNHEDANGCINYEELIRAILNG

Sequenced Peptides LSFGKCGDVMR

gi|37362252|gb|AAQ91254.1| myosin light chain alkali, smooth-muscle isoform [Danio rerio]

MSDFSEDQILEFKEAFLLFDRTGDGKITYNQCGDVMRALGQNPVNAEVLKVLGNPKAEEMNHKLLDFEQFLPMLQ
AIAKNKDQGTFEDFVEGLRVFDKEGNGTVMGAELRHVLTTLGEKMTEEEVETLLAGHEDANGCINYEELVRMVMS
G

Sequenced Peptides MTEEEVETLLAHGWDQGCLNYRWQR

Spot 3159 gi|51261923 Myosin alkali light chain 6, smooth muscle form [Xenopus tropicalis]

MCDYSDDQIADYKESFQLFDRVGDGKILFGQCGDVMRALGQNPTNAEVMKVLGNPKPEDMNIKTLDFEQFLPMM
QTVAKNRDVPGLEDIIEGLRVFDKEGNGTVMGSELRHVLVSLGEKMTDDEVETLLSNHEDANGCINYEELIRAILNG

Sequenced Peptides LSFGQCGDVMR

gi|37362252| myosin light chain alkali, smooth-muscle isoform [Danio rerio]

MSDFSEDQILEFKEAFLLFDRTGDGKITYNQCGDVMRALGQNPVNAEVLKVLGNPKAEEMNHKLLDFEQFLPMLQ
AIAKNKDQGTFEDFVEGLRVFDKEGNGTVMGAELRHVLTTLGEKMTEEEVETLLAGHEDANGCINYEELVRMVMS
G

Sequenced Peptides TVFLLFDK WGGSMEDFVEGLR

Spot 3233 >gi|45501160|gb|AAH67152.1| Profilin 2 [Danio rerio]

MSWASYVENLMSDGSCQDAAIVGCTAEAKYVWGAQEGGTFANITPTEIDVLVGKDRQSFFTNGLTLGSKKCSVIR
DNLTTEGDWTMDIRTKSQGGEPTYNIAVGKATKTLIMVKGKEGIHGGQLNKKTYTMAEYLRRSGY

Sequenced Peptides ESFFTNGLTLGSK AYEMADYLR

>gi|47228591|emb|CAG05411.1| unnamed protein product [Tetraodon nigroviridis]
(Sperm Polypeptide Vb of theCytochrome C Oxidase)

MAAGGIPTDEEQATGLEKIILTAMKEGADPYSMMKPKEYAGSKTDPHLVPSITNKRIVGCVCEEDNTAVVWFWLHE
GEPQRCPSCGAHYKLVHHHLPH

Sequenced Peptides AAGGMPTDEEQATGLER

Spot 3649 >gi|57157761|dbj|BAD83853.1| apolipoprotein A-I [Takifugu rubripes]

MKFVVLALALLLAVGSQAASLMADPPSELEHFRSALSMYLDRAKERAHSALATLDDAEYKELKDRLAQRVDDIHSQ
IKTLQGSVSPITDSVVSTISDATSELRTSIQTDFKTLQDETAAQREKLRAVVEQHLSEYRTLLQPIVSEYQAKHKEEM
DALKLKLDPVMEELHKKIAVNVEETKGALMPIVEKVHTKLAEYVEQIKAVVTPYVNEYKEELRDTYIRAMSLSRDDLD
AMRSKIDPIVEVIKEKVGEIGQIVSSTFSKS

Sequenced Peptides QVSPVTDSVVTTLAEATRGKK

>gi|52430350|gb|AAU50536.1| apolioprotein A1 [Fundulus heteroclitus]
DALKIKLQPVVEAMKTSVTANVEETKTALMPILESVRAKLSERLENLKEMATPYVEEYKEQLKEAYGQAQSVKPEDL
TALKEKITPMAEEVRAKVTEMFEAIAATFKRS

Sequenced Peptides TAYTQAQSVNAEKLKSLR

>gi|47215998|emb|CAF96246.1| unnamed protein product [Tetraodon nigroviridis]
Serin protease 35

SALDDEYTWPQWKVPLVRNRRTVSLSSPRFSARPQPEPNGVCGIECQRRLPAASLDDLENFLSYETVYENGSRT
YTSVAVEGLSEAAAWPRNASSRSRHKREVYGTDTRFTISDKQFSTKYPFSTSVKISTGCSGVLVSPKHVLTAAHCI
HDGKDYLDGVQKLRVGILKEKSRRGKGERRGGRGKGRGRKGDKEREEAADKEESGGKGERRGRGKGRKNRSR
RSVESEKPSFRWTRVKKSQVPKGWFKGVSGGLKADYDYAVLELKRPPKVKHMDVGVIPSLKKIPAGRIHFSGFDD
DVPATWSTASAPSRRNPTTWCTSTATPNPAPAAPASTSASRSPARRSGRGRSSGSSRVISGWM

Sequenced Peptides GGQAASLDDVENPLGYK

Spot 3690 >gi|37681911|gb|AAQ97833.1| proteasome subunit, alpha type, 5 [Danio rerio]

MFLTRSEYDRGVNTFSPEGRLFQVEYAIEAIKLGSTAIGIQTSEGVCLAVEKRITSPLMEPSSIEKIVEIDSHIGCAMS
GLIADAKTLIDKARVETQNHWFTYNETMTVESVTQAVSNLALQFGEEDADPGAMSRPFGVALLFGGVDEKGPQLY
HMDPSGTFVQCDARAIGSASEGAQSSLQEVYHKSMTLKDAIKSSLTILKQVMEEKLNATNIELATVEPGKTFHMYT
KEELEDVIKDI

Sequenced Peptides LFQVEYALERR SGRVNLELATVVRR

Annex II.2.- *Variation between experimental and theoretical Mr and pI values*. Experimental (Exper) and theoretical (Theor) Mr and pI values of each protein were measured with software analysis and Expasy Mw/pI tool, respectively. Variation [Δ (Exp-Theor)] was calculated as (Exper-Theor)) value and normalization [Norm Δ] as (Exper value-Theor value)/ (Exper value+Theor value). For spots 2587, 2723, 3233 and 3649, which couldn't be assigned univocally, values from both candidates are considered.

Spot ID	Prot ID	*Mr*				*pI*		
		Exper	Theor	Δ (Exp-Theor)	Norm Δ	Exper	Theor	Δ (Exp-Theor)
1942	Phosphoserine aminotransferase 1	55	40	15	0,158	6,9	8	-1,1
1963	Olfactory receptor Olr653	54	35	19	0,213	4,8	8,8	-4,0
1966	Serine (or cysteine) proteinase inhibitor	53	43	10	0,104	5,7	9	-3,3
2055	Isocitrate dehydrogenase 3 (NAD+) alpha	51	40	11	0,121	6,5	7,1	-0,6
2126	Malate dehydrogenase 1	49	36	13	0,153	6,6	7	-0,4
2174	Polymerase (RNA) II (DNA directed) polypeptide C	49	31	18	0,225	4,6	4,8	-0,2
2176	Acidic ribosomal phosphoprotein P0	49	21	28	0,400	5,6	9,4	-3,8
2243	Uridine phosphorylase 1	37	38	-1	-0,013	6,5	6,1	0,4
2275	Pyruvate dehydrogenase E1-beta subunit	47	39	8	0,093	5,6	6,2	-0,6
2339	Hydroxysteroid (17-beta) dehydrogenase 4	45	73	-28	-0,237	5,7	8,9	-3,2
2499	14-3-3 protein (Tyrosine 3-monooxygenase)	42	29	13	0,183	4,5	4,8	-0,3
2521	6-phosphogluconolactonase	41	26	15	0,224	5,1	4,9	0,2
2578	Carbonic anhydrase	39	28	11	0,164	4,4	5,2	-0,8
2587	Purine-nucleoside phosphorylase	39	32	7	0,098	6,4	6	0,4
	Proteasome subunit alpha	39	27	12	0,182	6,4	6,4	0
2591	Carbonic anhydrase	39	28	11	0,164	4,5	5,2	-0,7
2603	Methionine sulfoxide reductase A	39	26	13	0,200	7,9	7,7	0,2
2650	Glutathione S-transferase	38	26	12	0,188	6,3	6,7	-0,4
2667	Ubiquitin C-terminal hydrolase	37	24	13	0,213	5,3	5,51	-0,2
2685	Glutathione peroxidase	36	27	9	0,143	6,3	5,6	0,7
2723	Peroxiredoxin 3	36	27	9	0,142	6,6	9,2	2,6
	Translin	36	26	10	0,161	6,6	5,8	0,8

Annex II.2.- *Variation between experimental and theoretical Mr and pI values* (continuation).

Spot ID	Prot ID	*Mr*				*pI*		
		Exper	Theor	Δ (Exp-Theor)	Norm Δ	Exper	Theor	Δ (Exp-Theor)
2738	Proteasome subunit beta	36	23	13	0,220	7,7	6,3	1,4
2759	Apolipoprotein A-IV4	35	28	7	0,111	4,4	4,8	-0,4
2778	Proteasome beta 4 subunit	36	28	8	0,125	7,0	8,4	-1,4
2837	Heterochromatin-specific nonhistone protein	29	17	12	0,261	4,6	4,8	-0,2
2877	Histidyl-tRNA synthetase	35	23	12	0,207	4,1	6	-1,9
2897	Cofilin	22	18	4	0,100	6,0	6,8	-0,8
2898	Cofilin 2	22	19	3	0,073	6,4	7,6	-1,2
2908	Myosin regulatory light chain 2	22	15	7	0,189	4,5	4,7	-0,2
2909	Unnamed protein product	22	20	2	0,048	6,4	5,3	1,1
2918	Myosin light chain	22	20	2	0,048	4,3	4,7	-0,4
2972	Cofilina2	19	19	0	0,000	5,7	7,6	-1,9
3013	Transgelina 2	18	22	-4	-0,100	5,9	8,6	-2,7
3089	Nucleoside diphosphate kinase	15	16	-1	-0,032	6,7	6,1	0,6
3122	Myosin light chain alkali	13	17	-4	-0,133	3,8	4,5	-0,7
3159	Myosin alkali light chain 6	11	17	-4	-0,214	3,9	4,4	-0,5
3233	Profilin 2	18	15	3	0,091	5,6	7,7	-2,1
	Cytochrome c oxidase subunit Vb	18	11	7	0,241	5,6	6	-0,4
3649	Apolipoprotein A1	39	29	10	0,147	4,9	5,4	-0,5
	Serin protease 35	39	39	0	0	4,9	10	-5,1
3690	Proteasome subunit, alpha	41	26	15	0,224	4,4	4,7	-0,3

Annex II.3.- Variation between experimental *pI* value of the identified proteins measured with the IMP software and the theoretical *pI* calculated with Expasy tools. The experimental *pI* of every identified spot was plotted against the theoretical *pI* (down).

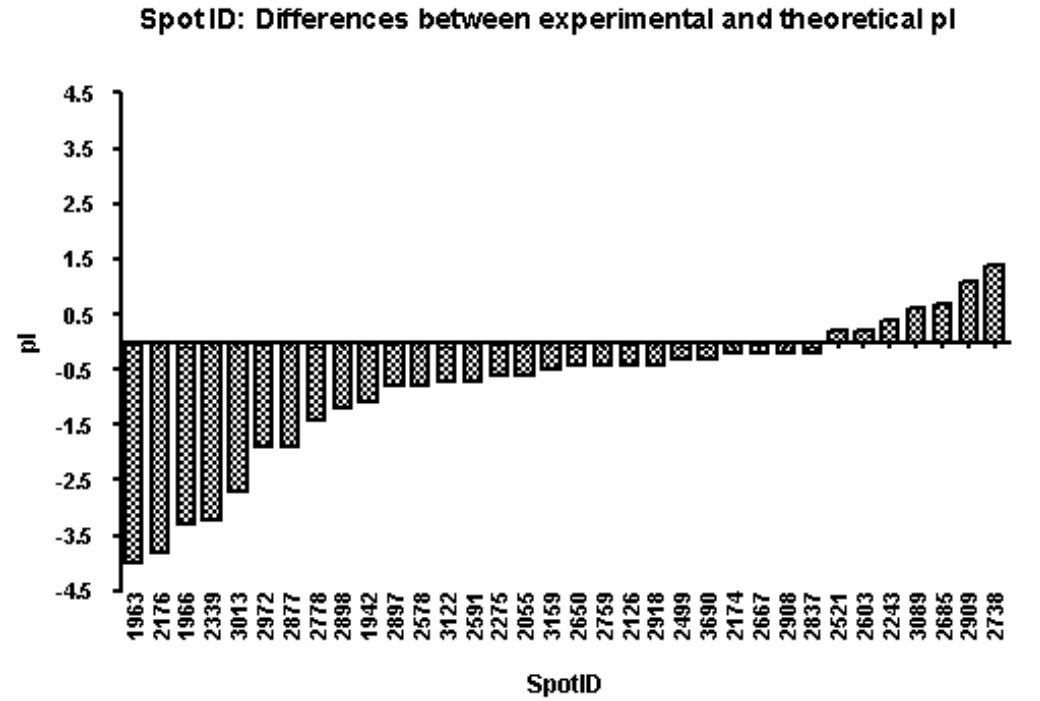

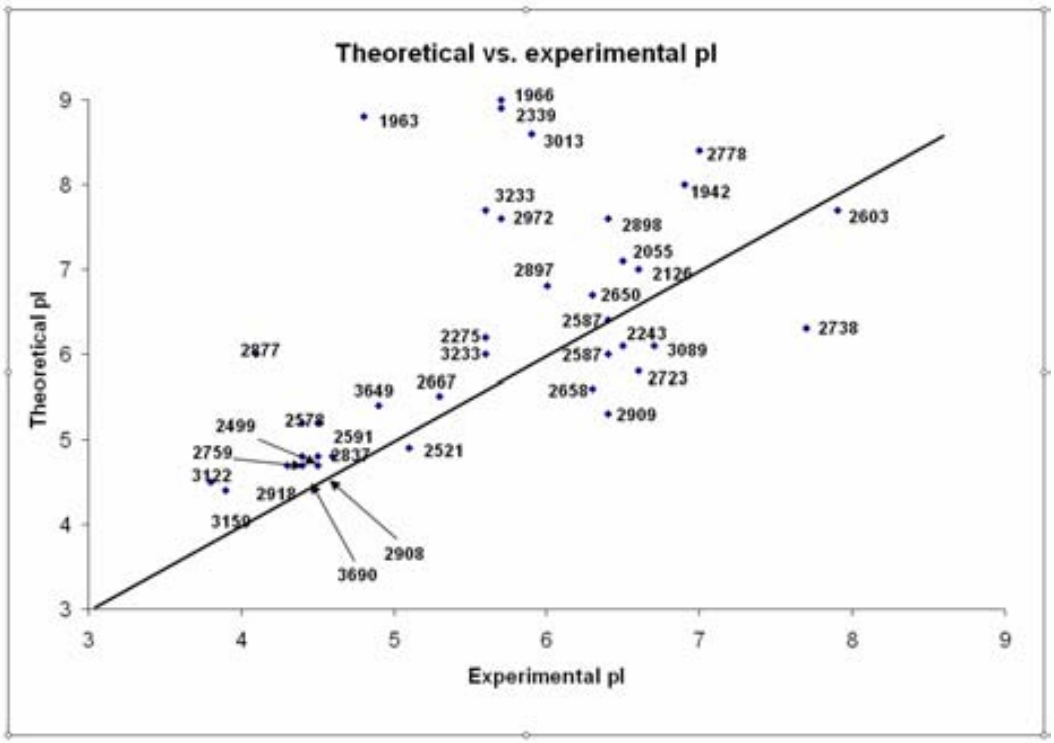

Annex II.4 .- Variation between experimental *Mr* value of the identified proteins measured with the IMP software and the theoretical *Mr* calculated with Expasy tools. The experimental *Mr* of every identified spot was plotted against the theoretical *Mr* (down).

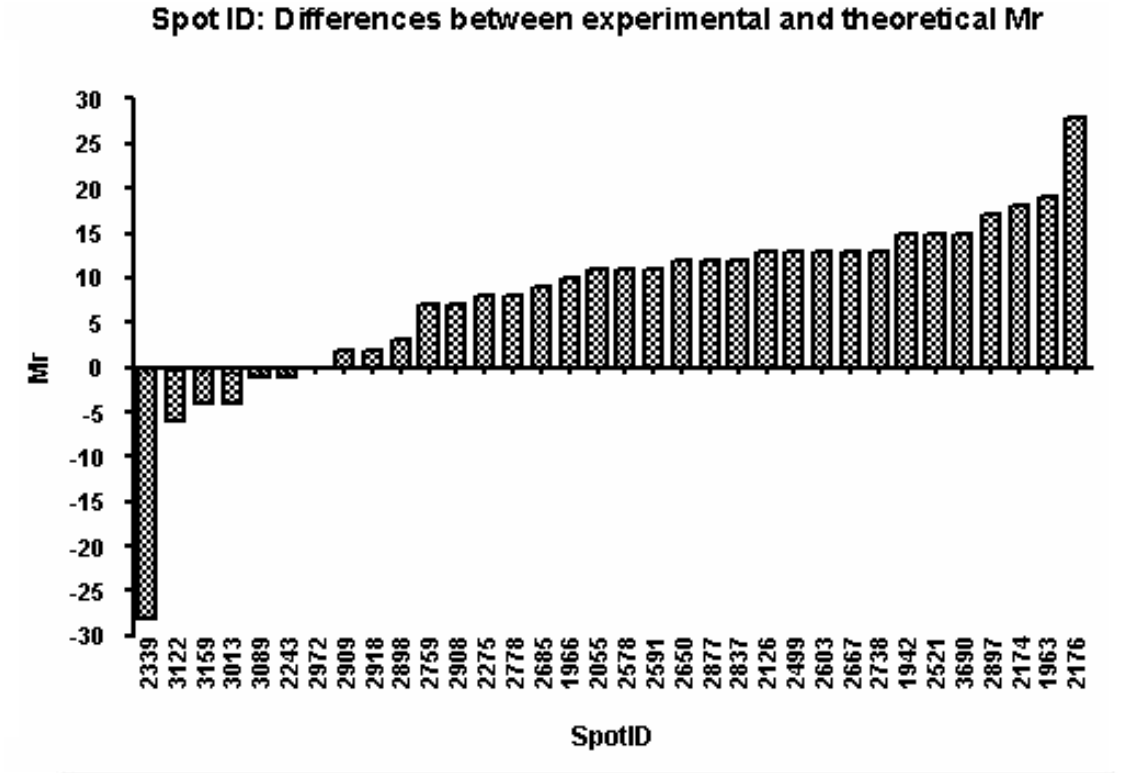

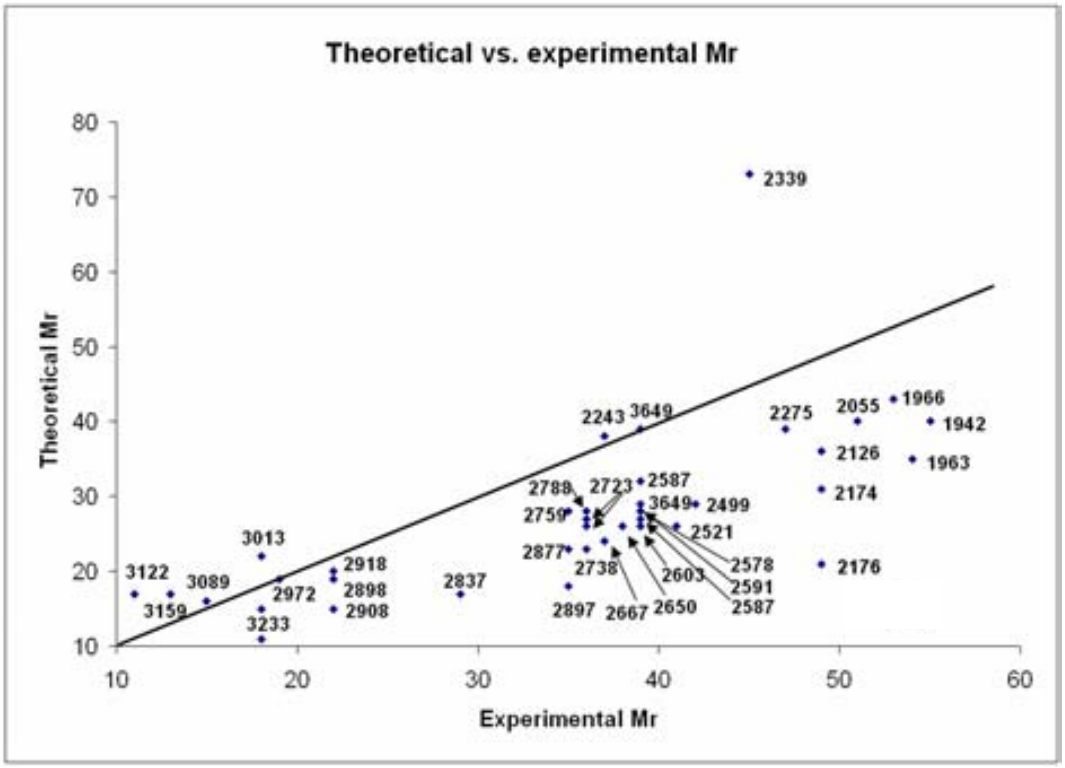

Annex III.1.- Effect of GnRHa (50 µg kg-1) with or without OA on GSI, milt production and sperm motility in the Senegal sole.

Hormone treament	Control				
No. fish	4	20	22	Mean	MSD
Animal Weight (gr)	833,0	714,0	1004,0	850,3	84,2
Both gonads weight (gr)	0,75	0,47	0,71	0,64	0,09
GSI	0,09	0,07	0,07	0,08	0,01
Sperma Volume (µl)	5,0	2,0	6,0	4,3	1,2
Spz/ml sperma ·10e9	2,5	3,3	2,9	2,9	0,2
Spz/gr testis ·10e6	32,9	20,2	54,5	35,9	10,0
Movility (s)	211,0	155,0	193,0	186,3	16,5

Hormone treament	GnRHa				
No. fish	8	24	25	Mean	MSD
Animal Weight (gr)	866,2	723,0	771,2	786,8	42,1
Both gonads weight (gr)	0,59	0,43	0,40	0,47	0,06
GSI	0,07	0,06	0,05	0,06	0,00
Sperma Volume (µl)	12,0	13,0	9,0	11,3	1,2
Spz/ml sperma ·10e9	1,4	2,1	1,6	1,7	0,2
Spz/gr testis ·10e6	45,8	98,8	71,7	72,1	15,3
Movility (s)	244,0	217,0	179,0	213,3	18,9

Hormone treament	GnRHa+OA				
No. fish	18	33	34	Mean	MSD
Animal Weight (gr)	917,6	959,8	800,2	892,5	47,7
Both gonads weight (gr)	0,30	0,60	0,46	0,45	0,08
GSI	0,03	0,06	0,06	0,05	0,01
Sperma Volume (µl)	1,0	2,0	3,0	2,0	0,6
Spz/ml sperma ·10e9		1,4	6,8	4,1	2,7
Spz/gr testis ·10e6		7,5	62,9	35,2	27,7
Movility (s)	600,0	605,0	392,0	532,3	70,2

Annex III.2.-

The NCBI protein identification and sequence, sequenced peptides and their situation in the homologous protein (red letters) from the identified spots in the hormone treatment study in chapter 3.

Spots 240, 250, 253, 261 263, 265, 267 gi|47224921 alpha-2-macroglobulin-1 [Tetraodon nigroviridis]

MALPGSRARMWALFLCLNWIFTDGAAAGPQFMVAIPAVMEAGAESRLCISLLQPNETLAVTAKLVFEDKATVIFER
SSDKEFHQCAVFQAPEVETPEVHALLVTVRGDQFHSVESRKVMFKSYKPETFVQTDKPIYLPGQTVHFRVVTLDS
MFRPANGLFHTIKILDSHQNRIGQWLNATTDGDILQLSFPLSAEAREGYYSISVWMEQSQVTRRFKVEKYVLPKFE
VTIEMADQVSVGQEEIDVDVCAKYTYGQPVPATVTVEMCRKLRSSSDTLIQVPCFEEEKKTSAAAPNSPPACTLFS
KQKRVELSFIIGKLFFVDTPNSYNEGSMLEGKIKVVHYNDTPIADKQIQLLNDKSWQGHVLQNLTTDADGIATFSLNT
TLFNGEEIQLRALVPEPEPYAQKPKFESAHHRASLYQPPSPHSKSVSSLTVSNTETPLLCEGDETLSIDYAFVGETA
GTVNLMYLIVSRGKIVTQGVQTVQILTDPTTEGSISFTLKMSPEFSPALQVVAYTILPSEHVIAHKADLAVTKCFLNKV
SVEFSPTSAVPGDDTTLKVKALPDSLCGVSAIDQSVLVKEPGNTLTPEQIFNMLPVRKVSSIPYEVEDAVPCLRVRQ
KRYIGRRRRPDDVNDAYSVFEGIGLKVATNLLFRMPSCVNFRGLEFHRGFVLYRESVPYIMAMKQKGTGAAPGGG
VIETIRTFFPETWVWKLVKVGESGETDVALTVPDTITTWETEAFCVSPQGFGLAPRKEITVFQPFFLELSLPYSIVRG
EQFELKATVFNYQTSCMMVSVKTAKSEDYTLTPLSANEYTSCLCGNERKTLSWTMLPSVIGVVSVTVTAEAVASHA
SCDNEIVSVPERGRTDTVTRSLIVKAEGTEMTKIHNWLLCPKEEPLKEEVELDLPANVIDGSARALVSVLGDILGRAL
KNLDGLLRMPYGCGEQNMALLAPNIYILQYLKSTGQLTDTILKKATHFLTSGYQRQLNYKHSNGAFSTFGTGSGNT
WLTAFVVRSFAKAKTFVYIDEAKMLGLQKLAAAEAEPRRLFPAVWKTLQQQDEGRRFRRSDAQRLHHGRLPGDG
HVAHRPGDPQEHAVPQRLRQQPEQHLHHGSAGLRLLPGWRHEDAGFPPAAPGHGGLRASLLYWSQSAEDQSS
SLSVEISSYVLLAKLSSSPTAEDLGYASRIVRWLTGQQNYYGGFSSTQDTVVALQALALYSTLVFSPAGSSTVTVQA
PSGQLVFDVNQDNKLLYQEKTLQDLKGTISLEAAGSMCASIQISLHYNIPTPTDTNIFSISVKPECSSEKNRVTLQLM
SQYSGKDITTNMVILDVKMLSGFVPDPESVNSAVRCSWIGLKRRRREFSSTSESC

Sequenced Peptides LLQLSYSLNSEAR MQHSLCGLSALDKWEPK
MRAPTAEDLGYWGLVR

Spot 261 gi|47224921 alpha-2-macroglobulin-1 [Tetraodon nigroviridis]

MAPPGSQMWTWSLCVLLSWTLFDHVAADPQYMLAVPAILEAGEESKFCISFLEPNETMTVTVSLKSKDFN
TTLMQMVSKQDFHECRSFEAPSVEKDHVMELEVEVQADTFYSKGARKVLIRQFNPESFIQTDKPLYLPGQ
TVQFRVVSLDSKLRPSALKYSVIELKDPSGNRIGQWLNQTTENAILQLSHQLNSEAPEGSYEIRTEADGK
QAL……SWETVLLLTGEMPE

Sequenced Peptides LLQLSYSLNSEAR

Spot 267 >gi|55667245| Alpha-2-macroglobulin precursor (Alpha-2-M) [Pan troglodytes]

MWAQLLLGMLALSPAIAEELPNYLVTLPARLNFPSVQKVCLDLSPGYSDVKFTVTLETKDKTQKLLEYSGLKKRHLH
CISFLVPPPAGGTEEVATIRVSGVGNNISFEEKKKVLIQRQGSGTFVQTDKPLYTPGQQVYFRIVTMDSNFVPVNDK
YSLVELQDPNSNRIAQWLEVVPEQGIVDLSFQLAPEAMLGTYTVAVAEGKTFGTFSVEEYVLPKFKVEVVEPKELS
TVQESFLVKICCRYTYGKPMLGAVQVSMCQKANTYWYREVELEQLPDKCRNLSGQTDKTGCFSAPVDMATFDLI
GYAYSHQINIVATVVEEGTGVEANATQNIYISPQMGSMTFEDTSNFYHPNFPFSGKIRVRGHDDSFLKNHLVFLVIY
GTNGTFNQTLVTDNNGLAPFTLETSGWNGTDISLEGKFQMEDLVYNPEQVPRYYQNAYLHLRPFYSTTRSFLGIH
RLNGPLKCGQPQEVLVDYYIDPADASPDQEISFSYYVRPGNGDGNSGKEAVHVTVPDAITEWKAMSFCTSQSRGF
GLSPTVGLTAFKPFFVDLTLPYSVVRGESFRLTATIFNYLKDCIRVQTDLAKSHEYQLESWADSQTSSCLCADEAKT
HHWNITAVRLGHINFTISTKILDSNEPCGGQKGFVPQKGQSDTLIKPVLVKPEGVLVEKTHSSLLCPKGKVASESVS
LELPVDVVPDSTKAYVTVLGDIMGTALQNLDGLVQMPSGCGEQNMVLFAPIIYVLQYLEKAGLLTEEIRSRAVGFLEI
GYQKELMYKHSNGSYSAFGERDGNGNTWLTAFVTKCFGQAQKFIFIDPKNIQDALKWMAGNQLPSGCYANVGNL
LHTAMKGVDDEVSLTAYVTAALLEMGKDVDDPMVSQGLRCLKNSATSTTNLYTQALLAYIFSLAGEMDIRNILLKQL
DQQAIISGESIHWSQKPTPSSNASPWSEPAAVDVELTAYALLAQLTKPSLTQKEIAKATSTVAWLAKQRNAYGGFS
STQDTVVALQALAKYATTAYMPSEEINLVVKSTENFQRTFNIQSVNRLVFQQDTLPNVP
GMYTLEASGQGCVYVQLLQQPLVKKVEFGTDTLNIYLDELIKNTQTYTFTISQSVLVTNLKPATIKVYDYYLPDEQAT
IQYSDPCE

Sequenced Peptides AQSFLFLDPK

>gi|47224921 alpha-2-macroglobulin-1 [Tetraodon nigroviridis]

MALPGSRARMWALFLCLNWIFTDGAAAGPQFMVAIPAVMEAGAESRLCISLLQPNETLAVTAKLVFEDKATVIFER
SSDKEFHQCAVFQAPEVETPEVHALLVTVRGDQFHSVESRKVMFKSYKPETFVQTDKPIYLPGQTVHFRVVTLDS
MFRPANGLFHTIKILDSHQNRIGQWLNATTDGDILQLSFPLSAEAREGYYSISVWMEQSQVTRRFKVEKYVLPKFE
VTIEMADQVSVGQEEIDVDVCAKYTYGQPVPATVTVEMCRKLRSSSDTLIQVPCFEEEKKTSAAAPNSPPACTLFS
KQKRVELSFIIGKLFFVDTPNSYNEGSMLEGKIKVVHYNDTPIADKQIQLLNDKSWQGHVLQNLTTDADGIATFSLNT
TLFNGEEIQLRALVPEPEPYAQKPKFESAHHRASLYQPPSPHSKSVSSLTVSNTETPLLCEGDETLSIDYAFVGETA
GTVNLMYLIVSRGKIVTQGVQTVQILTDPTTEGSISFTLKMSPEFSPALQVVAYTILPSEHVIAHKADLAVTKCFLNKV
SVEFSPTSAVPGDDTTLKVKALPDSLCGVSAIDQSVLVKEPGNTLTPEQIFNMLPVRKVSSIPYEVEDAVPCLRVRQ
KRYIGRRRRPDDVNDAYSVFEGIGLKVATNLLFRMPSCVNFRGLEFHRGFVLYRESVPYIMAMKQKGTGAAPGGG
VIETIRTFFPETWVWKLVKVGESGETDVALTVPDTITTWETEAFCVSPQGFGLAPRKEITVFQPFFLELSLPYSIVRG
EQFELKATVFNYQTSCMMVSVKTAKSEDYTLTPLSANEYTSCLCGNERKTLSWTMLPSVIGVVSVTVTAEAVASHA
SCDNEIVSVPERGRTDTVTRSLIVKAEGTEMTKIHNWLLCPKEEPLKEEVELDLPANVIDGSARALVSVLGDILGRAL
KNLDGLLRMPYGCGEQNMALLAPNIYILQYLKSTGQLTDTILKKATHFLTSGYQRQLNYKHSGAFSTFGTGSGNTW
LTAFVVRSFAKAKTFVYIDEAKMLGLQKLAAAEAEPRRLFPAVWKTLQQQDEGRRFRRSDAQRLHHGRLPGDGH
VAHRPGDPQEHAVPQRLRQQPEQHLHHGSAGLRLLPGWRHEDAGFPPAAPGHGGLRASLLYWSQSAEDQSSS
LSVEISSYVLLAKLSSSPTAEDLGYASRIVRWLTGQQNYYGGFSSTQDTVVALQALALYSTLVFSPAGSSTVTVQAP
SGQLVFDVNQDNKLLYQEKTLQDLKGTISLEAAGSMCASIQISLHYNIPTPTDTNIFSISVKPECSSEKNRVTLQLMS
QYSGKDITTNMVILDVKMLSGFVPDPESVNSAVRCSWIGLKRRRREFSSTSESC

Sequenced Peptides MPSCLSFR MRAPTAEDLGYWGLVR RFFLTSPPQR

Spot 277

gi|47224921|emb|CAG06491.1| unnamed protein product [Tetraodon nigroviridis] alpha-2-macroglobulin-1

MALPG……..EQNMALLAPNIYILQYLKSTGQLTDTILKKATHFLTSGYQRQLNYKHSNGAFSTFGTGSGNTWL
TAFVVRSFAKAKTFVYIDEAKMLGLQKLAAAEAEPRRLFPAVWKTLQQQDEGRRFRRSDAQRLHHGRLPGDGHV
AHRPGDPQEHAVPQRLRQQPEQHLHHGSAGLRLLPGWRHEDAGFPPAAPGHGGLRASLLYWSQSAEDQSSSL
SVEISSYVLLAKLSSSPTAEDLGYASRIVRWLTGQQNYYGGFSSTQDTVVALQALALYSTLVFSPAGSSTVTVQAP
SGQLVFDVNQDNKLLYQEKTLQDLKGTISLEAAGSMCASIQISLHYNIPTPTDTNIFSISVKPECSSEKNRVTLQLMS
QYSGKDITTNMVILDVKMLSGFVPDPESVNSAVRCSWIGLKRRRREFSSTSESC

Sequenced Peptides MRAPTAEDLGYWGLVR MGNFLTSPPQR

Spot 284

>gi|47224921|emb|CAG06491.1| unnamed protein product [Tetraodon nigroviridis] alpha-2-macroglobulin-1

MALPGS……PGHGGLRASLLYWSQSAEDQSSSLSVEISSYVLLAKLSSSPTAEDLGYASRIVRWLTGQN
YYGGFSSTQDTVVALQALALYSTLVFSPAGSSTVTVQAPSGQLVFDVNQDNKLLYQEKTLQDLKGTISLEAAGSMC
ASIQISLHYNIPTPTDTNIFSISVKPECSSEKNRVTLQLMSQYSGKDITTNMVILDVKMLSGFVPDPESVNSAVRCSWI
GLKRRRREFSSTSESC

Sequenced Peptides MRAPTAEDLGYWGLVR

Spot 298 >gi|31323728|gb|AAP47138.1| chaperone protein GP96 [Danio rerio]

MRRLWIIGLLCALLAFASVKADDDVDIDGTVEEDLGKSRDGSRTDDEVVQREEEAIQLDGLNTSQLKEIRDKAEKHA
FQAEVNRMMKLIINSLYKNKEIFLRELISNASDALDKIRLLSLTNEDALAGNEELTIKIKSDKEKNMLHITDTGIGMTKE
ELVKNLGTIAKSGTSEFLNKMTEVQDDSQSTSELIGQFGVGFYSAFLVADKVIVTSKHNNDTQHMWESDSNQFSVI
EDPRGDTLGRGTTITLVMKEEASDYLELETIKNLVKKYSQFINFPIYVWSSKTETVEEPIEDEAEAEKEEATEDEAEV
EEEEEDKDKPKTKKVEKTVWDWELMNDIKPIWQRPAKEVEEDEYTAFYKTFSRDTDEPLSHIHFTAEGEVTFKSILF
VPASAPRGLFDEYGTKKNDFIKLFVRRVFITDDFHDMMPKYLNFIKGVVDSDDLPLNVSRETLQQHKLLKVIRKKLV
RKTLDMIKKIAEEQYNDKFWKEFGTNIKLGVIEDHSNRTRLAKLLRFQTSHSDTVLSSLEQYVERMKEKQDKIYFMA
GTSRKEAESSPFVEKLLKKGYEVVYLTEPVDEYCIQALPEFDGKRFQNVAKEGVKFDESDKAKEKREALEKEFEPL
TTWMKDKALKEQIEKAVLSQRLTNSPCALVASQYGWSGNMERIMKAQAYQTGKDISTNYYASQKKTLEINPKHPLI
KEMLRRVNEDAEDKTAADLAVVLFETATLRSGYQLQDTKAYGERIERMLRLSMNVDLDAQVEEEPEEEPEEQTEE
AEDEEEVQADEAEEESEATSKDEL

Sequenced Peptides YEHP(CamC)ALVASQYGWSGNPYR RVDSDLDPLNVSR

Spots 424 , 431, 438, 531 >gi|74096001|ref|NP_001027856.1| Hemopexin [Takifugu rubripes]

MKLLTQVLCLALAVTWAHCNSHASAVLDRCLGLEMDAVAVNEVGIPYFFKGDHLFKGFHGKAELSNESFAELDDH
HHLGHVDAAFRMHFENSTDHDHLFFFLDHSVFSYYQHKLEQGYPKKISEVFPGIPDHLDAAVECPHPECEEDSVIF
FKGDEIYHYNVRTQAVDEKEFKDMPNCTSAFRFMEHFYCFHGHMFSKFDPKTGEVLGKYPKEARDYFMRCAKFS
EESDPVERERCSRVHLDAVTSDNAGNKYAFRGHHFLFKEEANDTLKADTIENAFKELHSDVDAVFSYQDHLYMIKN
DKIHIYKTGTAHTHLEGYPKPLKEELGIEGPIDAAFVCGDHHIAHLIKGQKMYDVDLKSSQRVADNERPISLFQKIDA
AICDGEGLKVIVGNHYYHFDSPMLFIAGRALPEQRRVSLELFGCDH

Sequenced Peptides VLVGNHYYTFESLK VSGADLFGCDH

Spot 531 >gi|74096001|ref|NP_001027856.1| Hemopexin [Takifugu rubripes]

MDLFSKTLLLCLLLILTDAAPAPQDAAEKDNISEVKEEDSGPALPDRCAGIEFDAITPDEKGKTLFFKGAYMWKDFH
GPAQLVSESFKEIDDIPNAGSISAAFRMHNKANPDDHDRIYLFLEDKVFSYYEQVLEEGYPKHINEEFPGVPTHLDA
AVECPKGECMADSVLFFKGQDVHMYDLSTKTVKTKTWSHLPACTSAFRWLEHYYCFHGHNFTRFNPISGEVNGT
YPKDARHYFMRCPNFGHGGGYNIPKCSEVKIDAITVDEAGRMYAFAGPIYMRLDTRRDGFHAFPITRQWKEVVGK
VDAVFSYGDKMYLIKGKQVYIYKGGAHYTLVEGYPKTLEEELGVEGPVDAAFVCPGQHTVHIIQGERFLDVSLTATP
RVVARNLPFVLSDIDAAYCDAKGVKLFSGSKYYQYASVTILALSKIAALAEPITSEMLGCQD

Sequenced Peptides W(CamC)TADSVLFFK HGPAKLRADSFK

Spot 540 >gi|59710087|ref|NP_001011879.1| keratin [Takifugu rubripes]

MSVRAVKTTTLSSVSTSRGPSQGFSSRSFSGYGGYGVGGGRQSFAVRSSYGGLGSSGAAVGAGGFKVVGGYV
GGAGNRVGGLECGYIGFGGGVAGGMGNDVVAPITAVTVNKSLLAPLNLEIDPTIQAIRTQEKEQIKTLNNRFASFIK
VRFLEQQNKMLETKWKLLQEQTTSRSNIDMMFEAYIANLRKHLDNLGHEKVKLESDLHHMDLVEDYKTRYEDEINK
RTDCENNFVLIKKDADAAYMNKVDLETQVTALSDELDFLRQIYDVEIQELQGQIKDTCVVVEMDNSRDLDMDSIVAE
VRAQYEDVANRSRAEAETWYQTKYAEMQQSAGRYGDDLKLSKAEISDMNRRIMRLQSEIDMVKSQKNHLEAQIA
ESEERGELAVTDAKHRIRELEEALQRAKQDMTMQVRQYQELMNVKLALDIEIATYRKLLEGEEDRLATGIKTTVSKQ
TSMNFSAYGLESSRTPSYVSSSFGAVKISGGPVSAQEATAMEHINKTETKVIKAEGAQKEEQVAQEVSAAVEEQTS
EEKQEQKQEQQVVEAEAVVEE

Sequenced Peptides TQSMNYSAYGLES(CamC)R VKDMVTVVAEVR

Spot 541 >gi|59710087|ref|NP_001011879.1| keratin [Takifugu rubripes]

MSVRAVKTTTLSSVSTSRGPSQGFSSRSFSGYGGYGVGGGRQSFAVRSSYGGLGSSGAAVGAGGFKVVGGYVA
GGAGNRVGGLECGYIGFGGGVAGGMGNDVVAPITAVTVNKSLLAPLNLEIDPTIQAIRTQEKEQIKTLNNRFASFID
KVRFLEQQNKMLETKWKLLQEQTTSRSNIDMMFEAYIANLRKHLDNLGHEKVKLESDLHHMTDLVEDYKTRYEDEI
NKRTDCENNFVLIKKDADAAYMNKVDLETQVTALSDELDFLRQIYDVEIQELQGQIKDTCVVVEMDNSRDLDMDSIV
AEVRAQYEDVANRSRAEAETWYQTKYAEMQQSAGRYGDDLKLSKAEISDMNRRIMRLQSEIDMVKSQKNLEAQIA
ESEERGELAVTDAKHRIRELEEALQRAKQDMTMQVRQYQELMNVKLALDIEIATYRKLLEGEEDRLATGIKTTVSKQ
TSMNFSAYGLESSRTPSYVSSSFGAVKISGGPVSAQEATAMEHINKTETKVIKAEGAQKEEQVAQEVSAAVEEQTS
EEKQEQKQEQQVVEAEAVVEE

Sequenced Peptides QTSMNYSAYGLES(CamC)R

Spot 581 >gi|39645432|gb|AAH63955.1| Keratin [Danio rerio]

MSGGMGGGMGGGIRKNFSSMSTSAVPMGSRSSVSFRRSGGGGGGGGFGAGSGGSFSYSMGGGGGGGGSGF
GGGFGSGGGFGSGGGFGGGAGFGGGSAYGGGAGFGGGFGPGGVVPITAVTVNQNLLAPLNLEIDPNIQVVRTQ
EKEQIKTLNNRFASFIDKVRFLEQQNKVLETKWSLLQEQTTTRSNIDAMFEAYIANLRRQLDGLGNEKMKLEGELKN
MQNLVEDFKNKYEDEINKRAAVENEFVLLKKDVDAAYMNKVELEAKVDSLQDEINFLRAIFEEELRELQSQIKDTSV
VVEMDNSRNLDMDAIVAEVRAQYEDIANRSRAEAESWYKQKFEEMQSSAGKYGDDLRNTKAEIADLNRMISRLQN
EIEAVKGQRANLEAQIAEAEERGELAVKDAKLRIKDLEDALQRAKQDMARQVREYQELMNVKLALDIEIATYRKLLE
GEESRIASGGNTATIHIQESSSSSGGGGGGFGYGGGSGYGGGSGFGGGSGYGGGSGFGGGSGFGYGGGSGM
SIGGGSGMSMSGGGGGQISMSRSSIVSSQKRRF

Sequenced Peptides DMDALVAEVR DTWVVEMDNSR LLALDLELATYR

>gi|59710087|ref|NP_001011879.1| keratin [Takifugu rubripes]

MSVRAVKTTTLSSVSTSRGPSQGFSSRSFSGYGGYGVGGGRQSFAVRSSYGGLGSSGAAVGAGGFKVVGGYVA
GGAGNRVGGLECGYIGFGGGVAGGMGNDVVAPITAVTVNKSLLAPLNLEIDPTIQAIRTQEKEQIKTLNNRFASFID
KVRFLEQQNKMLETKWKLLQEQTTSRSNIDMMFEAYIANLRKHLDNLGHEKVKLESDLHH
MTDLVEDYKTRYEDEINKRTDCENNFVLIKKDADAAYMNKVDLETQVTALSDELDFLRQIYDVEIQELQG
QIKDTCVVVEMDNSRDLDMDSIVAEVRAQYEDVANRSRAEAETWYQTKYAEMQQSAGRYGDDLKLSKAEISDMN
RRIMRLQSEIDMVKSQKNHLEAQIAESEERGELAVTDAKHRIRELEEALQRAKQDMTMQVRQYQELMNVKLALDIE
IATYRKLLEGEEDRLATGIKTTVSKQTSMNFSAYGLESSRTPSYVSSSFGAVKISGGPVS
AQEATAMEHINKTETKVIKAEGAQKEEQVAQEVSAAVEEQTSEEKQEQKQEQQVVEAEAVVEE

Sequenced Peptides MPGLSDELDFLR YGGLGSSGAAV QTSMNYSAYGLES(CamC)R

Spot 801 >gi|37362196|gb|AAQ91226.1| cytosolic nonspecific dipeptidase [Danio rerio]

MSYLPNLFKYVDEHQNEYVERLAQWVAVQSVSAWPEKRGEIKKIMEMAGKDIERLGGTVELVDIGMQKLP
SGEEIPLPPIVLGRLGSDPGKKTVCIYGHLDVQPASIEDGWDSQPFILEERDGKMYGRGSTDDKGPVLAW
FNIIEAYQKIGQELPINIKFCFEGMEESGSEGLDDLVFSRKDTFFKDVDYVCISDNYWLGKTKPCITYGL
RGICYFFIEMECCDKDLHSGVFGGSVHEAMTDLIALMGTLVDNKGKIKVPGIYDQVAKLTDEEKKLYEKI
EFDLEEYAKDVGAGKLMHDTKEQILMHRWRYPSLSLHGIEGAFSEAGAKTVIPRKVIGKFSIRLVPDMDP
KVVEKQVISHLEKTFAELKSSNQPEVATGPWTKAGWSDFNHPHYMAGRKGHETVFGVEPDLTREGGSIPVTLTFQ
EATGQNVMLLPVGSSDDGAHSQNEKLNRSNYIQGTKMLGAYFYEVSQLS

Sequenced Peptides VVEEQVLSHLEK WDH(CamC)EVQSVSAWPERK NLTVEMVDLGK
EWQPVTLTFG(CamC)RLR

Spot 851b , 851a

>gi|47218629|emb|CAG04958.1| ATP synthase β-subunit [Tetraodon nigroviridis]

MLGAVGRCCTGALQALKPGVQPLKALVGSPAVLARRDYVAPAAAAATANGRIVAVIGAVVDVQFDEGLPP
ILNALEVAGRDSRLVLEVAQHLGENTVRTIAMDGTEGLVRGQKVLDTGAPIRIPVGPETLGRIMNVIGEPIDERGPIT
TKQTAPIHAEAPEFTDMSVEQEILVTGIKVVDLLAPYAKGGKIGLFGGAGVGKTVLIMELINNVAKAHGGYSVFAGV
GERTREGNDLYHEMIESGVINLKDTTSKVALVYGQMNEPPGARARVALTGLTVAEYFRDQEGQDVLLFIDNIFRFT
QAGSEVSALLGRIPSAVGYQPTLATDMGTMQERITTTKKGSITSVQAIYVPADDLTDPAPATTFAHLDATTVLSRAIA
ELGIYPAVDPLDSTSRIMDPNIVGAEHYDVARGVQKILQDYKSLQDIIAILGMDELSEEDKLTVARARKIQRFLSQPF
QVAEVFTGHLGKLVPLKETIKGFQSILAGEYDALPEQAFYMVGPIEEVVQKAKKLVEEQS

Sequenced Peptides LTAMDGTEGLVR TGLTVAEYFR FTQAGSEVSALLGR
FAAHMELLNNVAK LVLEVAQHLWRWK MLDPNLVGAEHYDLAR
LMNVLGEPLDER

Spot 1017 >gi|61403546| 3-hydroxyisobutyryl-Coenzyme A hydrolase [Danio rerio]

MSLIIFTSAQRLRSVCRLQRIHGHMMSSKAGSEVLFEKVGKAGVITLNRPKALNALTLNMIRHIYPQLKKWDKDSET
DIVIIKGAGEKAFCAGGDIRAIAEAGKAGNLLSQVFFREEYILNNTIGTYQKPYVALINGITMGGGVGLSVHGQFRVA
TEKTLFAMPETGIGLFPDVGGGYFLPRLQGKLGLFLALTGFRLKGRDVQRVGVATHFVQSEKIESLEKDLVDLKSP
SISDVAQLLDSYQEQSHLDAEKPFVLQEQTEAIDRLFSAGSVEEIVENLKKDGSAFALKQAETLAKMSPTSLKLTFR
QIEEGARMSLQEVFMMEYRLSQACMNGHDFYEGVRAVLIDKDQSPKWKPSTLAGVSEQFVDKCFSSLDERDLKL

Sequenced Peptides LGLFLALTGFR EEYLLNNALGSYR

>gi|89268269| 3-hydroxyisobutyryl-Coenzyme A hydrolase [Xenopus tropicalis]

MSLGLLESQLRLKVFGRLQVIRQHLRMTNHTVKDGECLLTKAGCAGVITLNRPKALNALNLGMIRLIYPQLGLWEED
PETYLVIIKGVGGKAFCAGGDIRAVTDAGKAGDRLAQDFFREEYILNNAIGTYKKPYVALIDGITMGGGVGLSVHGH
FRVASENTLFAMPETAIGLFPDVGGGYFLPRLPGKLGLYLALTGFRLKGSDVQKAGIATHFVESEKIPSLEQDLVAM
KCPSKENVADVLDSYHNKSYAAQDKPFVLAEHLDKINSLFSASSVEAIIENLRCDGSSFALKQLQTLSTMSPTSLKIT
FRQLKEGSSMSLQEVLTMEYRLSQACMKGYDFYEGVRAVLIDKNQNAKWNPELLEEVTDDYIDSYFTSLGNSDLK
L

Sequenced Peptides RDSLAQDFFR

Spot 1030, 1031 >gi|47212109|emb|CAF96691.1| keratin 18 [Tetraodon nigroviridis]

MSFRKTTMVSIPSTRISLTRSTPQYGSSASIYGGAGGQGARTSSVSASLLRSNTPMVASSSSFKLSSALGGGAGG
SKVTGAGIIGDERGAMQNLNDRLANYIETVRNLELANKELEQKIMLAMEKGGPQTRDYSKYESIIEDLRRKIFDSITD
NARLVLQIDNARLAADDFKVKFDNEMAIRQSVEAEMAGLKKVIDDTNMNRMNIEGEIEAVREELAYLKKNHENDVM
ELRHQISRSGVQVDVDAPKGQDLAQIMEDMRANYEKIGAKNAEDLKRWHENQIADVQVQVSQNTEALQGAQMEI
GDLSRQLQTLEIELASQQSLKASLEDTLRNTELRSNMEMEKYNAITMRLEEELTKLRANIQNQTQDYEVLLNMKMK
LEAEISTYKVLLDGGDFKLQDALDELAGTA

Sequenced Peptides (1030) NHENEVMELR VQVSLEAPK KGDLAQLMEDMR
Y(CamC)FLELELASQQSLK

Sequenced Peptides (1031) KGDLAQLMEDMR Y(CamC)FLELELASQQSLK

Spot 1032 >gi|54035446| 26S protease regulatory subunit S10B [Danio rerio]

MAENREKGLQDYRKKLLEHKEIDGRLKELREQLKELTKQYEKSENDLKALQSVGQIVGEVLKQLTEEKFI
VKATNGPRYVVGCRRQLDKSKLKPGTRVALDMTTLTIMRYLPREVDPLVYNMSHEDPGSVSYSEIGGLSE
QIRELREVIELPLTNPELFQRVGIIPPKGCLLYGPPGTGKTLLARAVASQLDCNFLKVVSSSIVDKYIGE
SARLIREMFNYARDHQPCIIFMDEIDAIGGRRFSEGTSADREIQRTLMELLNQMDGFDTLHRVKMIMATN
RPDTLDPALLRPGRLDRKIHIELPNEQARLDILKIHSGPITKHGDIDYEAIVKLSDGFNGADLRNVCTEA
GMFAIRADHEYVTQEDFMKAVRKVADSKKLESKLDYKPV

Sequenced Peptides EVLELPLTNPELFKR NV(CamC)TEAGLFALR LGASKLD(CamC)NFLK

Spot 1102 >gi|56718619|gb|AAW28030.1| Glyceraldehyde 3-phosphate dehydrogenase [Danio rerio]

MSELCVGINGFGRIGRLVLRACLQKGIKVTAINDPFIDLQYMVYMFKYDSTHGRYKGEVHMEDGKLIVDGQAISVFQ
CMKPAEIPWGDAGALYVVESTGVFLSIEKASAHIQGGAKRVVVSAPSPDAPMFVMGVNQDKYDPSSMTIVSNASC
TTNCLAPLAKVIHDNFGIEEALMTTVHAYTATQKTVDGPSAKAWRDGRGAHQNIIPASTGAAKAVGKVIPELNGKLT
GMAFRVPVADVSVVDLTCRLTRPASYANIKESVKKAAHGPMKGILGYTEDSVVSSDFVGDTHSSIFDAGAGISLND
NFVKLISWYDNEFGYSHRVADLLMYMHSKE

Sequenced Peptides VPVADVWVDLT(CamC)R YYEPSPDAPMFVMRA(CamC)VK

Spot 1106 >gi|37682099|gb|AAQ97976.1| keratin 8 [Danio rerio]

MSTYSKKTSYTVKSSSSGSIPRNFSSLSYSGPSMSRQSYSARSSYGGVNRGMGAGMGGGSGFISSSSAYGLGG
MGTGMGAGVVAPIQAVTVNKSLLAPLNLEIDPNIQIVRTQEKEQIKTLNNRFASFIDKVRFLEQQNKMLETKWSLLQ
NQTATRSNIDAMFEAYIANLRRQLDSLGNDKMKLEADLHNMQGLVEDFKNKYEDEINKRTECENEFVLIKKDVDEA
YMNKVELEAKLESLTDEINFLRQIFEEEIRELQSQIKDTSVVVEMDNSRNLDMDAIVAEVRAQYEDIANRSRAEAEM
WYKSKYEEMQTSANKYGDDLRSTKTEIADLNRMIQRLQSEIDAVKGQRANLENQIAEAEERGEMAVRDAKGRIKD
LEDALQRAKQDMARQIREYQDLMNVKLALDIEIATYRKLLEGEEDRLATGIKAINISKQSTSYGGYPMESAGSSYST
YSSGYSSGLSGGYGGGYSGGYSGGYSSGSGYSDTVSQTKKSVVIKMIETKDGRVVSESSEVVQD

Sequenced Peptides QNSLTDELNFLR

Spot 1119 >gi|28557116|dbj|BAC57564.1| tropomyoshin1-1 [Takifugu rubripes]

MDAIKKKMQMLKLDKENALDRAEQAETDKKAAEDRSKQLEDELRELEKKLRVTEDERDRVTEEFQTAEEKLLTAE
EVATKAEAEVASLNRRIQLVEEELDRAQERLGTALTKLEEAEKAADESERGMKVIENRAMKDEEKMELQEIQLKEA
KHIAEEADRKYEEVARKLVIIEGDLERTEERAELAESKCAELEEELKTVTNNLKSLEAQAEKYSQKEDKYEEEIKVLT
DKLKEAETRAEFAERTVAKLEKTIDDLEDELYSQKLKYKAISEELDHALNDMTSI

Sequenced Peptides LDQENALDR QDVFEEFKTAEEK EP(CamC)VASLNR
VEEFQTAEEK LQLVEEELDR MELQELKLK LLEGDLER

Spot 1123 >gi|15028982| type I keratin S8 [Oncorhynchus mykiss]

MSYYSYKSSSGGGPMNFSGGSNIMSSRVGYVSSAPKAFSVYGGGSGGGTRISSSSVRSVSSGYGGGAGFGGGY
GSGGGGYGSGGGGYGSGGGGGFNLSSALDGGAIHLNEKATMQNLNDRLSTYLDKVRSLEEANSKLEIQIREYKK
GPAAERDYSKYWAIINDLKDKINGATCNNANILLQIDNSKLAADDFQTKFEHELMMRQSVEADIANLRRLLDQTTLT
KADLEMQIEGLQDELAYLKKNHIEELAAMRAQLTGTVNVEVDAAPQQDMSRTMEEIRTQYEGIIDKHRRDQEAWF
NDKSANLSKEVATSTEIIQTTKTEINDLRRTMQGLEIELQSQLSMKAALENTLRETDGRYSAMLSGYQNQIDMLEQE
LNRVRQSIETQGHDYKMLLDIKSRLEQEIATYRGLLEGEESRTVGSGGSKTTVTTSTVRSSS

Sequenced Peptides QSVEADLANLR WWNTLNVEVDASPKQRWK

Spot 1134 >gi|47216949|emb|CAG04891.1| annexin A3t [Tetraodon nigroviridis] annexin A3

MSVWDDLDLLLDSPSSITVNSNTKGTVKDKKDFKVEEDVSALRKAIEGLGTTETTLIEVLTQRSNNQRQLIAKAYEK
ATGRTLVADLEGDTHGDFEDLLVALVTPPDVFDCQEVIRAIKGAGTTESTLTEIFASRSNRQIKGLSEAYLAETGRSV
IHDLQSEVSGDYGKALLILAEGKRDESTSADAAKAKAEAKELYNAGEKKWGTDEAKFIDILCHRSVPQLRQTLVEYK
SMSKKTLQESIESEMSGNLQKLLVAVVKCVKNVPAYFAEKLFKAMKGAGTTESILTRILVSRSEIDLSDIKAEYKKLF
GSSLYSQLESEVSGSYGDALKSLCGQED

Sequenced Peptides K[158.0]TECTLTELFSSR SPSEAYKAETGK
FF(CamC)LLYSQLESEVSGDYVMPR

Spot 1139 >gi|74310597|rNADH dehydrogenase subunit 5 [Cylindrophis ruffus]

MNTITPTLTVTIFMSLTLLIMKLLIKKTQNLTHTKHIMMLMFIISLIPLSLLLNNENETMLSSPPIIYMTTTNISISLILDTFS
LTFIPVSLFITWSIVEFSIWYMSTDPYINKFIKHLLTFLIAMLIIITANNMIQLFVGWEGVGIMSFLLIGWWYARSDANSA
ALQAIIYNRIGDIGLIMTTAWLMSSSSMNMQELFTQHETMSIIPLMGLVGAAAGKSAQFGLHPWLPAAMEGPTPVSA
LLHSSTMVVAGVFLLIRLHPIMQNNITSTTCLILGATTTLFAAASAITQHDIKKIIALSTTSQLGLMMTMIGLNQPKLAFL
HMAMHSFFKALLFLCSGSFIHNLGGEQDIRKMGNLNKNLPMTSSMITIASLSLMGMPFLSGFYSKDTIIETMTISHIN
SWALMLTLVATMLSAMYSMRIINFTLTNFPRTKQKIHQENKTLAKPTLRLTLGSILAGTMTKLSTLQTTSTMTMPTTI
KLSALTITIAGILLSTDLMFLSPHQPPKKPKTLTLFFNQLAFFNMIHRAAPMKTLKFGQQISTELVDLWALENYGPKGL
SNSTIKMIHTTTQQKNLIKNYLTTFTLTIILTLVLMMSK

Sequenced Peptides AQVLWALESYGR

Spot 1146 >gi|66792936| tropomyosin 4 isoform 1 [Danio rerio]

MEAIKKKMQMLKLDKENAIDRAEQAETEQKAAEDKCKQLDDELVGLQKKLRQTEDELDKYSEALKDAQEKLELSE
KKAADAEGDVAALNRRIQLVEEELDRAQERLGTALQKLEEAEKAADESERGMKVIENRAMKDEEKMEIQEMQLKE
AKHIAEEADRKYEEVARKLVILEGELERAEERAEVAECKASDLEEELKNVTNNLKSLEAQAEKYSEKEDKYEEEIKV
LSDKLKEAETRAEFAERTVAKLEKSIDDLEDELYAQKLKYKAISEELDHALND
TTSL

Sequenced Peptides LQLVEEELDR QQDAEEGVAALNR EQLVLEELDRAEKR
LVVLEGELEKAEER

Spot 1147 >gi|74136103|ref|NP_001027910.1| tropomyosin2 [Takifugu rubripes]

MEAIKKKMQMLKLDKENAIDRAEQAEGDKKGAEDKCKQLEEELLGLQKKLKGVEDELDKYSESLKDAQEKLEQAE
KKAADAEAEVASLNRRIQLVEEELDRAQERLATALQKLEEAEKAADESERGMKVIENRASKDEEKMEIQEMQLKEA
KHIAEEADRKYEEVARKLVILEGDLERSEERAEVAEAKSGDLEEELKNVTNNLKSLEAQAEKYSQKEDKYEEEIRVL
TDKLKEAETRAEFAERSVAKLEKTIDDLEEKLAQAKEENLDMHQVLDQTLLELNNL

Sequenced Peptides NNKENALDR LQEEELLGLKK QLLVEEELDR REDELDQYSESLK
LVLLEGDLER QMLEEELGANVTNLNK VDDDLEENLAQAK

Spot 1189 >gi|41054657| HEAT-like (PBS lyase) repeat containing 1 [Danio rerio]

MANDKDIAAVGSILVNTKQDLTTRFRALFTLRNLGGAEAVKWISEAFVDESALLKHELAYCLGQMQDESAIPTLEAV
LKDTNQEPMVRHEAGEALGAIGNPKVLELLKKYAEDPVIEVAETCQLAVKRLEWLMNGGEQTKDGTDENPYCSVD
PAPPAQRKSVPELRTQLLDETLPLFDRYRAMFALRNLGTEEAVLALGDGLQCSSALFRHEIGYVLGQIQHEASIPQL
QAALEKMDENAMVRHECAEALGSIGKEPCVQILERYRKDQERVVKESCEVALDMLEYENSSQFQYADGLLRLQSA
H

Sequenced Peptides WLLDDTLPLFER WWKWVLALGGLDQ(CamC)SYWPK

Spot 1204 >gi|68372040| oxidative-stress responsive 1 [Danio rerio]

MSEDPSSQPWSIDKDDYELQEVIGSGATAVVQAAYCKPRKEKVAIKRINLEKCQTSMDELLKEIQAMSQCHHPNIV
SYYTSFVVKDELWLVMKLLSGGSVLDFIKYIISKGEHKSGVMDEPSIATILREVLEGLEYLHKNGQIHRDVKAGNILL
GEDGSVQIADFGVSAFLATGGDMTRNKVRKTFVGTPCWMAPEVMEQVRGYDFKADLWSFGITAIELATGAAPYH
KYPPMKVLMLTLQNDPPCLETGVTDKEMVKKYGKSFRKMISLCLQKDPEKRPTAAELLKHKFFTKAKNTDYLKEKL
LERAPTIGERSRKVRRVPGSSGRLHKTEDGEWEWSDDELDVESEEGKAAVAALRSPRVKEEAVPNAEVRVHFFFI
LPTKICAESSGFLQPAAVGQPEVPHAADDTATISASQAVAGPTTTGQDSAKIPISLVLRLRNTKKELNDIRFEFMPGR
DTADGVSQELVSAGLVDGRDLVIVAANLQKIVDDPQTHKNVTFKLYNYSSLLRLLLSWTIMANFGEILEAIGDFGLFQ
KLLLFALCFPNLILPFQLSSLVFNHADTNHHCNTDWILKADPNLTKEEQLNLTLPRLSDGSFNPCQMYKPVDWNLSA
IQEYGLNQTTTCTDGWVHNDTIYEATIVTDVFGFLPESARWLLDRGRTKDAKKLIQKAAAVNKRAVPESLVEEVLKE
KPVEKGGIKILFGSRVLRKYFLAITFAWCALNLAYYSLSLNVGKFGLDIFLTQLIFGLSEIPVHFLCMWSLEVVGRKPS
LIVSLVLGGCLCLLTVAVPQTWYGNLSVSSKNRLSSLVKVAGKIIGFNQTGLMDLKWDVHIDSIVKKAQQRLYFLQQ
LSKFNLPQELLVQFYSSTHLLSSNPSSALRLSCQNQPP

Sequenced Peptides SVPESLLEEVLASR

Spot 1294 >gi|94482754|gb|ABF22374.1| 3-hydroxyisobutyrate dehydrogenase [Takifugu rubripes]

MAAVFRVTRNALLKRKNNIDTACGLSRSMASKTPVGFIGLGNMGSPMAKNLLKNGYPIIATDLFPESCKELQDIGAQ
VVDSPGEVAERADRIITMLPSTPNVLEVYTGPNGILKKVKKGTLLIDSSTIDPAVSKEMAVAAEKMGAVFMDAPVTG
GVGAASLAKLSFMVGGVEEEYQAAQELLTCMGANVVYCGQVGTGQAAKICNNMLLAIGMIGTAETMNLGIRLGLD
PKLLTKILNMSSGRCWSSDTYNPVPGVMEGVPSANNYQGGFGTTLMAKDLGLAQNTATNTKTPIPLGSLAHQIFR
VMCSRGYANKDFSSVFQFLREEEGQ

Sequenced Peptides MNLFMDAPVTGRKWRR MPGLAQNTATDTK
DWPLSSLAHKLYR

Spot 1393 >gi|47937924 Short-chain dehydrogenase/reductase [Danio rerio]

MFSWIKAQHKGVDVCINNAGLALPEPLLNGKTSGWRTMMNVNVIGLAVCTREAYQSMKERNIDDGHIININSMSGH
RVVNSAFTHFYTATKYAVTALTEGLRQELREAKTHIRATSISPGLVETEFAYRLFSENQDKASATYKSIKCLQPDDLA
NAVVYVLSAPHHVQIGDIQMRPVEQLT

Sequenced Peptides YAVTALTEGLR VTSLSPGLVETEFAFR

>gi|47227808| short-chain dehydrogenase/reductase[Tetraodon nigroviridis]

MERWRGRVALVTGASVGIGAATAVALVRSGMKVVGCARDVDKVQKLSTECQVRGHSGVLVPFKCDLSNEEEILA
MFAAIKAQHGGVDVCINNAGLAHPEPLLNGKTSGWKNMLDVNVLALCVCTREAYQSMKERNVDDGHIIHINSMSG
HRVVPSADIHFYSATKYAVTALTEGLRQELRDANTHIRVTVRWEFLLVWWKQNLLPDCTVMTLTKLLLCTLNLSLW
TLSMSPTLSFTPWVPLLMCRLVTFRCGLWGRCHSDTTWEFFF

Sequenced Peptides VALVTGASVGLGAATAR MQESNEEELLSMFRDK
WGDDVNVLALPVHRK YAVTALTEGLR

Spot 1409 >gi|51858534|gb|AAH81655.1| LRP16 protein [Danio rerio]

MSARPELNLESDRSDWKQAKTKLCSMDKEKRRELYRVDFIPLEDVPVWSPSGDSSCKPRCEVNEELNMKVSLFG
GDITKLEIDAVANAANKTLLGGGGVDGAIHRGAGPLLRKECATLNGCETGEAKITGAYGLPARYVI
HTVGPIVHDSVGEREEEALRNCYYNCLHTATKHHLRTVAFPCISTGVYGYPPDQAVEVALKTVRDYLEQN
PEKLDRVIFCVFLKSDKQLYENLLPAYFPRGSPPKSKL

Sequenced Peptides WAFP(CamC)LSTGLYGYHWK

Spot 1411 >gi|37362126| Glutathione S-transferase [Micropterus salmoides]

MAKDMTLLWGSGSPPCWRVQIALEEKSLQGYNQKLLRFDKMEHKSQEVMDMNPRGQLPAFKHGNNVLNESYAA
CLYLESEFKSQGNKLIPDCSAEKALMYQRMFEGLTLNQKMADVIYYNWKVPEGERHDSAVKRNRDVLSAEVKLW
EGYLQKASGSFFAGKNFSLADVTVYPSIAYLFHFGLCEERYPKLAAYYNSNKDRPSIKATWPPTWLENPQGQDQL
KDI

Sequenced Peptides SS(CamC)MMLRKALMYQR

>gi|64236|emb|CAA45293.1| glutathione-S-transferase [Pleuronectes platessa]

MAKDMTLLWGSGSPPCWRVMIVLEEKNLQAYNSKLLSFEKGEHKSAEVMSMNPRGQLPSFKHGSKVLNESYAAC
MYLESQFKSQGNKLIPDCPAEQAMMYQRMFEGLTLAQKMADVIYYSWKVPEAERHDSAVKRNKENLSTELKLWE
EYLQKTSGSFVAGKSFSLADVSVFPGVAYLFRFGLTEERYPQLTAYYNSLKERPSIKASWPPTWLESPQGQDMLK
DV

Sequenced Peptides LFHLYYSWYVPEEER

Spot 1422 >gi|56789119|gb|AAH88077.1| Peroxiredoxin 6 [Xenopus tropicalis]

MSVLLGSVFPNFEAETTVGKIKFHDWLGDSWGILFSHPKDYTPVCTTELGRVVQLLDEFKKREIKLIAVS
CDSVKDHEGWSEDILSYVGSTGTFPYPIIADPDRKLAKELGMIDPDEKDSTGMPLTARAVFIVGSDKRLK
LSILYPATTGRNFDEILRVIDSLKLTARQKVATPVDWQPGKPCMVVPNLSNEEAKKLFPNYEQKTVPSGK
NYLRFTPDY

Sequenced Peptides VLDSLKLTAQK

Spot 1424

>gi|47193903|emb|CAF91861.1| Peroxiredoxin 6 [Tetraodon nigroviridis]

SWGILFSHPKDFTPVCTTELARAAKLSEEFKKRDVKMIALSIDSVEDHCSWSKDVMALNAEPKRPLPYPIIADDKRQ
LSVQLGMLDPDELDKDGIPLTARCVFVIGPDKKLKLSILYPATTGRNFDELLRVIDSLQLTAQKKVATPVDWK

Sequenced Peptides VLDSLQLTAKK

>gi|37748290|gb|AAH59671.1| Peroxiredoxin 6 [Danio rerio]

MPGILLGDVFPNFEADTTIGKIKFHEFLGNSWGILFSHPRDFTPVCTTELARAAKLHEEFKKRDVKMIALSIDSVEDH
RKWSEDILAFNQDKACCPMPFPIIADDKRELSVLLGMLDPDERDKDGMPLTARCVFVVGPDKRLKLSILYPATTGR
NFDEILRVVDSLQLTATKKVATPVDWKPGQEVMVIPSLSDEEANKLFPAGFTLKEVPSGKKYIRYTKP

Sequenced Peptides LSLLYPATWK RLLLGDVFPNPFVDGLFSK DFTPVCTTELACAAK
NFDELLR VLDSLQLTAKK

Spot 1439 >gi|57157763|dbj|BAD83854.1| apolipoprotein A-IV1 [Takifugu rubripes]

MKVLAVLVLALFSGVNANILWQQPPKSNLDMVKDAFWDYVAKVTLTAEESLNQIRQSELGQEVNAKFSES
ADKVNQYVVALRTQATPLTQDFITRVSQEAEQLKTRLETELSAMTTNLQPYSDMLVKLQTQLEEMKKETA
SLAEAMDAEALKTILQHKSHELKKQLEHNAKELQAQMVPYTEEMKNKMEQSLEDFHSSLMPIAQSFESQL
NQKTQEIQQSLIPYGEELKAKLDSSAQDVQAQLAALWEAFTKTQ

Sequenced Peptides DGWVD(CamC)VNKYVVALR MQWVEAQMTPYTKEMR

Spot 1439b >gi|68400425|Proteasome subunit beta type 5 precursor [Danio rerio]

MALQDVCGLLEPPLFPQWTAPLSQSFMPEDSTHLFGGGIYGEAFSSWVPRRSGLNPLEFYMPISEYITKS
PINFGQTPQSSNLLDVDHMHPTLPYISQSGALPFTLSHGTTTLGFAFQGGVIAAADTRSSCAGKVACPASPKVLPIH
SHLVGTTSGTSADCALWKRILARELRLYQLRHRRRLSTGGAAKLLSHMLHPFKGTELCVAATLCGWDGDEDQDN
AQPMTERYANTTLTSKSSSQSAASSGLSGVRGPRVVYVCSDGLRLQGALFSVGSGSPYAYSILDGGVRWGMSAQ
EAAAVAREAVYRPTYRDAYSGNNVDLYHVTAKGWRRRERENLKEEYYREKERRAQNNTGEKSIHSIK

Sequenced Peptides WQAPLSQDFMTYEPR VEVWGENMQPYALYYSK

Spot 1440 >gi|47211292| ubiquitin C-terminal hydrolase L1; UCH-L1t [Tetraodon nigroviridis]

MEWTPMELNPEMLNMLMTSLGVNESWRFVDVVGLESEQLSAVPKPCCALMLLFPLTQQHESFRKQQADIVEETG
VYFLKQMAPNSCGTVALLHAVANNKGKLTFASDSVLQKFLDETADMSSDDRAKHLEKN

Sequenced Peptides LFDETANFSADDR MAKFMAVAVLALLHAVANNKSK

>gi|37722017 ubiquitin C-terminal hydrolase L1; UCH-L1 [Danio rerio]

MEWKPMEINPEMLNKVLSKLGVGSKWRFVDVLGLEDESLSGVPSPCCAMMLLFPLTQQHEDFRSKQSVGDCKD
VYFLKQTVVNSCGTVGLVHAVANNQDSIDFDNNSALKKFLEATSGMSPAERAKELEQNKAIQETHDAVADEGQCR
PEADKVNFHFITFVNVNGRLYELDGRIDGPVSHGPTKPDSFVMDAARVCREFMEREKGEVRFSAVALCKA

Sequenced Peptides FSAVAL(CamC)R LFDETANFSADDR VDVNGQLYEFDGR
YS(CamC)NS(CamC)GTLALLHAVANDWR

Spot 1507 >gi|67772036 Ferritin middle subunit [Siniperca chuatsi]

MESQVRQNYHRDCEAAINRMVNMELFASYTYTSMAFYFSRDDVALPGFTHFFKENSEEEREHAQKLLSFQNNRG
GRIFLQDIKKPERDEWGSGLEAMQCALQLEKNVH

Sequenced Peptides LLSFKNNR

>gi|51858515|gb|AAH81630.1| Zgc:92245 [Danio rerio] Ferritin heavy polypeptide

MSSQVRQNFHQECEAAINRQIYLELYASYVYLSMGYYFDRDDKSLPNFAKFFRDQSKEEREHAEKLMSLQ
NQRGGRIFLQDIKKPDRDEWGSGLEALECALALEKSVNLSLLELHKVATQHNDPHVCDFLETHYLDEQVK
SIKELSDWVGSLRRMGAPQNNMAEYLFDRHTLGKESS

Sequenced Peptides MAEYLFSR

>gi|47939430|gb|AAH71455.1| Zgc:56095 protein [Danio rerio] Ferritin lower subunit

MSLIKQNLHSNNEANINKLINLKLTASYVYLSLGMYFDRDDVALPNFSKFFLERSHKERDHAEDLLEYQN
TRGGRILLQTVAKPSRDDWKGGIDALAFSLEHQKSINRSLLEVHRVAGDHSDPHLSDFLEGKFFTDSHET
IKTLGDYLGSLSRITSSDPHGKMAEYLFDKHTLSSTQIS

Sequenced Peptides MAEYLFSR LGDYLGTLTR

Spot 1512

>gi|37779086|gb|AAP20203.1| putative transient receptor protein 2 [Pagrus major]

HEGAKGKTTKKRPQRATSNVFAMFDQSQIQEFKEAFNMIDQNRDGFIDKEDLHDMLASLGKNPSDEYLEGMMSE
APGPINFTMFLTMFGERLNGTDPEDVIRNAFACFDEEGSGVIHEDHLRELLTTMGDRFTDEEVDELFREAPIDKKG
NFNYAEFTRILKHGAKDKDDE

>gi|47213295|emb|CAG12377.1| unnamed protein product [Tetraodon nigroviridis]

MSSKRAKGKTTKKRPQRATSNVFAMFDQSQIQEFKEAFNMIDQNRDGFIDKEDLHDMLASLGKNPSDEYLEGMM
AEAPGPINFTMFLTMFGERLNGTDPEDVIRNAFACFDEEGSGVIHEDHLRELLTTMGDRFTDEEVDELFREAPIDKK
GNFNYAEFTRILKHGAKDKDD

>gi|33991794|gb|AAH56526.1| Myosin light chain (19.9 kD) (mlc-4) [Danio rerio]

MSSKRAKGKITKKRPQRATSNVFAMFDQSQIQEFKEAFNMIDQNRDGFIDKEDLHDMLASLGKNPADDYLEAMMT
EAPGPINFTMFLTMFGEKLNGTDPEEVIRNAFACFDEEGTGFIHEDYLRELLTTMGDRFTDEEVDELFREAPIDKKS
NFNYVEFTRILKHGAKDKDD

Sequenced Peptides EAFNMLDQNR ARGTDMLPVLR FTDEEVDELFR GNFNYAEFTR

Annex III.3.- *Variation between experimental and theoretical Mr and pI values*. Experimental (Exper) and theoretical (Theor) Mr and pI values of each protein were measured with software analysis and Expasy Mw/pI tool, respectively. Variation [Δ (Exp-Theor)] was calculated as (Exper-Theor)) value and normalization [Norm Δ] as (Exper value-Theor value)/ (Exper value+Theor value).

Spot ID	**Prot ID**	***Mr***				***pI***		
		Exp.	**Theor.**	**Δ(Exp-Theo)**	**Norm Δ**	**Exp.**	**Theor.**	**Δ(Exp-Theo)**
240	Alpha-2-macroglobulin-1	92	150	-58	-0,240	4,31	6,23	-1,9
250	Alpha-2-macroglobulin-1	92	150	-58	-0,240	4,38	6,23	-1,9
253	Alpha-2-macroglobulin-1	91	150	-59	-0,245	4,45	6,23	-1,8
261	Alpha-2-macroglobulin-1	90	150	-60	-0,250	4,52	6,23	-1,7
263	Alpha-2-macroglobulin-1	89	150	-61	-0,255	4,58	6,23	-1,7
265	Alpha-2-macroglobulin-1	88	150	-62	-0,261	4,65	6,23	-1,6
267	Alpha-2-macroglobulin-1	88	150	-62	-0,261	4,72	6,23	-1,5
277	Alpha-2-macroglobulin-1	88	150	-62	-0,261	4,78	6,23	-1,5
284	Alpha-2-macroglobulin-1	87	150	-63	-0,266	4,86	6,23	-1,4
298	Chaperone protein GP96	85	91	-6	-0,034	4,38	4,77	-0,4
424	Hemopexin	77	49	28	0,222	4,36	5,66	-1,3
431	Hemopexin	76	49	27	0,216	4,44	5,66	-1,2
438	Hemopexin	75	49	26	0,210	4,52	5,66	-1,1
531	Hemopexin	71	49	22	0,183	5,28	5,66	-0,4
540	Keratin	70	61	9	0,069	4,84	5,04	-0,2
541	Keratin	70	61	9	0,069	4,91	5,04	-0,1
581	Keratin	68	61	7	0,054	4,71	5,04	-0,3
801	Cytosolic nonspecific dipeptidase	58	53	5	0,045	5,27	5,18	0,1
851a	ATP synthase β-subunit	56	55	1	0,009	4,64	5,09	-0,5
851b	ATP synthase β-subunit	55	55	0	0,000	4,63	5,09	-0,5
932	Interferon induced protein 56	53	50	3	0,029	7,59	6,48	1,1
1017	3-hydroxyisobutyryl-Coenzyme A hydrolase	49	42	7	0,077	6,32	7,66	-1,3
1030	Keratin 18	48	45	3	0,032	4,62	5,02	-0,4

Annex III.3.- *Variation between experimental and theoretical Mr and pI values* (continuation).

Spot ID	Prot ID	*Mr*				*pI*		
		Exp.	Theor.	Δ(Exp-Theo)	Norm Δ	Exp.	Theor.	Δ(Exp-Theo)
1031	Keratin 18	48	45	3	0,032	4,54	5,02	-0,5
1032	Proteasome 26S subunit ATPase 6	48	44	4	0,043	7,37	7,1	0,3
1102	Glyceraldehyde 3-phosphate dehydrogenase	44	36	8	0,100	7,45	6,55	0,9
1106	Keratin 8	44	58	-14	-0,137	4,41	5,15	-0,7
1119	Tropomyosin	43	33	10	0,132	4,03	4,67	-0,6
1123	Keratin S8 type I	43	79	-36	-0,295	4,49	5,14	-0,6
1134	Annexin A3	42	37	5	0,063	5,16	5,13	0,0
1139	NADH dehydrogenase 5	42	66	-24	-0,222	6,19	9,76	-3,6
1146	Tropomyosin 4 isoform 1	41	33	8	0,108	3,91	4,66	-0,8
1147	Tropomyosin 2	41	33	8	0,108	4,02	4,68	-0,7
1189	HEAT-like repeat containing 1	39	34	5	0,068	4,05	4,77	-0,7
1204	similar to oxidative-stress responsive 1	39	98	-59	-0,431	6,66	7,24	-0,6
1294	3-hydroxyisobutyrate dehydrogenase	28	35	-7	-0,111	7,95	8,09	-0,1
1393	Short-chain dehydrogenase/reductase	27	20	7	0,149	8,3	7,78	0,5
1409	LRP16 protein	26	28	-2	-0,037	5,7	6,6	-0,9
1411	Glutathione S-transferase	26	25	1	0,020	6,04	7,63	-1,6
1422	Peroxiredoxin 6	26	25	1	0,020	6,54	6	0,5
1424	Peroxiredoxin 6	25	25	0	0,000	3,89	6,1	-2,2
1439	Apolipoprotein A-IV1	24	29	-5	-0,094	4,01	4,95	-0,9
1439b	Proteasome subunit beta type 5	23	40	-17	-0,270	4,13	8,76	-4,6
1440	Ubiquitin C-terminal hydrolase	25	24	1	0,020	5,02	5,2	-0,2
1507	Ferritin subunits (H, M, L)	19	21	-2	-0,050	5,22	5,51	-0,3
1512	Putative transient receptor protein 2 or Myosin light chain	19	20	-1	-0,026	4,23	4,67	-0,4

Annex III.4.- Variation between experimental *pI* value of the identified proteins measured with the Decyder software and the theoretical *pI* calculated with Expasy tools. The experimental *pI* of every identified spot was plotted against the theoretical *pI* (down).

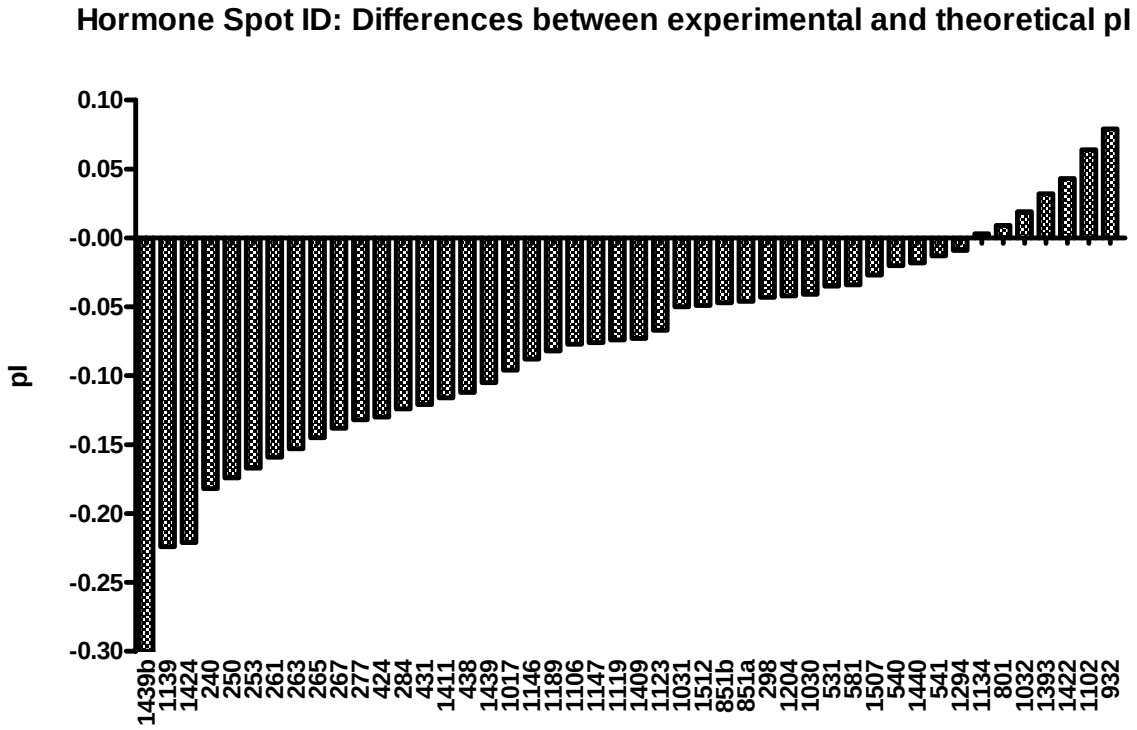

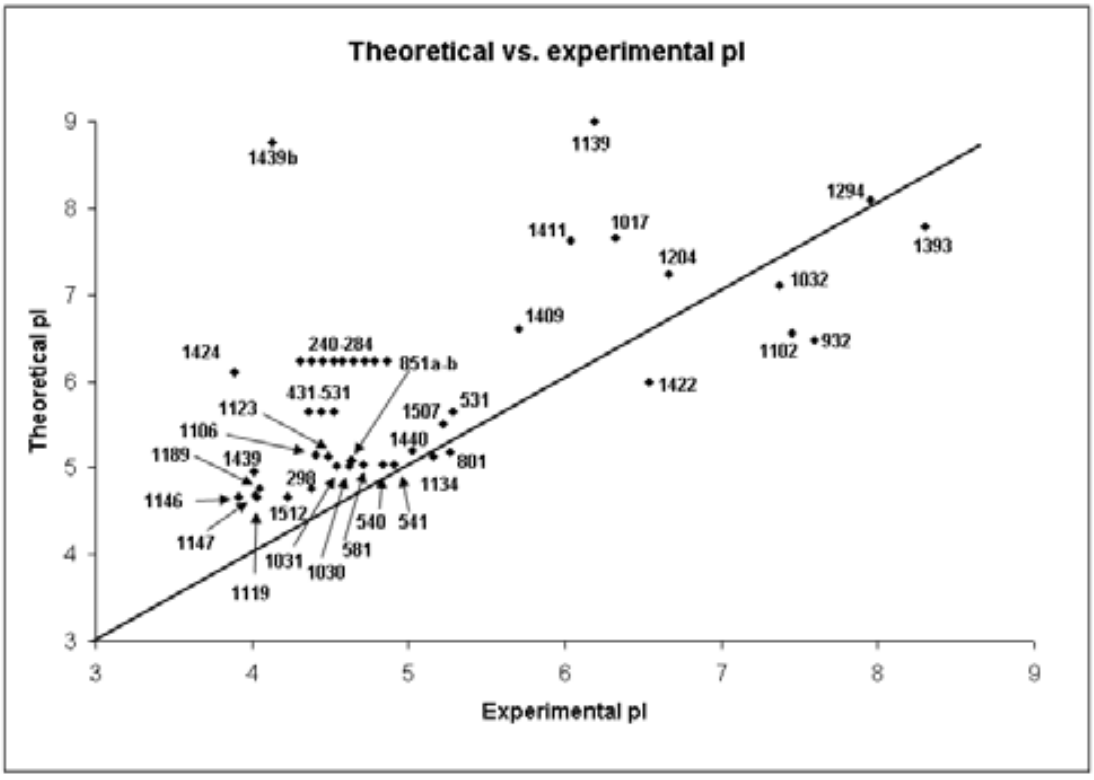

Annex III.5- Variation between experimental Mr value of the identified proteins measured with the Decyder software and the theoretical Mr calculated with Expasy tools. The experimental *Mr* of every identified spot was plotted against the theoretical *Mr* (down).

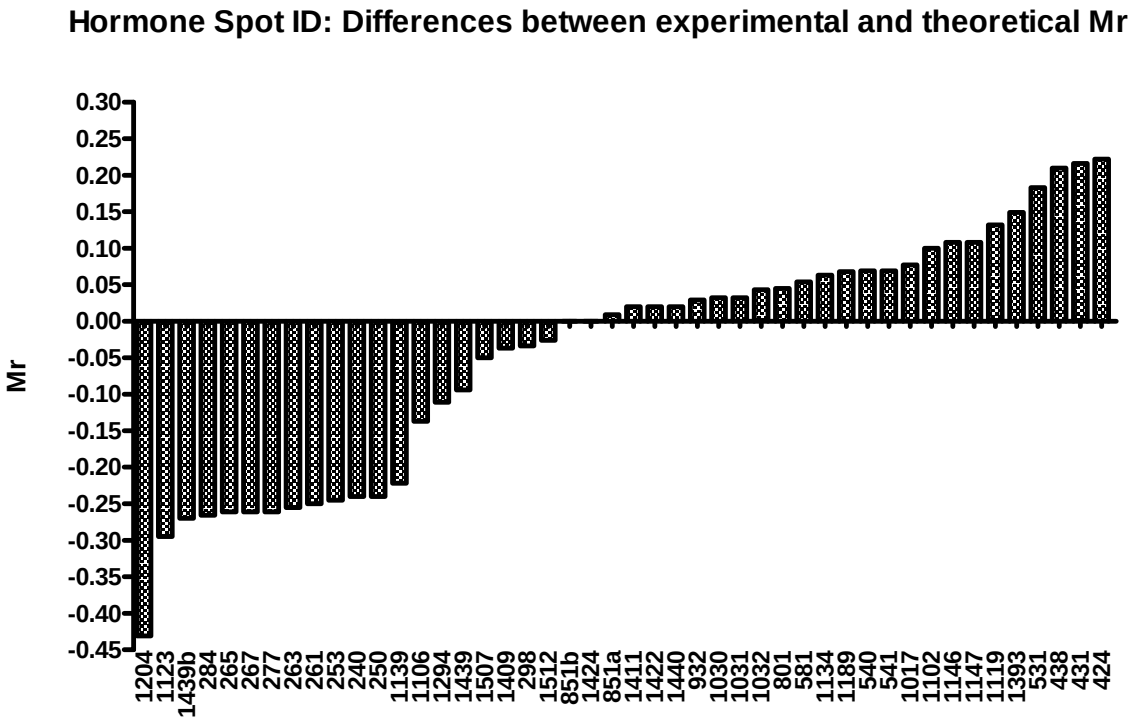

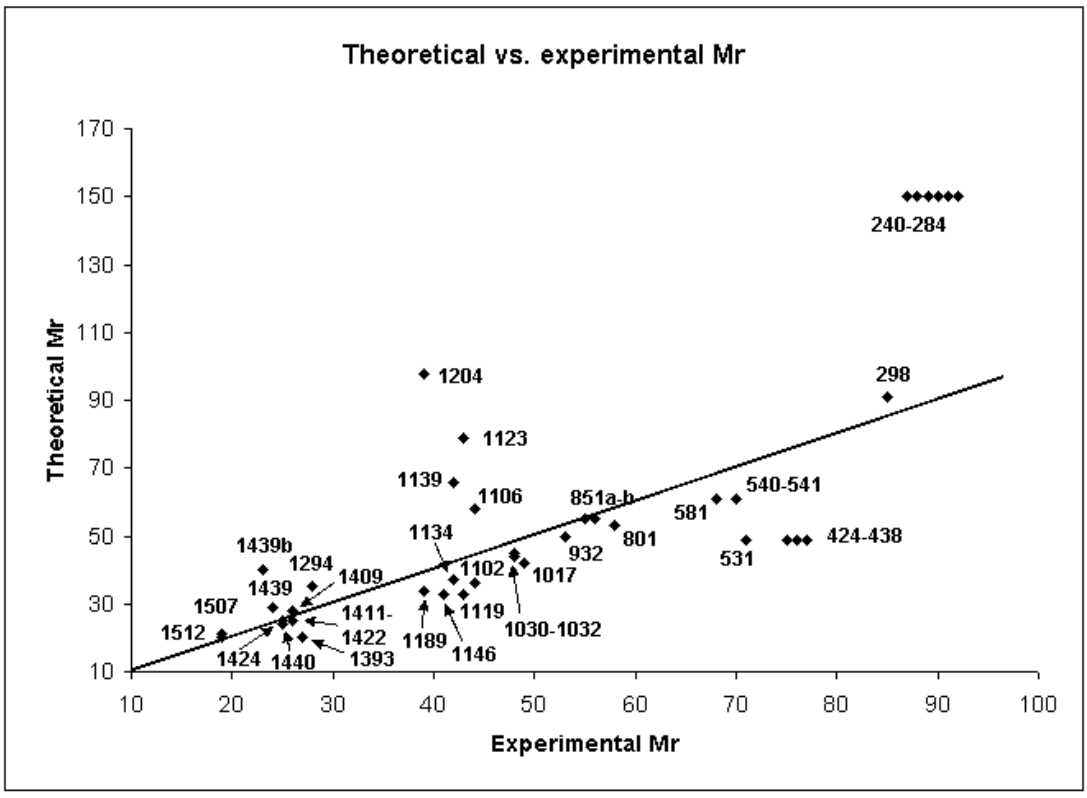

Annex III.6.- Detailed results for the transcriptomic analysis performed using the testis tissue from F1 *S.senegalensis* (Control, GnRHa treated, GnRHA +OA treated). Two different comparisons were performed in triplicate in an array composed of 5087 transcripts: F1 GnRHa vs. F1 Control and F1 GnRHa vs. F1 GnRHa+OA.

Replicate Fold Change Results

The results of the expression analysis are presented after processing the average population values for each gene.

In this report, we concentrate on the genes and pathways that were significantly regulated across the different analyses.

First we list the associated pathways that contain al least one gene with significant regulation (including all the genes in the array that are inside the same pathway) and at the end the up-regulated and down-regulated gene lists. The gene lists contain the fold change value, the associated p-value and finally the mean control value for each regulated gene.

A fold change value of +1.2 reflects a 20% up regulation, while -1.4 means a 40% down-regulation.

The *p-values* are calculated according to the absolute value of the *regularized t-statistic (Baldi and Long ,2001)* which uses a Bayesian framework to derive the following formula:

$$t_R = \frac{\overline{x_n}}{\sqrt{\frac{v_0 \widetilde{s_0^2} + (n-1)\widetilde{s_n^2}}{v_0+n-1}}}$$

where v_0 is a tunable parameter that determines the relative contributions of gene specific and global variances. This leads to a *t-student* distribution with $v_0 + n - 1$ degrees of freedom. $v_0 = 1$ is the value used in our analysis, as when we have a small number of replicates (2 or 3) helps to slightly increase the degrees of freedom while with more than 3 replicates, quickly decreases the importance of the population statistics as it grows the reliability of the $\widetilde{s_n}$ estimate. *p-values* were calculated as two-tailed tests from the t-distribution under the null hypothesis M=0. A typical treshhold for the *p-value* is being lower than 0.05 - means 5% of probability that that gene is not regulated. The absence of the *p-value* reflects the situation wherein replica data were discarded and a single value was retained.

The mean expression level of the control value was included to permit to assess the absolute gene expression level in addition to the gene expression changes.

3.1 Group #1 - IR-Ct-0306_Cy5 vs IR-Gn-0306_Cy3 : IR-Ct-0306_Cy5 vs IR-Gn-0306_Cy3

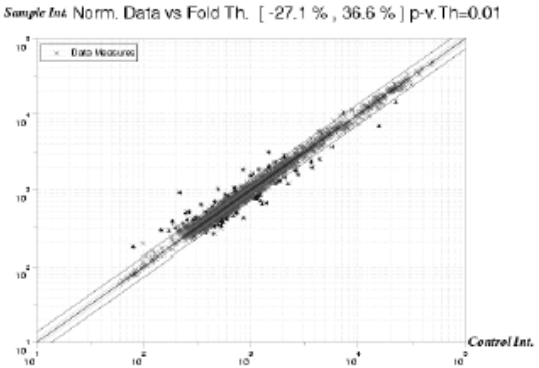

(a) Normalized Data *vs* Fold Change Threshold

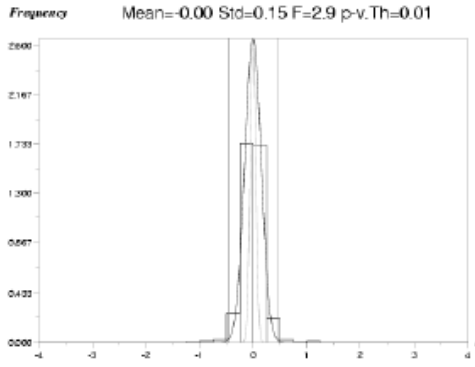

(b) log(Control/Sample) Histogram

Replicate Number = 3	log(Ratio)	Fold Ch.
Robust Mean	-0.004	-1.003
Robust Std	0.150	
Upper Cut-off Th.	3.000 σ	1.362
Lower Cut-off Th.	-3.000 σ	-1.370
P-Value Th.	0.01	1.00%
Up-Regulated Gene #	32	
Down-Regulated Gene #	38	
Total Regulated Gene #	70	

(c) Fold Change Statistics

Figure 3.1: Fold Change Data for *IR-Ct-0306_Cy5 vs IR-Gn-0306_Cy3* Group.

3.1.1 Regulated Pathways List

NOTE: Take into account that the information contained in the Pathways just accounts for *102* genes of all the *5087* transcripts available on the array. That means that they only can reflect *2.01%* of the DNA array available information.

PATHWAY	DESCRIPTION	GENES IN ARRAY
dre03010:G1	Ribosome - Danio rerio (zebrafish)	Chimera, (-1.1)fau, Hypothetical-protein, -2-6, LOC554630, LOC554792, LOC567951, LOC573049, putative-protein-(5I806)-(LOC568650)-Danio-rerio, rpl10, (-1.1)(-1.1)rpl12, rpl13, (+1.1)rpl13a, (-1.2)rpl19, (+1.1)rpl26, (-1.1)rpl27, (+1.1)rpl34, (-1.1)rpl35, (-1.1)rpl36, (+1.1)rpl5b, (-1.1)rpl7a, (-1.1)rps10, (+1.1)rps14, (+1.1)rps15a, (-1.1)(-1.1)rps18, (-1.2)rps2, rps21, rps26, (-1.1)rps29, (+1.1)rps3, (-1.1)rps5, rps7, (-1.1)rpsa, (+1.5)(+1.1)zgc

3.1.2 Up-Regulated Gene List

ID	FOLD	NAME	P-VALUE	CTRL	DESCRIPTION
PGSP0013L19-T7.AB1	+4.32	pgsP0013L19-T7.ab1	0.00024960		
CL799CONTIG1-ENSDARG00000038434	+2.22	zp2	0.00583460		zona pellucida glycoprotein 2.2 Source: RefSeq-peptide NP-571902
CONS-PGSP0029K08-T7.AB1-ENSDARG00000036518	+2.18	ba1l	0.0000130		Hemoglobin beta-1 subunit (Hemoglobin beta-1 chain) (Beta-1-globin) (Beta-A1-globin). Source: Uniprot/SWISSPROT Q90486
PGSP0029K08-T7.AB1-ENSDARG00000036518	+2.16	ba1l	0.00003190		Hemoglobin beta-1 subunit (Hemoglobin beta-1 chain) (Beta-1-globin) (Beta-A1-globin). Source: Uniprot/SWISSPROT Q90486
PGSP0030K15-T7.AB1-ENSDARG00000012199	+2.04	SP-Q6K0C3-SPAAU	0.00007650		Q6k0c3 sparus aurata (gilthead sea bream). cytosolic alanine aminotransferase. 7/2004 Length = 491-GO:0016847; F:1-aminocyclopropane-1-carboxylate synthase . . .; IEA GO:0009058; P:biosynthesis; IEA
CL244CONTIG1-ENSDARG00000019357	+2.04	LOC557510	0.00147650		PREDICTED: similar to liver fatty acid binding protein Source: RefSeq-peptide-predicted XP-685682
CL489CONTIG1-ENSDARG00000013430	+2.03	zgc	0.00042160		betaine-homocysteine methyltransferase Source: RefSeq-peptide NP-001012498
CL510CONTIG1-ENSDARG00000044638	+2.01	zgc	0.00388320		hypothetical protein LOC393268 Source: RefSeq-peptide NP-956592
CL154CONTIG1	+1.96	SP-Q9W7D4-ORYLA	0.00167290		Q9w7d4 oryzias latipes (medaka fish) (japanese ricefish). hypothetical protein. 3/2004 Length = 199-
PGSP0020G15-T7.AB1	+1.83	pgsP0020G15-T7.ab1	0.00020380		
CL29CONTIG1-ENSDARG00000017299	+1.70	zgc	0.00004570		peripheral myelin protein 2 Source: RefSeq-peptide NP-001004682
CL1186CONTIG1	+1.64	SP-Q6DHD6-BRARE	0.00023160		Q6dhd6 brachydanio rerio (zebrafish) (danio rerio). zgc:92501. 10/2004 Length = 342-GO:0004034; F:aldose 1-epimerase activity; IEA GO:0006012; P:galactose metabolism; IEA
PGSP0023I15-T7.AB1	+1.62	SP-Q9IA80-XENLA	0.00006310		Q9ia80 xenopus laevis (african clawed frog). securin. 3/2003 Length = 188-GO:0005737; C:cytoplasm; IEA GO:0000067; P:DNA replication and chromosome cycle; IEA
PGSP0021L12-T7.AB1	+1.59	pgsP0021L12-T7.ab1	0.00076670		
PGSP0002A05-T7.AB1-ENSDARG00000043153	+1.57	ZFIN	0.00007830		cyclin B1 Source: RefSeq-peptide NP-571588
PGSP0016J04-T7.AB1	+1.56	pgsP0016J04-T7.ab1	0.00006730		
CL636CONTIG1	+1.52	CL636Contig1	0.00081580		
CL465CONTIG1-ENSDARG00000035756	+1.52	zgc	0.00536760		hypothetical protein LOC393818 Source: RefSeq-peptide NP-957139
PGSP0011F09-T7.AB1	+1.51	SP-Q9SPM1-LYCES	0.0004470		Q9spm1 lycopersicon esculentum (tomato). extensin-like protein. 3/2004 Length = 711-GO:0005199; F:structural constituent of cell wall; IEA

PGSP0001P08-T7.AB1	+1.50	pgsP0001P08-T7.ab1	0.00009090		
PGSP0027B10-T7.AB1	+1.48	pgsP0027B10-T7.ab1	0.00119250		
PGSP0019H08-T7.AB1-ENSDARG00000045946	+1.43	LOC570543	0.00046010		PREDICTED: similar to Protein transport protein Sec24D (SEC24-related protein D) Source: RefSeq-peptide-predicted XP-699130
PGSP0013I09-T7.AB1	+1.43	pgsP0013I09-T7.ab1	0.00030580		
CL232CONTIG1	+1.41	CL232Contig1	0.00051840		
CL257CONTIG1	+1.40	CL257Contig1	0.00168120		
CL771CONTIG1-ENSDARG00000005454	+1.39	tacc3	0.00081980		transforming acidic coiled coil 3 protein Source: RefSeq-peptide NP-997746
PGSP0027I03-T7.AB1	+1.39	pgsP0027I03-T7.ab1	0.00118930		
CL1100CONTIG1-ENSDARG00000007219	+1.38	ACTN1-HUMAN	0.00076080		P12814 homo sapiens (human). alpha-actinin 1 (alpha-actinin cytoskeletal isoform) (non-muscle alpha-actinin 1) (f-actin cross linking protein). 5/2005 Length = 892-GO:0015629; C:actin cytoskeleton; TAS GO:0017166; F:vinculin binding; IPI
PGSP0016B19-T7.AB1-ENSDARG00000036995	+1.38	LOC573495	0.00032140		hypothetical protein LOC415167 Source: RefSeq-peptide NP-001002077
CL135CONTIG1-ENSDARG00000005221	+1.38	LOC564420	0.00033540		PREDICTED: similar to desmin Source: RefSeq-peptide-predicted XP-692850
PGSP0004L20-T7.AB1	+1.37	pgsP0004L20-T7.ab1	0.00025190		
PGSP0016M23-T7.AB1-ENSDARG00000029798	+1.37	SP-Q5BJ65-XENTR	0.00094480		CONS Q5bj65 xenopus tropicalis (western clawed frog) (silurana tropicalis). hypothetical protein. 5/2005 Length = 128- Q5bj65 xenopus tropicalis (western clawed frog) (silurana tropicalis). hypothetical protein. 5/2005 Length = 128-

3.1.3 Down-Regulated Gene List

ID	FOLD	NAME	P-VALUE	CTRL	DESCRIPTION
CL1051CONTIG1	-2.24	CL1051Contig1	0.00002710		
CONS-PGSP0021E08-T7.AB1-ENSDARG00000033009	-2.07	zgc	0.00020460		hypothetical protein LOC336231 Source: RefSeq-peptide NP-956297
PGSP0012I19-T7.AB1	-2.01	pgsP0012I19-T7.ab1	0.00002190		
PGSP0015N21-T7.AB1	-1.91	pgsP0015N21-T7.ab1	0.00071030		
R-CL491CONTIG1	-1.90	CL491Contig1	0.00003410		
CONS-PGSP0021E08-T7.AB1-ENSDARG00000033009	-1.83	zgc	0.00037760		hypothetical protein LOC336231 Source: RefSeq-peptide NP-956297
CL973CONTIG1-ENSDARG00000043625	-1.71	SP-Q6DCC9-XENLA	0.00007580		Q6dcc9 xenopus laevis (african clawed frog). mgc83638 protein. 10/2004 Length = 494-GO:0008757; F:S-adenosylmethionine-dependent methyltransf. . .; IEA GO:0009312; P:oligosaccharide biosynthesis; IEA
PGSP0009K11-T7.AB1	-1.70	pgsP0009K11-T7.ab1	0.00004140		
CL382CONTIG1-ENSDARG00000044734	-1.70	ZFIN	0.00007780		actin related protein 2/3 complex, subunit 3 Source: RefSeq-peptide NP-001002114
R-PGSP0029F18-T7.AB1	-1.70	pgsP0029F18-T7.ab1	0.0006520		
PGSP0008G07-T7.AB1-ENSDARG00000018263	-1.59	LOC558994	0.00113510		hypothetical protein LOC394023 Source: RefSeq-peptide NP-957342
PGSP0028F14-T7.AB1-ENSDARG00000040768	-1.54	SP-Q5VWP7-HUMAN	0.00018920		Q5vwp7 homo sapiens (human). putative homeodomain transcription factor 1. 2/2005 Length = 762-
PGSP0010D14-T7.AB1	-1.53	pgsP0010D14-T7.ab1	0.00043150		
PGSP0028O03-T7.AB1	-1.52	pgsP0028O03-T7.ab1	0.00020360		
PGSP0015M22-T7.AB1	-1.52	pgsP0015M22-T7.ab1	0.00130840		
PGSP0001K12-T7.AB1	-1.48	pgsP0001K12-T7.ab1	0.00048160		
PGSP0021M24-T7.AB1	-1.48	CALD1-CHICK	0.0001150		P12957 gallus gallus (chicken). caldesmon (cdm). 2/2005 Length = 771-
CL380CONTIG1	-1.46	CL380Contig1	0.00127160		
PGSP0013L11-T7.AB1-ENSDARG00000015239	-1.46	prp19	0.00086840		PRP19/PSO4 homolog Source: RefSeq-peptide NP-958875

PGSP0018A16-T7.AB1	-1.45	SP-Q5BKP5-MOUSE	0.00446730		Q5bkp5 mus musculus (mouse). ddx50 protein. 5/2005 Length = 734-GO:0005524; F:ATP binding; IEA GO:0000166; F:nucleotide binding; IEA
PGSP0028P13-T7.AB1-ENSDARG00000029072	-1.44	LOC554994	0.00026710		Kruppel-like factor 6 Source: RefSeq-peptide NP-958869
PGSP0022D02-T7.AB1	-1.43	pgsP0022D02-T7.ab1	0.00025110		
PGSP0028G10-T7.AB1	-1.42	pgsP0028G10-T7.ab1	0.00036970		
CL1080CONTIG1	-1.42	CL1080Contig1	0.00034050		
PGSP0016C15-T7.AB1	-1.41	pgsP0016C15-T7.ab1	0.00366230		
R-PGSP0014K04-T7.AB1	-1.41	pgsP0014K04-T7.ab1	0.0002930		
PGSP0022B09-T7.AB1	-1.40	pgsP0022B09-T7.ab1	0.0009470		
PGSP0020E17-T7.AB1	-1.39	pgsP0020E17-T7.ab1	0.0003250		
PGSP0013O08-T7.AB1-ENSDARG00000015279	-1.39	SP-Q5ZMW0-CHICK	0.00641870		Q5zmw0 gallus gallus (chicken). hypothetical protein. 10/2004 Length = 794-
PGSP0002N07-T7.AB1-ENSDARG00000044619	-1.39	birc2	0.00151650		baculoviral IAP repeat-containing 2 Source: RefSeq-peptide NP-919376
PGSP0001K20-T7.AB1-ENSDARG00000039702	-1.38	LOC567628	0.00141950		eukaryotic translation initiation factor 3, subunit 10 (theta) Source: RefSeq-peptide NP-956114
R-PGSP0001M02-T7.AB1	-1.38	pgsP0001M02-T7.ab1	0.00031720		
PGSP0016C07-T7.AB1	-1.38	pgsP0016C07-T7.ab1	0.00267910		
PGSP0025E18-T7.AB1-ENSDARG00000040530	-1.38	NP-001015066.1 (RefSeq peptide ID) . To view all Ensembl genes linked to the name click here.	0.00049530		beta3-glucuronyltransferase Source: RefSeq-peptide NP-001015066
PGSP0013I17-T7.AB1-ENSDARG00000039849	-1.38	serpinb1l4	0.00330980		serpin peptidase inhibitor, clade B (ovalbumin), member 1, like 4 Source: RefSeq-peptide NP-956235
PGSP0013D15-T7.AB1	-1.38	pgsP0013D15-T7.ab1	0.00206710		

3.2 Group #2 - IR-GnOA-0306_Cy5 vs IR-Gn-0306_Cy3 : IR-GnOA-0306_Cy5 vs IR-Gn-0306_Cy3

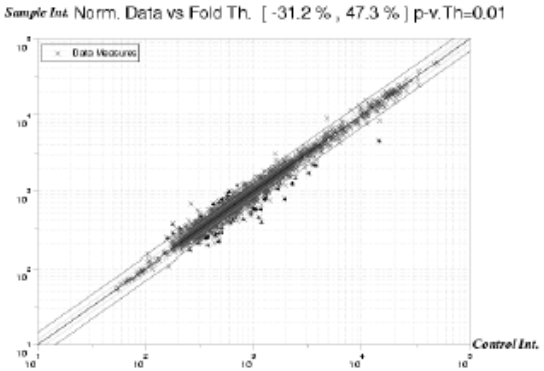

(a) Normalized Data *vs* Fold Change Threshold

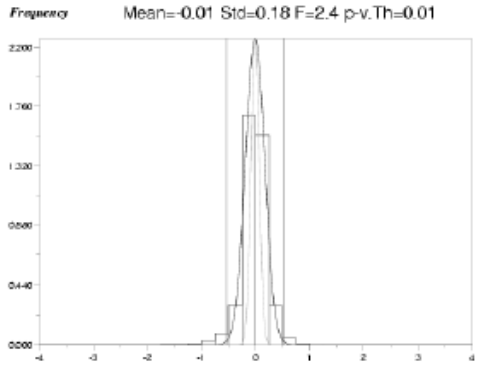

(b) log(Control/Sample) Histogram

Replicate Number = 3	log(Ratio)	Fold Ch.
Robust Mean	-0.008	-1.006
Robust Std	0.176	
Upper Cut-off Th.	3.000 σ	1.435
Lower Cut-off Th.	-3.000 σ	-1.451
P-Value Th.	0.01	1.00%
Up-Regulated Gene #	11	
Down-Regulated Gene #	34	
Total Regulated Gene #	45	

(c) Fold Change Statistics

Figure 3.3: Fold Change Data for *IR-GnOA-0306_Cy5 vs IR-Gn-0306_Cy3* Group.

3.2.1 Regulated Pathways List

NOTE: Take into account that the information contained in the Pathways just accounts for *102* genes of all the *5087* transcripts available on the array. That means that they only can reflect *2.01%* of the DNA array available information.

PATHWAY	DESCRIPTION	GENES IN ARRAY
dre00590:G2	Arachidonic acid metabolism - Danio rerio (zebrafish)	(+1.1)mest, (+1.1)(+1.6)(+1.3)(-1.6)zgc
dre00625:G2	Tetrachloroethene degradation - Danio rerio (zebrafish)	(+1.1)mest, (+1.1)(+1.6)(+1.3)(-1.6)zgc
dre00980:G2	Metabolism of xenobiotics by cytochrome P450 - Danio rerio (zebrafish)	(+1.1)adh5, (+1.1)mest, (+1.1)(+1.6)(+1.3)(-1.6)zgc
dre03010:G2	Ribosome - Danio rerio (zebrafish)	Chimera, fau, Hypothetical-protein, -2-6, (-1.1)LOC554630, LOC554792, (-1.1)LOC567951, LOC573049, putative-protein-(5I806)-(LOC568650)-Danio-rerio, rpl10, (-1.2)(-1.1)rpl12, rpl13, rpl13a, (-1.2)(-1.1)rpl19, (+1.1)rpl26, rpl27, (+1.1)rpl34, rpl35, rpl36, (+1.2)rpl5b, (-1.3)rpl7a, (-1.4)rps10, (-1.1)rps14, (+1.2)rps15a, (+1.1)rps18, (-1.2)rps2, rps21, (+1.1)rps26, rps29, (+1.1)rps3, rps5, (-1.1)rps7, (-1.1)(-1.4)rpsa, (+1.1)(+1.6)(+1.3)(-1.6)zgc

3.2.2 Up-Regulated Gene List

ID	FOLD	NAME	P-VALUE	CTRL	DESCRIPTION
CL244CONTIG1-ENSDARG00000019357	+2.09	LOC557510	0.00232530		PREDICTED: similar to liver fatty acid binding protein Source: RefSeq-peptide-predicted XP-685682
PGSP0020E10-T7.AB1	+1.67	SP-Q68G59-MOUSE	0.00616630		Q68g59 mus musculus (mouse). ai849286 protein (fragment). 10/2004 Length = 1209-GO:0005634; C:nucleus; IDA
PGSP0001P08-T7.AB1	+1.66	pgsP0001P08-T7.ab1	0.0018990		
PGSP0011F09-T7.AB1	+1.63	SP-Q9SPM1-LYCES	0.0003890		Q9spm1 lycopersicon esculentum (tomato). extensin-like protein. 3/2004 Length = 711-GO:0005199; F:structural constituent of cell wall; IEA
CL465CONTIG1-ENSDARG00000035756	+1.58	zgc	0.00079390		hypothetical protein LOC393818 Source: RefSeq-peptide NP-957139
PGSP0027B10-T7.AB1	+1.56	pgsP0027B10-T7.ab1	0.00219940		
CL636CONTIG1	+1.55	CL636Contig1	0.00126340		
CL29CONTIG1-ENSDARG00000017299	+1.54	zgc	0.00567060		peripheral myelin protein 2 Source: RefSeq-peptide NP-001004682
PGSP0021L12-T7.AB1	+1.53	pgsP0021L12-T7.ab1	0.00494340		
PGSP0008L06-T7.AB1	+1.52	pgsP0008L06-T7.ab1	0.00655050		
PGSP0027I03-T7.AB1	+1.47	pgsP0027I03-T7.ab1	0.00070360		

3.2.3 Down-Regulated Gene List

ID	FOLD	NAME	P-VALUE	CTRL	DESCRIPTION
CL1051CONTIG1	-3.17	CL1051Contig1	0.00522310		
CONS-PGSP0021E08-T7.AB1-ENSDARG00000033009	-2.98	zgc	0.00283720		hypothetical protein LOC336231 Source: RefSeq-peptide NP-956297
CONS-PGSP0021E08-T7.AB1-ENSDARG00000033009	-2.41	zgc	0.00235020		hypothetical protein LOC336231 Source: RefSeq-peptide NP-956297
CL382CONTIG1-ENSDARG00000044734	-2.41	ZFIN	0.00755080		actin related protein 2/3 complex, subunit 3 Source: RefSeq-peptide NP-001002114
PGSP0028F14-T7.AB1-ENSDARG00000040768	-2.14	SP-Q5VWP7-HUMAN	0.00890090		Q5vwp7 homo sapiens (human). putative homeodomain transcription factor 1. 2/2005 Length = 762-
PGSP0015N21-T7.AB1	-1.98	pgsP0015N21-T7.ab1	0.00011120		
PGSP0012P10-T7.AB1-ENSDARG00000044307	-1.95	SP-Q66HV8-BRARE	0.00252180		Q66hv8 brachydanio rerio (zebrafish) (danio rerio). phosphofructokinase, muscle. 10/2004 Length = 784- GO:0005945; C:6-phosphofructokinase complex; IEA GO:0006096; P:glycolysis; IEA
PGSP0008G07-T7.AB1-ENSDARG00000018263	-1.90	LOC558994	0.00121870		hypothetical protein LOC394023 Source: RefSeq-peptide NP-957342
PGSP0015M22-T7.AB1	-1.89	pgsP0015M22-T7.ab1	0.00278350		
PGSP0013L11-T7.AB1-ENSDARG00000015239	-1.86	prp19	0.00502010		PRP19/PSO4 homolog Source: RefSeq-peptide NP-958875
R-PGSP0029F18-T7.AB1	-1.82	pgsP0029F18-T7.ab1	0.00474720		
R-PGSP0001M02-T7.AB1	-1.79	pgsP0001M02-T7.ab1	0.00994340		
PGSP0021M24-T7.AB1	-1.73	CALD1-CHICK	0.00323680		P12957 gallus gallus (chicken). caldesmon (cdm). 2/2005 Length = 771-
PGSP0009K11-T7.AB1	-1.72	pgsP0009K11-T7.ab1	0.00020420		
PGSP0001K20-T7.AB1-ENSDARG00000039702	-1.72	LOC567628	0.004720		eukaryotic translation initiation factor 3, subunit 10 (theta) Source: RefSeq-peptide NP-956114
PGSP0013O08-T7.AB1-ENSDARG00000015279	-1.69	SP-Q5ZMW0-CHICK	0.00289040		Q5zmw0 gallus gallus (chicken). hypothetical protein. 10/2004 Length = 794-

PGSP0028P13-T7.AB1-ENSDARG00000029072	-1.65	LOC554994	0.00346930		Kruppel-like factor 6 Source: RefSeq-peptide NP-958869
PGSP0002N07-T7.AB1-ENSDARG00000044619	-1.64	birc2	0.00264550		baculoviral IAP repeat-containing 2 Source: RefSeq-peptide NP-919376
CL380CONTIG1	-1.60	CL380Contig1	0.00041460		
PGSP0030P13-T7.AB1-ENSDARG00000042854	-1.60	zgc	0.0043160		hypothetical protein LOC394043 Source: RefSeq-peptide NP-957362
R-CL491CONTIG1	-1.60	CL491Contig1	0.00715160		
PGSP0015N22-T7.AB1-ENSDARG00000014139	-1.59	ZFIN	0.00910040		Srp72 protein (Fragment). Source: Uniprot/SPTREMBL Q32PT8
PGSP0002A05-T7.AB1-ENSDARG00000043153	-1.59	ZFIN	0.00570830		cyclin B1 Source: RefSeq-peptide NP-571588
CONS-PGSP0002P03-T7.AB1-ENSDARG00000041553	-1.59	mt2	0.00621130		Metallothionein-2 (MT-2). Source: Uniprot/SWISSPROT Q7ZSY6
PGSP0028G05-T7.AB1-ENSDARG00000035622	-1.55	ZFIN	0.00694720		X-box binding protein 1 (xbp1), mRNA Source: RefSeq-dna NM-131874
CL931CONTIG1	-1.53	CL931Contig1	0.0043150		
PGSP0013N18-T7.AB1	-1.52	SP-Q800F9-TETNG	0.0081510		Q800f9 tetraodon nigroviridis (green puffer). gart protein. 2/2005 Length = 992-GO:0005737; C:cytoplasm; IEA GO:0009113; P:purine base biosynthesis; IEA
PGSP0014D23-T7.AB1	-1.52	pgsP0014D23-T7.ab1	0.00501950		
PGSP0001M17-T7.AB1	-1.51	SP-Q6NYM8-BRARE	0.00339530		Q6nym8 brachydanio rerio (zebrafish) (danio rerio). hypothetical protein zgc:77479. 7/2004 Length = 471-GO:0005506; F:iron ion binding; IEA GO:0008152; P:metabolism; IEA
CL448CONTIG1	-1.49	CL448Contig1	0.00355260		
PGSP0014L16-T7.AB1	-1.48	pgsP0014L16-T7.ab1	0.00192450		
PGSP0022I07-T7.AB1	-1.48	pgsP0022I07-T7.ab1	0.00823430		
PGSP0016I17-T7.AB1	-1.47	pgsP0016I17-T7.ab1	0.00802160		
PGSP0013D15-T7.AB1	-1.45	pgsP0013D15-T7.ab1	0.00186560		